frontiers | Research Topics

Progression to diabetes: Molecular and cellular mechanisms

Edited by
Carlos Guillén and Adolfo Garcia-Ocana

Published in
Frontiers in Endocrinology

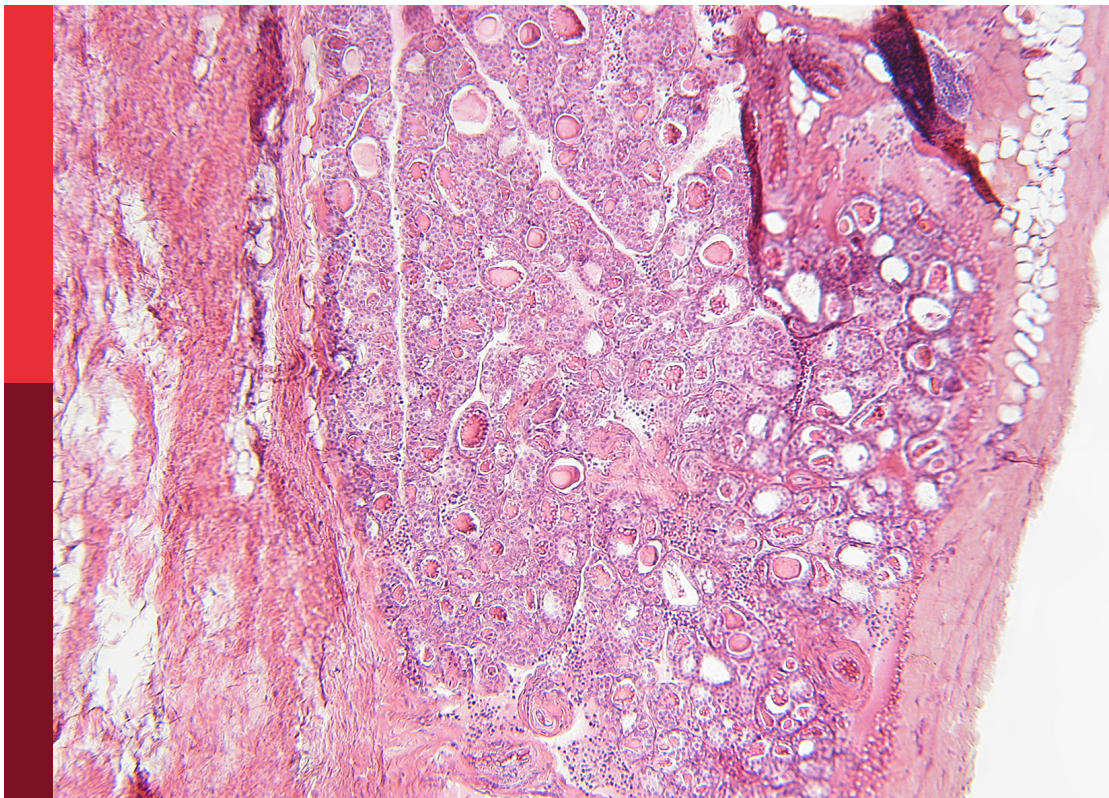

ISSN 1664-8714
ISBN 978-2-83251-722-2
DOI 10.3389/978-2-83251-722-2

About Frontiers

Frontiers is more than just an open access publisher of scholarly articles: it is a pioneering approach to the world of academia, radically improving the way scholarly research is managed. The grand vision of Frontiers is a world where all people have an equal opportunity to seek, share and generate knowledge. Frontiers provides immediate and permanent online open access to all its publications, but this alone is not enough to realize our grand goals.

Frontiers journal series

The Frontiers journal series is a multi-tier and interdisciplinary set of open-access, online journals, promising a paradigm shift from the current review, selection and dissemination processes in academic publishing. All Frontiers journals are driven by researchers for researchers; therefore, they constitute a service to the scholarly community. At the same time, the *Frontiers journal series* operates on a revolutionary invention, the tiered publishing system, initially addressing specific communities of scholars, and gradually climbing up to broader public understanding, thus serving the interests of the lay society, too.

Dedication to quality

Each Frontiers article is a landmark of the highest quality, thanks to genuinely collaborative interactions between authors and review editors, who include some of the world's best academicians. Research must be certified by peers before entering a stream of knowledge that may eventually reach the public - and shape society; therefore, Frontiers only applies the most rigorous and unbiased reviews. Frontiers revolutionizes research publishing by freely delivering the most outstanding research, evaluated with no bias from both the academic and social point of view. By applying the most advanced information technologies, Frontiers is catapulting scholarly publishing into a new generation.

What are Frontiers Research Topics?

Frontiers Research Topics are very popular trademarks of the *Frontiers journals series*: they are collections of at least ten articles, all centered on a particular subject. With their unique mix of varied contributions from Original Research to Review Articles, Frontiers Research Topics unify the most influential researchers, the latest key findings and historical advances in a hot research area.

Find out more on how to host your own Frontiers Research Topic or contribute to one as an author by contacting the Frontiers editorial office: frontiersin.org/about/contact

Progression to diabetes: Molecular and cellular mechanisms

Topic editors
Carlos Guillén — Complutense University, Spain
Adolfo Garcia-Ocana — Icahn School of Medicine at Mount Sinai, United States

Topic coordinator
Ana García Aguilar — Complutense University of Madrid, Spain

Citation
Guillén, C., Garcia-Ocana, A., eds. (2023). *Progression to diabetes: Molecular and cellular mechanisms*. Lausanne: Frontiers Media SA.
doi: 10.3389/978-2-83251-722-2

Table of contents

04 Editorial: Progression to Diabetes: Molecular and cellular mechanisms
Carlos Guillén and Adolfo Garcia-Ocana

06 Magnesium increases insulin-dependent glucose uptake in adipocytes
Lynette J. Oost, Steef Kurstjens, Chao Ma, Joost G. J. Hoenderop, Cees J. Tack and Jeroen H. F. de Baaij

18 Regulation of Pdx1 by oxidative stress and Nrf2 in pancreatic beta-cells
Sharon Baumel-Alterzon and Donald K. Scott

27 Contribution of mitochondrial gene variants in diabetes and diabetic kidney disease
Meng Li, Siqian Gong, Xueyao Han, Lingli Zhou, Simin Zhang, Qian Ren, Xiaoling Cai, Yingying Luo, Wei Liu, Yu Zhu, Xianghai Zhou, Yufeng Li and Linong Ji

46 Pancreatic β-cell hyper-O-GlcNAcylation leads to impaired glucose homeostasis *in vivo*
Seokwon Jo, Samantha Pritchard, Alicia Wong, Nandini Avula, Ahmad Essawy, John Hanover and Emilyn U. Alejandro

57 Targeting pancreatic beta cell death in type 2 diabetes by polyphenols
Ana García-Aguilar and Carlos Guillén

67 ADAR1-dependent editing regulates human β cell transcriptome diversity during inflammation
Florian Szymczak, Roni Cohen-Fultheim, Sofia Thomaidou, Alexandra Coomans de Brachène, Angela Castela, Maikel Colli, Piero Marchetti, Erez Levanon, Decio Eizirik and Arnaud Zaldumbide

79 The progress and challenges of circRNA for diabetic foot ulcers: A mini-review
Deer Li, Jiaxing Guo, Xiyu Ni, Guanwen Sun and Huhe Bao

90 Systematic review of transcriptome and microRNAome associations with gestational diabetes mellitus
Kimberly A. Lewis, Lisa Chang, Julinna Cheung, Bradley E. Aouizerat, Laura L. Jelliffe-Pawlowski, Monica R. McLemore, Brian Piening, Larry Rand, Kelli K. Ryckman and Elena Flowers

112 Improving human mesenchymal stem cell-derived hepatic cell energy metabolism by manipulating glucose homeostasis and glucocorticoid signaling
Joana Saraiva Rodrigues, Andreia Faria-Pereira, Sérgio Póvoas Camões, Ana Sofia Serras, Vanessa Alexandra Morais, Jorge Lira Ruas and Joana Paiva Miranda

frontiers | Frontiers in Endocrinology

TYPE Editorial
PUBLISHED 07 February 2023
DOI 10.3389/fendo.2023.1141337

OPEN ACCESS

EDITED AND REVIEWED BY
Jared Rutter,
The University of Utah, United States

*CORRESPONDENCE
Carlos Guillén
cguillen@ucm.es

SPECIALTY SECTION
This article was submitted to Diabetes: Molecular Mechanisms, a section of the journal Frontiers in Endocrinology

RECEIVED 10 January 2023
ACCEPTED 26 January 2023
PUBLISHED 07 February 2023

CITATION
Guillén C and Garcia-Ocana A (2023) Editorial: Progression to Diabetes: Molecular and cellular mechanisms. *Front. Endocrinol.* 14:1141337. doi: 10.3389/fendo.2023.1141337

Editorial: Progression to Diabetes: Molecular and cellular mechanisms

Carlos Guillén[1,2]* and Adolfo Garcia-Ocana[3]

[1]Department of Biochemistry and Molecular Biology, Faculty of Pharmacy, Complutense University, Madrid, Spain, [2]Centro de Investigación Biomédica en Red (CIBER) de Diabetes y Enfermedades Metabólicas Asociadas, Instituto de Salud Carlos III, Madrid, Spain, [3]Medicine, Endocrinology, Diabetes and Bone Disease, Icahn School of Medicine at Mount Sinai, New Yor, NY, United States

KEYWORDS

pancreatic beta (β) cells, type 1 diabetes mellitus, gestational diabetes – mellitus, type 2 (non-insulin-dependent) diabetes mellitus, diabetic patient

Editorial on the Research Topic
Progression to Diabetes: Molecular and cellular mechanisms

Diabetes represents a group of heterogeneous metabolic diseases, which share the appearance of hyperglycemia. The main goal of this Research Topic is to describe different biological processes and molecular mechanisms regulating pancreatic β cell homeostasis with a special emphasis on:

1. Post-translational modifications of different proteins involved in metabolism.
2. Signaling pathways altered during the progression of the disease (mainly in T1DM, T2DM, and gestational diabetes or GDM).
3. Cellular mechanisms that could explain the progression of the disease.
4. Metabolic and epigenetic changes occurring during the progression of diabetes (T1DM, T2DM, and GDM).

This special issue contains nine papers in total: five original research papers presenting novel data about some of the items previously indicated, three mini-reviews, and one systematic review.

In the first of the original papers published in this special issue (Szymczak et al.), the authors report that an enzyme involved in RNA editing, the RNA-specific adenosine deaminase 1 (ADAR1) involved in the transformation of adenine into inosine, plays an important role, favoring a mispairing of adenosine and avoiding an uncontrolled immune response after IFN-γ stimulation. These findings are uncovered using human β cells and human islets. Importantly, ADAR1 is proposed as a novel regulator of pancreatic β cell transcriptome under inflammatory conditions, potentially playing a role in understanding T1DM.

In the second manuscript (Rodrigues et al.), the authors describe a new method for generating a hepatocyte-like cell (HLC) from stem cells. This method is based on the modulation of glucose metabolism and the control of mitochondrial function using insulin, glucose, and dexamethasone. The authors analyze the effect of different concentrations of these agents on the improvement of the hepatic phenotype of these cells, which could serve as a platform for understanding and modeling energy metabolism-related alterations.

In the third paper (Jo et al.), the authors explore the role of posttranslational modification (PTM), called O-GlcNacylation, in different nutrient and stress conditions, in pancreatic β cells. This PTM is controlled by the action of two opposite groups of enzymes, O-GlcNAc transferase (OGT) and O-GlcNAcase (OGA). The findings of this study suggest that a reduction in the action of OGT and the hyperactivity of OGA are deleterious for pancreatic β cells.

In the fourth manuscript of this Research Topic (Oost et al.), the authors describe that magnesium ion, which is commonly defective in T2DM patients, has beneficial effects on adipocytes, increasing the glucose uptake in response to insulin as well as insulin signaling, favoring insulin sensitivity. These results point to the important contribution of this ion in the reduction of insulin resistance in T2DM patients.

In the last original research manuscript (Li et al.), the authors report the effect of several variants of the mitochondrial DNA (mtDNA) associated with diabetes and diabetic kidney disease (DKD) using next-generation sequencing (NGS) from different cohorts of patients. The authors demonstrate a connection between some variants of the mtDNA with either diabetes or DKD, suggesting potential implications on individual therapy for these patients that derives from alterations in mtDNA.

In the first mini-review (García-Aguilar et al.), the authors review the role of polyphenols as a potential treatment for improving pancreatic β cell homeostasis; restoring important cellular processes, such as autophagy; and reducing ER stress and mitochondrial dysfunction, among others. These alterations are commonly observed during the progression of T2DM, suggesting that this group of compounds has therapeutic potential for maintaining healthier pancreatic β cells.

In the second mini-review (Li et al.), the authors review the involvement of circular RNAs (circRNA for short) in the appearance of diabetic foot ulcers (DFU). It has been shown that circRNAs are differentially expressed when diabetic and non-diabetic patients are compared. Therefore, circRNAs could be a potential diagnostic marker and a therapeutic target for treating DFU more effectively.

In the last mini-review (Baumel-Alterzon S et al.), the authors review the role of oxidative stress in the control of one of the master regulators of pancreatic β cell differentiation, Pdx1. It describes the importance of nuclear factor erythroid 2-related factor (Nrf2), as a key molecule involved in the generation of the antioxidant response and the induction of Pdx1, suggesting that pharmacological intervention aimed at modulating Nrf2 and the antioxidant response in pancreatic β cells can lead to the restoration of Pdx1 levels and pancreatic β cell differentiation in diabetes.

In the systematic review by Lewis et al., the authors analyze the changes in the transcriptome and in the miRNAome that could potentially participate in the pathogenesis of gestational diabetes (GDM). This information is valuable for improving the diagnosis, prevention, and treatment of patients with GDM.

Author contributions

All authors listed have made a substantial, direct, and intellectual contribution to the work and approved it for publication.

Acknowledgments

We appreciate all authors who submitted their research articles and all reviewers for their contributions to this Research Topic.

Conflict of interest

The authors declare that the research was conducted in the absence of any commercial or financial relationships that could be construed as a potential conflict of interest.

Publisher's note

frontiers | Frontiers in Endocrinology

TYPE Original Research
PUBLISHED 25 August 2022
DOI 10.3389/fendo.2022.986616

OPEN ACCESS

EDITED BY
Carlos Guillén,
Department of Biochemistry and Molecular Biology, Complutense University, Spain

REVIEWED BY
Rudy M. Ortiz,
University of California, Merced, United States
Daniel John Fazakerley,
University of Cambridge, United Kingdom

*CORRESPONDENCE
Jeroen H. F. de Baaij
jeroen.debaaij@radboudumc.nl

SPECIALTY SECTION
This article was submitted to Diabetes: Molecular Mechanisms, a section of the journal Frontiers in Endocrinology

RECEIVED 05 July 2022
ACCEPTED 03 August 2022
PUBLISHED 25 August 2022

CITATION
Oost LJ, Kurstjens S, Ma C, Hoenderop JGJ, Tack CJ and de Baaij JHF (2022) Magnesium increases insulin-dependent glucose uptake in adipocytes.
Front. Endocrinol. 13:986616.
doi: 10.3389/fendo.2022.986616

Magnesium increases insulin-dependent glucose uptake in adipocytes

Lynette J. Oost[1], Steef Kurstjens[1,2], Chao Ma[1,3], Joost G. J. Hoenderop[1], Cees J. Tack[4] and Jeroen H. F. de Baaij[1*]

[1]Department of Physiology, Radboud Institute for Molecular Life Sciences, Radboud University Medical Center, Nijmegen, Netherlands, [2]Laboratory of Clinical Chemistry and Hematology, Jeroen Bosch Hospital, 's-Hertogenbosch, Netherlands, [3]Beijing Tongren Hospital Beijing Institute of Ophthalmology, Beijing Ophthalmology and Visual Science Key Laboratory, Beijing Tongren Eye Center, Capital Medical University, Beijing, China, [4]Department of Internal Medicine, Radboud Institute for Molecular Life Sciences, Radboud University Medical Center, Nijmegen, Netherlands

Background: Type 2 diabetes (T2D) is characterized by a decreased insulin sensitivity. Magnesium (Mg^{2+}) deficiency is common in people with T2D. However, the molecular consequences of low Mg^{2+} levels on insulin sensitivity and glucose handling have not been determined in adipocytes. The aim of this study is to determine the role of Mg^{2+} in the insulin-dependent glucose uptake.

Methods: First, the association of low plasma Mg^{2+} with markers of insulin resistance was assessed in a cohort of 395 people with T2D. Secondly, the molecular role of Mg^{2+} in insulin-dependent glucose uptake was studied by incubating 3T3-L1 adipocytes with 0 or 1 mmol/L Mg^{2+} for 24 hours followed by insulin stimulation. Radioactive-glucose labelling, enzymatic assays, immunocytochemistry and live microscopy imaging were used to analyze the insulin receptor phosphoinositide 3-kinases/Akt pathway. Energy metabolism was assessed by the Seahorse Extracellular Flux Analyzer.

Results: In people with T2D, plasma Mg^{2+} concentration was inversely associated with markers of insulin resistance; i.e., the lower Mg^{2+}, the more insulin resistant. In Mg^{2+}-deficient adipocytes, insulin-dependent glucose uptake was decreased by approximately 50% compared to control Mg^{2+}condition. Insulin receptor phosphorylation Tyr1150/1151 and PIP3 mass were not decreased in Mg^{2+}-deficient adipocytes. Live imaging microscopy of adipocytes transduced with an Akt sensor (FoxO1-Clover) demonstrated that FoxO1 translocation from the nucleus to the cytosol was reduced, indicting less Akt activation in Mg^{2+}-deficient adipocytes. Immunocytochemistry using a Lectin membrane marker and at the membrane located Myc epitope-tagged glucose transporter 4 (GLUT4) demonstrated that GLUT4 translocation was diminished in insulin-stimulated Mg^{2+}-deficient adipocytes compared to control conditions. Energy metabolism in Mg^{2+} deficient adipocytes was characterized by decreased glycolysis, upon insulin stimulation.

10.3389/fendo.2022.986616

Conclusions: Mg^{2+} increases insulin-dependent glucose uptake in adipocytes and suggests that Mg^{2+} deficiency may contribute to insulin resistance in people with T2D.

KEYWORDS

Magnesium, type 2 diabetes, insulin resistance, glycemic control, glucose transporter 4

Introduction

T2D is a chronic condition that is characterized by insulin resistance and relative insulin deficiency (1), leading to microvascular and macrovascular complications (2–4). Insulin resistance enhances the hepatic glucose production and diminishes glucose uptake in insulin-sensitive cells, including adipose tissue, skeletal muscle and liver tissue (5). Reduced insulin action can be compensated by increased insulin secretion, but when insulin production capacity is jeopardized, chronic hyperglycemia will develop (6).

In healthy people, high glucose levels induce the secretion of insulin. Upon insulin binding autophosphorylation of the insulin receptor (IR) occurs and the phosphoinositide 3-kinases/Akt (PI3K/Akt) pathway is activated resulting in GLUT4-mediated glucose uptake in adipocytes and skeletal muscle cells (7–9). The insulin receptor substrates (IRS) active the PI3K enzyme, which converts phosphatidylinositol-2,4,5-triphosphate (PIP2) to phosphatidylinositol-3,4,5-triphosphate (PIP3) (10). Subsequently, PIP3 interacts with Akt to phosphorylate Akt substrate of 160 kDa (AS160) resulting in translocation of GLUT4 to the cell membrane (11). Insulin resistance decreases glucose uptake that may be attributed, at least partially, to defects in PI3K/Akt signaling and GLUT4 translocation (9, 12, 13).

The prevalence of hypomagnesemia (plasma/serum Mg^{2+}< 0.7 mmol/L) in T2D is between 9.1–47.7%, which is tenfold higher compared to the healthy population (14–21). Hypomagnesemia may contribute to insulin resistance, as Mg^{2+} supplementation enhances insulin sensitivity and glucose profiles both in people with and without diabetes (22–25). Supplementation of Mg^{2+} increases IR and GLUT4 levels in rat skeletal muscle (26, 27). However, the mechanism of Mg^{2+} in the insulin-dependent glucose uptake has not been studied in adipocytes.

In this study we aimed to unravel the role of Mg^{2+} deficiency in insulin-dependent glucose uptake. We first studied the association of plasma Mg^{2+} with insulin resistance markers in people with T2D. Next, we assessed the molecular mechanism of Mg^{2+} on IR phosphorylation, PIP3 mass generation, Akt activation, GLUT4 translocation and energy homeostasis in mature 3T3-L1 adipocytes.

Materials and methods

Type 2 diabetes cohort statistics

Details about the Diabetes Pearl Cohort have previously been reported (18). In short, 395 people with T2D were included and plasma samples were taken after an overnight fasting period and immediately analyzed for laboratory parameters (glycated hemoglobin (HbA_{1c}), plasma glucose, creatinine, total cholesterol, triglycerides (Ty), high-density lipoprotein (HDL), low-density lipoprotein (LDL) and magnesium. Body mass index (BMI) was calculated as kilograms per body mass. Waist circumference was measured after normal exhalation in duplicate and repeated if the difference was >1.0 cm. For this study we used the Triglyceride Glucose-Body Mass Index (TyG-BMI), Triglyceride Glucose-Waist Circumference (TyG-WC) and Triglyceride HDL (Ty/HDL) ratio as surrogate markers for insulin resistance by using the following calculations: TyG-BMI=Ln [Ty (mg/dL) * plasma glucose (mg/dL)/2] * BMI, TyG-WC= Ln [Ty (mg/dL) * plasma glucose (mg/dL)/2] × WC (cm) and Ty/HDL ratio= Ty (mg/dL)/HDL (mg/dL) (28).

Cell culture

The 3T3-L1 fibroblasts (ATCC, CL-173) were cultured in Dulbecco's modified Eagle's medium (DMEM) (Lonza Westburg, Leusden, the Netherlands) supplemented with 4 mmol/L L-glutamine (GE healthcare Life Sciences, Logan, UT, USA), MEM Non-Essential Amino Acids (Lonza Westburg) and 10% (v/v) fetal bovine serum (FBS) (Greiner Bio One, Alphen aan den Rijn, the Netherlands), at 37°C in a humidified atmosphere of 5% (v/v) CO_2 in air. Cells were induced two days post-confluence by adding 1 µg/ml bovine insulin (Sigma-Aldrich, St. Louis, MO, USA), 0.5 mmol/L 3-isobutyl-1-methylxanthine (IBMX) (Sigma-Aldrich), and 1 µM

dexamethasone (Sigma-Aldrich) for 3 days. Cells were incubated for 4 days with cultured medium supplemented with 1 µg/ml bovine insulin only (refreshed after 2 days) to obtain fully differentiated adipocytes. Adipocytes were maintained another 48 hours in culture medium followed by a 24 hour incubation with either 1 or 0 mmol/L Mg^{2+} (Sigma-Aldrich) DMEM medium (containing 25 mmol/L D-glucose, 0.04 mmol/L Phenol Red, 1 mmol/L sodium pyruvate, 1.8 mmol/L CaCl2, 0.00025 mmol/L Fe(NO3)3, 17.9 mmol/L NaHCO3, 5.3 mmol/L KCl, 110.3 mmol/L NaCl, 0.9 mmol/L NaH2PO4, 0.4 mmol/L glycine, 0.4 mmol/L L-Arginine hydrochloride, 0.2 mmol/L L-Cystine 2HCl, 4 mmol/L L-Glutamine, 0.2 mmol/L L-Histidine hydrochloride, 0.8 mmol/L L-Isoleucine, 0.8 mmol/L L-Leucine, 0.8 mmol/L L-Lysine hydrochloride, 0.2 mmol/L L-Methionine, 0.4 mmol/L L-Phenylalanine, 0.4 mmol/L L-Serine, 0.8 mmol/L L-Threonine, 0.08 mmol/L L-Tryptophan, 0.4 mmol/L L-Tyrosine disodium salt dihydrate, 0.8 mmol/L L-Valine, MEM Vitamin Solution (Thermo Fisher Scientific, Waltham, MA USA) and 10% (v/v) FBS). Cells were cultured without FBS after 18 hours of incubation, 6 hours prior to the experiment.

To transduce 3T3-L1 adipocytes with FoxO1-Clover and Myc-GLUT4-mCherry DNA, lentiviruses were generated using HEK293-FT cells. HEK293-FT cells (kind gift from Translational Metabolic Laboratory, Radboud University Medical Center, bought at Thermo Fisher Scientific, R70007) were grown in DMEM (Lonza Westburg) supplemented with 6 mmol/L L-glutamine (GE healthcare Life Sciences), MEM Amino Acids (Lonza Westburg), 10% (v/v) FBS (Greiner Bio One), 1 mmol/L sodium pyruvate and 1% (v/v) penicillin/streptomycin (10,000 units/10 mg). Cells were maintained at 37°C in a humidified atmosphere of 5% (v/v) CO_2 in air.

Radioactive $_3$H-2-deoxyglucose uptake

The 3T3-L1 fibroblasts were seeded on coated Poly-L-lysine (PLL) (Sigma-Aldrich) dishes and differentiated. Mature 3T3-L1 adipocytes were washed twice with warm Krebs–Ringer–phosphate–HEPES (KRPH) buffer (20 mmol/L HEPES, 5 mmol/L KH_2PO_4, 1 mmol/L $CaCl_2$, 136 mmol/L NaCl, and 4.7 mmol/L KCl set at pH 7.4 with NaOH) containing either 1 or 0 mmol/L Mg^{2+}. Cells were incubated without or with 10 nmol/L human insulin (Sigma-Aldrich) and 0 or 1 mmol/L Mg^{2+} for 0, 10, 20 or 30 minutes at 37°C in radioactive buffer containing 5 mmol/L 2-deoxyglucose (2DG) (Sigma-Aldrich) and 1 µCi ^{3}H-2DG (PerkinElmer, Hoogvliet Rotterdam, the Netherlands). The incubation was stopped by washing with cold KRPH buffer and cells were lysed with 0.05% (w/v) SDS (MP Biomedicals) in dH_2O. Cell lysates were added to Opti-Fluor O scintillation liquid (PerkinElmer) and counted using the Hidex 600 SL. Radioactive counts were corrected for the background count in each of the incubation buffers. The assay was repeated without the addition of ^{3}H-2DG to correct for protein concentrations using the bicinchoninic acid (BCA) assay (Thermo Fisher Scientific) according to the manufacturer's protocol.

ELISA assays

3T3-L1 fibroblasts were seeded and differentiated in PLL coated 10 cm dishes or T-175 flasks. Mature adipocytes were stimulated with or without 10 nmol/L human insulin (Sigma-Aldrich) 30 minutes at 37°C. One confluent 10 cm dish per experimental condition was used for the Phospho-Insulin Receptor b (Tyr1150/1151) Sandwich ELISA (Cell Signaling Technology, Leiden, the Netherlands) and one confluent T-175 flask per experimental condition was used for the PIP3 Mass Elisa (Echelon Biosciences, Salt Lake City, UT, USA) were used according to the manufacturer's protocol.

Production of recombinant lentivirus

The pLenti-FoxO1-Clover (Addgene, Cambridge, MA, USA) and pLenti-Myc-GLUT4-mCherry (Addgene, Cambridge, MA, USA) plasmids were used as template. The packaging plasmids pLP1, pLP2 and pLP/VSVG were a kind gift from the Translational Metabolic Laboratory, Radboud University Medical Center. HEK293-FT cells were seeded at 70% confluence in Petri dishes coated with 20 µg/ml collagen (Thermo Fisher Scientific) per cm^2. After cell attachment medium was switched to advanced DMEM (Thermo Fisher Scientific) supplemented with 6 mmol/L L-glutamine (GE healthcare Life Sciences), 2% (v/v) FBS (Greiner Bio One) and 10 µmol/L water-soluble cholesterol (Sigma-Aldrich). After 24 hours of incubation with cholesterol containing medium, HEK293-FT cells were transduced by incubating overnight in Opti-MEM I (Thermo Fisher Scientific) containing 3 µg lentiviral vector and packaging plasmids combined with a 1:3 DNA-reagent ratio Lipofectamine 2000 (Thermo Fisher Scientific) per 100 mm plate. The following morning medium was switched to cholesterol containing medium and incubated 48 hours at 37°C in a humidified atmosphere of 5% (v/v) CO_2 in air. Lentivirus was harvested by collecting the medium supernatant, followed by centrifugation 5 minutes, 2000 xg at 4°C. The supernatant was filtered using sterile low protein binding 0.45 µm filters (Sigma-Aldrich) and concentrated using Lenti-X Concentrator (Takara Bio, Saint-Germain-en-Laye, France), according to the manufacturer's protocol. Viral titer was determined using Lenti-X GoStix Plus (Takara Bio), according to the manufacturer's protocol.

Lentivirus transduction

Viral supernatants containing FoxO1-Clover or Myc-GLUT4-mCherry were added to fresh medium supplemented with 8 µg/ml Polybrene (Sigma-Aldrich). Mature 3T3-L1

adipocytes were incubated with approximately 40 ng p24 particles per 96 well or 120 ng p24 particles per 24 well and incubated overnight. The next day, the medium was replaced with fresh medium. Microscopy experiments were performed 4 to 6 days post transduction.

Akt sensor

3T3-L1 fibroblasts were differentiated on fibronectin (Roche Applied Science, Almere, the Netherlands) coated 96 well plates and differentiated. Mature adipocytes were transduced with Lentivirus particles containing FoxO1-Clover. FoxO1 is a direct and specific target of Akt; FoxO1 rapidly translocate from the nucleus to the cytoplasm in response to Akt activation (29). The transduction was followed by a 24 hour incubation with 0 or 1 mmol/L Mg^{2+} of which the last 6 hours adipocytes where incubated without FBS. Medium was replaced 30 minutes prior to starting live imaging; containing 0 or 1 mmol/L Mg^{2+}, FBS free, phenol-free, supplemented with 1 µg/ml Hoechst 33342 (Sigma-Aldrich). Live imaging was performed using a ZEISS Axio Observer light microscope. Adipocytes were imaged for 30 minutes with a photo interval per 30 seconds. The cells were stimulated using a final concentration of 10 nM human insulin (Sigma-Aldrich) which was added between 30-60 seconds after the start of visualization. The relative intensity of fluorescent units in the cytosol/nucleus was analyzed by the following formula:

$$((\text{cytosol flourescence} - \text{background flourescence}) * \text{area cytosol}) - \frac{((\text{nuclues flourescence} - \text{background flourescence}) * \text{area nucleus})}{((\text{nucleus flourescence} - \text{background flourescence}) * \text{area nucleus})}$$

All values are normalized by dividing by the first measurement (t=0). Data was fitted using the four-parameter sigmoid dose-response curve. The maximum top value of this function was used as the fluorescent unit's cytosol/nucleus ratio.

Immunocytochemistry of endogenously expressed GLUT4

3T3-L1 fibroblasts were seeded on fibronectin (Sigma-Aldrich) coated glass coverslips in 6 well plates. After 24 hours of 0 or 1 mmol/L Mg^{2+} incubation, adipocytes were stimulated with or without 10 nM human insulin (Sigma-Aldrich) 30 minutes at 37°C and subsequently cooled on ice. Subsequently, adipocytes were rinsed in PBS and incubated 10 minutes with 5 ug/ml Lectin Alexa 680 (Thermo Fisher Scientific) in DMEM supplemented with 30 mmol/L HEPES (Sigma-Aldrich), rinsed with PBS and fixated with 4% (w/v) PFA methanol-free formaldehyde solution (Thermo Fisher Scientific). The fixation solution was removed by rinsing with PBS. Adipocytes were permeabilized in 0.3% (v/v) Triton X-100 (Sigma-Aldrich) with 0.1% (w/v) BSA (Sigma-Aldrich) in PBS for 10 minutes. Quenching was done by 50 mmol/L NH_4Cl in PBS for 10 minutes and followed by washing with PBS. Adipocytes were incubated in 16% (v/v) goat serum (Vector Laboratories, Amsterdam, the Netherlands) with 0.3% (v/v) Triton X-100 (Sigma-Aldrich) for 30 minutes and, subsequently, incubated with primary 1:200 GLUT4 (Santa Cruz Biotechnology, Heidelberg Germany) overnight at 4°C. The following day, cells were rinsed with PBS and incubated with 1:300 secondary Goat anti-Mouse IgG Alexa 488 (Thermo Fisher Scientific) in 16% (v/v) goat serum with 0.3% (v/v) Triton X-100 for 1 hour at room temperature, followed by PBS washing. Nuclei were stained using 0.1 ug/ml DAPI (Thermo Fisher Scientific) for 10 minutes at room temperature, followed by PBS washing and mounting using Fluoromount-G (SouthernBiotech, Birmingham, AL, USA). Fluorescence confocal microscopy was performed with a Zeiss LSM880 and images were taken with the Zeiss Zen software. Co-localization of GLUT4 and Lectin was quantified using ImageJ (JACop) software with the Mander's coefficient.

Immunocytochemistry of overexpressed GLUT4

Differentiated 3T3-L1 were seeded on fibronectin (Roche Applied Science) coated glass coverslips in 24 well plates. Adipocytes were transduced with Lentivirus particles containing Myc-GLUT4-mCherry. After 24 hours of 0 or 1 mmol/L Mg^{2+} incubation, adipocytes were stimulated with or without 10 nmol/L human insulin (Sigma-Aldrich) 30 minutes at 37°C and subsequently cooled on ice. The adipocytes were fixated with 4% (w/v) PFA methanol-free formaldehyde solution (Thermo Fisher Scientific). Quenching was done by 50 mmol/L NH_4Cl in PBS for 10 minutes, followed by washing with PBS. Adipocytes were incubated in 16% (v/v) goat serum (Vector Laboratories) with 0.3% (v/v) Triton X-100 (Sigma-Aldrich) for 30 minutes and, subsequently incubated with 1:200 c-Myc Antibody (Santa Cruz Biotechnology). The following day adipocytes were incubated with 1:500 secondary antibody Goat anti-Mouse IgG Alexa 488 (Thermo Fisher Scientific) in 16% (v/v) goat serum with 0.3% (v/v) Triton X-100 for 1 hour at room temperature. Nuclei were stained using 0.1 ug/ml DAPI (Thermo Fisher Scientific) for 10 minutes at room temperature, followed by PBS washing and mounting using Flouromount-G (SouthernBiotech). Fluorescence confocal microscopy was performed with a Zeiss LSM880 and images were taken with the Zeiss Zen software. Co-localization of Myc and GLUT4-mCherry was quantified using ImageJ (JACop) software with the Mander's coefficient.

Seahorse XF Glycolytic Stress Test

3T3-L1 fibroblasts were differentiated in fibronectin coated XF96 Cell Culture Seahorse plates (Agilent Technologies, Amstelveen, the Netherlands). The sensor cartridge was hydrated 24 hours in XF Calibrant at 37°C in a non-CO_2 incubator overnight. The culture medium was replaced 1 hour before the Seahorse run with 0 or 1 mmol/L Mg^{2+} DMEM (recipe described in section **Cell Culture**), containing no glucose or pyruvate sources and 5 mmol/L HEPES. The XF96 cell plate was incubated at 37°C in a non-CO_2 environment for 1 hour before starting the glycolytic stress test. During the run, cells were sequentially treated with or without 10 nmol/L human insulin (Sigma-Aldrich), 10 mmol/L D-glucose, 1 µM oligomycin (Sigma-Aldrich) and 50 mmol/L 2DG (Sigma-Aldrich). Protein concentration was measured using the U/CSF protein kit (Thermo Fischer Scientific). Adhered cells were stored at -80°C until measurement in 0.33% (v/v) Triton X-100 dissolved in 10 mmol/L Tris-HCl (pH 7.6). On the day of measurement, U/CSF protein quantification solution was added to the well. After 10 minutes of incubation at 37°C, absorbance was measured at 600 nm. Protein concentrations in wells containing samples were obtained using the concentration calculated from the sCal (Thermo Fischer Scientific) calibration curve included in each plate. All data was normalized for the amount of protein in each well. The non-glycolytic acidification rate was calculated by: the average of the last rate measurement prior to insulin injection. Glycolysis was calculated by: (maximum rate measurement before oligomycin injection) – (last rate measurement before glucose injection). The glycolytic capacity was calculated by: (maximum rate measurement after oligomycin injection) – (last rate measurement before glucose injection).

Statistical analyses

All *in vitro* data are presented as mean ± SEM. Statistical significance was evaluated using Two-Way Analysis of Variance (ANOVA) or by a Student's T-Test when comparing only two groups. Pearson correlations were performed using SPSS for Windows (V25.0.0.1 IBM) to determine the association between plasma Mg^{2+} concentration and fasting glucose and the insulin resistance markers: TyG-BMI, TyG-WC and Ty/HDL. Normal distribution of data was verified by calculating the quotient of the skewness divided by its standard error. Variables that were not normally distributed were log transformed. Statistical significance set at *P<0.05; **P<0.01; and ***P<0.001.

Results

The plasma magnesium concentration is inversely associated with insulin resistance

Previously, we demonstrated that plasma triglycerides and fasting glucose levels are major determinants of the plasma Mg^{2+} concentration (18). The negative association of plasma Mg^{2+} concentration with fasting glucose levels is visualized in Figure 1A. Figures 1B–D shows the negative association of plasma Mg^{2+} and markers of insulin resistance, confirming the association between low Mg^{2+} levels and insulin resistance in people with T2D.

Magnesium increases insulin-dependent glucose uptake

To determine the potential causative relationship between Mg^{2+} and insulin resistance, the effects of Mg^{2+} on insulin sensitivity and glucose handling were further examined *in vitro*. Radioactive ^{3}H-2DG uptake was measured in mature 3T3-L1 adipocytes that were Mg^{2+}-deficient (0 mmol/L Mg^{2+}) or incubated with its physiological concentration (1 mmol/L Mg^{2+}). In Mg^{2+}-deficient adipocytes, insulin-stimulated glucose uptake was decreased by 50% at 20 and 30 minutes compared to adipocytes with a physiological Mg^{2+} concentration ($P< 0.001$) (Figure 2).

Magnesium increases translocation of endogenous and overexpressed GLUT4 upon insulin-stimulation

Insulin-dependent glucose uptake is mainly mediated by GLUT4 in adipocytes (9, 30). GLUT4 expression at the plasma membrane was increased in insulin-stimulated adipocytes with physiological Mg^{2+} compared to insulin-stimulated Mg^{2+}-deficient adipocytes (Figures 3A, B). The GLUT4 co-localization with membrane marker Lectin was increased twofold in insulin-stimulated adipocytes incubated with physiological Mg^{2+} compared to Mg^{2+}-deficient adipocytes ($P< 0.05$). The effect of insulin on the translocation of endogenous GLUT4 was almost completely abolished in Mg^{2+}-deficient adipocytes (Figure 3C). In adipocytes that overexpressed Myc-GLUT4-mCherry and were stimulated with insulin, there was less GLUT4 translocation to the plasma membrane in Mg^{2+}-deficient adipocytes compared to controls ($P< 0.001$), but was not completely abolished (Figure 3D). The GLUT4 translocation to the plasma membrane was increased by threefold in insulin-stimulated Mg^{2+}-deficient adipocytes and increased by fourfold in insulin-stimulated controls, compared to non-insulin stimulated adipocytes (Figure 3D).

Magnesium is not involved in the autophosphorylation of the insulin receptor

Phosphorylation of IR tyrosine residues is the first essential requirement for insulin signaling, with phosphorylation of

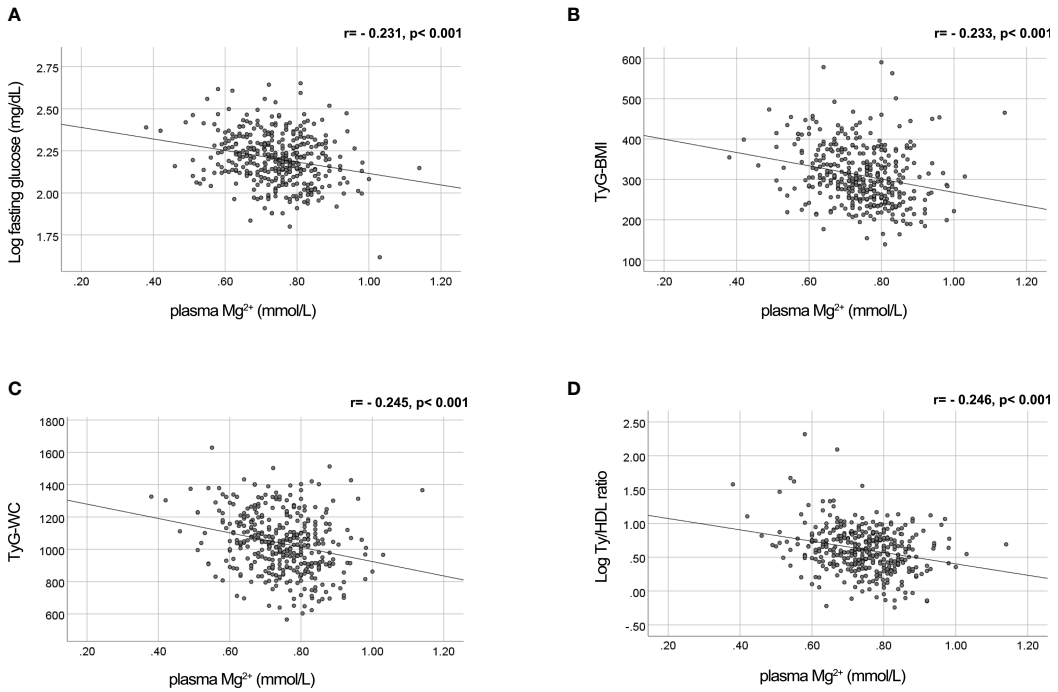

FIGURE 1
Mg^{2+} is negatively correlated with fasting glucose levels and insulin resistance markers TyG-WC, TyG-BMI and Ty/HDL ratio in people with T2D. Plasma Mg^{2+} concentration scatter plotted versus **(A)** Log fasting glucose (n=382); **(B)** TyG-BMI (n=379); **(C)** TyG-WC (n=376); and **(D)** Log Ty/HDL ratio (n=384) in people with T2D. Statistically analyzed using Pearson correlation. Mg^{2+}, magnesium; T2D, type 2 diabetes; TyG-BMI, Triglyceride Glucose-Body Mass Index; TyG-WC, Triglyceride Glucose-Waist Circumference; Ty/HDL, Triglyceride High Density Lipoprotein.

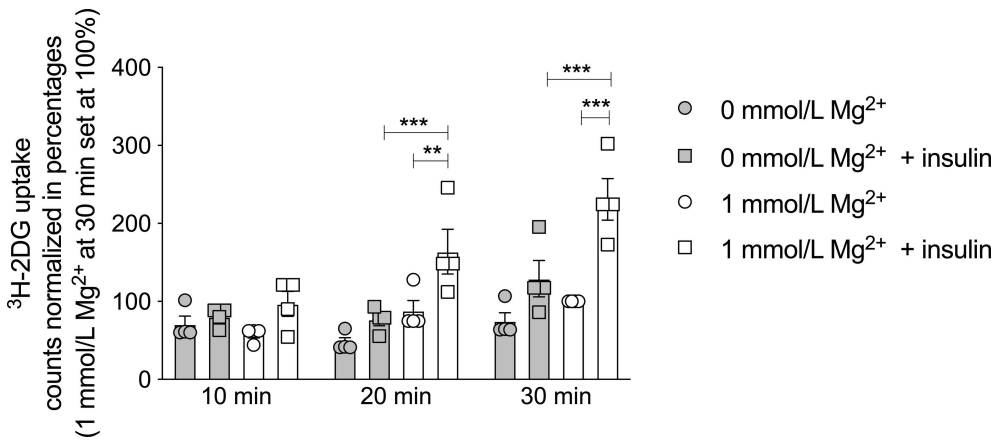

FIGURE 2
Effect of Mg^{2+} on insulin-dependent glucose uptake in 3T3-L1 adipocytes. ^{3}H-2DG uptake for 10, 20 or 30 minutes in 3T3-L1 adipocytes that were incubated with 0 or 1 mmol/L Mg^{2+} for 24 hours (n=4). Legend: circle is without insulin, square is with insulin, grey color is 0 mmol/L Mg^{2+} and white color is 1 mmol/L Mg^{2+}. Data are shown as mean ± S.E.M. Statistically analyzed with Two-Way ANOVA. Significance **p<0.01; ***p< 0.001. 2DG = 2-deoxyglucose, Mg^{2+}, magnesium; min, minutes.

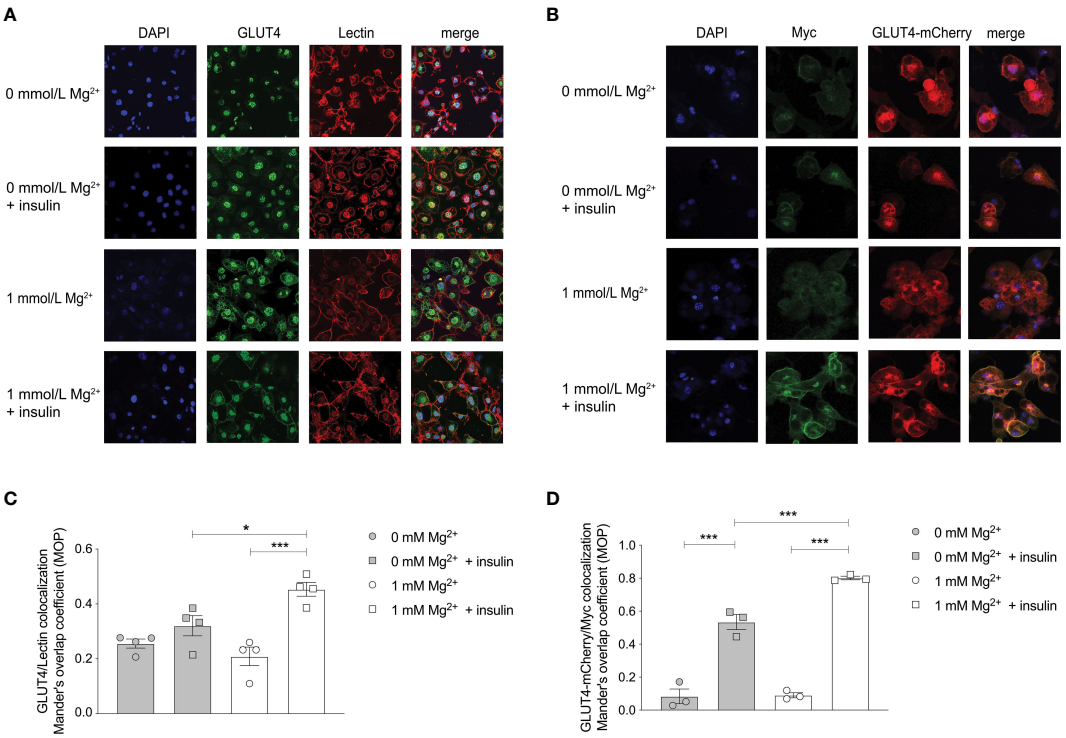

FIGURE 3
Effect of Mg^{2+} on insulin-dependent localization of the GLUT4 transporter to the cell membrane in 3T3-L1 adipocytes. **(A)** Immunocytochemistry staining of DAPI, GLUT4 and the cell membrane marker Lectin in insulin-stimulated 3T3-L1 adipocytes that are incubated with 0 or 1 mmol/L Mg^{2+} (n=4). GLUT4 signal was assessed at the plasma membrane, since GLUT4 antibody did result in non-specific nuclear staining. **(B)** Immunocytochemistry staining of DAPI, anti-myc and GLUT4-mCherry in insulin-stimulated 3T3-L1 adipocytes that were transduced with pLenti-Myc-GLUT4-mCherry, incubated 0 or 1 mmol/L Mg^{2+} (n=3). **(C)** Quantification of the immunocytochemistry staining by co-localization GLUT4 and Lectin at the plasma membrane compared to total cytosol expression (n=4). **(D)** Quantification of the ratio of cell surface Myc signal to total mCherry signal in 3T3-L1 adipocytes transduced with pLenti-myc-GLUT4-mCherry (n=3). Legend: circle is without insulin, square is with insulin, grey color is 0 mmol/L Mg^{2+} and white color is 1 mmol/L Mg^{2+}. Data are shown as mean ± S.E.M. Statistically analyzed with Two-Way ANOVA. Significance *p<0.05; ***p< 0.001. GLUT4, glucose transporter 4; Mg^{2+}, magnesium.

Tyr1150/Tyr1151 predominant for activation *in vivo* (31, 32). Insulin increased Tyr1150/1151 autophosphorylation in adipocytes (P< 0.001), though this increase was similar in adipocytes with a physiological Mg^{2+} concentration compared to Mg^{2+}-deficient adipocytes (Figure 4A). Mg^{2+} *per se* had no effect on Tyr1150/1151 autophosphorylation, with and without insulin stimulation. The positive control, DMAQ-B1, a selective stimulator of IR tyrosine kinase phosphorylation, resulted in specific response by increasing Tyr1150/1151 phosphorylation almost threefold compared to the physiological condition (1 mmol/L Mg^{2+} without insulin stimulation) (P< 0.01) (33).

PIP3 generation is not increased by magnesium

Cell lipid extractions for enzymatic assays were performed to measure PIP3 mass of 3T3-L1 adipocytes incubated with a physiological Mg^{2+} concentration versus Mg^{2+}-deficient. Mg^{2+} did not increase PIP3 mass generation. PIP3 mass was not increased in insulin-stimulated adipocyte conditions, with and without Mg^{2+}. The positive control, the PI3K enzyme inhibitor wortmannin, decreased PIP3 mass by approximately 80% compared to the physiological condition (1 mmol/L Mg^{2+} without insulin stimulation) (P< 0.05) (Figure 4B).

Magnesium is essential for insulin-stimulated Akt activation

Adipocytes were overexpressed with the Akt sensor (FoxO1-Clover) and stimulated with insulin. The translocation of FoxO1 from the nucleus to the cytosol was diminished in the Mg^{2+}-deficient adipocytes compared to adipocytes incubated with a physiological Mg^{2+} concentration (P< 0.01) (Figure 5).

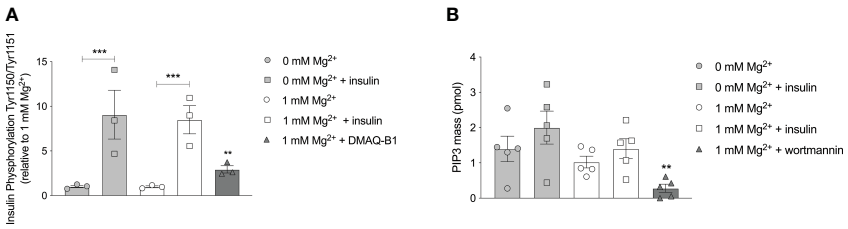

FIGURE 4
Effect of Mg^{2+} on the auto phosphorylation of the IR at residue Tyr1150/1151 and PI3K kinase regulatory subunits that phosphorylate PIP2 to PIP3. **(A)** The phosphorylation of Tyr 1150/115 in 3T3-L1 adipocytes incubated with 0 or 1 mmol/L Mg^{2+}. DMAQ-B1 is used as positive control to mimic IR phosphorylation (n=3). **(B)** PIP3 mass in 3T3-L1 adipocytes incubated with 1 or 0 mmol/L Mg^{2+}. Wortmannin is used as positive control to inhibit PI3K enzyme activity (n=5). Legend: circle is without insulin, square is with insulin, grey color is 0 mmol/L Mg^{2+}, white color is 1 mmol/L Mg^{2+} and rectangles are positive controls. Data are shown as mean ± S.E.M. Statistically analyzed with Two-Way ANOVA. Positive controls are analyzed with Student t-test, compared to 1 mmol/L Mg^{2+} condition. **p<0.01; ***p< 0.001. Mg^{2+}, magnesium; PIP3, phosphatidylinositol-3,4,5-trisphosphate; DMAQ-B1, demethylasterriquinone B1.

Magnesium increases the insulin-stimulated glycolytic respiration rate

The effect of Mg^{2+} on the intracellular energy metabolism was assessed using the Seahorse XF Glycolytic Stress Test. The glycolytic stress test curve demonstrated that the glycolysis is increased in insulin-stimulated adipocytes with a physiological level of Mg^{2+} compared to Mg^{2+}-deficient adipocytes (Figure 6A). Oxygen consumption rate (OCR) was measured simultaneously and Mg^{2+} nor insulin-stimulation did not alter OCR rate (data not shown). The basal non-glycolytic acidification was higher in Mg^{2+}-deficient adipocytes compared to adipocytes incubated with physiological Mg^{2+} concentration ($P< 0.05$) (Figure 6B), which suggests that increased glycolysis may have compensated for basal energy homeostasis. The glycolysis was enhanced in insulin-stimulated adipocytes compared to insulin-stimulated Mg^{2+}-deficient adipocytes ($P< 0.05$) (Figure 6C). The glycolytic capacity (Figure 6D) remained the same in adipocytes incubated with and without Mg^{2+}, with and without insulin stimulation.

Discussion

The study demonstrated that Mg^{2+} plays an important role in insulin-dependent glucose uptake by increasing Akt activation and GLUT4 translocation to the plasma membrane. This may provide a mechanism by which a low Mg^{2+} may result in insulin resistance and explain the inverse association between, plasma Mg^{2+} concentration and insulin resistance in people with T2D.

Our results demonstrate that Mg^{2+} acts downstream of the IR and PI3K by activating Akt and/or GLUT4. Previous studies that investigated the effect of HIV1-protease inhibitors on insulin resistance are in agreement with our findings and demonstrated only signaling effects that are downstream of PI3K, in 3T3-L1 adipocytes and skeletal muscle (34–36). In non-insulin-stimulated macrophages and osteoblasts, Mg^{2+} activated Akt for anti-inflammatory properties and growth signaling (37, 38). All together, these findings suggest that insulin-dependent glucose uptake can be improved without

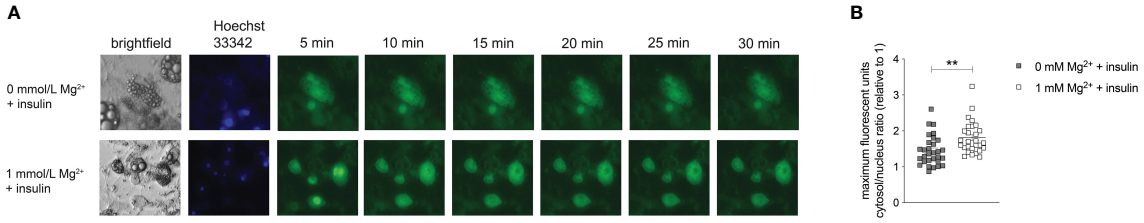

FIGURE 5
Effect of Mg^{2+} on insulin-dependent Akt activation. Live imaging of insulin-stimulated 3T3-L1 adipocytes transduced with pLenti-FoxO1-Clover and incubated with 0 or 1 mmol/L Mg^{2+}. **(A)** Live images showing Brightfield, Hoechst 33342 and Clover signal in 3T3T-L1 adipocytes stimulated with insulin. **(B)** Quantified maximal mean intensity ratio of the cytosol in 3T3-L1 adipocytes stimulated with insulin (n=5, 3–10 cells analyzed per biological replicate). Statistically analyzed with Student's T-Test. grey color is 0 mmol/L Mg^{2+} and white color is 1 mmol/L Mg^{2+}. Mg^{2+}, magnesium; min, minutes. **p<0.01.

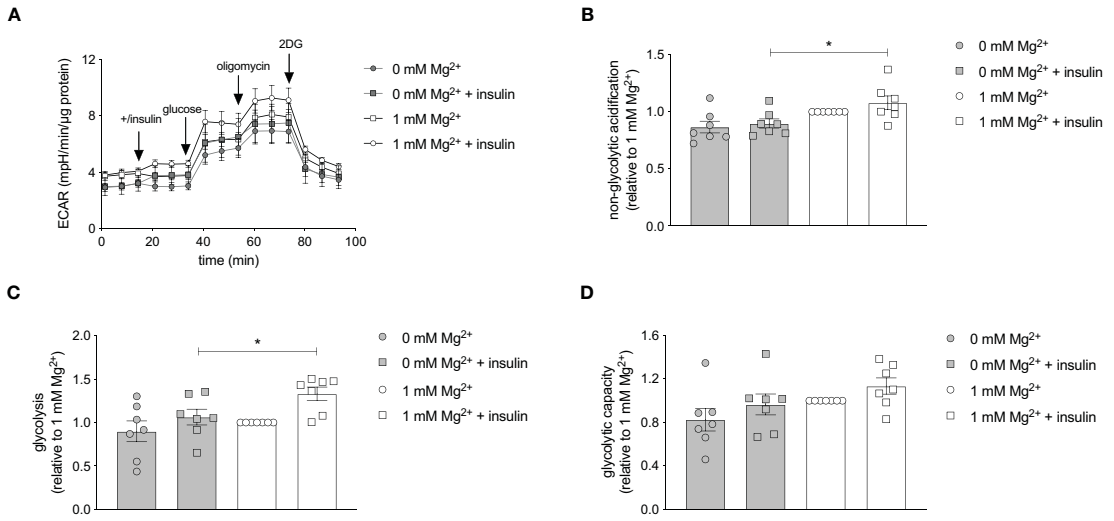

FIGURE 6
Effect of Mg^{2+} on insulin-stimulated glycolytic respiration rate in 3T3-L1 adipocytes. Glycolytic Stress Test in insulin-stimulated 3T3-L1 adipocytes incubated with 0 or 1 mmol/L Mg^{2+}. **(A)** Representative raw Glycolytic Stress Test curve in 3T3-L1 adipocytes. Quantification of the **(B)** non-glycolytic acidification, **(C)** glycolysis and **(D)** glycolytic capacity in 3T3-L1 adipocytes (n=7). All data adjusted for protein. Legend: circle is without insulin, square is with insulin, grey color is 0 mmol/L Mg^{2+} and white color is 1 mmol/L Mg^{2+}. Data are shown as mean ± S.E.M. Statistically analyzed with Two-Way ANOVA. *p<0.05. 2DG, 2-deoxyglucose; ECAR, extracellular acidification rate; Mg^{2+}, magnesium; min, minutes.

affecting IR phosphorylation but can be driven by Akt activation and GLUT4 translocation. The functionality of Akt and GLUT4 have shown to be essential for preventing insulin resistance (39–41).

Animal studies that assessed the role of Mg^{2+} on PI3K/Akt signaling are limited and show inconsistent results. For instance, rats that are fed with a low Mg^{2+} diet showed diminished IR phosphorylation in skeletal muscle after only 4 days (42). While Reis et al. showed no differences on IR phosphorylation in skeletal muscle after a longer period of 11 weeks (43). Supplementation of Mg^{2+} in T2D rats did increase IR and GLUT4 expression levels in skeletal muscle (26, 27). However, these studies did not examine the intermediate PI3K/Akt signal transduction thoroughly in the skeletal muscle, thereby failed to show on which key proteins Mg^{2+} exerts in the skeletal muscle. We suggest that Mg^{2+} has a selective regulation of Akt-dependent processes that is cell-specific and differ in adipocytes compared to skeletal muscle (5).

The exact metabolic exertion of Mg^{2+} remains to be elucidated, but it is suggested that Mg^{2+} and ATP act together in the IR-PI3K-Akt pathway as a kinase substrate (44). Mg-ATP serves as substrate in the phosphoryl transfer reaction in the phosphorylation of proteins (45, 46). Additionally, Mg^{2+} may induce an electrostatic interaction, which enhances the binding affinity and stability of ATP to protein kinases (47). It has been established that Rab GTPases also have Mg^{2+}-binding motifs (48), which may stimulate AS160 phosphorylation and GLUT4 translation.

The impaired glucose uptake caused by low intracellular Mg^{2+} affects the metabolism of the adipocyte. It has been well established that Mg-ATP acts as a co-factor for many key enzymes involved in glycolysis (49–51). In our study, glycolysis was decreased in Mg^{2+}-deficient adipocytes compared to adipocytes incubated with a physiological Mg^{2+} concentration. In adipocytes, insulin stimulates the insulin-dependent glucose uptake and hexokinase and 6-phosphofructokinase activity, which both enhance glycolysis (52). The enhanced glycolysis could be related to increased activity of glycolytic enzymes (49), or can be a consequence of the increased insulin-dependent glucose uptake. We therefore suggest that the increased glycolysis, which may be a consequence of insulin-dependent glucose uptake, requires Mg^{2+} as a co-factor.

To date, Mg^{2+} studies have focused primarily on studying the insulin-dependent glucose uptake in skeletal muscles (26, 27, 42, 43). In contrast, we used mature 3T3-L1 adipocytes. The severity of insulin resistance in adipose tissue may even proceed skeletal muscle (53, 54), emphasizing the importance of identifying insulin sensitive mechanisms in adipose tissue. To our knowledge, there is one previous study demonstrating that Mg^{2+} deficiency reduced insulin-dependent glucose metabolism in isolated rat adipocytes, but this study did not assess the IR-PI3K-Akt pathway (55).

Our results suggest that Mg^{2+} deficiency in adipocytes exaggerates insulin resistance in people with T2D. Screening for hypomagnesemia and providing Mg^{2+} supplementation may improve insulin sensitivity, which prevents the development of T2D (23, 56).

A strength of our study is that we examined a large part of the IR-PI3K-Akt pathway. On the other hand, a limitation of our approach is that only two concentrations of Mg^{2+} was used in our study, namely a cell physiological concentration (1 mmol/L Mg^{2+}) and Mg^{2+}-deficient (0 mmol/L Mg^{2+}). Additionally, the intracellular Mg^{2+} concentration and other electrolytes were not measured, limiting conclusions on the direct metabolic effect of Mg^{2+}. It should be noted that a short-term (24 hours) incubation with 0 mmol/L Mg^{2+} was selected to cause a significant reduction of the intracellular Mg^{2+} concentration. Experiments in HEK293 cells have demonstrated that intracellular Mg^{2+} levels are generally decreased within a few hours (57). Furthermore, a reduction of intracellular Mg^{2+} is observed when incubating myocytes (58), Madin-Darby Canine Kidney (MDKC) (59), mouse distal convoluted tubule (60), or breast cancer MDA-MB-231 cells (57) for 16-24 hours with 0 mmol/L Mg^{2+} (61). As such, our approach could be representative for the chronic low cytosolic free intracellular Mg^{2+} levels in people with T2D and hypomagnesemia.

In summary, Mg^{2+} acts on Akt and GLUT4 to improve insulin signaling and glucose uptake in adipocytes; thereby controlling extracellular glucose levels. The increased availability of glucose is translated into an increased glycolysis in adipocytes. The defects in Akt and GLUT4 signaling by Mg^{2+} deficiency could be the fundamental reason for the negative association of hypomagnesemia and insulin resistance in people with T2D.

Data availability statement

The original contributions presented in the study are included in the article/supplementary material. Further inquiries can be directed to the corresponding author.

Ethics statement

The studies involving human participants were reviewed and approved by the Ethics committee of the Radboud University Medical Center. The patients/participants provided their written informed consent to participate in this study.

Author contributions

LO and SK performed together the radioactive glucose uptake experiments. LO performed all the other experiments described in the manuscript. SK and CM did preliminary analysis that were essential for the set-up of this study. LO and JB wrote the manuscript. JH, CT, and JB supervised the study. All authors reviewed and approved the final version of the manuscript. JB is the guarantor of this work and had full access to all the data in the study and takes responsibility for the integrity of the data.

Funding

This research was funded by the Dutch Diabetes Research Foundation (2017–81–014).

Conflict of interest

The authors declare that the research was conducted in the absence of any commercial or financial relationships that could be construed as a potential conflict of interest.

Publisher's note

References

1. Smushkin G, Vella A. What is type 2 diabetes? *Med (Baltimore)* (2010) 38:597–601. doi: 10.1016/j.mpmed.2010.08.008

2. Ormazabal V, Nair S, Elfeky O, Aguayo C, Salomon C, Zuñiga FA. Association between insulin resistance and the development of cardiovascular disease. *Cardiovasc Diabetol* (2018) 17:1–14. doi: 10.1186/s12933-018-0762-4

3. Meigs JB, Rutter MK, Sullivan LM, Fox CS, D'Agostino RB, Wilson PWF. Impact of insulin resistance on risk of type 2 diabetes and cardiovascular. *Diabetes Care* (2007) 30:1219–25. doi: 10.2337/dc06-2484

4. Duckworth WC. Hyperglycemia and cardiovascular disease. *Curr Atheroscler Rep* (2001) 3:383–91. doi: 10.1007/s11883-001-0076-x

5. Fazakerley DJ, Krycer JR, Kearney AL, Hocking SL, James DE. Muscle and adipose tissue insulin resistance: malady without mechanism? *J Lipid Res* (2019) 60:1720–32. doi: 10.1194/jlr.R087510

6. American Diabetes Association. Diagnosis and classification of diabetes mellitus. *Diabetes Care* (2008) 31:S62–7. doi: 10.2337/dc14-S081

7. Minokoshi Y, Kahn CR, Kahn BB. Tissue-specific ablation of the GLUT4 glucose transporter or the insulin receptor challenges assumptions about insulin action and glucose homeostasis. *J Biol Chem* (2003) 278:33609–12. doi: 10.1074/jbc.R300019200

8. Huang S, Czech MP. The GLUT4 glucose transporter. *Cell Metab* (2007) 5:237–52. doi: 10.1016/j.cmet.2007.03.006

9. Govers R. Molecular mechanisms of GLUT4 regulation in adipocytes. *Diabetes Metab* (2014) 40:400–10. doi: 10.1016/j.diabet.2014.01.005

10. Okada T, Kawano Y, Sakakibara T, Hazeki O, Ui M. Essential role of phosphatidylinositol 3-kinase in insulin-induced glucose transport and antilipolysis in rat adipocytes. *Stud Selective Inhibitor Wortmannin J Biol Chem* (1994) 269:3568–73. doi: 10.1016/S0021-9258(17)41901-6

11. Tan S-X, Ng Y, Burchfield JG, Ramm G, Lambright DG, Stöckli J, et al. The rab GTPase-activating protein TBC1D4/AS160 contains an atypical phosphotyrosine-binding domain that interacts with plasma membrane phospholipids to facilitate GLUT4 trafficking in adipocytes. *Mol Cell Biol* (2012) 32:4946–59. doi: 10.1128/MCB.00761-12

12. Deshmukh AS. Insulin-stimulated glucose uptake in healthy and insulin-resistant skeletal muscle. *Horm Mol Biol Clin Investig* (2016) 26:13–24. doi: 10.1515/hmbci-2015-0041

13. Hotamisligil G k. S, Peraldi P, Budavari A, Ellis R, White MF, Spiegelman BM. IRS-1-Mediated inhibition of insulin receptor tyrosine kinase activity in TNF-alpha- and obesity-induced insulin resistance. *Sci (80)* (1996) 271:665–70. doi: 10.1126/science.271.5249.665

14. Haque WMM, Khan A, Nazimuddin K, Musa A, Ahmed AS, Sarker RSC. Frequency of hypomagnesemia in hospitalized diabetic hypokalemic patients. *J Bangladesh Coll Physicians Surg* (1970) 26:10–3. doi: 10.3329/jbcps.v26i1.4227

15. Simmons D, Joshi S, Shaw J. Hypomagnesaemia is associated with diabetes: Not pre-diabetes, obesity or the metabolic syndrome. *Diabetes Res Clin Pract* (2010) 87:261–6. doi: 10.1016/J.DIABRES.2009.11.003

16. Oost LJ, van der Heijden AAWA, Vermeulen EA, Bos C, Elders PJM, Slieker RC, et al. Serum magnesium is inversely associated with heart failure, atrial fibrillation, and microvascular complications in type 2 diabetes. *Diabetes Care* (2021) 44:1757–65. doi: 10.2337/dc21-0236

17. Waanders F, Dullaart RPF, Vos MJ, Hendriks SH, van Goor H, Bilo HJG, et al. Hypomagnesaemia and its determinants in a contemporary primary care cohort of persons with type 2 diabetes. *Endocrine* (2020) 67:80–6. doi: 10.1007/s12020-019-02116-3

18. Kurstjens S, de Baaij JHF, Bouras H, Bindels RJM, Tack CJJ, Hoenderop JGJ. Determinants of hypomagnesemia in patients with type 2 diabetes mellitus. *Eur J Endocrinol* (2017) 176:11–9. doi: 10.1530/EJE-16-0517

19. De Lima ML, Cruz T, Pousada JC, Rodrigues LE, Barbosa K, Canguçu V. The effect of magnesium supplementation in increasing doses on the control of type 2 diabetes. *Diabetes Care* (1998) 21:682–6. doi: 10.2337/diacare.21.5.682

20. Tosiello L. Hypomagnesemia and diabetes mellitus: A review of clinical implications. *Arch Intern Med* (1996) 156:1143–8. doi: 10.1001/archinte.156.11.1143

21. Ahmed F, Mohammed A. Magnesium: The forgotten electrolyte–a review on hypomagnesemia. *Med Sci* (2019) 7:56. doi: 10.3390/medsci7040056

22. Song Y, He K, Levitan EB, Manson JE, Liu S. Effects of oral magnesium supplementation on glycaemic control in type 2 diabetes: A meta-analysis of randomized double-blind controlled trials. *Diabetes Med* (2006) 23:1050–6. doi: 10.1111/j.1464-5491.2006.01852.x

23. Guerrero-Romero F, Tamez-Perez H, González-González G, Salinas-Martínez A, Montes-Villarreal J, Treviño-Ortiz J, et al. Oral magnesium supplementation improves insulin sensitivity in non-diabetic subjects with insulin resistance. *A Double-blind Placebo-controlled Randomized Trial Diabetes Metab* (2004) 30:253–8. doi: 10.1016/S1262-3636(07)70116-7

24. Mooren FC, Krüger K, Völker K, Golf SW, Wadepuhl M, Kraus A. Oral magnesium supplementation reduces insulin resistance in non-diabetic subjects - a double-blind, placebo-controlled, randomized trial. *Diabetes Obes Metab* (2011) 13:281–4. doi: 10.1111/j.1463-1326.2010.01332.x

25. Guerrero-Romero F, Simental-Mendía LE, Hernández-Ronquillo G, Rodriguez-Morán M. Oral magnesium supplementation improves glycaemic status in subjects with prediabetes and hypomagnesaemia: A double-blind placebo-controlled randomized trial. *Diabetes Metab* (2015) 41:202–7. doi: 10.1016/j.diabet.2015.03.010

26. Morakinyo AO, Samuel TA, Adekunbi DA. Magnesium upregulates insulin receptor and glucose transporter-4 in streptozotocin-nicotinamide-induced type-2 diabetic rats. *Endocr Regul* (2018) 52:6–16. doi: 10.2478/enr-2018-0002

27. Sohrabipour S, Sharifi MR, Sharifi M, Talebi A, Soltani N. Effect of magnesium sulfate administration to improve insulin resistance in type 2 diabetes animal model: using the hyperinsulinemic-euglycemic clamp technique. *Fundam Clin Pharmacol* (2018) 32:603–16. doi: 10.1111/fcp.12387

28. Zheng S, Shi S, Ren X, Han T, Li Y, Chen Y, et al. Triglyceride glucose-waist circumference, a novel and effective predictor of diabetes in first-degree relatives of type 2 diabetes patients: Cross-sectional and prospective cohort study. *J Transl Med* (2016) 14:1–10. doi: 10.1186/s12967-016-1020-8

29. Gross SM, Rotwein P. Akt signaling dynamics in individual cells. *J Cell Sci* (2015) 128:2509–19. doi: 10.1242/jcs.168773

30. Rudich A, Konrad D, Török D, Ben-Romano R, Huang C, Niu W, et al. Indinavir uncovers different contributions of GLUT4 and GLUT1 towards glucose uptake in muscle and fat cells and tissues. *Diabetologia* (2003) 46:649–58. doi: 10.1007/s00125-003-1080-1

31. White MF, Shoelson SE, Keutmann H. Kahn CR. *A Cascade Tyrosine Autophosphorylation β-Subunit Activates Phosphotransferase Insulin Receptor J Biol Chem* (1988) 263:2969–80. doi: 10.1016/S0021-9258(18)69163-X

32. Wilden PA, Backer JM, Kahn CR, Cahill DA, Schroeder GJ, White MF. The insulin receptor with phenylalanine replacing tyrosine-1146 provides evidence for separate signals regulating cellular metabolism and growth. *Proc Natl Acad Sci U.S.A.* (1990) 87:3358–62. doi: 10.1073/pnas.87.9.3358

33. Webster NJG, Park K, Pirrung MC. Signaling effects of demethylasterriquinone B1, a selective insulin receptor modulator. *ChemBioChem* (2003) 4:379–85. doi: 10.1002/cbic.200200468

34. Haugaard SB, Andersen O, Madsbad S, Frøsig C, Iversen J, Nielsen JO, et al. Skeletal muscle insulin signaling defects downstream of phosphatidylinositol 3-kinase at the level of akt are in HIV lipodystrophy. *Diabetes* (2005) 54:3474–83. doi: 10.2337/diabetes.54.12.3474

35. Rudich A, Vanounou S, Riesenberg K, Porat M, Tirosh A, Harman-Boehm I, et al. The HIV protease inhibitor nelfinavir induces insulin resistance and increases basal lipolysis in 3T3-L1 adipocytes. *Diabetes* (2001) 50:1425–31. doi: 10.2337/diabetes.50.6.1425

36. Ben-Romano R, Rudich A, Tirosh A, Potashnik R, Sasaoka T, Riesenberg K, et al. Nelfinavir-induced insulin resistance is associated with impaired plasma membrane recruitment of the PI 3-kinase effectors Akt/PKB and PKC-ζ. *Diabetologia* (2004) 47:1107–17. doi: 10.1007/s00125-004-1408-5

37. Su NY, Peng TC, Tsai PS, Huang CJ. Phosphoinositide 3-kinase/Akt pathway is involved in mediating the anti-inflammation effects of magnesium sulfate. *J Surg Res* (2013) 185:726–32. doi: 10.1016/j.jss.2013.06.030

38. Wang J, Ma XY, Feng YF, Ma ZS, Ma TC, Zhang Y, et al. Magnesium ions promote the biological behaviour of rat calvarial osteoblasts by activating the PI3K/Akt signalling pathway. *Biol Trace Elem Res* (2017) 179:284–93. doi: 10.1007/s12011-017-0948-8

39. George S, Rochford JJ, Wolfrum C, Gray SL, Schinner S, Wilson JC, et al. A family with severe insulin resistance and diabetes due to a mutation in AKT2. *Sci (80)* (2004) 304:1325–8. doi: 10.1126/science.1096706

40. Cho H, Mu J, Kim JK, Thorvaldsen JL, Chu Q, Crenshaw EB, et al. Insulin resistance and a diabetes mellitus-like syndrome in mice lacking the protein kinase Akt2 (PKBβ). *Sci (80)* (2001) 292:1728–31. doi: 10.1126/science.292.5522.1728

41. Miura T, Suzuki W, Ishihara E, Arai I, Ishida H, Seino Y, et al. Impairment of insulin-stimulated GLUT4 translocation in skeletal muscle and adipose tissue in the tsumura Suzuki obese diabetic mouse: A new genetic animal model of type 2 diabetes. *Eur J Endocrinol* (2001) 145:785–90. doi: 10.1530/eje.0.1450785

42. Suárez A, Pulido N, Casla A, Casanova B, Arrieta FJ, Rovira A. Impaired tyrosine-kinase activity of muscle insulin receptors from hypomagnesaemic rats. *Diabetologia* (1995) 38:1262–70. doi: 10.1007/BF00401757

43. Reis MAB, Reyes FGR, Saad MJA, Velloso LA. Magnesium deficiency modulates the insulin signaling pathway in liver but not muscle of rats. *J Nutr* (2000) 130:133–8. doi: 10.1093/jn/130.2.133

44. Kostov K. Effects of magnesium deficiency on mechanisms of insulin resistance in type 2 diabetes: Focusing on the processes of insulin secretion and signaling. *Int J Mol Sci* (2019) 20:2–15. doi: 10.3390/ijms20061351

45. Henkelman G, LaBute MX, Tung CS, Fenimore PW, McMahon BH. Conformational dependence of a protein kinase phosphate transfer reaction. *Proc Natl Acad Sci U.S.A.* (2005) 102:15347–51. doi: 10.1073/pnas.0506425102

46. Zhao Y, Liu Y, Gao X, Xu P. *Phosphorus chemistry*. Berlin/Munich/Boston: Walter de Gruyter GmbH (2019). pp. 67–80. doi: 10.1515/9783110562552-005.

47. Yu L, Xu L, Xu M, Wan B, Long Y, Huang Q. Role of Mg2+ ions in protein kinase phosphorylation: insights from molecular dynamics simulations of ATP-kinase complexes. *Mol Simul* (2011) 37:1143–50. doi: 10.1080/08927022.2011.561430

48. Pylypenko O, Hammich H, Yu IM, Houdusse A. Rab GTPases and their interacting protein partners: Structural insights into rab functional diversity. *Small GTPases* (2018) 9:22–48. doi: 10.1080/21541248.2017.1336191

49. Laughlin MR, Thompson D. The regulatory role for magnesium in glycolytic flux of the human erythrocyte. *J Biol Chem* (1996) 271:28977–83. doi: 10.1074/jbc.271.46.28977

50. Pasternak K, Joanna K, Anna H. Biochemistry of magnesium. *J Elem* (2020) 15:601–16. doi: 10.1111/j.1749-6632.1969.tb13003.x

51. Cronin CN, Tipton KF. The roles of magnesium ions in the reaction catalysed by phosphofructokinase from trypanosoma brucei. *Biochem J* (1987) 247:41–6. doi: 10.1042/bj2470041

52. Dimitriadis G, Mitrou P, Lambadiari V, Maratou E, Raptis SA. Insulin effects in muscle and adipose tissue. *Diabetes Res Clin Pract* (2011) 93 Suppl 1:S52–9. doi: 10.1016/S0168-8227(11)70014-6

53. Turner N, Kowalski GM, Leslie SJ, Risis S, Yang C, Lee-Young RS, et al. Distinct patterns of tissue-specific lipid accumulation during the induction of insulin resistance in mice by high-fat feeding. *Diabetologia* (2013) 56:1638–48. doi: 10.1007/s00125-013-2913-1

54. Burchfield JG, Kebede MA, Meoli CC, Stöckli J, Whitworth PT, Wright AL, et al. High dietary fat and sucrose results in an extensive and time-dependent deterioration in health of multiple physiological systems in mice. *J Biol Chem* (2018) 293:5731–45. doi: 10.1074/jbc.RA117.000808

55. Kandeel FR, Balon E, Scott S, Nadler JL. Magnesium deficiency and glucose metabolism in rat adipocytes. *Metabolism* (1996) 45:838–43. doi: 10.1016/S0026-0495(96)90156-0

56. Rodríguez-Morán M, Guerrero-Romero F. Oral magnesium supplementation improves insulin sensitivity and metabolic control in type 2 diabetic subjects a randomized double-blind controlled trial. *Diabetes Care* (2003) 26:1147–52. doi: 10.2337/diacare.26.4.1147

57. Hardy S, Kostantin E, Wang SJ, Hristova T, Galicia-Vázquez G, Baranov PV, et al. Magnesium-sensitive upstream ORF controls PRL phosphatase expression to mediate energy metabolism. *Proc Natl Acad Sci U.S.A.* (2019) 116:2925–34. doi: 10.1073/pnas.1815361116

58. Quamme GA, Rabkin SW. Cytosolic free magnesium in cardiac myocytes: Identification of a Mg2+ influx pathway. *Biochem Biophys Res Commun* (1990) 167:1406–12. doi: 10.1016/0006-291X(90)90679-H

59. Quamme GA, Dai LJ. Presence of a novel influx pathway for Mg2+ in MDCK cells. *Am J Physiol Cell Physiol* (1990) 259:C521–5. doi: 10.1152/ajpcell.1990.259.3.c521

60. Dai LJ, Friedman PA, Quamme GA. Phosphate depletion diminishes Mg2+ uptake in mouse distal convoluted tubule cells. *Kidney Int* (1997) 51:1710–8. doi: 10.1038/ki.1997.236

61. Romani AMP. Intracellular magnesium homeostasis. *Magnes Cent Nerv Syst* (2011) 512:13–58. doi: 10.1017/UPO9780987073051.003

frontiers | Frontiers in Endocrinology

TYPE Mini Review
PUBLISHED 15 September 2022
DOI 10.3389/fendo.2022.1011187

OPEN ACCESS

EDITED BY
Carlos Guillén,
Department of Biochemistry and Molecular Biology (UCM), Spain

REVIEWED BY
Teresa Pereira,
Uppsala University, Sweden

*CORRESPONDENCE
Sharon Baumel-Alterzon
sharon.alterzon@mssm.edu

SPECIALTY SECTION
This article was submitted to Diabetes: Molecular Mechanisms, a section of the journal Frontiers in Endocrinology

RECEIVED 03 August 2022
ACCEPTED 26 August 2022
PUBLISHED 15 September 2022

CITATION
Baumel-Alterzon S and Scott DK (2022) Regulation of Pdx1 by oxidative stress and Nrf2 in pancreatic beta-cells. *Front. Endocrinol.* 13:1011187. doi: 10.3389/fendo.2022.1011187

Regulation of Pdx1 by oxidative stress and Nrf2 in pancreatic beta-cells

Sharon Baumel-Alterzon[1,2*] and Donald K. Scott[1,2]

[1]Diabetes, Obesity and Metabolism Institute, Icahn School of Medicine at Mount Sinai, New York, NY, United States, [2]Mindich Child Health and Development Institute, Icahn School of Medicine at Mount Sinai, New York, NY, United States

The beta-cell identity gene, pancreatic duodenal homeobox 1 (*Pdx1*), plays critical roles in many aspects of the life of beta-cells including differentiation, maturation, function, survival and proliferation. High levels of reactive oxygen species (ROS) are extremely toxic to cells and especially to beta-cells due to their relatively low expression of antioxidant enzymes. One of the major mechanisms for beta-cell dysfunction in type-2 diabetes results from oxidative stress-dependent inhibition of PDX1 levels and function. ROS inhibits Pdx1 by reducing *Pdx1* mRNA and protein levels, inhibiting PDX1 nuclear localization, and suppressing PDX1 coactivator complexes. The nuclear factor erythroid 2-related factor (*Nrf2*) antioxidant pathway controls the redox balance and allows the maintenance of high Pdx1 levels. Therefore, pharmacological activation of the *Nrf2* pathway may alleviate diabetes by preserving Pdx1 levels.

KEYWORDS

Pdx1, ROS, Nrf2, oxidative-stress, beta-cells, diabetes

Introduction

Since its first introduction into the scientific community in 1945, reactive oxygen species (ROS) have been the focus of numerous studies (1). ROS are defined as oxygen-derived atoms or molecules that possess one or more unpaired electrons, making them highly reactive (2). While the cytoplasm, cell membrane, endoplasmic reticulum (ER) and peroxisome are capable of producing ROS, up to 90% of cellular ROS (composed mostly of H_2O_2 andO_2^-) are generated in the mitochondria due to incomplete reduction of oxygen to water in the electron transport chain (ETC) (3). High levels of ROS are extremely toxic to the cell, leading to DNA breaks, lipid peroxidation, protein aggregation, protein denaturation and protein fragmentation (4). Therefore, most cells are equipped with a battery of antioxidant genes that have the power to neutralize this threat, maintaining a fine equilibrium between ROS production and an antioxidant defense. In cases where ROS levels exceed the cell's ability to detoxify it and the

equilibrium is breached, the cell enters into a pathophysiological condition called "oxidative stress" (5). Oxidative stress takes part in the etiology of many diseases, contributing to the initiation and progression of cancer, vascular-related diseases, respiratory diseases, neurodegenerative disorders, digestive diseases, kidney diseases, chronic inflammatory disorders, aging and diabetes (5–7). Diabetes is linked to various cellular stresses that generate ROS, such as hyperglycemia, hyperlipidemia, hypoxia, inflammation, and ER stress (8, 9) (Figure 1). Indeed, pancreatic islets of type-2 diabetic patients often present increased levels of oxidative stress markers (such as oxidative DNA damage marker, 8-hydroxy-2′-deoxyguanosine) and this, at least in part, is due to the fact that beta-cells express low levels of several antioxidant genes, making them highly vulnerable to increased ROS levels (7, 10). In line with that, high ROS levels reduce functional beta-cell mass by increasing beta-cell apoptosis, reducing beta-cell proliferation, and damaging beta-cell function (7). Therefore, and perhaps as a compensatory mechanism, beta-cells protect themselves against oxidative stress by activating the nuclear factor erythroid 2-related factor (*Nrf2*) antioxidant signaling pathway. This activation is performed by ROS which oxidize critical cysteine in the NRF2 inhibitor, KEAP1, thus inhibiting NRF2 degradation (7, 11). Remarkably, apart from providing protection against oxidative stress, NRF2 regulates beta-cell mitochondrial biogenesis and activity, provides anti-inflammatory effects, promotes beta-cell function and stimulates beta-cell proliferation (7, 11).

Beta-cells express a unique set of key marker genes that define their identity and function by contributing to the expression and secretion of insulin (12). One of these genes is the duodenal homeobox 1 (*Pdx1*), a protein that plays many distinct roles in the life of a beta-cell, including involvement in beta-cell differentiation, beta-cell function, beta-cell survival and beta-cell proliferation (13–18). To do so, PDX1 controls the expression of other genes that play important roles in the beta-cell fate. These genes include insulin (*Ins1*, *Ins2*), neurogenin 3 (*Ngn3*), SRY-box transcription factor 9 (*Sox9*), hepatocyte nuclear factor 6 and 1b (*Hnf6, Hnf1b*), forkhead box protein a2 (*Foxa2*), V-Maf musculoaponeurotic fibrosarcoma oncogene homolog A (*MafA*), NK2 homeobox 2 (*Nkx2.2*), neurogenic differentiation (*NeuroD*), solute carrier family 2 member 2 (Glut2, *Slc2a2*), glucokinase (*Gck*), islet amyloid polypeptide (*Iapp*), NK6 homeobox 1 (*Nkx6.1*), cyclin D1 (*Ccnd1*), cyclin D2 (*Ccnd2*), and the transient receptor potential cation channel family 3 and 6 (*Trpc3,6*) (13, 16, 17, 19). In agreement with these findings, homozygous *Pdx1* knockout ($Pdx1^{-/-}$) mice exhibit pancreatic agenesis while heterozygous *Pdx1* knockout ($Pdx1^{+/-}$) mice present with beta-cell ER stress, beta-cell apoptosis, impaired insulin secretion, decreased beta-cell proliferation and reduced beta-cell mass (20–25). Additionally, tamoxifen-inducible beta-cell specific *Pdx1* deletion in adult mice results in hyperglycemia and transdifferentiation of beta-cells into alpha-like cells (26). In humans, 5% of diagnosed type-2 diabetes patients present with genetic defects in *PDX1* and mutations in *PDX1* define a subset of maturity-onset diabetes of the young 4 (MODY 4) (27, 28).

Defective expression of *Pdx1* has been documented in diabetes and this is attributed to oxidative stress (9, 29–31). Beta-cell specific deletion of *Nrf2* in mice under diabetogenic situation results in increased oxidative stress and reduced Pdx1 expression. Conversely, activation of NRF2 using genetic or pharmacological approaches increases *Pdx1* expression (11). These findings suggest that the NRF2 pathway is essential for preserving PDX1 levels, thus contributing to the maintenance of functional beta-cell mass. In this review, we aim to bring together all the current knowledge about the effect of physiological changes in redox balance on beta-cell fate *via* regulation on PDX1 levels.

Regulation of PDX1 levels by ROS during embryonic beta-cell development

During embryogenesis, *Pdx1* is expressed in two waves. The first wave begins at early stages of pancreatic development (E8.5 in mouse, gestational week 4 in human), with the appearance of dorsal and ventral foregut endoderm buds that later transform into a fully developed pancreas. At that stage, PDX1 is detected in the pancreas epithelium (13, 32–34). Mutations and deletions of *Pdx1* during the first wave results in pancreas agenesis in both mice and humans. Accordingly, *Pdx1* deletion does not affect the development of the endoderm buds. Rather, deletion of *Pdx1* inhibits the morphogenesis of the buds creating defects in the development of pancreatic epithelium (13, 20, 35, 36). Interestingly, the appearance of early premature insulin and glucagon positive cells in cells that lack PDX1 suggests that unlike in the second wave of *Pdx1* expression, the first wave of *Pdx1* expression is not involved in the development of endocrine cells (34, 36).

At the second wave of *Pdx1* expression, which occurs at late gestation (beginning at E13.5 in mouse, gestational week 12 in human), PDX1 stimulates the expression of another developmental factor, *Ngn3*. NGN3 levels, which significantly increase in mouse at E13.5 and reach maximal levels at E15.5, are responsible for the specification of endocrine progenitors into endocrine cells that will later form the pancreatic islets (13, 37, 38). Inducible *Pdx1* deletion at these ages blocks the formation of acinar cells and islets in mouse embryos (35). Additionally, beta-cell specific *Pdx1* deletion increases glucagon and somatostatin positive cells at the expense of insulin positive cells resulting in diabetes (34). Following the second wave of *Pdx1* expression, PDX1 levels remain constant towards and during adulthood (in healthy non-diabetic settings). In adults, PDX1 is restricted to beta-cells where it works to maintain beta-cell maturity and function (13, 33).

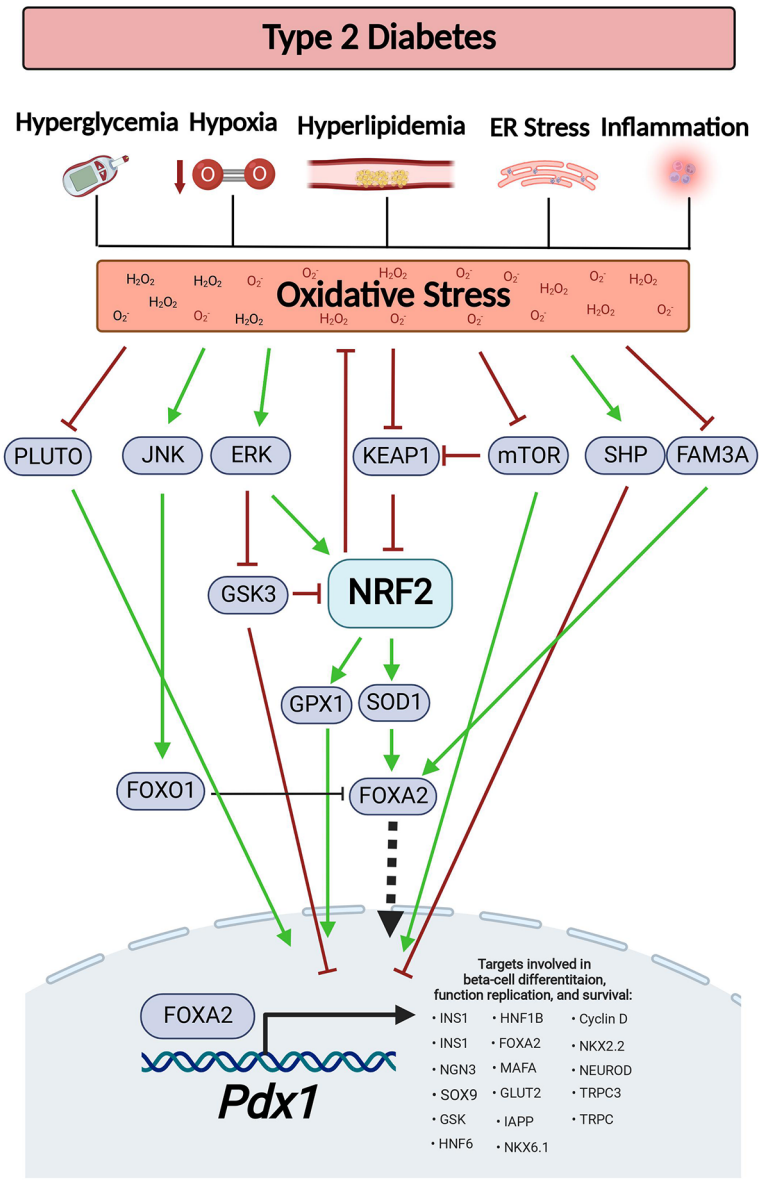

FIGURE 1
Oxidative stress-dependent pathways affect Pdx1 levels during diabetes. Type-2 diabetes is associated with various pathological conditions that generate ROS, such as hyperglycemia, hyperlipidemia, hypoxia, inflammation, and ER stress. This results in oxidative stress. Oxidative stress reduces the expression level of *PLUTO* lncRNA, stimulates JNK-dependent FOXO1 activation, inhibits mTOCR signaling, increases SHP expression and reduces FAM3A levels, all of which results in decreased PDX1 levels. On the other hand, in order to maintain ROS at appropriate levels, oxidative stress also serves as a signal for Nrf2 activation by inhibition of Keap1 and by activation of the ERK signaling. This results in increased expression of the Nrf2 target genes, *Sod1* and *Gpx, which* restore PDX1 levels. This figure was generated using BioRender.com.

Some levels of ROS are necessary for normal cellular function. For example, moderate levels of ROS (up to ~100 nM H_2O_2) are needed for stem cells to maintain their ability to go through cell differentiation and to keep their "stemness". The underlying mechanism involves the oxidation of tyrosine and cysteine residues which activates protein kinases, protein phosphatases, and signaling factors that take part in cell differentiation (39). This might explain the formation of moderated ROS levels (starting at E12.5 and peaking at E15.5) by NADPH oxidase 4 (*Nox4*) activity during the development of embryonic mouse pancreas (40). Nevertheless, accumulation of higher ROS levels (above ~100 μM H_2O_2) may lead to cell senescence or death (39). Furthermore, prompt increase of oxidative stress may pose a risk on normal pancreatic development since PDX1 levels are negatively regulated by ROS (for further details on the mechanisms see Figure 1 and

Table 1 below) (41–45). This highlights the need to maintain ROS at appropriate levels to support pancreatic development and differentiation without damaging the cells. Surprisingly two NRF2 antioxidant target genes, catalase (*Cat*) and superoxide dismutase 1 (*Sod1*), are upregulated during pancreatic development (40). This suggests that NRF2 helps maintaining the required redox balance in the embryonic pancreas, a theory that has not been tested yet. In support of that, SOD1 stimulates *Pdx1* expression by increasing the expression of Forkhead Box Protein A2 (*Foxa2*), one of the main *Pdx1* transcriptional regulators (46). SOD1 can also support *Pdx1* transcription by increasing H3 acetylation and H3K4 methylation on the *Pdx1* promoter, thus providing an open active chromatin (46). Intriguingly, during pancreatic development, ROS activates the ERK signaling pathway which can further activate the NRF2 pathway and increase *Pdx1* expression, resulting in differentiation of endocrine progenitors into beta-cells (47–49). Overall, these findings suggest that by maintaining normal redox balance, the NRF2 pathway supports appropriate PDX1 levels that promote normal pancreatic development.

Regulation of PDX1 levels by ROS during postnatal ages and adulthood

After birth, both mouse and human neonates exhibit a sharp burst of beta-cell proliferation. This peak of proliferation, which is temporary, substantially declines with age (50). Weaning is believed to be the main trigger for the loss of beta-cell proliferative capabilities, and it coincides with the gradual maturation of beta-cells (51, 52). Mechanistically, the transition from fat-rich maternal milk to carbohydrate-rich diet inhibits the proliferative factor, mammalian target of rapamycin complex1 (mTORC1) and activates 5'-adenosine monophosphate–activated protein kinase (AMPK), which promotes beta-cell maturity. On the other hand, continuous supplementation of milk-fat rich diet to mice during weaning into adulthood maintains high mTORC1 levels and beta-cell proliferation (53). Consistent with these findings, beta-cell specific deletion of *mtorc1* in mice leads to impaired beta-cell proliferation, reduced beta-cell survival and decreased beta-cell mass (54), while activation of mTORC1 stimulates mouse beta-cell proliferation by increasing cyclin D2 expression (55). Interestingly, branched chain amino acids can activate the mTORC1-Rab1A axis to maintain PDX1 protein stability and increase its nuclear localization (56, 57). Moreover, beta-cell-specific overexpression of kinase-dead mTOR mutants results in decreased *Pdx1* mRNA and protein levels (58). These findings link mTOR-stimulated beta-cell proliferation during postnatal ages with PDX1 activity. Oxidative stress and conditions that generate ROS such as ER stress and hypoxia, can inhibit mTOR signaling (59). In postnatal Akita mice, ER stress inhibits mTORC1 leading to reduced beta-cell proliferation, as well to decreased PDX1 protein levels and downregulation of PDX1 target genes. However, restoration of mTORC1 activity in these mice did not affect PDX1 protein levels, suggesting that ER stress affects PDX1 levels by mTORC1-independent mechanisms (60). Although the exact mechanism by which mTORC1 regulates *Pdx1* is unknown, mTORC1 can control NRF2 levels by p62-dependent degradation of its inhibitor, KEAP1 (7, 61), suggesting that NRF2 might be involved.

PDX1 binding sites are found in several genes that are associated with cell replication, such as *Nasp, Bard1, Mnx1*, and *Mcm7* (17). This suggest that PDX1 on its own can stimulate beta-cell proliferation. Accordingly, overexpression of *Pdx1* in primary rat islets increases beta-cell proliferation by upregulation of cyclin *D1* and *D2* expression (16), which are essential for beta-cell proliferation during postnatal ages (62, 63), over-nutrition (64, 65), and pregnancy (66). Interestingly, oxidative stress reduces cyclins *D1* and *D2* expression while activation of the NRF2 antioxidant pathway increases cyclin D1 (9, 11). On the other hand, mice expressing mutated PDX1 develop diabetes at weaning concomitantly with reduced beta-cell proliferation and beta-cell area (17). Thus, regulation of redox-balance is important for PDX1-stimulated beta-cell proliferation.

During adulthood, PDX1 switches roles and takes part in beta-cell identity and maturation. For example, PDX1 controls insulin gene transcription by forming a transcriptional activation complex with neuronal differentiation 1 (*Neurod1*) and by upregulation of *MafA* and *Ngn3* expression, which are needed for insulin transcription (13). MAFA can further enhance glucose-stimulated insulin secretion (GSIS) to maintain glucose homeostasis (67). PDX1 can also upregulate the expression of other factors that are necessary for GSIS, such as *Glut2* and glucokinase (28). Indeed, two missense mutations in the *Pdx1* transactivation domain inhibit GSIS (68). Lastly, as previously mentioned, PDX1 positively regulates the expression of various beta-cell identity genes (13, 16, 17, 19). This might explain why beta-cell specific *Pdx1* deletion results in an altered transcriptional profile that resembles alpha-like cells. This includes downregulation of *Ins1* and *Glut2* genes while upregulation of *Gcg* (glucagon) and *MafB* (26). These findings suggest that physiological situations that increase oxidative stress may inhibit PDX1 from maintaining beta-cell identity and function, and eventually lead to diabetes (as described in part 4).

Regulation of PDX1 levels by ROS in beta-cells during diabetes

One of the major mechanisms for beta-cell dysfunction in type-2 diabetes involves the inhibition of *Pdx1* by oxidative stress (41–44). For example, chronic exposure of syrian hamster

islet cell line HIT-T15 to high glucose concentrations reduces *Pdx1* mRNA and protein levels (44, 69). Additionaly, type-2 diabetic rodent models, such as db/db mice as well as mice and rats fed on high fat diet (HFD), display reduced *Pdx1* mRNA and/or protein expression as well as decreased PDX1 nuclear localization (53, 70–72). Similarly, beta-cell specific deletion of Nrf2 in mice fed on HFD results in increased oxidative stress, reduced *Pdx1* mRNA levels and inhibition of PDX1 translocation into the nucleus (11). Conversely, treatment of obese diabetic C57BL/KsJ-db/db mice or Zucker diabetic rats with antioxidant agents restores PDX1 nuclear localization and PDX1 transcriptional activity (73, 74). Likewise, overexpression of glutathione peroxidase 1 (*Gpx1*), a Nrf2 antioxidant target gene, increases *Pdx1* mRNA and protein levels in mouse beta-cells (75).

The mechanisms behind ROS-dependent reduction of PDX1 levels vary (Figure 1 and Table 1). For example, oxidative stress can lead to activation of forkhead box protein O1 (FOXO1) by c-Jun N-terminal kinase (JNK) or by acetylation of FOXO1. As a result, FOXO1 goes through phosphorylation, nuclear translocation and subsequent activation (76, 88). FOXO1 then mediates inhibition of FOXA2-transcriptional activation of *Pdx1* and inhibits PDX1 nuclear translocation (76, 89–91). Moreover, islets from mice fed on HFD exhibit nuclear exclusion and reduced activity of FOXA2 (92) and db/db mouse islets show reduced levels of family with sequence similarity 3 member A (FAM3A), a factor that upregulates PDX1 levels *via* activation of CaM-FOXA2 pathway (85). Oxidative stress can reduce PDX1 levels by additional mechanisms. For example, during conditions that generate ROS, such as high glucose concentrations, ER stress and treatment with streptozotocin (STZ) (7), orphan nuclear receptor small heterodimer partner (SHP) downregulates Pdx1 at the mRNA levels (78, 82, 84). In addition, mutations in *Klf11* transcription factor which are associated with maturity-onset diabetes of the young 7 (MODY7), lead to promoter repression of the antioxidant gene catalase 1 (*Cat1*), and to a reduction in *Pdx1* transcription in beta-cells (93, 94). Saturated fatty-acids, such as palmitic-acid, can stimulate the production of H_2O_2 in beta-cells, leading to beta-cell death (95). Interestingly, recent findings show that incubation of beta-cells with palmitic acid leads to sequestration of PDX1 into stress-granules. This sequestration prevents PDX1 from translocating to the nucleus and transcribing its target genes. Moreover, inhibition of the

TABLE 1 Ros-dependent mechanisms that reduce Pdx1 levels and activity during diabetes.

Diabetic situations associated with oxidative stress	Mechanisms	Reduced Pdx1 RNA levels	Reduced PDX1 protein levels	Reduced PDX1 nuclear localization	Reduced PDX1 transcriptional activity	Citations
Hydrogen peroxide (H_2O_2)	• Phosphorylation of PDX1 Serine 61/66 by GSK3. • Reduced H3 and H4 histone acetylation in *Pdx1* promoter. • Activation of FOXO1 inhibits FOXA2.	X	X	X		(75–77)
Chronic exposure to high glucose concentration	• Hypermethylation at CpG sites on *Pdx1* promoter. • Phosphorylation of PDX1 Serine 268 by Gsk3. • Reduced PDX1-P300 interaction. • Reduced *Pdx1* and *p300* expression by SHP.	X	X		X	(44, 53, 69, 78–80)
Palmitic acid	• Sequestration of PDX1 into stress-granules in a PI3K/EIF2α dependent manner.			X		(81)
Streptozotocin (STZ)	• Reduced *Pdx1* expression by SHP.	X				(82)
High fat diet (HFD)	• Reduced PDX1-CHD4 interaction.	X		X	X	(70, 71, 83)
ER stress	• Reduced *Pdx1* expression by SHP.		X			(60, 84)
db/db diabetic mice	• Phosphorylation of PDX1 Serine 269 by GSK3. • Reduced *Fam3a* expression inactivates CaM-FOXA2 pathway.	X	X	X		(53, 72, 73, 85)
Type 2 diabetic human islets	• Hypermethylation at CpG sites on *PDX1* promoter. • Reduced *PLUTO* lncRNA. • Reduced PDX1-CHD4 interaction. • Reduced expression of *p300*. • Reduced PDX1-SWI/SNF interaction.	X			X	(79, 80, 83, 86, 87)

stress-granules formation in HFD fed mice results in increased PDX1 nuclear localization and improved glucose tolerance as well as GSIS (81).

At the post-transcriptional level, oxidative stress increases activity of glycogen synthase kinase 3 (GSK3), a known NRF2 inhibitor, which then phosphorylates PDX1 serine 61 and/or serine 66 resulting in PDX1 protein degradation (7, 77). Additionally, INS1e rat beta-cell-like insulinoma cells and human islets chronically exposed to high glucose display GSK3-mediated phosphorylation of PDX1 serine 268, resulting in PDX1 degradation and reduced expression of PDX1 target genes (53). Oxidative stress also reduces H3 and H4 histone acetylation in the *Pdx1* promoter, leading to transcriptional silencing due to tightly packed chromatin (75). Islets from type-2 diabetic donors show higher methylation status at ten CpG sites on the *PDX1* promoter. This is associated with reduced *PDX1* mRNA levels. The same phenomenon is observed in rat insulinoma beta-like cells (INS 832/13) incubated chronically at high glucose concentrations (19, 79). Additionally, treatment of human stem cells with the DNA methylation inhibitor, 5-aza-2′-deoxycytidine, increases PDX1 nuclear levels (19, 96). Human and mouse pancreatic islets express hundreds of long non-coding RNAs (lncRNAs), some of which are playing important roles in beta-cell differentiation and function. One of the most characterized ones is a beta-cell specific lncRNA called *PLUTO*, which positively regulates *PDX1* transcription. *PLUTO*, exhibits a marked reduction of expression in islets from type-2 diabetic donors, positioning it as another mechanism for reducing PDX1 levels under ROS-associated pathological conditions (86).

Apart from affecting PDX1 abundance, conditions associated with increased ROS can affect PDX1 transcriptional activity by targeting coactivator complexes associated with PDX1 (97). For example, decreased interaction between PDX1 and the chromodomain helicase DNA-binding 4 (CHD4) ATPase subunit of the NuRD complex is observed in both islets of type-2 donors and in mice fed on HFD (83). Similarly, in human type-2 diabetic beta-cells, there is a significant reduction in PDX1 binding to the ATP-dependent SWI/SNF chromatin remodeling complex, a complex that is needed for pancreas development and beta-cell identity (87, 98). PDX1 also interacts with histone acetyltransferases p300 and CBP (p300/CBP) to stimulate expression of PDX1 target genes, including insulin (99). INS-1E cells incubated in high glucose concentrations and islets from type-2 donors display reduced levels of p300 due to protein degradation (80), a situation that may hamper PDX1 transcriptional activity.

Based on their ability to reduce hyperglycemia and body weight, the U.S. food and drug administration (FDA) approved the use of Glucagon-like peptide-1 receptor (GLP-1R) agonists as a treatment for type-2 patients (100). Interestingly, treatments of islets from a rat model of intrauterine growth retardation (IUGR) or from a "catch up growth" Wistar rat model with the GLP-1R agonists, Exendin 4 and Liraglutide, increase Pdx1 transcription by increasing H3 histone acetylation, increasing H3K4me3 levels and by reducing H3K9me2 levels in Pdx1 promoter (101, 102). Additionally, GLP-1 itself stimulates PDX1 nuclear translocation *via* cAMP-dependent PKA pathway and activates NRF2 through the PKA-dependent ERK activation pathway, suggesting that NRF2 might be involved in this regulation (7, 103).

Concluding remarks

To conclude, published data indicate that alteration in redox-balance leads to dysregulated PDX1 levels and activity, which can result in diabetes. Expression of several NRF2 target genes, as well as treatment with CDDO-Me, an NRF2 pharmacological activator, maintain PDX1 abundance by reducing oxidative stress (11, 40, 75, 104). These findings suggest that activation of the NRF2 pathway may alleviate diabetes by preserving PDX1 levels. Additional studies are needed to further explore the role of NRF2 in maintaining PDX1 levels during embryonic, postnatal and adult life. Interestingly, CDDO derivatives were also shown to contribute to the maintenance of functional beta-cell mass by promoting beta-cell proliferation, reducing beta-cell oxidative damages, increasing islet cell viability, improving insulin content, stimulating insulin secretion and reducing secretion of proinflammatory cytokines (7, 11). Furthermore, treatment of db/db and streptozotocin-induced diabetic mouse models with CDDO derivatives improves diabetes outcome (105–107) and these compounds have been tested under several clinical trials to improve chronic kidney disease in diabetic patients (7).This places NRF2 as a potential therapeutic target for type-2 diabetes.

Author contributions

SB-A designed content, wrote text, and produced the figure. DKS reviewed and edited the manuscript. All authors contributed to the article and approved the submitted version.

Funding

This work was supported by the National Institutes ofHeath/The National INstitute of Diabetes Digestive and Kidney Diseases R01DK114338 andR01DK130300 (to DKS) and K01128387 (to SB-A).

Conflict of interest

The authors declare that the research was conducted in the absence of any commercial or financial relationships that could be construed as a potential conflict of interest.

Publisher's note

References

1. Alfadda AA, Sallam RM. Reactive oxygen species in health and disease. *J BioMed Biotechnol* (2012) 2012:936486. doi: 10.1155/2012/936486

2. Zhang C, Wang X, Du J, Gu Z, Zhao Y. Reactive oxygen species-regulating strategies based on nanomaterials for disease treatment. *Adv Sci (Weinh)* (2021) 8 (3):2002797. doi: 10.1002/advs.202002797

3. Tirichen H, Yaigoub H, Xu W, Wu C, Li R, Li Y. Mitochondrial reactive oxygen species and their contribution in chronic kidney disease progression through oxidative stress. *Front Physiol* (2021) 12:627837. doi: 10.3389/fphys.2021.627837

4. Len JS, Koh WSD, Tan SX. The roles of reactive oxygen species and antioxidants in cryopreservation. *Biosci Rep* (2019) 39(8):BSR20191601. doi: 10.1042/BSR20191601

5. Pizzino G, Irrera N, Cucinotta M, Pallio G, Mannino F, Arcoraci V, et al. Oxidative stress: Harms and benefits for human health. *Oxid Med Cell Longev* (2017) 2017:8416763. doi: 10.1155/2017/8416763

6. Liu Z, Ren Z, Zhang J, Chuang CC, Kandaswamy E, Zhou T, et al. Role of ros and nutritional antioxidants in human diseases. *Front Physiol* (2018) 9:477. doi: 10.3389/fphys.2018.00477

7. Baumel-Alterzon S, Katz LS, Brill G, Garcia-Ocana A, Scott DK. Nrf2: The master and captain of beta cell fate. *Trends Endocrinol Metab* (2020) 32(1):7–19. doi: 10.1016/j.tem.2020.11.002

8. Galicia-Garcia U, Benito-Vicente A, Jebari S, Larrea-Sebal A, Siddiqi H, Uribe KB, et al. Pathophysiology of type 2 diabetes mellitus. *Int J Mol Sci* (2020) 21 (17):6275. doi: 10.3390/ijms21176275

9. Wang J, Wang H. Oxidative stress in pancreatic beta cell regeneration. *Oxid Med Cell Longev* (2017) 2017:1930261. doi: 10.1155/2017/1930261

10. Del Guerra S, Lupi R, Marselli L, Masini M, Bugliani M, Sbrana S, et al. Functional and molecular defects of pancreatic islets in human type 2 diabetes. *Diabetes* (2005) 54(3):727–35. doi: 10.2337/diabetes.54.3.727

11. Baumel-Alterzon S, Katz LS, Brill G, Jean-Pierre C, Li Y, Tse I, et al. Nrf2 regulates beta-cell mass by suppressing beta-cell death and promoting beta-cell proliferation. *Diabetes* (2022) 71(5):989–1011. doi: 10.2337/db21-0581

12. Mostafa D, Yanagiya A, Georgiadou E, Wu Y, Stylianides T, Rutter GA, et al. Loss of beta-cell identity and diabetic phenotype in mice caused by disruption of Cnot3-dependent mrna deadenylation. *Commun Biol* (2020) 3(1):476. doi: 10.1038/s42003-020-01201-y

13. Zhu Y, Liu Q, Zhou Z, Ikeda Y. Pdx1, neurogenin-3, and mafa: Critical transcription regulators for beta cell development and regeneration. *Stem Cell Res Ther* (2017) 8(1):240. doi: 10.1186/s13287-017-0694-z

14. Yao X, Li K, Liang C, Zhou Z, Wang J, Wang S, et al. Tectorigenin enhances Pdx1 expression and protects pancreatic beta-cells by activating erk and reducing er stress. *J Biol Chem* (2020) 295(37):12975–92. doi: 10.1074/jbc.RA120.012849

15. Fujimoto K, Polonsky KS. Pdx1 and other factors that regulate pancreatic beta-cell survival. *Diabetes Obes Metab* (2009) 11 Suppl 4:30–7. doi: 10.1111/j.1463-1326.2009.01121.x

16. Hayes HL, Moss LG, Schisler JC, Haldeman JM, Zhang Z, Rosenberg PB, et al. Pdx-1 activates islet alpha- and beta-cell proliferation *Via* a mechanism regulated by transient receptor potential cation channels 3 and 6 and extracellular signal-regulated kinases 1 and 2. *Mol Cell Biol* (2013) 33(20):4017–29. doi: 10.1128/MCB.00469-13

17. Spaeth JM, Gupte M, Perelis M, Yang YP, Cyphert H, Guo S, et al. Defining a novel role for the Pdx1 transcription factor in islet beta-cell maturation and proliferation during weaning. *Diabetes* (2017) 66(11):2830–9. doi: 10.2337/db16-1516

18. Zhu X, Oguh A, Gingerich MA, Soleimanpour SA, Stoffers DA, Gannon M. Cell cycle regulation of the Pdx1 transcription factor in developing pancreas and insulin-producing beta-cells. *Diabetes* (2021) 70(4):903–16. doi: 10.2337/db20-0599

19. Liu J, Lang G, Shi J. Epigenetic regulation of pdx-1 in type 2 diabetes mellitus. *Diabetes Metab Syndr Obes* (2021) 14:431–42. doi: 10.2147/DMSO.S291932

20. Vinogradova TV, Sverdlov ED. Pdx1: A unique pancreatic master regulator constantly changes its functions during embryonic development and progression of pancreatic cancer. *Biochem (Mosc)* (2017) 82(8):887–93. doi: 10.1134/S000629791708003X

21. Sachdeva MM, Claiborn KC, Khoo C, Yang J, Groff DN, Mirmira RG, et al. Pdx1 (Mody4) regulates pancreatic beta cell susceptibility to er stress. *Proc Natl Acad Sci U.S.A.* (2009) 106(45):19090–5. doi: 10.1073/pnas.0904849106

22. Brissova M, Blaha M, Spear C, Nicholson W, Radhika A, Shiota M, et al. Reduced pdx-1 expression impairs islet response to insulin resistance and worsens glucose homeostasis. *Am J Physiol Endocrinol Metab* (2005) 288(4):E707–14. doi: 10.1152/ajpendo.00252.2004

23. Brissova M, Shiota M, Nicholson WE, Gannon M, Knobel SM, Piston DW, et al. Reduction in pancreatic transcription factor pdx-1 impairs glucose-stimulated insulin secretion. *J Biol Chem* (2002) 277(13):11225–32. doi: 10.1074/jbc.M111272200

24. Sun J, Mao L, Yang H, Ren D. Critical role for the Tsc1-Mtorc1 pathway in beta-cell mass in Pdx1-deficient mice. *J Endocrinol* (2018) 238(2):151–63. doi: 10.1530/JOE-18-0015

25. Jara MA, Werneck-De-Castro JP, Lubaczeuski C, Johnson JD, Bernal-Mizrachi E. Pancreatic and duodenal homeobox-1 (Pdx1) contributes to beta-cell mass expansion and proliferation induced by Akt/Pkb pathway. *Islets* (2020) 12 (2):32–40. doi: 10.1080/19382014.2020.1762471

26. Gao T, McKenna B, Li C, Reichert M, Nguyen J, Singh T, et al. Pdx1 maintains beta cell identity and function by repressing an alpha cell program. *Cell Metab* (2014) 19(2):259–71. doi: 10.1016/j.cmet.2013.12.002

27. Urakami T. Maturity-onset diabetes of the young (Mody): Current perspectives on diagnosis and treatment. *Diabetes Metab Syndr Obes* (2019) 12:1047–56. doi: 10.2147/DMSO.S179793

28. Kushner JA, Ye J, Schubert M, Burks DJ, Dow MA, Flint CL, et al. Pdx1 restores beta cell function in Irs2 knockout mice. *J Clin Invest* (2002) 109(9):1193–201. doi: 10.1172/JCI14439

29. Moin ASM, Butler AE. Alterations in beta cell identity in type 1 and type 2 diabetes. *Curr Diabetes Rep* (2019) 19(9):83. doi: 10.1007/s11892-019-1194-6

30. Robertson RP, Harmon J, Tran PO, Tanaka Y, Takahashi H. Glucose toxicity in beta-cells: Type 2 diabetes, good radicals gone bad, and the glutathione connection. *Diabetes* (2003) 52(3):581–7. doi: 10.2337/diabetes.52.3.581

31. Guo S, Dai C, Guo M, Taylor B, Harmon JS, Sander M, et al. Inactivation of specific beta cell transcription factors in type 2 diabetes. *J Clin Invest* (2013) 123 (8):3305–16. doi: 10.1172/JCI65390

32. Astro V, Adamo A. Epigenetic control of endocrine pancreas differentiation in vitro: Current knowledge and future perspectives. *Front Cell Dev Biol* (2018) 6:141. doi: 10.3389/fcell.2018.00141

33. Jorgensen MC, Ahnfelt-Ronne J, Hald J, Madsen OD, Serup P, Hecksher-Sorensen J. An illustrated review of early pancreas development in the mouse. *Endocr Rev* (2007) 28(6):685–705. doi: 10.1210/er.2007-0016

34. Gannon M, Ables ET, Crawford L, Lowe D, Offield MF, Magnuson MA, et al. Pdx-1 function is specifically required in embryonic beta cells to generate appropriate numbers of endocrine cell types and maintain glucose homeostasis. *Dev Biol* (2008) 314(2):406–17. doi: 10.1016/j.ydbio.2007.10.038

35. Holland AM, Hale MA, Kagami H, Hammer RE, MacDonald RJ. Experimental control of pancreatic development and maintenance. *Proc Natl Acad Sci U.S.A.* (2002) 99(19):12236–41. doi: 10.1073/pnas.192255099

36. Ahlgren U, Jonsson J, Edlund H. The morphogenesis of the pancreatic mesenchyme is uncoupled from that of the pancreatic epithelium in Ipf1/Pdx1-deficient mice. *Development* (1996) 122(5):1409–16. doi: 10.1242/dev.122.5.1409

37. Oliver-Krasinski JM, Kasner MT, Yang J, Crutchlow MF, Rustgi AK, Kaestner KH, et al. The diabetes gene Pdx1 regulates the transcriptional network of pancreatic endocrine progenitor cells in mice. *J Clin Invest* (2009) 119(7):1888–98. doi: 10.1172/JCI37028

38. White P, May CL, Lamounier RN, Brestelli JE, Kaestner KH. Defining pancreatic endocrine precursors and their descendants. *Diabetes* (2008) 57(3):654–68. doi: 10.2337/db07-1362

39. Sies H, Jones DP. Reactive oxygen species (Ros) as pleiotropic physiological signalling agents. *Nat Rev Mol Cell Biol* (2020) 21(7):363–83. doi: 10.1038/s41580-020-0230-3

40. Liang J, Wu SY, Zhang D, Wang L, Leung KK, Leung PS. Nadph oxidase-dependent reactive oxygen species stimulate beta-cell regeneration through differentiation of endocrine progenitors in murine pancreas. *Antioxid Redox Signal* (2016) 24(8):419–33. doi: 10.1089/ars.2014.6135

41. Yaribeygi H, Sathyapalan T, Atkin SL, Sahebkar A. Molecular mechanisms linking oxidative stress and diabetes mellitus. *Oxid Med Cell Longev* (2020) 2020:8609213. doi: 10.1155/2020/8609213

42. Kaneto H, Matsuoka TA. Involvement of oxidative stress in suppression of insulin biosynthesis under diabetic conditions. *Int J Mol Sci* (2012) 13(10):13680–90. doi: 10.3390/ijms131013680

43. Newsholme P, Keane KN, Carlessi R, Cruzat V. Oxidative stress pathways in pancreatic beta-cells and insulin-sensitive cells and tissues: Importance to cell metabolism, function, and dysfunction. *Am J Physiol Cell Physiol* (2019) 317(3): C420–C33. doi: 10.1152/ajpcell.00141.2019

44. Robertson R, Zhou H, Zhang T, Harmon JS. Chronic oxidative stress as a mechanism for glucose toxicity of the beta cell in type 2 diabetes. *Cell Biochem Biophys* (2007) 48(2-3):139–46. doi: 10.1007/s12013-007-0026-5

45. Kawamori D, Kajimoto Y, Kaneto H, Umayahara Y, Fujitani Y, Miyatsuka T, et al. Oxidative stress induces nucleo-cytoplasmic translocation of pancreatic transcription factor pdx-1 through activation of c-jun Nh(2)-terminal kinase. *Diabetes* (2003) 52(12):2896–904. doi: 10.2337/diabetes.52.12.2896

46. Wang X, Vatamaniuk MZ, Roneker CA, Pepper MP, Hu LG, Simmons RA, et al. Knockouts of Sod1 and Gpx1 exert different impacts on murine islet function and pancreatic integrity. *Antioxid Redox Signal* (2011) 14(3):391–401. doi: 10.1089/ars.2010.3302

47. Hoarau E, Chandra V, Rustin P, Scharfmann R, Duvillie B. Pro-Oxidant/Antioxidant balance controls pancreatic beta-cell differentiation through the Erk1/2 pathway. *Cell Death Dis* (2014) 5:e1487. doi: 10.1038/cddis.2014.441

48. Liang C, Hao F, Yao X, Qiu Y, Liu L, Wang S, et al. Hypericin maintians Pdx1 expression *Via* the erk pathway and protects islet beta-cells against glucotoxicity and lipotoxicity. *Int J Biol Sci* (2019) 15(7):1472–87. doi: 10.7150/ijbs.33817

49. Papaiahgari S, Kleeberger SR, Cho HY, Kalvakolanu DV, Reddy SP. Nadph oxidase and erk signaling regulates hyperoxia-induced Nrf2-are transcriptional response in pulmonary epithelial cells. *J Biol Chem* (2004) 279(40):42302–12. doi: 10.1074/jbc.M408275200

50. Gregg BE, Moore PC, Demozay D, Hall BA, Li M, Husain A, et al. Formation of a human beta-cell population within pancreatic islets is set early in life. *J Clin Endocrinol Metab* (2012) 97(9):3197–206. doi: 10.1210/jc.2012-1206

51. Jacovetti C, Matkovich SJ, Rodriguez-Trejo A, Guay C, Regazzi R. Postnatal beta-cell maturation is associated with islet-specific microrna changes induced by nutrient shifts at weaning. *Nat Commun* (2015) 6:8084. doi: 10.1038/ncomms9084

52. Jaafar R, Tran S, Shah AN, Sun G, Valdearcos M, Marchetti P, et al. Mtorc1 to ampk switching underlies beta-cell metabolic plasticity during maturation and diabetes. *J Clin Invest* (2019) 129(10):4124–37. doi: 10.1172/JCI127021

53. Sacco F, Seelig A, Humphrey SJ, Krahmer N, Volta F, Reggio A, et al. Phosphoproteomics reveals the Gsk3-Pdx1 axis as a key pathogenic signaling node in diabetic islets. *Cell Metab* (2019) 29(6):1422–32.e3. doi: 10.1016/j.cmet.2019.02.012

54. Blandino-Rosano M, Barbaresso R, Jimenez-Palomares M, Bozadjieva N, Werneck-de-Castro JP, Hatanaka M, et al. Loss of Mtorc1 signalling impairs beta-cell homeostasis and insulin processing. *Nat Commun* (2017) 8:16014. doi: 10.1038/ncomms16014

55. Balcazar N, Sathyamurthy A, Elghazi L, Gould A, Weiss A, Shiojima I, et al. Mtorc1 activation regulates beta-cell mass and proliferation by modulation of cyclin D2 synthesis and stability. *J Biol Chem* (2009) 284(12):7832–42. doi: 10.1074/jbc.M807458200

56. Zhang X, Wang X, Yuan Z, Radford SJ, Liu C, Libutti SK, et al. Amino acids-Rab1a-Mtorc1 signaling controls whole-body glucose homeostasis. *Cell Rep* (2021) 34(11):108830. doi: 10.1016/j.celrep.2021.108830

57. Fan J, Yuan Z, Burley SK, Libutti SK, Zheng XFS. Amino acids control blood glucose levels through mtor signaling. *Eur J Cell Biol* (2022) 101(3):151240. doi: 10.1016/j.ejcb.2022.151240

58. Alejandro EU, Bozadjieva N, Blandino-Rosano M, Wasan MA, Elghazi L, Vadrevu S, et al. Overexpression of kinase-dead mtor impairs glucose homeostasis by regulating insulin secretion and not beta-cell mass. *Diabetes* (2017) 66(8):2150–62. doi: 10.2337/db16-1349

59. Wang J, Yang X, Zhang J. Bridges between mitochondrial oxidative stress, er stress and mtor signaling in pancreatic beta cells. *Cell Signal* (2016) 28(8):1099–104. doi: 10.1016/j.cellsig.2016.05.007

60. Riahi Y, Israeli T, Yeroslaviz R, Chimenez S, Avrahami D, Stolovich-Rain M, et al. Inhibition of Mtorc1 by er stress impairs neonatal beta-cell expansion and predisposes to diabetes in the akita mouse. *Elife* (2018) 7:e38472. doi: 10.7554/eLife.38472

61. Kageyama S, Saito T, Obata M, Koide RH, Ichimura Y, Komatsu M. Negative regulation of the Keap1-Nrf2 pathway by a P62/Sqstm1 splicing variant. *Mol Cell Biol* (2018) 38(7):e00642-17. doi: 10.1128/MCB.00642-17

62. Kushner JA, Ciemerych MA, Sicinska E, Wartschow LM, Teta M, Long SY, et al. Cyclins D2 and D1 are essential for postnatal pancreatic beta-cell growth. *Mol Cell Biol* (2005) 25(9):3752–62. doi: 10.1128/MCB.25.9.3752-3762.2005

63. Tschen SI, Zeng C, Field L, Dhawan S, Bhushan A, Georgia S. Cyclin D2 is sufficient to drive beta cell self-renewal and regeneration. *Cell Cycle* (2017) 16 (22):2183–91. doi: 10.1080/15384101.2017.1319999

64. Lakshmipathi J, Alvarez-Perez JC, Rosselot C, Casinelli GP, Stamateris RE, Rausell-Palamos F, et al. Pkczeta is essential for pancreatic beta-cell replication during insulin resistance by regulating mtor and cyclin-D2. *Diabetes* (2016) 65 (5):1283–96. doi: 10.2337/db15-1398

65. Stamateris RE, Sharma RB, Hollern DA, Alonso LC. Adaptive beta-cell proliferation increases early in high-fat feeding in mice, concurrent with metabolic changes, with induction of islet cyclin D2 expression. *Am J Physiol Endocrinol Metab* (2013) 305(1):E149–59. doi: 10.1152/ajpendo.00040.2013

66. Salazar-Petres ER, Sferruzzi-Perri AN. Pregnancy-induced changes in beta-cell function: What are the key players? *J Physiol* (2022) 600(5):1089–117. doi: 10.1113/JP281082

67. Aguayo-Mazzucato C, Koh A, El Khattabi I, Li WC, Toschi E, Jermendy A, et al. Mafa expression enhances glucose-responsive insulin secretion in neonatal rat beta cells. *Diabetologia* (2011) 54(3):583–93. doi: 10.1007/s00125-010-2026-z

68. Wang X, Sterr M, Ansarullah, Burtscher I, Bottcher A, Beckenbauer J, et al. Point mutations in the Pdx1 transactivation domain impair human beta-cell development and function. *Mol Metab* (2019) 24:80–97. doi: 10.1016/j.molmet.2019.03.006

69. Olson LK, Redmon JB, Towle HC, Robertson RP. Chronic exposure of hit cells to high glucose concentrations paradoxically decreases insulin gene transcription and alters binding of insulin gene regulatory protein. *J Clin Invest* (1993) 92(1):514–9. doi: 10.1172/JCI116596

70. Reimer MK, Ahren B. Altered beta-cell distribution of pdx-1 and glut-2 after a short-term challenge with a high-fat diet in C57bl/6j mice. *Diabetes* (2002) 51 Suppl 1:S138–43. doi: 10.2337/diabetes.51.2007.s138

71. Glavas MM, Hui Q, Tuduri E, Erener S, Kasteel NL, Johnson JD, et al. Early overnutrition reduces Pdx1 expression and induces beta cell failure in Swiss Webster mice. *Sci Rep* (2019) 9(1):3619. doi: 10.1038/s41598-019-39177-3

72. Bosma KJ, Andrei SR, Katz LS, Smith AA, Dunn JC, Ricciardi VF, et al. Pharmacological blockade of the Ep3 prostaglandin E2 receptor in the setting of type 2 diabetes enhances beta-cell proliferation and identity and relieves oxidative damage. *Mol Metab* (2021) 54:101347. doi: 10.1016/j.molmet.2021.101347

73. Kaneto H, Kajimoto Y, Miyagawa J, Matsuoka T, Fujitani Y, Umayahara Y, et al. Beneficial effects of antioxidants in diabetes: Possible protection of pancreatic beta-cells against glucose toxicity. *Diabetes* (1999) 48(12):2398–406. doi: 10.2337/diabetes.48.12.2398

74. Tanaka Y, Gleason CE, Tran PO, Harmon JS, Robertson RP. Prevention of glucose toxicity in hit-T15 cells and zucker diabetic fatty rats by antioxidants. *Proc Natl Acad Sci U.S.A.* (1999) 96(19):10857–62. doi: 10.1073/pnas.96.19.10857

75. Wang XD, Vatamaniuk MZ, Wang SK, Roneker CA, Simmons RA, Lei XG. Molecular mechanisms for hyperinsulinaemia induced by overproduction of selenium-dependent glutathione peroxidase-1 in mice. *Diabetologia* (2008) 51 (8):1515–24. doi: 10.1007/s00125-008-1055-3

76. Kawamori D, Kaneto H, Nakatani Y, Matsuoka TA, Matsuhisa M, Hori M, et al. The forkhead transcription factor Foxo1 bridges the jnk pathway and the transcription factor pdx-1 through its intracellular translocation. *J Biol Chem* (2006) 281(2):1091–8. doi: 10.1074/jbc.M508510200

77. Boucher MJ, Selander L, Carlsson L, Edlund H. Phosphorylation marks Ipf1/Pdx1 protein for degradation by glycogen synthase kinase 3-dependent mechanisms. *J Biol Chem* (2006) 281(10):6395–403. doi: 10.1074/jbc.M511597200

78. Park KG, Lee KM, Seo HY, Suh JH, Kim HS, Wang L, et al. Glucotoxicity in the ins-1 rat insulinoma cell line is mediated by the orphan nuclear receptor small heterodimer partner. *Diabetes* (2007) 56(2):431–7. doi: 10.2337/db06-0753

79. Yang BT, Dayeh TA, Volkov PA, Kirkpatrick CL, Malmgren S, Jing X, et al. Increased DNA methylation and decreased expression of pdx-1 in pancreatic islets from patients with type 2 diabetes. *Mol Endocrinol* (2012) 26(7):1203–12. doi: 10.1210/me.2012-1004

80. Ruiz L, Gurlo T, Ravier MA, Wojtusciszyn A, Mathieu J, Brown MR, et al. Proteasomal degradation of the histone acetyl transferase P300 contributes to beta-cell injury in a diabetes environment. *Cell Death Dis* (2018) 9(6):600. doi: 10.1038/s41419-018-0603-0

81. Zhang M, Yang C, Zhu M, Qian L, Luo Y, Cheng H, et al. Saturated fatty acids entrap Pdx1 in stress granules and impede islet beta cell function. *Diabetologia* (2021) 64(5):1144–57. doi: 10.1007/s00125-021-05389-4

82. Noh JR, Hwang JH, Kim YH, Kim KS, Gang GT, Kim SW, et al. The orphan nuclear receptor small heterodimer partner negatively regulates pancreatic beta cell survival and hyperglycemia in multiple low-dose streptozotocin-induced type 1 diabetic mice. *Int J Biochem Cell Biol* (2013) 45(8):1538–45. doi: 10.1016/j.biocel.2013.05.004

83. Davidson RK, Weaver SA, Casey N, Kanojia S, Hogarth E, Schneider Aguirre R, et al. The Chd4 subunit of the nurd complex regulates Pdx1-controlled genes involved in beta-cell function. *J Mol Endocrinol* (2022) 69 (2):329–41. doi: 10.1530/JME-22-0011

84. Seo HY, Kim YD, Lee KM, Min AK, Kim MK, Kim HS, et al. Endoplasmic reticulum stress-induced activation of activating transcription factor 6 decreases insulin gene expression *Via* up-regulation of orphan nuclear receptor small heterodimer partner. *Endocrinology* (2008) 149(8):3832–41. doi: 10.1210/en.2008-0015

85. Yang W, Chi Y, Meng Y, Chen Z, Xiang R, Yan H, et al. Fam3a plays crucial roles in controlling Pdx1 and insulin expressions in pancreatic beta cells. *FASEB J* (2020) 34(3):3915–31. doi: 10.1096/fj.201902368RR

86. Akerman I, Tu Z, Beucher A, Rolando DMY, Sauty-Colace C, Benazra M, et al. Human pancreatic beta cell lncrnas control cell-specific regulatory networks. *Cell Metab* (2017) 25(2):400–11. doi: 10.1016/j.cmet.2016.11.016

87. McKenna B, Guo M, Reynolds A, Hara M, Stein R. Dynamic recruitment of functionally distinct Swi/Snf chromatin remodeling complexes modulates Pdx1 activity in islet beta cells. *Cell Rep* (2015) 10(12):2032–42. doi: 10.1016/j.celrep.2015.02.054

88. Kitamura YI, Kitamura T, Kruse JP, Raum JC, Stein R, Gu W, et al. Foxo1 protects against pancreatic beta cell failure through neurod and mafa induction. *Cell Metab* (2005) 2(3):153–63. doi: 10.1016/j.cmet.2005.08.004

89. Kitamura T, Nakae J, Kitamura Y, Kido Y, Biggs WH3rd, Wright CV, et al. The forkhead transcription factor Foxo1 links insulin signaling to Pdx1 regulation of pancreatic beta cell growth. *J Clin Invest* (2002) 110(12):1839–47. doi: 10.1172/JCI16857

90. Glauser DA, Schlegel W. The emerging role of foxo transcription factors in pancreatic beta cells. *J Endocrinol* (2007) 193(2):195–207. doi: 10.1677/JOE-06-0191

91. Kikuchi O, Kobayashi M, Amano K, Sasaki T, Kitazumi T, Kim HJ, et al. Foxo1 gain of function in the pancreas causes glucose intolerance, polycystic pancreas, and islet hypervascularization. *PloS One* (2012) 7(2):e32249. doi: 10.1371/journal.pone.0032249

92. Ohtsubo K, Chen MZ, Olefsky JM, Marth JD. Pathway to diabetes through attenuation of pancreatic beta cell glycosylation and glucose transport. *Nat Med* (2011) 17(9):1067–75. doi: 10.1038/nm.2414

93. Fernandez-Zapico ME, van Velkinburgh JC, Gutierrez-Aguilar R, Neve B, Froguel P, Urrutia R, et al. Mody7 gene, Klf11, is a novel P300-dependent regulator of pdx-1 (Mody4) transcription in pancreatic islet beta cells. *J Biol Chem* (2009) 284 (52):36482–90. doi: 10.1074/jbc.M109.028852

94. Neve B, Fernandez-Zapico ME, Ashkenazi-Katalan V, Dina C, Hamid YH, Joly E, et al. Role of transcription factor Klf11 and its diabetes-associated gene variants in pancreatic beta cell function. *Proc Natl Acad Sci U.S.A.* (2005) 102 (13):4807–12. doi: 10.1073/pnas.0409177102

95. Elsner M, Gehrmann W, Lenzen S. Peroxisome-generated hydrogen peroxide as important mediator of lipotoxicity in insulin-producing cells. *Diabetes* (2011) 60(1):200–8. doi: 10.2337/db09-1401

96. Elsharkawi I, Parambath D, Saber-Ayad M, Khan AA, El-Serafi AT. Exploring the effect of epigenetic modifiers on developing insulin-secreting cells. *Hum Cell* (2020) 33(1):1–9. doi: 10.1007/s13577-019-00292-y

97. Davidson RK, Kanojia S, Spaeth JM. The contribution of transcriptional coregulators in the maintenance of beta-cell function and identity. *Endocrinology* (2021) 162(2):bqaa213. doi: 10.1210/endocr/bqaa213

98. Spaeth JM, Liu JH, Peters D, Guo M, Osipovich AB, Mohammadi F, et al. The Pdx1-bound Swi/Snf chromatin remodeling complex regulates pancreatic progenitor cell proliferation and mature islet beta-cell function. *Diabetes* (2019) 68(9):1806–18. doi: 10.2337/db19-0349

99. Mosley AL, Corbett JA, Ozcan S. Glucose regulation of insulin gene expression requires the recruitment of P300 by the beta-Cell-Specific transcription factor pdx-1. *Mol Endocrinol* (2004) 18(9):2279–90. doi: 10.1210/me.2003-0463

100. Latif W, Lambrinos KJ, Rodriguez R. *Compare and contrast the glucagon-like peptide-1 receptor agonists (Glp1ras)*. Treasure Island (FL: Statpearls (2022).

101. Gao M, Deng XL, Liu ZH, Song HJ, Zheng J, Cui ZH, et al. Liraglutide protects beta-cell function by reversing histone modification of pdx-1 proximal promoter in catch-up growth Male rats. *J Diabetes Complications* (2018) 32 (11):985–94. doi: 10.1016/j.jdiacomp.2018.08.002

102. Pinney SE, Jaeckle Santos LJ, Han Y, Stoffers DA, Simmons RA. Exendin-4 increases histone acetylase activity and reverses epigenetic modifications that silence Pdx1 in the intrauterine growth retarded rat. *Diabetologia* (2011) 54 (10):2606–14. doi: 10.1007/s00125-011-2250-1

103. Wang X, Zhou J, Doyle ME, Egan JM. Glucagon-like peptide-1 causes pancreatic duodenal homeobox-1 protein translocation from the cytoplasm to the nucleus of pancreatic beta-cells by a cyclic adenosine Monophosphate/Protein kinase a-dependent mechanism. *Endocrinology* (2001) 142(5):1820–7. doi: 10.1210/endo.142.5.8128

104. Muscogiuri G, Salmon AB, Aguayo-Mazzucato C, Li M, Balas B, Guardado-Mendoza R, et al. Genetic disruption of Sod1 gene causes glucose intolerance and impairs beta-cell function. *Diabetes* (2013) 62(12):4201–7. doi: 10.2337/db13-0314

105. Uruno A, Furusawa Y, Yagishita Y, Fukutomi T, Muramatsu H, Negishi T, et al. The Keap1-Nrf2 system prevents onset of diabetes mellitus. *Mol Cell Biol* (2013) 33(15):2996–3010. doi: 10.1128/MCB.00225-13

106. Masuda Y, Vaziri ND, Li S, Le A, Hajighasemi-Ossareh M, Robles L, et al. The effect of Nrf2 pathway activation on human pancreatic islet cells. *PloS One* (2015) 10(6):e0131012. doi: 10.1371/journal.pone.0131012

107. Li S, Vaziri ND, Masuda Y, Hajighasemi-Ossareh M, Robles L, Le A, et al. Pharmacological activation of Nrf2 pathway improves pancreatic islet isolation and transplantation. *Cell Transplant* (2015) 24(11):2273–83. doi: 10.3727/096368915X686210

frontiers | Frontiers in Endocrinology

TYPE Original Research
PUBLISHED 12 October 2022
DOI 10.3389/fendo.2022.953631

OPEN ACCESS

EDITED BY
Carlos Guillén,
Complutense University, Spain

REVIEWED BY
Andrei I. Tarasov,
Ulster University, United Kingdom
Lili Ding,
Shanghai University of Traditional Chinese Medicine, China

*CORRESPONDENCE
Linong Ji
jiln@bjmu.edu.cn

†These authors have contributed equally to this work

‡These authors have contributed equally to this work

SPECIALTY SECTION
This article was submitted to Diabetes: Molecular Mechanisms, a section of the journal Frontiers in Endocrinology

RECEIVED 26 May 2022
ACCEPTED 04 August 2022
PUBLISHED 12 October 2022

CITATION
Li M, Gong S, Han X, Zhou L, Zhang S, Ren Q, Cai X, Luo Y, Liu W, Zhu Y, Zhou X, Li Y and Ji L (2022) Contribution of mitochondrial gene variants in diabetes and diabetic kidney disease.
Front. Endocrinol. 13:953631.
doi: 10.3389/fendo.2022.953631

Contribution of mitochondrial gene variants in diabetes and diabetic kidney disease

Meng Li[1†], Siqian Gong[1†], Xueyao Han[1‡], Lingli Zhou[1], Simin Zhang[1], Qian Ren[1], Xiaoling Cai[1], Yingying Luo[1], Wei Liu[1], Yu Zhu[1], Xianghai Zhou[1], Yufeng Li[2] and Linong Ji[1*‡]

[1]Department of Endocrinology and Metabolism, Peking University People's Hospital, Peking University Diabetes Center, Beijing, China, [2]Department of Endocrinology, Pinggu Teaching Hospital, Capital Medical University, Beijing, China

Objectives: Mitochondrial DNA (mtDNA) plays an important role in the pathogenesis of diabetes. Variants in mtDNA have been reported in diabetes, but studies on the whole mtDNA variants were limited. Our study aims to explore the association of whole mtDNA variants with diabetes and diabetic kidney disease (DKD).

Methods: The whole mitochondrial genome was screened by next-generation sequencing in cohort 1 consisting of 50 early-onset diabetes (EOD) patients with a maternally inherited diabetes (MID) family history. A total of 42 variants possibly associated with mitochondrial diseases were identified according to the filtering strategy. These variants were sequenced in cohort 2 consisting of 90 EOD patients with MID. The association between the clinical phenotype and these variants was analyzed. Then, these variants were genotyped in cohort 3 consisting of 1,571 type 2 diabetes mellitus patients and 496 subjects with normal glucose tolerance (NGT) to analyze the association between variants with diabetes and DKD.

Results: Patients with variants in the non-coding region had a higher percentage of obesity and levels of fasting insulin (62.1% vs. 24.6%, P = 0.001; 80.0% vs. 26.5% P < 0.001). The patients with the variants in rRNA had a higher prevalence of obesity (71.4% vs. 30.3%, P = 0.007), and the patients with the variants in mitochondrial complex I had a higher percentage of the upper tertile of FINS (64.3% vs. 34.3%, P = 0.049). Among 20 homogeneous variants successfully captured, two known variants (m.A3943G, m.A10005G) associated with other mitochondrial diseases were only in the diabetic group, but not in the NGT group, which perhaps indicated its possible association with diabetes. The prevalence of DKD was significantly higher in the group with the 20 variants than those without these variants (18.7% vs. 14.6%, P = 0.049) in the participants with diabetes of cohort 3.

10.3389/fendo.2022.953631

Conclusion: MtDNA variants are associated with MID and DKD, and our findings advance our understanding of mtDNA in diabetes and DKD. It will have important implications for the individual therapy of mitochondrial diabetes.

KEYWORDS

mitochondrial DNA, mitochondrial diabetes, diabetes, diabetic kidney disease, insulin resistance

1 Introduction

Mitochondrial diseases are a clinically heterogeneous cluster of inherited metabolic disease that could affect the function of the mitochondrial respiratory chain and oxidative phosphorylation system (1). Diabetes is the most well-described form of endocrine dysfunction in mitochondrial diseases. The mitochondrial genome is a maternally inherited 16,569-bp circular double-stranded DNA molecule that contains two ribosomal RNA genes, 22 transfer RNA (tRNA) genes, and 13 genes for the proteins of the oxidative phosphorylation system (2). Mitochondria are important for the synthesis of ATP and synthesis of the hormone. The mitochondrial DNA (mtDNA) variants possibly lead to the lack of ATP and impair hormone production when mitochondrial dysfunction occurs. In the process of insulin synthesis, mitochondria not only provide the necessary ATP for insulin exocytosis but also have a core function in glucose sensing and the induction of triggering and amplifying signals that adjust insulin secretion to glycaemia. Variants in the mitochondrial genomes are related to a cluster of metabolic diseases, including mitochondrial diabetes, insulin resistance (IR), non-alcoholic fatty liver disease (NAFLD), and metabolic syndrome (MetS) (3–6). Single mtDNA variants are associated with type 2 diabetes mellitus (T2DM). An mtDNA genome-wide association analysis indicated a potential role for mtDNA in diabetic kidney disease (DKD). As we know, the m.A3243G variant is the most common heteroplasmic mtDNA variant associated with mitochondrial diabetes. The m.A3243G variant reduced the synthesis of mtDNA-encoded proteins, which resulted in an imbalance within the mitochondrion between nuclear and mitochondrial encoded oxidative phosphorylation subunits (7, 8). Multisystemic disease manifestations can precede the onset of diabetes in patients with mitochondrial diseases (9). For example, sensorineural deafness and a family history of maternal inheritance should raise suspicion that the patient might have a mitochondrial disease. Other mtDNA variants associated with diabetes include point variants in the tRNA genes MT–TL1, MT–TK, MT–TS2, and MT–TE, as well as the variants in MT–ND6, which encodes the NADH-ubiquinone oxidoreductase chain 6 (10–12). Furthermore, IR also plays a key role in the development of T2DM and DKD. There is a clear evidence of an association between skeletal muscle IR and abnormalities in mitochondrial oxidative metabolism (13). However, most studies just focused on the association among single mtDNA loci and diabetes and DKD, and studies on the whole mtDNA gene with diabetes and DKD were limited. In addition, high-throughput sequencing could enhance the ability to identify mitochondrial respiratory chain complex deficiencies (14). Therefore, the study was designed as follows: to screen the whole mitochondrial gene variants in early-onset diabetes with the maternal family history using next-generation sequencing (NGS) and then to explore the mtDNA variants with diabetes and DKD. The study aims to help us elucidate novel insights into mitochondrial genetic etiology.

Abbreviations: mtDNA, mitochondrial DNA; NGS, next-generation sequencing; EOD, early-onset diabetes; MID, maternally inherited diabetes; DKD, diabetic kidney disease; tRNA, transfer RNA; IR, insulin resistance; NAFLD, non-alcoholic fatty liver disease; MetS, metabolic syndrome; FINS, fasting insulin; FPG, fasting plasma glucose; HOMA, homeostasis model assessment; HbA1c, hemoglobin A1c; LHON, Leber hereditary optic neuropathy.

2 Materials and methods

2.1 Study overview

This study was conducted in compliance with the Declaration of Helsinki. The study protocol was approved by the Ethics Committee of Peking University People's Hospital. Written informed consent was obtained from all the study participants. A flowchart of the study is shown in Figure 1. The study was divided into three groups (1): The whole mitochondrial genome was screened by NGS in cohort 1 consisting of 50 early-onset diabetes (EOD) patients. The variants possibly associated with mitochondrial diseases were identified according to the filtering strategy. (2) The above variants were sequenced in cohort 2 with 90 EOD patients, and the clinical phenotypic features of patients with potential pathogenic variants were analyzed. (3) Cohort 3 was a case–control study that included 1,571 patients with T2DM and 496

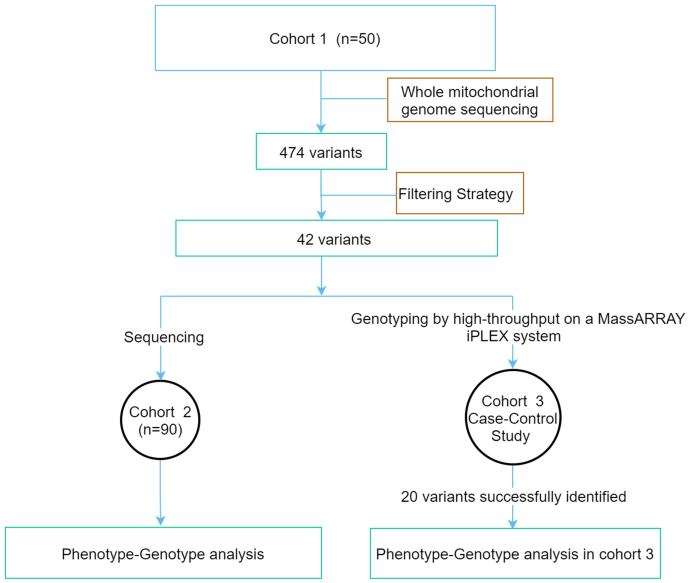

FIGURE 1
The flowchart of the study.

healthy individuals with normal glucose tolerance (NGT) to analyze the different features of the patients with variants and without these variants.

2.2 Screening of the mitochondrial gene in the patients with early-onset diabetes (cohort 1 and cohort 2)

Cohort 2 with 50 unrelated Chinese patients with EOD who had a maternally inherited diabetes (MID) family history were included from the inpatient and outpatient populations of the Department of Endocrinology and Metabolism at Peking University People's Hospital from January 2013 to December 2017. Then, 40 unrelated EOD patients with MID were recruited to identify the potential disease-associated variants. Cohort 2 included the above 90 patients. All the patients were of northern Han Chinese ancestry and residents of Beijing. They have been diagnosed with diabetes according to the 1999 World Health Organization criteria (15). The inclusion criteria for the EOD patients were as follows: (1) diagnosed with T2DM ≤40 years, (2) patients with the typical clinical features of type 1 diabetes or other specific forms of diabetes (e.g., chronic pancreatitis) and those who were positive for anti-glutamic acid decarboxylase antibodies, anti-islet cell antibodies were excluded, and (3) without the m. A3243G variant. The clinical information of 90 EOD patients was collected, including demographics, initial presentation, the treatment of diabetes, physical examination results, and laboratory test results, which are summarized at the time of enrollment in Table 1. The patients were diagnosed as being overweight or obese, based on the criteria: overweight was defined as a body mass index (BMI) ≥24 kg/m^2 and <28 kg/m^2, and obesity was defined as a BMI ≥28 kg/m^2. Coronary heart disease (CHD) was determined as a history of the disease. Cerebrovascular disease was determined as a history of transient ischemic attack or ischemic or hemorrhagic stroke. Hypertension was determined as a systolic blood pressure ≥140 mmHg and/or diastolic blood pressure ≥90 mmHg or the current treatment of hypertension. Dyslipidemia was defined as total cholesterol ≥5.18 mmol/L, triglycerides ≥1.70 mmol/L, LDL-c ≥3.37 mmol/L, HDL-c1.3 mmol/L in women or HDL-c<1.04 mmol/L in men, or treatment with antihyperlipidemic agents (16). Diabetic kidney disease (DKD) was defined as having a urinary albumin-to-creatinine ratio ≥30 mg/g or an estimated glomerular filtration rate (eGFR) <60 ml/min/1.73 m^2. Patients diagnosed as having a urinary tract infection, other glomerular diseases, or gross hematuria were excluded. Homeostasis model assessment (HOMA) was used to evaluate β-cell function and insulin sensitivity. IR index (HOMA-IR) = [fasting insulin (Fins, mIU/L) × fasting plasma glucose (FPG,

TABLE 1 The clinical characteristics of the patients from cohort 1 and cohort 2.

Characteristics	cohort 1 (n=50)	cohort 2 (n=90)
Sex, male/female	35/15	59/31
Age, years	34.7 ± 8.4	35.3 ± 7.1
Age at diagnosis, years	29.9 ± 7.0	30.2 ± 6.0
Duration, years	3.5 (0.0, 7.0)	4.0 (1.0, 7.3)
BMI, kg/m^2	28.5 ± 4.5	26.9 ± 4.2
WC, cm		
Male	99.1 ± 11.9	94.8 ± 11.1
Female	92.1 ± 11.8	88.8 ± 10.0
SBP, mmHg	130 ± 17	126 ± 16
DBP, mmHg	84 ± 11	83 ± 11
Laboratory examination		
FPG, mmol/l	9.1 ± 3.2	8.7 ± 3.5
FINS, μU/ml	16.2 (9.9, 27.8)	12.5 (7.8, 21.5)
HbA1c, %	8.9 ± 1.9	8.5 ± 2.1
LDL, mmol/l	2.7 ± 0.9	2.8 ± 0.8
HDL, mmol/l		
Male	0.9 (0.8, 1.0)	0.9 (0.8, 1.0)
Female	1.0 (0.9, 1.1)	1.0 (0.9, 1.2)
TC, mmol/l	4.9 ± 1.2	4.7 ± 1.1
TG, mmol/l	2.1 (1.4, 4.2)	1.8 (1.2, 2.8)
UA, umol/l		
Male	393.2 ± 80.3	374.5 ± 82.2
Female	337.8 ± 75.2	328.0 ± 86.9
ALT, U/l	29.5 (19.5, 46.8)	24.0 (16.0, 40.0)
AST, U/l	22.5 (18.0, 32.5)	20.0 (16.0, 27.5)
CRE, μmol/l	66.8 ± 28.1	63.7 ± 23.3
eGFR, ml/min/1.73 m^2	167.9 ± 54.9	158.7 ± 46.8
ACR, mg/g	74.5 (9.7, 190.8)	17.8 (3.0, 93.8)
DKD (n, %)	35 (70.0)	40 (44.4)
DR (n, %)	12 (24.0)	17 (18.9)
Family history of MID (n, %)	50 (100.0)	90 (100.0)

BMI, body mass index; WC, waist circumference; SBP, systolic blood pressure; DBP, diastolic blood pressure; FPG, fasting plasmatic glucose; FINS, fasting insulin; HbA1c, hemoglobin A1c; LDL, low-density lipoprotein; HDL, high-density lipoprotein; TC, total cholesterol; TG, triacylglycerol; UA, uric acid; CRE, creatinine; eGFR, estimated glomerular filtration rate; ACR, albumin-to-creatinine ratio; DKD, diabetic kidney disease; DR, diabetic retinopathy; MID, maternal inherited diabetes.
Values are means ± SDs, and medians (interquartile range) were for non-normally distributed data.

mmol/L)]/22.5, and β-cell function (HOMA-β) = [Fins (mIU/L) × 20]/[FPG (mmol/L) — 3.5] (17). When assessing the levels of HOMA-IR and HOMA-β, we excluded patients who were using insulin. MetS was assessed based on the International Diabetes Federation (IDF 2005) criteria: the diagnosis of central obesity (WC ≥ 90 cm in men or ≥ 80 cm in women), plus any two of the following four factors: (1) TG levels ≥ 1.7 mmol/L, (2) HDL-C < 1.03 mmol/L in men or < 1.29 mmol/L in women, (3) SBP ≥ 130 mmHg or DBP ≥ 85 mmHg or previous diagnosis with hypertension, (4) FBG ≥ 5.6 mmol/L, or previous diagnosis with type 2 diabetes mellitus (18).

2.3 The methods for screening the mitochondrial gene in cohort 1 and cohort 2

DNA was extracted from peripheral blood using standard procedures. The whole mitochondrial DNA of 50 patients in cohort 1 was used with NGS. For them, the Agilent Sureselect XT2 capture chip was used for the mitochondrial gene (accession number: NC_012920.1). A HiSeq 2500 Sequencing System (Illumina, San Diego, CA, USA) was adopted for sequencing. Sequencing data were obtained with the target

region coverage (~100%) and the sequencing depth on target > 2,000. All rare variants of mtDNA were validated by Sanger sequencing.

2.4 Annotation and filtration of the mitochondrial DNA variants possibly associated with mitochondrial diseases

The criteria for selecting the mtDNA variants possibly associated with mitochondrial diseases from the NGS data were as follows: (1) variant frequency in the cohort 1 was <20%; (2) sequencing depth >400 ×; (3) we searched the variants in the MITOMAP database (https://www.mitomap.org/MITOMAP) and selected the mtDNA variants that were possibly disease related based on the database. (4) The potential disease-related variants were validated by Sanger sequencing.

2.5 Screening of potential disease-related variants from cohort 1 in cohort 2

The potential disease-related variants screened and identified from cohort 1 were verified in cohort 2 by Sanger sequencing. PCR amplification was performed using PCR Enzyme Mix. The 24 pairs of mitochondrial primers are shown in Supplementary Table 1. The conditions for the PCR were as follows: initial denaturation at 94°C for 1 min, followed by 35 cycles of denaturation at 94°C for 30 s, primer annealing for 45 s at 61°C, and primer extension at 72°C for 2 min. A final extension was at 72°C for 5 min. The direct sequencing of PCR products was purified using a gel extraction kit (Axygen, California, USA) and performed with the ABI 3730xl DNA sequencer (Applied Biosystems) (19).

2.6 The analysis of sequencing data from cohort 2

The sequencing data from cohort 2 were analyzed. The pathogenicity of these variants in the coding area and tRNA were evaluated by HmtVar (https://www.hmtvar.uniba.it/). The pathogenicity of non-synonymous CDS variants were classified into four categories: (1) polymorphic: disease score (DS) < 0.43, allele frequency (AF) > 0.003264; (2) likely polymorphic: DS < 0.43, AF ≤ 0.003264; (3) likely pathogenic: DS ≥ 0.43, AF > 0.003264; and (4) pathogenic: DS ≥ 0.43, AF ≤ 0.003264. The pathogenicity of tRNA variants was classified into four categories: (1) polymorphic: DS < 0.35, AF > 0.005020; (2) likely polymorphic: DS < 0.35, AF ≤ 0.005020; (3) likely pathogenic: DS ≥ 0.35, AF > 0.005020; (4) pathogenic: DS ≥ 0.35, AF ≤ 0.005020. The DS was evaluated according to the software of MutPred, Polyphen2, Panther, PhD SNP, and SNPs & GO.

2.7 Screening for the potential disease-related variants in the expanded samples (cohort 3)

2.7.1 The participants for the case–control study (cohort 3)

A total of 1,571 T2DM patients and 496 healthy individuals with NGT were also enrolled in the case–control study. The inclusion criteria for the control samples were as follows: normal glucose tolerance confirmed *via* a 75 g oral glucose tolerance test according to the 1999 World Health Organization criteria (15); at the age of over 40; and hemoglobin A1c (HbA1c) <6%. Their clinical features are also summarized in Table 2.

2.7.2 The methods for genotyping the mtDNA in cohort 3

The above selected mtDNA variants were screened in the case–control cohort (cohort 3) using high-throughput genotyping on a MassARRAY platform (Sequenom) to genotype the mtDNA variants. Duplicate DNA samples and wild genotypes confirmed by sequencing were simultaneously genotyped as quality controls.

2.8 Statistical analysis

Statistical tests were performed with the SPSS software 23.0 (Chicago, IL, USA). Continuous variables are presented as the means and standard deviations (means ± standard deviations) for normally distributed data or as medians (interquartile range) for non-normally distributed data. Categorical variables are presented as numbers and percentages. Student's *t*-tests, Fisher's exact tests, and chi-square tests were performed to compare the clinical difference. The Mann–Whitney rank-sum test was used to make comparisons for the non-normally distributed variable. When we analyzed the metabolic features between patients with 42 variants and without those variants in cohort 2 and cohort 3, the levels of FINS, HOMA-IR, and HOMA-β were grouped according to the tertiles. An ordered-classification chi-square test was used to compare the differences between groups. Logistic regression analysis was conducted to address the relation between variables. $P < 0.05$ was considered statistically significant.

TABLE 2 Characteristics of the subjects of type 2 diabetes or normal glucose tolerance in cohort 3.

Characteristic	Controlsn=496	Patients with DM n=1,571	P-value
Sex, male/female	248/248	898/673	0.005
Age, years	52.0 ± 8.6	52.6 ± 11.8	0.247
Duration, years	–	1.0 (0.1, 6.0)	–
BMI, kg/m^2	25.7 ± 3.3	25.8 ± 3.5	0.808
WC, cm			
Male	89.5 ± 8.9	92.8 ± 10.3	<0.001
Female	84.8 ± 9.3	87.8 ± 9.7	<0.001
SBP, mmHg	131 ± 17	129 ± 16	0.003
DBP, mmHg	86 ± 12	83 ± 13	<0.001
Hypertension	136 (27.5)	319 (50.9)	0.000
Dyslipidemia	387 (78.0)	734 (87.3)	0.000
Laboratory examination			
FPG, mmol/l	5.4 ± 0.4	8.7 ± 2.4	<0.001
FINS, μU/ml	7.1 (4.9, 10.2)	8.8 (5.9, 13.6)	<0.001
HbA1c, %	5.4 ± 0.3	8.2 ± 1.9	<0.001
LDL, mmol/l	2.9 ± 0.7	3.0 ± 0.9	0.085
HDL, mmol/l			
Male	1.1 ± 0.3	1.0 ± 0.3	0.005
Female	1.2 ± 0.2	1.2 ± 0.3	0.848
TC, mmol/l	4.9 ± 0.8	4.9 ± 1.3	0.467
TG, mmol/l	1.1 (0.7, 1.6)	1.7 (1.3, 2.5)	<0.001
UA, μmol/l	269 ± 74	327 ± 91	0.000
Male	307.0 ± 71.3	347.5 ± 89.9	<0.001
Female	231.7 ± 54.9	296.6 ± 82.9	<0.001
ALT, U/l	19.0 (14.3, 25.0)	22.0 (16.0, 35.0)	<0.001
AST, U/l	21.0 (18.0, 24.0)	1.7 (1.3, 2.5)	0931
CRE, μmol/l	61.9 ± 28.3	65.7 ± 18.8	0.003
eGFR, ml/min/1.73 m^2	129.3 ± 31.4	125.5 ± 37.5	0.063
HOMA-IR	1.7 (1.1, 2.4)	3.3 (2.1, 5.1)	<0.001

BMI, body mass index; WC, waist circumference; SBP, systolic blood pressure; DBP, diastolic blood pressure; FPG, fasting plasmatic glucose; FINS, fasting insulin; HbA1c, hemoglobin A1c; LDL, low-density lipoprotein; HDL, high-density lipoprotein; TC, total cholesterol; TG, triacylglycerol; UA, urine acid; CRE, creatinine; eGFR, estimated glomerular filtration rate; HOMA-IR, homeostasis model assessment insulin resistance index.
Values are means ± SDs or numbers of subjects (percentages), and medians (interquartile range) were for non-normally distributed data. Student's t-tests, and chi-square tests were performed to compare the clinical difference between two groups. The Mann–Whitney rank-sum test was used to make comparisons for the non-normally distributed variable.

3 Results

3.1 Characteristics of the study participants

The clinical characteristics of the enrolled participants are shown in Table 1. The whole mitochondrial genome was screened by NGS in cohort 1. In addition, the cohort 2 including 90 EOD patients was sequenced to analyze the variants possibly associated with metabolic diseases. The 90 patients had an MID family history, of which 59 (65.6%) were men and the average age at diagnosis was 30.2 ± 6.0 years. The mean BMI was 26.9 ± 4.2 kg/m^2, and the average HbA1c was 8.5 ± 2.1%. The clinical characteristic features of cohort 3 are shown in Table 2.

3.2 The analysis of mtDNA variants in the mitochondrial gene in cohort 1 and cohort 2

Through the whole mitochondrial genome sequencing of 50 patients with MID, the mean coverage of the target genes was above 95.0%, and the mean depth was above 400 ×. In total, 474 variants on mtDNA were identified, including 225 variants in the coding region and 249 variants in the non-coding region. Among the coding region, 150 synonymous variants, one non-sense variant, and 74 non-synonymous variants were identified. According to the filtering strategy in the method, 42 mtDNA variants are identified in Table 3. Then, these 42 mtDNA variants were screened in cohort 2, and the frequency of these variants in cohort 2 are displayed in Table 3. Among

TABLE 3 The rare mitochondrial DNA (mtDNA) variants from cohort 2 possibly associated with mitochondrial disease (n=42).

No.	Base change	Frequency in cohort 2	Amino acid change	hom/ het	Locus Type	Locus	Prediction	Associated disease	Reference
1	C150T	8 (8.9)	/	hom	MT-DLOOP	/	/	Longevity/cervical carcinoma/HPV infection risk	(20, 21)
2	T195C	4 (4.3)	/	hom	MT-DLOOP	/	/	BD-associated/melanoma	(22, 23)
3	A663G	4 (4.3)	/	hom	rRNA	MT-RNR1	/	Coronary atherosclerosis risk	(24)
4	A827G	2 (2.2)	/	hom	rRNA	MT-RNR1	/	Deaf	(25)
5	T1005C	4 (4.4)	/	hom	rRNA	MT-RNR1	/	Deaf	(26)
6	C1048T	2 (2.2)	/	hom	rRNA	MT-RNR1	/	Deaf	(27)
7	G1719A	1 (1.1)	/	hom	rRNA	MT-RNR2	/	Ischemic stroke	(28)
8	C2835T	1 (1.1)	/	hom	rRNA	MT-RNR2	/	Rett syndrome	(29, 30)
9	A3397G	2 (2.2)	Met31Val	hom	CDS	MT-ND1	Likely Polymorphic	AD, PD	(31–33)
10	T3398C	2 (2.2)	Met31Thr	hom	CDS	MT-ND1	Polymorphic	DM/GDM/possibly LVNC cardiomyopathy-associated	(34–36)
11	C3497T	2 (2.2)	Ala64Val	hom	CDS	MT-ND1	Likely Polymorphic	LHON	(33)
12	A3943G	1 (1.1)	Iie213Val	hom	CDS	MT-ND1	Likely Polymorphic	Aging	(37)
13	A4833G	4 (4.4)	Thr122Ala	hom	CDS	MT-ND2	Likely Pathogenic	DM; AD, PD	(38, 39)
14	A5466G	1 (1.1)	Thr333Ala	hom	CDS	MT-ND2	Likely Polymorphic	DM; deafness; cardiomyopathy	(40)
15	G7598A	1(1.1)	Ala5Thr	hom	CDS	MT-CO2	Polymorphic	Possible LHON helper variant; Deafness	(41, 42)
16	C8414T	9 (1.0)	Leu17Phe	hom	CDS	MT-ATP6	Likely Pathogenic	Longevity	(43)
17	C8794T	3 (3.3)	His90Tyr	hom	CDS	MT-ATP6	Polymorphic	Exercise endurance/coronary Atherosclerosis risk	(24, 44)
18	A10005G	1 (1.1)	/	hom	tRNA	MT-TG	Likely Polymorphic	Hearing loss	(45)
19	T10084C	1 (1.1)	Iie9Thr	hom	CDS	MT-ND3	Polymorphic	Mitochondrial encephalomyopathy	(46)
20	A10086G	1 (1.1)	Asn10Asp	hom	CDS	MT-ND3	Likely Pathogenic	Hypertensive end-stage renal disease	(47)
21	A11084G	1 (1.1)	Thr109Ala	hom	CDS	MT-ND4	Pathogenic	MELAS	(46)
22	T11204C	1 (1.1)	Phe149Leu	hom	CDS	MT-ND4	Likely Polymorphic	Head and neck cancer	(48)
23	A12026G	1 (1.1)	Ile423Val	hom	CDS	MT-ND4	Polymorphic	DM	(49)
24	G12192A	1 (1.1)	/	hom	tRNA	MT-TH	Likely Polymorphic	Cardiomyopathy; LHON; deaf	(50, 51)
25	T12338C	3 (3.3)	Met1Thr	hom	CDS	MT-ND5	Likely Pathogenic	Lebers optic atrophycardiomyopathy	(52–54)
26	A12361G	2 (2.2)	Thr9Ala	hom	CDS	MT-ND5	Polymorphic	Non-alcoholic fatty liver disease	(4)
27	T12811C	1 (1.1)	Tyr159His	hom	CDS	MT-ND5	Polymorphic	LHON	(55)

(Continued)

TABLE 3 Continued

No.	Base change	Frequency in cohort 2	Amino acid change	hom/ het	Locus Type	Locus	Prediction	Associated disease	Reference
28	G13135A	1 (1.1)	Ala267Thr	hom	CDS	MT-ND5	Polymorphic	HCM	(56)
29	G13708A	3 (3.3)	Ala458Thr	hom	CDS	MT-ND5	Polymorphic	LHON	(57)
30	T14502C	1 (1.1)	Ile58Val	hom	CDS	MT-ND6	Likely Polymorphic	LHON	(58)
31	T14674C	1 (1.1)	/	hom	tRNA	MT-TE	Pathogenic	Reversible COX deficiency myopathy	(59)
32	A14693G	3 (3.3)	/	hom	tRNA	MT-TE	Likely Polymorphic	MELAS; LHON; deaf	(60–62)
33	A14927G	1 (1.1)	Thr61Ala	hom	CDS	MT-CYB	Likely Polymorphic	Cardiomyopathy	(63)
34	A15218G	1 (1.1)	Thr158Ala	hom	CDS	MT-CYB	Likely Pathogenic	Possible LHON modulator; epilepsy, sensorineural hearing impairment or DM	(64, 65)
35	G15497A	1 (1.1)	Gly251Ser	hom	CDS	MT-CYB	Polymorphic	Obesity	(66)
36	G15927A	2 (2.2)	/	hom	tRNA	MT-TT	Likely Pathogenic	Deafness	(54)
37	A15951G	1 (1.1)	/	hom	tRNA	MT-TT	Polymorphic	LHON	(47, 67)
38	T16093C	4 (4.4)	/	hom	Regulatory Sequence	MT-DLOOP	/	Breast cancer	(68)
39	G16129A	7 (7.8)	/	hom	Regulatory Sequence	MT-DLOOP	/	Breast cancer	(68)
40	A16183C	2 (2.2)	/	het	Regulatory Sequence	MT-DLOOP	/	Breast cancer; hypertension	(68, 69)
41	C16192T	1 (1.1)	/	hom	Regulatory Sequence	MT-DLOOP	/	Malignant melanoma	(22)
42	A16300G	1 (1.1)	/	hom	Regulatory Sequence	MT-DLOOP	/	Head/neck tumor	(70)

Het, heterozygote; Hom, homozygote; BD, bipolar disorder; AD, Alzheimer disease; PD, Parkinson disease; DM, diabetes mellitus; GDM, gestational diabetes mellitus; LVNC, left ventricular non-compaction; LHON, Leber hereditary optic neuropathy; MELAS, mitochondrial encephalopathy lactic acidosis and stroke-like episodes; HCM, hypertrophic cardiomyopathy.

them, seven variants were located in the D-loop, four variants in MT-ND1, two variants in MT-ND2, one in MT-CO2, two in MT-ATP6, two variants in MT-ND3, three variants in MT-ND4, five variants in MT-ND5, and one variant in MT-ND6. In addition, three variants were in MT-CYB, and six variants in tRNA, and six variants were in rRNA. The above 42 variants were located in complex I, complex III, complex IV, complex V and a non-coding area (including ND6 and D-loop), tRNA, and rRNA.

Among the 42 mtDNA variants, five variants (m.T3398C, m.A4833G, m.A5466G, m.A12026G, m.A15218G) have been reported to be possibly associated with diabetes (Figure 2).

3.3 The comparison of metabolic features between patients with 42 variants and without those variants in cohort 2

Compared with the patients without 42 variants, the patients with these variants had higher levels of FINS and HOMA-IR with a significant difference [14.6 (10.0, 26.7) vs. 8.1 (5.8, 13.4), $P = 0.006$; 6.5 (3.2, 10.2) vs. 3.3 (1.8, 4.3), $P = 0.002$]. There was no difference between the two groups of BMI, waist circumference, and HbA1c. In addition, the prevalence of DKD was significantly higher in the group with the variants than those without the variants (48.4% vs. 20.0%, P = 0.001) in Table 4.

A total of 42 mtDNA variants were in different domains of mitochondria including complex I, complex III, complex IV, complex V, non-coding region, rRNA, and tRNA. Patients with variants in the non-coding region had a higher percentage of obesity and levels of FINS than those without these variants with significant difference (62.1% vs. 24.6%, P = 0.001; 80.0% vs. 26.5% P < 0.001). The patients with the variants in rRNA had a higher prevalence of obesity (71.4% vs. 30.3%, P = 0.007), and the patients with the variants in complex I had a higher level of FINS (64.3% vs. 34.3%, P = 0.049). There was no significant difference on the frequency of different BMIs and levels of FINS, HOMA-IR, and HOMA-β of the patients with variants in other domains of mitochondria in Tables 5, 6.

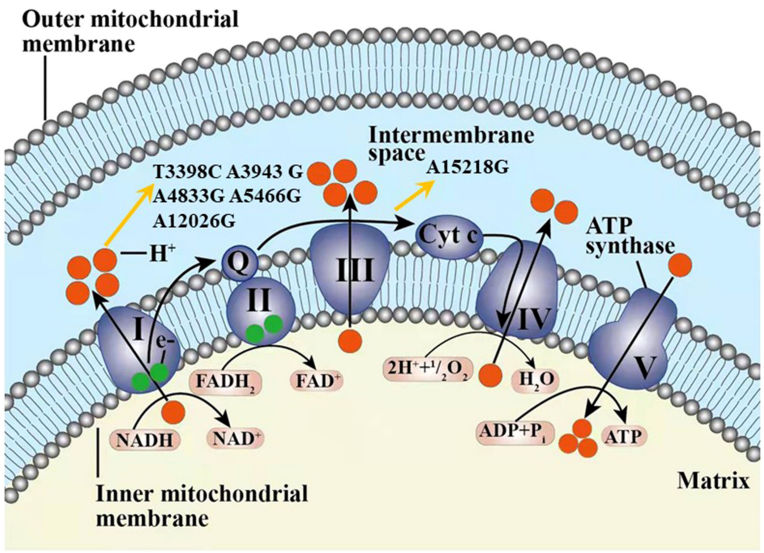

FIGURE 2
The six variants from cohort 2 and one variant from cohort 3 found in our study possibly associated with diabetes in our study displayed in the electron transport chain of mitochondria, including T3398C, A3943G, A4833G, A5466G, A12026G, and A15218G. The complexes I-V marked as I-V were included in the respiratory chain and oxidative phosphorylation system. Q, coenzyme Q10; Cyt c, cytochrome c; e-, electron.

3.4 The high-throughput genotyping results of mtDNA variants in cohort 3

In cohort 3, 42 mtDNA variants were screened using high-throughput genotyping, to investigate the phenotype and genotype of mtDNA variants. After the sequencing, 20 homogeneous variants associated with mitochondrial diseases were successfully captured and met the criteria of quality control in Table 7 and Figure 3. Excluding the variant of m.C3497T, there was no significant difference on the frequency of the mtDNA variants in the diabetic group and NGT group. We further enlarged 200 NGT subjects to screen the m.C3497T variant and found that there was no significant difference between the two groups.

Among the 20 homogeneous variants, two variants of m.A3943G (Figure 3) and m.A10005G were just found in the diabetic group and did not exist in the NGT group. The detailed clinical features are shown in Supplementary Table 2.

3.5 The comparison of metabolic features between patients with the 20 mtDNA variants and without those variants in diabetic patients from cohort 3

In the diabetic group, the levels of FINS, BMI, HOMA-IR, and HOMA-β were similar between the group with the 20 variants and those without the variants. The prevalence of MetS was similar in the two groups (56.8% vs. 57.2%, P = 0.886). The prevalence of DKD was significantly higher in the group with the variants than those without the variants (18.7% vs. 14.6%, P = 0.049) in Table 8.

We divided the patients into two groups: (1) without variants and (2) with one-to-three variants. In the logistic regression analysis, compared with the group without the variants, the OR of DKD for the group with one-to-three variants was 1.422 (95% CI: 1.055, 1.915, P = 0.021). After adjustments for age, the OR was 1.434 (95% CI: 1.061, 1.937, P = 0.019). In the adjusted model 3 that was further fitted with age and sex, the OR of DKD for the group with one-to-three variants was 1.433 (95% CI: 1.060, 1.936, P = 0.019).

The 20 mtDNA variants were in six domains of mitochondria including complex I, complex III, complex V, non-coding, rRNA, and rRNA. There was no significant difference of the prevalence of patients with normal BMI/overweight/obesity, FINS tertiles, HOMA-IR tertiles, and HOMA-β tertiles between patients with variants in these domains of mitochondria and without these variants in Supplementary Table 3 and Table 4.

4 Discussion

In our study, we analyzed whole mitochondrial DNA sequence variants in EOD with MID. We identified that seven variants, of which five variants were in complex I of mitochondrial, one variant in complex III, and one in tRNA

TABLE 4 Comparison of subjects with the 42 variants of mtDNA with the subjects without those variants in cohort 2.

Characteristics	without variants n=25	with variants n=65	P
Sex, male/female	13/12	47/28	0.067
Age, years	35.2 ± 6.4	35.4 ± 7.4	0.901
BMI, kg/m^2	25.5 ± 2.7	27.4 ± 4.5	0.060
WC, cm			
Male	93.0 ± 10.8	95.4 ± 11.2	0.505
Female	86.5 ± 5.5	90.1 ± 11.9	0.351
SBP, mmHg	115 ± 17	112 ± 26	0.690
DBP, mmHg	86 ± 11	86 ± 13	0.106
Hypertension, n (%)	13 (23.6)	15 (23.1)	0.942
MetS, n (%)	27 (49.1)	38 (58.5)	0.305
DR, n (%)	4 (16.7)	13 (21.0)	0.653
DKD, n (%)	11 (20.0)	31 (48.4)	0.001
FPG, mmol/l	8.2 ± 3.5	8.8 ± 3.5	0.464
FINS, μU/ml	8.1 (5.8, 13.4)	14.6 (10.0, 26.7)	0.006
HbA1c, %	8.4 ± 2.0	8.5 ± 2.1	0.872
LDL, mmol/l	3.0 ± 0.8	2.7 ± 0.8	0.133
HDL, mmol/l			
Male	0.9 ± 0.2	1.0 ± 0.3	0.486
Female	1.1 ± 0.2	1.0 ± 0.2	0.256
TC, mmol/l	5.0 ± 1.1	4.8 ± 0.9	0.368
TG, mmol/l	1.9 (1.0, 2.6)	1.8 (1.2, 3.3)	0.692
UA, μmol/l			
Male	377.8 ± 85.2	373.6 ± 82.3	0.873
Female	323.0 ± 105.0	331.4 ± 75.7	0.801
ALT, U/l	19.5 (12.5, 34.5)	25.0 (17.0, 29.5)	0.253
AST, U/l	18.0 (15.3, 24.8)	21.0 (17.0, 29.5)	0.093
CRE, μmol/l	57.1 ± 16.0	66.2 ± 25.2	0.096
eGFR, ml/min*1.73m^2	156.5 ± 37.5	159.5 ± 50.2	0.788
ACR, mg/g	7.9 (1.9, 65.2)	21.8 (3.0, 106.4)	0.077
HOMA-IR	3.3 (1.8, 4.3)	6.5 (3.2, 10.2)	0.002
HOMA-β	61.1 (24.0, 110.7)	72.8 (38.3, 120.6)	0.126

BMI, body mass index; WC, waist circumference; SBP, systolic blood pressure; DBP, diastolic blood pressure; MetS, metabolic syndrome; FPG, fasting plasmatic glucose; FINS, fasting insulin; HbA1c, hemoglobin A1c; LDL, low-density lipoprotein; HDL, high-density lipoprotein; TC, total cholesterol; TG, triacylglycerol; UA, uric acid; CRE, creatinine; eGFR, estimated glomerular filtration rate; ACR, albumin-to-creatinine ratio; DKD, diabetic kidney disease; DR, diabetic retinopathy. HOMA-IR, homeostasis model assessment insulin resistance index. HOMA-β, homeostasis model assessment β-cell function.
Values are means ± SDs or numbers of subjects (percentages), and medians (interquartile range) were for non-normally distributed data. Student's t-tests, and chi-square tests were performed to compare the clinical difference between two groups. The Mann–Whitney rank-sum test was used to make comparisons for the non-normally distributed variable.

from cohort 2 and cohort 3, were possibly diabetes associated. Patients with variants in the non-coding region had a higher percentage of obesity and levels of FINS. The patients with 20 homozygous variants had a significantly higher prevalence of DKD than those without these variants in diabetic patients. As we know, it was the first study to investigate the whole mtDNA sequence variants with diabetes and DKD in the Chinese population, and our study has provided a new insight into the mitochondrial genetic role in diabetes and its complication *via*.

Mitochondria are essential in energy metabolism and cellular survival and play a central role in numerous metabolic processes. IR plays a key role in the development of T2DM and DKD. Several abnormalities in mitochondrial oxidative metabolism, including the reduced content and size of mitochondria (11), impaired mitochondrial respiration, and reduced electron transport chain activity (11, 12, 17), as well as the transcriptional downregulation of genes involved in mitochondrial oxidative metabolism (13, 14, 19), have been associated with obesity, T2DM, and aging in human skeletal muscle. These alterations are collectively termed mitochondrial dysfunction and are often associated with an impaired insulin-mediated increase in transcript levels and ATP synthesis in the mitochondria of skeletal muscle in insulin-resistant individuals (9, 38). Skeletal muscle is essential for metabolism because of its role in glucose uptake and its importance in exercise. It plays an important role in peripheral IR (71). In our study of cohort 2, we

TABLE 5 Comparison of body mass index (BMI) and other traits among the patients with variants and without these variants in the complex I, III, IV, and V domains of mitochondria.

	Tertile/ Category	In Complex I		P-value	In Complex III		P-value	In Complex IV		P-value	In Complex V		P-value
		Without Variants	With variants		Without Variants	With variants		Without Variants	With variants		Without Variants	With variants	
BMI	normal	14/59 (23.7%)	7/31 (22.6%)	0.964	20/85 (23.5%)	1/5 (20.0%)	0.841	21/88 (23.9%)	0/2 (0.0%)	1.000	18/72 (25.0%)	3/18 (16.7%)	0.057
	overweight	23/59 (39.0%)	13/31 (41.9%)		33/85 (38.8%)	3/5 (60.0%)		35/88 (39.8%)	1/2 (50.0%)		32/72 (44.4%)	4/18 (22.2%)	
	obesity	22/59 (37.3%)	11/31 (35.5%)		32/85 (37.6%)	1/5 (20.0%)		32/88 (36.4%)	1/2 (50.0%)		22/72 (30.6%)	11/18 (61.1%)	
FINS*	T1	9/35 (25.7%)	0/14 (0.0%)	0.049	0/46 (0.0%)	0/3 (0.0%)	0.208	9/47 (19.1%)	0/2 (0.0%)	1.000	8/38 (21.1%)	1/11 (9.1%)	0.677
	T2	14/35 (40.0%)	5/14 (35.7%)		19/46 (41.3%)	0/3 (0.0%)		18/47 (38.3%)	1/2 (50.0%)		15/38 (39.5%)	4/11 (36.4%)	
	T3	12/35 (34.3%)	9/14 (64.3%)		18/46 (39.1%)	3/3 (100.0%)		20/47 (42.6%)	1/2 (50.0%)		15/38 (39.5%)	6/11 (54.5%)	
HOMA-IR*	T1	7/35 (20.0%)	0/13 (0.0%)	0.131	7/45 (15.6%)	0/3 (0.0%)	0.375	7/46 (15.2%)	0/2 (0.0%)	1.000	6/37 (16.2%)	1/11 (9.1%)	0.264
	T2	13/35 (37.1%)	4/13 (30.8%)		17/45 (37.8%)	0/3 (0.0%)		16/46 (34.8%)	1/2 (50.0%)		15/37 (40.5%)	2/11 (18.2%)	
	T3	15/35 (42.9%)	9/13 (69.2%)		21/45 (46.7%)	3/3 (100.0%)		23/46 (50.0%)	1/2 (50.0%)		16/37 (43.2%)	8/11 (72.7%)	
HOMA-β*	T1	17/35 (48.6%)	2/13 (15.4%)	0.101	18/45 (40.0%)	1/3 (33.3%)	1.000	19/46 (41.3%)	0/2 (0.0%)	0.512	13/37 (35.1%)	6/11 (54.5%)	0.125
	T2	8/35 (22.9%)	5/13 (38.5%)		12/45 (26.7%)	1/3 (33.3%)		12/46 (26.1%)	1/2 (50.0%)		9/37 (24.3%)	4/11 (36.4%)	
	T3	10/35 (28.6%)	6/13 (46.2%)		15/45 (33.3%)	1/3 (33.3%)		15/46 (32.6%)	1/2 (50.0%)		15/37 (40.5%)	1/11 (9.1%)	

BMI, body mass index; FINS, fasting insulin; HOMA-IR, homeostasis model assessment insulin resistance index; HOMA-β, homeostasis model assessment β-cell function; T, tertile. T1–3 were grouped according to tertile category of FINS, HOMA-IR. Ordered classification chi-square test was used to compare the differences between groups. When we analyzed the difference of FINS and HOMA-IR, patients using insulin were excluded. * means that the subjects who were treated with insulin were excluded. A P-value <0.05 was considered significant.

TABLE 6 Comparison of BMI and other traits among the patients with variants and without these variants in the non-coding region, transfer RNA, and rRNA of mitochondria.

	Tertile/Category	In non-coding		P-value	In rRNA		P-value	In tRNA		P-value
		Without variants	With Variants		Without variants	With Variant		Without variants	With Variants	
BMI	normal	15/61 (24.6%)	6/29 (20.7%)	0.001	18/76 (23.7%)	3/14 (21.4%)	0.007	19/79 (24.1%)	2/11 (18.2%)	0.799
	overweight	31/61 (50.8%)	5/29 (17.2%)		35/76 (46.1%)	1/14 (7.1%)		32/79 (40.5%)	4/11 (36.4%)	
	obesity	15/61 (24.6%)	18/29 (62.1%)		23/76 (30.3%)	10/14 (71.4%)		28/79 (35.4%)	5/11 (45.5%)	
FINS*	T1	6/34 (17.6%)	3/15 (20.0%)	<0.001	8/39 (20.5%)	1/10 (10.0%)	0.522	8/42 (19.0%)	1/7 (14.3%)	0.317
	T2	19/34 (55.9%)	0/15 (0.0%)		16/39 (41.0%)	3/10 (30.0%)		18/42 (42.9%)	1/7 (14.3%)	
	T3	9/34 (26.5%)	12/15 (80.0%)		15/39 (38.5%)	6/10 (60.0%)		16/42 (38.1%)	5/7 (71.4%)	
HOMA-IR*	T1	5/33 (15.2%)	2/15 (13.3%)	0.064	7/38 (18.4%)	0/10 (0.0%)	0.272	6/41 (14.6%)	1/7 (14.3%)	0.056
	T2	15/33 (45.5%)	2/15 13.3%		14/38 (36.8%)	3/10 (30.0%)		17/41 (41.5%)	0/7 (0.0%)	
	T3	13/33 (39.4%)	11/15 73.3%		17/38 (44.7%)	7/10 (70.0%)		18/41 (43.9%)	6/7 (85.7%)	
HOMA-β*	T1	17/38 (44.7%)	2/10 (20.0%)	0.364	17/38 (44.7%)	2/10 (20.0%)	0.364	16/41 (39.0%)	3/7 (42.9%)	1.000
	T2	9/38 (23.7%)	4/10 (40.0%)		9/38 (23.7%)	4/10 (40.0%)		11/41 (26.8%)	2/7 (28.6%)	
	T3	12/38 (31.6%)	4/10 (40.0%)		12/38 (31.6%)	4/10 (40.0%)		14/41 (34.1%)	2/7 (28.6%)	

BMI, body mass index; FINS, fasting insulin; HOMA-IR, homeostasis model assessment insulin resistance index; HOMA-β, homeostasis model assessment β-cell function; T, tertile.

TABLE 7 The analysis of 20 mtDNA variants in the case–control study from cohort 3.

No.	Variant	Position	Neurodisease	Amino change	Locus type	Locus	Prediction	Genotype distribution		MAF %		P-value *	Adjusted OR (95% CI) *
								NGT group	No. of diabetic patients of variant genotype/wild genotype	No. of NGT group of variant genotype/wild genotype	DM group		
1	C1048T	1048	No	–	rRNA	MT-RNR1	Unavailable	31/1,499	3/449	2	0.7	0.063	3.095 (0.942,10.172)
2	G1719A	1719	No	–	rRNA	MT-RNR1	Unavailable	22/1,517	10/474	1.4	2.1	0.330	0.687 (0.323, 1.462)
3	A3397G	3397	Yes	Met31Val	CDS	MT-ND1	Likely Polymorphic	14/1,492	1/494	0.9	0.2	0.139	4.635 (0.608, 35.340)
4	C3497T	3497	Yes	Ala64Val	CDS	MT-ND1	Likely Polymorphic	34/1,530	19/474	2.2	3.9	0.043	0.554 (0.313-0.981)
5	A3943G	3943	No	Iie213Val	CDS	MT-ND1	Likely Polymorphic	1/1,567	0/495	0.06	0	1.000	–
6	A5466G	5466	No	Thr333Ala	CDS	MT-ND2	Likely Polymorphic	12/1,555	1/495	0.8	0.2	0.198	3.820 (0.495, 29.451)
7	G7598A	7598	Yes	Ala-5Thr	CDS	MT-CO2	Polymorphic	8/1,539	1/493	0.5	0.2	0.376	2.563 (0.320, 20.540)
8	C8794T	8794	No	His-90Tyr	CDS	MT-ATP6	Polymorphic	117/1,445	41/452	7.5	8.3	0.549	0.893 (0.616, 1.294)
9	A10005G	10005	No	–	tRNA	MT-TG	Likely Polymorphic	1/1,514	0/493	0.1	0	1.000	–
10	A10086G	10086	No	Asn10Asp	CDS	MT-ND3	Likely Pathogenic	1/1,537	2/492	0.1	0.4	0.135	0.160 (0.014, 1.769)
11	A11084G	11084	Yes	Thr109Ala	CDS	MT-ND4	Pathogenic	12/1,499	9/483	0.8	1.8	0.073	0.449 (0.187,1.078)
12	T11204C	11204	No	Phe149Leu	CDS	MT-ND4	Likely Polymorphic	5/1,540	4/491	0.3	0.8	0.172	0.399 (0.107, 1.490)
13	G12192A	12192	No	–	tRNA	MT-TH	Likely Polymorphic	4/1,553	4/492	0.3	0.8	0.105	0.317 (0.079, 1,271)
14	T12338C	12338	Yes	Met1Thr	CDS	MT-ND5	Likely Pathogenic	70/1,400	21/472	4.8	4.3	0.646	1.124 (0.683, 1.850)
15	A12361G	12361	No	Thr9Ala	CDS	MT-ND5	Polymorphic	58/1,507	13/481	3.7	2.6	0.256	1.424 (0.774, 2.621)
16	T14502C	14502	Yes	Iie58Val	CDS	MT-ND6	Likely Polymorphic	30/1,506	6/489	2	1.2	0.282	1.624 (0.672, 3.924)

(Continued)

10.3389/fendo.2022.953631

TABLE 7 Continued

No.	Variant	Position	Neurodisease	Amino change	Locus type	Locus	Prediction	Genotype distribution		MAF %		P-value *	Adjusted OR (95% CI) *
								NGT group	No. of diabetic patients of variant genotype/wild genotype	No. of NGT group of variant genotype/wild genotype	DM group		
17	A14693G	14693	Yes	–	tRNA	MT-TE	Likely Polymorphic	18/1,545	6/490	1.2	1.2	0.916	0.951 (0.376, 2.410)
18	A14927G	14927	No	Thr61Ala	CDS	MT-CYB	Likely Polymorphic	20/1,545	7/489	1.3	1.4	0.820	0.904 (0.380, 2.151)
19	A15218G	15218	Yes	Thr158Ala	CDS	MT-CYB	Likely Pathogenic	26/1,513	7/486	1.7	1.4	0.681	1.193 (0.515, 2.766)
20	A15951G	15951	Yes	–	tRNA	MT-TT	Polymorphic	16/1,526	6/489	1	1.2	0.744	1.170 (0.455, 3.007)

NGT, normal glucose tolerance; MAF, major allele frequency.
Logistic regression analysis was used to compare the prevalence of mtDNA variants in diabetic patients and the subjects with normal glucose tolerance. *means that the results were analyzed by logistic regression with no adjustment.

10.3389/fendo.2022.953631

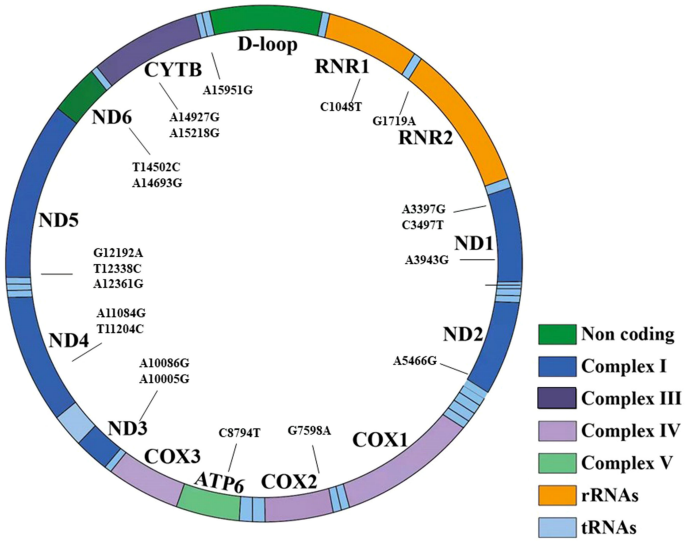

FIGURE 3
The 20 variants have been shown in the structure of the mitochondrial genes and different domains. It included seven regions: non-coding region, complex I, complex III, complex IV, complex V, transfer RNA, and rRNA.

found that 42 rare variants were associated with IR. In addition, patients with variants in the non-coding region had a higher percentage of obesity and higher FINS. These variants were in the D-loop region, and previously, variants in the D-loop have been shown to be associated with breast cancer and other tumors (22, 68–70). The D-loop is the main regulation region of mitochondrial transcription (72). In addition, variants in the 12S rRNA gene were found to have a higher percentage of obesity. These variants in the 12S rRNA gene have been reported to be associated with a coronary atherosclerosis risk, deafness, and ischemic stroke (24–28). These data strongly indicate that the D-loop region and 12S rRNA may be associated with obesity. After enlarging the sample size, we found that there was an association of mitochondrial variants with DKD. The levels of FINS and HOMA-IR had an upward trend in the group with 20 variants, although there was no significant statistical difference. This may be related to the heteroplasmy of mitochondria and the loss of information by high-throughput sequencing.

Mitochondrial respiratory Complex I plays an important role in the process of ATP synthesis, which is the rate-limiting enzyme in electron transport chain (ETC) (73, 74). Current evidence suggests that the defects in complex I may be associated with metabolic diseases, including diabetes, IR, and NAFLD (3–5). In addition, complex I is also a major source of reactive oxygen species (ROS) in mitochondria (75), which has been implicated in the pathology of Parkinson disease (76) and ageing (77). Previous studies have demonstrated that the pivotal role of the ND6 epigenetic network could regulate mitochondrial function and affect IR (5). It indicated that the function of complex I may be associated with IR. Five of the above seven mtDNA variants were found in complex I in our study, which were previously reported in patients with diabetes (34, 38, 40, 78). It may be due to the influence on the structure and the function of complex I, leading to IR and defecting the function of islets; thereby, these were considered to be possibly diabetes and DKD associated.

m.A10005G was previously reported to be possibly associated with hearing loss (45). m.A10005G is located in the D-loop and had a crucial role in tRNA recognition by cognate aminoacyl-tRNA synthetases (79). Another variant was the m.A15218G variant in MT-CYB. Previous research associated m.A15218G with epilepsy, diabetes, and Leber hereditary optic neuropathy (LHON) (78, 80). This variant led to the substitution of a conserved hydrophilic threonine by a hydrophobic alanine at position 159 of the cytochrome b subunit of complex III. In addition, the position was highly conservative (81). The cytochrome b subunit of complex III formed the catalytic core (82). The evolutionary conservation of the amino acid position, results from the prediction algorithms, and the homoplasic nature of the variant suggest that m.A15218G is mildly deleterious (64).

Current studies have shown that increased ROS was associated with diabetic kidney injury (83). Hyperglycemia would stimulate an increase in aerobic glycolysis with the resultant increase in substrate delivery to the mitochondria and a subsequent increase in mitochondrial activity (84). Increased tricarboxylic acid cycle (TCA) activity would produce more NADH and FADH2, which would then be used

TABLE 8 The comparison of the subjects without the 20 variants and with the 20 variants in normal glucose tolerance and diabetes mellitus groups from cohort 3.

Characteristics	NGT (n=496)			DM (n=1,571)		
	without variantsn=364	with variantsn=132	p	without variantsn=1,159	with variantsn=412	p
Sex, male/female	173/191	75/57	0.067	657/502	241/171	0.524
Age, years	52.1 ± 8.9	51.5 ± 8.0	0.468	52.6 ± 11.8	52.6 ± 11.8	0.980
BMI, kg/m^2	25.6 ± 3.3	26.1 ± 3.1	0.139	25.8 ± 3.5	25.7 ± 3.5	0.647
WC, cm						
Male	88.4 ± 8.3	91.2 ± 9.0	0.015	91.9 ± 10.0	92.0 ± 10.5	0.955
Female	84.6 ± 9.0	86.7 ± 8.4	0.12	89.4 ± 7.7	89.6 ± 8.7	0.957
SBP, mmHg	131 ± 16	131 ± 18	0.888	129 ± 16	128 ± 16	0.173
DBP, mmHg	86 ± 11	86 ± 12	0.747	84 ± 13	84 ± 14	0.288
CHD, n (%)	0 (0)	0 (0)	–	30 (2.6)	16 (3.9)	0.281
CBD, n (%)	0 (0)	0 (0)	–	24 (3)	17 (3)	0.180
Hypertension, n (%)	102 (28.0)	34 (25.0)	0.617	225 (19.4)	94 (22.8)	0.140
Dyslipidemia, n (%)	112 (30.8)	28 (21.2)	0.622	718 (61.9)	226 (54.9)	0.164
MetS, n (%)	128 (56.1)	58 (31.2)	0.074	663 (57.2)	234 (56.8)	0.886
DR, n (%)	–	–	–	332 (28.6)	113 (27.4)	0.797
DKD, n (%)	–	–	–	169 (14.6)	77 (18.7)	0.049
FPG, mmol/l	5.4 ± 0.4	5.4 ± 0.4	0.787	8.7 ± 2.4	8.8 ± 2.4	0.231
FINS, μU/ml	6.9 (4.8,9.8)	7.8 (4.9,11.2)	0.068	8.6 (5.8,13.5)	9.0 (5.8,13.7)	0.635
HbA1c, %	5.4 ± 0.3	5.4 ± 0.3	0.548	8.1 ± 1.9	8.2 ± 1.9	0.203
TC, mmol/l	4.9 ± 0.8	4.9 ± 0.8	0.954	5.0 ± 1.3	4.8 ± 1.1	0.001
HDL, mmol/l						
Male	1.1 ± 0.3	1.1 ± 0.2	0.5	1.0 ± 0.3	1.0 ± 0.3	0.364
Female	1.2 ± 0.2	1.2 ± 0.3	0.498	1.2 ± 0.3	1.28 ± 0.3	0.79
LDL, mmol/l	2.9 ± 0.7	2.9 ± 0.7	0.511	3.0 ± 0.9	2.9 ± 0.9	0.147
TG, mmol/l	1.0 (0.7,1.6)	1.1 (0.8,1.6)	0.221	1.8 (1.3,2.6)	1.7 (1.2,2.4)	0.119
UA, μmol/l						
Male	304.6 ± 73.8	312.4 ± 65.4	0.430	345.1 ± 91.8	353.8 ± 84.8	0.333
Female	231.9 ± 56.0	231.1 ± 51.2	0.925	290.4 ± 81.6	309.1 ± 85.4	0.07
ALT, U/l	18.0 (14.0, 24.0)	19.0 (15.0, 25.8)	0.178	22.0 (16.0, 35.0)	22.0 (15.8, 35.0)	0.570
AST, U/l	20.0 (18.0, 24.0)	21.0 (18.0, 25.0)	0.979	21.0 (17.0, 27.0)	20.0 (16.0, 28.0)	0.422
CRE, μmol/l	62.0 ± 32.0	61.7 ± 14.1	0.911	65.9 ± 19.0	65.3 ± 18.4	0.658
eGFR, ml/min*1.73 m^2	129.3 ± 32.1	129.2 ± 29.7	0.961	125.1 ± 37.6	126.7 ± 37.1	0.598
ACR, mg/g	5.1 (1.8,12.0)	4.8 (2.1,11.4)	0.992	10.0 (3.5,47.9)	13.3 (4.3,54.4)	0.214
HOMA-IR	1.6 (1.1,2.4)	1.9 (1.2,2.8)	0.084	3.3 (2.1,5.0)	3.3 (2.1,5.4)	0.254
HOMA-β	75.4 (52.7,110.2)	89.3 (53.0,117.9)	0.107	37.6 (21.7,67.4)	37.4 (21.1,66.7)	0.643

NGT, normal glucose tolerance; DM, diabetes mellitus; BMI, body mass index; WC, waist circumference; SBP, systolic blood pressure; DBP, diastolic blood pressure; CHD, coronary heart disease; CBD, cerebrovascular disease; DR, diabetic retinopathy; DKD, diabetic kidney disease; FPG, fasting plasma glucose; FINS, fasting insulin; HbA1c, hemoglobin A1c; TC, total cholesterol; HDL-C, high-density lipoprotein cholesterol; LDL-C, low-density lipoprotein cholesterol; TG, triglycerides; UA, uric acid; eGFR, estimated glomerular filtration rate; CRE, creatinine; ACR, albumin-to-creatinine ratio; HOMA-IR, homeostasis model assessment estimated insulin resistance; HOMA-β, homeostasis model assessment β function.
Values are means ± SDs or numbers of subjects (percentages), and medians (interquartile range) were for non-normally distributed data. Student's t-tests and chi-square tests were performed to compare the clinical difference between two groups. The Mann–Whitney rank-sum test was used to make comparisons for the non-normally distributed variable.

in the ETC in the mitochondria. The above evidence may partly explain the reason why the mtDNA variation could lead to DKD. The variety of mtDNA variants could alternate the structure of mitochondria and affect different aspects of mitochondrial function, thereby causing diabetes and DKD.

Diabetes due to mtDNA variants requires individualized treatment. Metformin is not recommended in the case of mitochondrial diabetes because it was shown to cause lactic acidosis. SGLT-2i could lead to lower blood sugar and body weight; reduced cardiovascular events risks; and the improvement of the inflammation status, liver steatosis, and uric acid concentrations (85). GLP-1 Ras also had the protective effect on the cardiovascular system. Since mtDNA variants are known to elevate the level of ROS, they are especially dangerous for the cardiovascular system, where they can cause cardiomyopathy, atherosclerosis, and hypertension. Diabetic patients with

identified mtDNA variants are considered a high-risk group for cardiovascular diseases. Therefore, the cardioprotective effects of SGLT-2i, GLP-1 RA, and related substances have significant benefits in comparison to alternative treatments (86). In addition, we also need to pay attention to new strategies aimed at restoring complex I activity, reducing oxidative stress in alleviating IR, and the treatment of diabetes.

There are also three limitations in our study. First, the software we used was aimed to evaluate the coding variants and tRNA, and the variants in rRNA were unavailable. The pathogenicity of these variants is needed to be further investigated. Secondly, the sample size to evaluate the potential disease-associated variants was limited; thus, a larger sample size of population is needed to further investigate the variants in the mitochondrial diabetes and DKD for future studies. Thirdly, the exact mechanism of the potential disease-associated variants that possibly cause disease is further needed for the research *in vivo* and *in vitro* studies.

5 Conclusions

In our study, we found that seven variants in mitochondrial complex I, D-loop, and complex I were possibly associated with diabetes and 20 mtDNA variants may be associated with a higher risk of DKD. Although it has been proposed that the variants might impair the function of mitochondrial complex I and elevate the levels of ROS, the molecular mechanism linking diabetes and DKD is further needed to be investigated. Prospective and larger-scale studies are needed to establish the clinical relevance of this association.

Data availability statement

The datasets presented in this article are not readily available due to ethical restrictions. Requests to access the datasets should be directed to the corresponding author.

Ethics statement

The studies involving human participants were approved by the Ethics Committee of Peking University People's Hospital. The patients/participants provided their written informed consent to participate in this study.

Author contributions

ML conducted this study, collected and explored the data, and completed the original manuscript. LJ contributed to the study design, critically revised the manuscript, and obtained the funding. XH also contributed to the study design and critically revised the manuscript. SG contributed to the sample collection and analysis of the data and reviewed the manuscript. LZ, SZ, QR, XC, YYL, WL, YZ, XZ, and YFL contributed to the data and sample collection and reviewed the manuscript. All authors read the final manuscript and approved final submission.

Funding

This research was supported by grants from National Key Research and Development Program of China (2016YFC1304901), Beijing Municipal Science and Technology Committee Funding (Z141100007414002 and D131100005313008), National High-Technology Research and Development Program of China (2012AA02A509), Bethune Merck Research Fund for young and middle-aged doctors (2119000314), and Major Chronic Non-communicable Disease Prevention and Control Research(2016YFC1305600).

Acknowledgments

We would like to express our gratitude to the subjects for their contributions to the study, as well as to all the physicians and nurses for their work in this procedure of the study.

Conflict of interest

The authors declare that the research was conducted in the absence of any commercial or financial relationships that could be construed as a potential conflict of interest.

Publisher's note

Supplementary material

The Supplementary Material for this article can be found online at: https://www.frontiersin.org/articles/10.3389/fendo.2022.953631/full#supplementary-material

References

1. Chinnery PF. Primary mitochondrial disorders overview. In: *GeneReviews*. Seattle: University of Washington Press (1993).

2. Calvo SE, Clauser KR, Mootha VK. MitoCarta2.0: an updated inventory of mammalian mitochondrial proteins. *Nucleic Acids Res* (2016) 44:D1251–1257. doi: 10.1093/nar/gkv1003

3. Sharma V, Sharma I, Singh VP, Verma S, Pandita A, Singh V, et al. mtDNA G10398A variation provides risk to type 2 diabetes in population group from the jammu region of India. *Meta Gene* (2014) 2:269–73. doi: 10.1016/j.mgene.2014.02.003

4. Lu MY, Huang JF, Liao YC, Bai RK, Trieu RB, Chuang WL, et al. Mitochondrial polymorphism 12361A>G is associated with nonalcoholic fatty liver disease. *Transl Res* (2012) 159:58–9. doi: 10.1016/j.trsl.2011.10.011

5. Cao K, Lv W, Wang X, Dong S, Liu X, Yang T, et al. Hypermethylation of hepatic mitochondrial ND6 provokes systemic insulin resistance. *Adv Sci (Weinh)* (2021) 8:2004507. doi: 10.1002/advs.202004507

6. Palmieri VO, De Rasmo D, Signorile A, Sardanelli AM, Grattagliano I, Minerva F, et al. T16189C mitochondrial DNA variant is associated with metabolic syndrome in Caucasian subjects. *Nutrition* (2011) 27:773–7. doi: 10.1016/j.nut.2010.08.016

7. Janssen GM, Maassen JA, van Den Ouweland JM. The diabetes-associated 3243 mutation in the mitochondrial tRNA(Leu(UUR)) gene causes severe mitochondrial dysfunction without a strong decrease in protein synthesis rate. *J Biol Chem* (1999) 274:29744–8. doi: 10.1074/jbc.274.42.29744

8. Maassen JA, t Hart LM, Janssen GM, Reiling E, Romijn JA, Lemkes HH. Mitochondrial diabetes and its lessons for common type 2 diabetes. *Biochem Soc Trans* (2006) 34:819–23. doi: 10.1042/bst0340819

9. Guillausseau PJ, Dubois-Laforgue D, Massin P, Laloi-Michelin M, Bellanné-Chantelot C, Gin H, et al. Heterogeneity of diabetes phenotype in patients with 3243 bp mutation of mitochondrial DNA (Maternally inherited diabetes and deafness or MIDD). *Diabetes Metab* (2004) 30:181–6. doi: 10.1016/s1262-3636(07)70105-2

10. Murphy R, Turnbull DM, Walker M, Hattersley AT. Clinical features, diagnosis and management of maternally inherited diabetes and deafness (MIDD) associated with the 3243A>G mitochondrial point mutation. *Diabetic Med J Br Diabetic Assoc* (2008) 25:383–99. doi: 10.1111/j.1464-5491.2008.02359.x

11. Kishimoto M, Hashiramoto M, Araki S, Ishida Y, Kazumi T, Kanda E, et al. Diabetes mellitus carrying a mutation in the mitochondrial tRNA(Leu(UUR)) gene. *Diabetologia* (1995) 38:193–200. doi: 10.1007/bf00400094

12. Whittaker RG, Schaefer AM, McFarland R, Taylor RW, Walker M, Turnbull DM. Prevalence and progression of diabetes in mitochondrial disease. *Diabetologia* (2007) 50:2085–9. doi: 10.1007/s00125-007-0779-9

13. Peppa M, Koliaki C, Nikolopoulos P, Raptis SA. Skeletal muscle insulin resistance in endocrine disease. *J BioMed Biotechnol* (2010) 2010:527850. doi: 10.1155/2010/527850

14. Kohda M, Tokuzawa Y, Kishita Y, Nyuzuki H, Moriyama Y, Mizuno Y, et al. A comprehensive genomic analysis reveals the genetic landscape of mitochondrial respiratory chain complex deficiencies. *PloS Genet* (2016) 12:e1005679. doi: 10.1371/journal.pgen.1005679

15. Alberti KG, Zimmet PZ. Definition, diagnosis and classification of diabetes mellitus and its complications. part 1: Diagnosis and classification of diabetes mellitus provisional report of a WHO consultation. *Diabetes Med* (1998) 15:539–53. doi: 10.1002/(sici)1096-9136(199807)15:7<539::Aid-dia668>3.0.Co;2-s

16. National Cholesterol Education Program (NCEP) Expert Panel on Detection, Evaluation, and Treatment of High Blood Cholesterol in Adults (Adult Treatment Panel III). Third report of the national cholesterol education program (NCEP) expert panel on detection, evaluation, and treatment of high blood cholesterol in adults (Adult treatment panel III) final report. *Circulation* (2002) 106:3143–421. doi: 10.1161/circ.106.25.3143

17. Matthews DR, Hosker JP, Rudenski AS, Naylor BA, Treacher DF, Turner RC. Homeostasis model assessment: insulin resistance and beta-cell function from fasting plasma glucose and insulin concentrations in man. *Diabetologia* (1985) 28:412–9. doi: 10.1007/bf00280883

18. Alberti KGMM, Zimmet P, Shaw J. Metabolic syndrome–a new world-wide definition. a consensus statement from the international diabetes federation. *Diabetes Med* (2006) 23:469–80. doi: 10.1111/j.1464-5491.2006.01858.x

19. Wang Q, Liu M, Xu C, Tang Z, Liao Y, Du R, et al. Novel CACNA1S mutation causes autosomal dominant hypokalemic periodic paralysis in a Chinese family. *J Mol Med (Berl)* (2005) 83:203–8. doi: 10.1007/s00109-005-0638-4

20. Niemi AK, Moilanen JS, Tanaka M, Hervonen A, Hurme M, Lehtimäki T, et al. A combination of three common inherited mitochondrial DNA polymorphisms promotes longevity in Finnish and Japanese subjects. *Eur J Hum Genet* (2005) 13:166–70. doi: 10.1038/sj.ejhg.5201308

21. Zhai K, Chang L, Zhang Q, Liu B, Wu Y. Mitochondrial C150T polymorphism increases the risk of cervical cancer and HPV infection. *Mitochondrion* (2011) 11:559–63. doi: 10.1016/j.mito.2011.02.005

22. Ebner S, Lang R, Mueller EE, Eder W, Oeller M, Moser A, et al. Mitochondrial haplogroups, control region polymorphisms and malignant melanoma: a study in middle European caucasians. *PloS One* (2011) 6:e27192. doi: 10.1371/journal.pone.0027192

23. Rollins B, Martin MV, Sequeira PA, Moon EA, Morgan LZ, Watson SJ, et al. Mitochondrial variants in schizophrenia, bipolar disorder, and major depressive disorder. *PloS One* (2009) 4:e4913. doi: 10.1371/journal.pone.0004913

24. Sawabe M, Tanaka M, Chida K, Arai T, Nishigaki Y, Fuku N, et al. Mitochondrial haplogroups a and M7a confer a genetic risk for coronary atherosclerosis in the Japanese elderly: an autopsy study of 1,536 patients. *J Atheroscler Thromb* (2011) 18:166–75. doi: 10.5551/jat.6742

25. Chaig MR, Zernotti ME, Soria NW, Romero OF, Romero MF, Gerez NM. A mutation in mitochondrial 12S rRNA, A827G, in argentinean family with hearing loss after aminoglycoside treatment. *Biochem Biophys Res Commun* (2008) 368:631–6. doi: 10.1016/j.bbrc.2008.01.143

26. Li Z, Li R, Chen J, Liao Z, Zhu Y, Qian Y, et al. Mutational analysis of the mitochondrial 12S rRNA gene in Chinese pediatric subjects with aminoglycoside-induced and non-syndromic hearing loss. *Hum Genet* (2005) 117:9–15. doi: 10.1007/s00439-005-1276-1

27. Abreu-Silva RS, Rincon D, Horimoto AR, Sguillar AP, Ricardo LA, Kimura L, et al. The search of a genetic basis for noise-induced hearing loss (NIHL). *Ann Hum Biol* (2011) 38:210–8. doi: 10.3109/03014460.2010.513774

28. Rosa A, Fonseca BV, Krug T, Manso H, Gouveia L, Albergaria I, et al. Mitochondrial haplogroup H1 is protective for ischemic stroke in Portuguese patients. *BMC Med Genet* (2008) 9:57. doi: 10.1186/1471-2350-9-57

29. Tang J, Qi Y, Bao XH, Wu XR. Mutational analysis of mitochondrial DNA of children with rett syndrome. *Pediatr Neurol* (1997) 17:327–30. doi: 10.1016/s0887-8994(97)00151-3

30. Cardaioli E, Dotti MT, Hayek G, Zappella M, Federico A. Studies on mitochondrial pathogenesis of rett syndrome: Ultrastructural data from skin and muscle biopsies and mutational analysis at mtDNA nucleotides 10463 and 2835. *J Submicrosc Cytol Pathol* (1999) 31:301–4.

31. Shoffner JM, Brown MD, Torroni A, Lott MT, Cabell MF, Mirra SS, et al. Mitochondrial DNA variants observed in Alzheimer disease and Parkinson disease patients. *Genomics* (1993) 17:171–84. doi: 10.1006/geno.1993.1299

32. Cavelier L, Erikson I, Tammi M, Jalonen P, Lindholm E, Jazin E, et al. MtDNA mutations in maternally inherited diabetes: presence of the 3397 ND1 mutation previously associated with alzheimer's and parkinson's disease. *Hereditas* (2001) 135:65–70. doi: 10.1111/j.1601-5223.2001.00065.x

33. Mitchell AL, Elson JL, Howell N, Taylor RW, Turnbull DM. Sequence variation in mitochondrial complex I genes: Mutation or polymorphism? *J Med Genet* (2006) 43:175–9. doi: 10.1136/jmg.2005.032474

34. Jaksch M, Hofmann S, Kaufhold P, Obermaier-Kusser B, Zierz S, Gerbitz KD. A novel combination of mitochondrial tRNA and ND1 gene mutations in a syndrome with MELAS, cardiomyopathy, and diabetes mellitus. *Hum Mutat* (1996) 7:358–60. doi: 10.1002/(sici)1098-1004(1996)7:4<358::Aid-humu11>3.0.Co;2-1

35. Tang S, Batra A, Zhang Y, Ebenroth ES, Huang T. Left ventricular noncompaction is associated with mutations in the mitochondrial genome. *Mitochondrion* (2010) 10:350–7. doi: 10.1016/j.mito.2010.02.003

36. Finsterer J, Bittner R, Bodingbauer M, Eichberger H, Stöllberger C, Blazek G. Complex mitochondriopathy associated with 4 mtDNA transitions. *Eur Neurol* (2000) 44:37–41. doi: 10.1159/000008190

37. Tranah GJ, Nalls MA, Katzman SM, Yokoyama JS, Lam ET, Zhao Y, et al. Mitochondrial DNA sequence variation associated with dementia and cognitive function in the elderly. *J Alzheimers Dis* (2012) 32:357–72. doi: 10.3233/jad-2012-120466

38. Ohkubo E, Aida K, Chen J, Hayashi JI, Isobe K, Tawata M, et al. A patient with type 2 diabetes mellitus associated with mutations in calcium sensing receptor gene and mitochondrial DNA. *Biochem Biophys Res Commun* (2000) 278:808–13. doi: 10.1006/bbrc.2000.3867

39. Takasaki S. Mitochondrial SNPs associated with Japanese centenarians, alzheimer's patients, and parkinson's patients. *Comput Biol Chem* (2008) 32:332–7. doi: 10.1016/j.compbiolchem.2008.03.014

40. Sakaue S, Ohmuro J, Mishina T, Miyazaki H, Yamaguchi E, Nishimura M, et al. A case of diabetes, deafness, cardiomyopathy, and central sleep apnea: Novel mitochondrial DNA polymorphisms. *Tohoku J Exp Med* (2002) 196:203–11. doi: 10.1620/tjem.196.203

41. Chen T, Liu Q, Jiang L, Liu C, Ou Q. Mitochondrial COX2 G7598A mutation may have a modifying role in the phenotypic manifestation of aminoglycoside antibiotic-induced deafness associated with 12S rRNA A1555G mutation in a han Chinese pedigree. *Genet Test Mol Biomarkers* (2013) 17:122–30. doi: 10.1089/gtmb.2012.0251

42. Zhadanov SI, Atamanov VV, Zhadanov NI, Schurr TG. *De novo* COX2 mutation in a LHON family of Caucasian origin: implication for the role of mtDNA polymorphism in human pathology. *J Hum Genet* (2006) 51:161–70. doi: 10.1007/s10038-005-0340-y

43. Jiang C, Cui J, Liu F, Gao L, Luo Y, Li P, et al. Mitochondrial DNA 10609T promotes hypoxia-induced increase of intracellular ROS and is a risk factor of high altitude polycythemia. *PloS One* (2014) 9:e87775. doi: 10.1371/journal.pone.0087775

44. Tanaka M, Takeyasu T, Fuku N, Li-Jun G, Kurata M. Mitochondrial genome single nucleotide polymorphisms and their phenotypes in the Japanese. *Ann N Y Acad Sci* (2004) 1011:7–20. doi: 10.1007/978-3-662-41088-2_2

45. Zheng J, Bai X, Xiao Y, Ji Y, Meng F, Aishanjiang M, et al. Mitochondrial tRNA mutations in 887 Chinese subjects with hearing loss. *Mitochondrion* (2020) 52:163–72. doi: 10.1016/j.mito.2020.03.005

46. Lertrit P, Noer AS, Jean-Francois MJ, Kapsa R, Dennett X, Thyagarajan D, et al. A new disease-related mutation for mitochondrial encephalopathy lactic acidosis and strokelike episodes (MELAS) syndrome affects the ND4 subunit of the respiratory complex I. *Am J Hum Genet* (1992) 51:457–68.

47. Levin L, Zhidkov I, Gurman Y, Hawlena H, Mishmar D. Functional recurrent mutations in the human mitochondrial phylogeny: Dual roles in evolution and disease. *Genome Biol Evol* (2013) 5:876–90. doi: 10.1093/gbe/evt058

48. Allegra E, Garozzo A, Lombardo N, De Clemente M, Carey TE. Mutations and polymorphisms in mitochondrial DNA in head and neck cancer cell lines. *Acta Otorhinolaryngol Ital* (2006) 26:185–90.

49. Tawata M, Ohtaka M, Iwase E, Ikegishi Y, Aida K, Onaya T. New mitochondrial DNA homoplasmic mutations associated with Japanese patients with type 2 diabetes. *Diabetes* (1998) 47:276–7. doi: 10.2337/diab.47.2.276

50. Shin WS, Tanaka M, Suzuki J, Hemmi C, Toyo-oka T. A novel homoplasmic mutation in mtDNA with a single evolutionary origin as a risk factor for cardiomyopathy. *Am J Hum Genet* (2000) 67:1617–20. doi: 10.1086/316896

51. Mimaki M, Ikota A, Sato A, Komaki H, Akanuma J, Nonaka I, et al. A double mutation (G11778A and G12192A) in mitochondrial DNA associated with leber's hereditary optic neuropathy and cardiomyopathy. *J Hum Genet* (2003) 48:47–50. doi: 10.1007/s100380300005

52. Liu Z, Song Y, Gu S, He X, Zhu X, Shen Y, et al. Mitochondrial ND5 12338T>C variant is associated with maternally inherited hypertrophic cardiomyopathy in a Chinese pedigree. *Gene* (2012) 506:339–43. doi: 10.1016/j.gene.2012.06.071

53. Zhang J, Ji Y, Lu Y, Fu R, Xu M, Liu X, et al. Leber's hereditary optic neuropathy (LHON)-associated ND5 12338T > C mutation altered the assembly and function of complex I, apoptosis and mitophagy. *Hum Mol Genet* (2018) 27:1999–2011. doi: 10.1093/hmg/ddy107

54. Chen B, Sun D, Yang L, Zhang C, Yang A, Zhu Y, et al. Mitochondrial ND5 T12338C, tRNA(Cys) T5802C, and tRNA(Thr) G15927A variants may have a modifying role in the phenotypic manifestation of deafness-associated 12S rRNA A1555G mutation in three han Chinese pedigrees. *Am J Med Genet Part A* (2008) 146a:1248–58. doi: 10.1002/ajmg.a.32285

55. Zhou HP, Ishikawa H, Yasumoto R, Sakurai K, Sawamura H. Leber hereditary optic neuropathy harboring a rare m.12811 T>C mitochondrial DNA mutation. *Can J Ophthalmol* (2021) 56:e82–4. doi: 10.1016/j.jcjo.2020.12.022

56. Wei YL, Yu CA, Yang P, Li AL, Wen JY, Zhao SM, et al. Novel mitochondrial DNA mutations associated with Chinese familial hypertrophic cardiomyopathy. *Clin Exp Pharmacol Physiol* (2009) 36:933–9. doi: 10.1111/j.1440-1681.2009.05183.x

57. Jha RK, Dawar C, Hasan Q, Pujar A, Gupta G, Vishnu VY, et al. Mitochondrial genetic heterogeneity in leber's hereditary optic neuropathy: Original study with meta-analysis. *Genes (Basel)* (2021) 12:1300. doi: 10.3390/genes12091300

58. Zhang J, Zhou X, Zhou J, Li C, Zhao F, Wang Y, et al. Mitochondrial ND6 T14502C variant may modulate the phenotypic expression of LHON-associated G11778A mutation in four Chinese families. *Biochem Biophys Res Commun* (2010) 399:647–53. doi: 10.1016/j.bbrc.2010.07.135

59. Horvath R, Kemp JP, Tuppen HA, Hudson G, Oldfors A, Marie SK, et al. Molecular basis of infantile reversible cytochrome c oxidase deficiency myopathy. *Brain* (2009) 132:3165–74. doi: 10.1093/brain/awp221

60. Young WY, Zhao L, Qian Y, Li R, Chen J, Yuan H, et al. Variants in mitochondrial tRNAGlu, tRNAArg, and tRNAThr may influence the phenotypic manifestation of deafness-associated 12S rRNA A1555G mutation in three han Chinese families with hearing loss. *Am J Med Genet Part A* (2006) 140:2188–97. doi: 10.1002/ajmg.a.31434

61. Tzen CY, Thajeb P, Wu TY, Chen SC. Melas with point mutations involving tRNALeu (A3243G) and tRNAGlu(A14693g). *Muscle Nerve* (2003) 28:575–81. doi: 10.1002/mus.10473

62. Tong Y, Mao Y, Zhou X, Yang L, Zhang J, Cai W, et al. The mitochondrial tRNA(Glu) A14693G mutation may influence the phenotypic manifestation of ND1 G3460A mutation in a Chinese family with leber's hereditary optic neuropathy. *Biochem Biophys Res Commun* (2007) 357:524–30. doi: 10.1016/j.bbrc.2007.03.189

63. Sun Y, Han X. Study progress in mitochondrial cardiomyopathy. *J Appl Clin Pediatr* (2011) 26:50–2. doi: 10.3969/j.issn.1003-515X.2011.01.019

64. Soini HK, Moilanen JS, Finnila S, Majamaa K. Mitochondrial DNA sequence variation in Finnish patients with matrilineal diabetes mellitus. *BMC Res Notes* (2012) 5:350. doi: 10.1186/1756-0500-5-350

65. Jancic J, Rovcanin B, Djuric V, Pepic A, Samardzic J, Nikolic B, et al. Analysis of secondary mtDNA mutations in families with leber's hereditary optic neuropathy: Four novel variants and their association with clinical presentation. *Mitochondrion* (2020) 50:132–8. doi: 10.1016/j.mito.2019.10.011

66. Liguori R, Mazzaccara C, Pasanisi F, Buono P, Oriani G, Finelli C, et al. The mtDNA 15497 G/A polymorphism in cytochrome b in severe obese subjects from southern Italy. *Nutr Metab Cardiovasc Dis* (2006) 16:466–70. doi: 10.1016/j.numecd.2005.06.009

67. Li R, Qu J, Zhou X, Tong Y, Hu Y, Qian Y, et al. The mitochondrial tRNA (Thr) A15951G mutation may influence the phenotypic expression of the LHON-associated ND4 G11778A mutation in a Chinese family. *Gene* (2006) 376:79–86. doi: 10.1016/j.gene.2006.02.014

68. Tommasi S, Favia P, Weigl S, Bianco A, Pilato B, Russo L, et al. Mitochondrial DNA variants and risk of familial breast cancer: An exploratory study. *Int J Oncol* (2014) 44:1691–8. doi: 10.3892/ijo.2014.2324

69. Buford TW, Manini TM, Kairalla JA, McDermott MM, Vaz Fragoso CA, Chen H, et al. Mitochondrial DNA sequence variants associated with blood pressure among 2 cohorts of older adults. *J Am Heart Assoc* (2018) 7:e010009. doi: 10.1161/jaha.118.010009

70. Fliss MS, Usadel H, Caballero OL, Wu L, Buta MR, Eleff SM, et al. Facile detection of mitochondrial DNA mutations in tumors and bodily fluids. *Sci (New York NY)* (2000) 287:2017–9. doi: 10.1126/science.287.5460.2017

71. Merz KE, Thurmond DC. Role of skeletal muscle in insulin resistance and glucose uptake. *Compr Physiol* (2020) 10:785–809. doi: 10.1002/cphy.c190029

72. Suzuki M, Toyooka S, Miyajima K, Iizasa T, Fujisawa T, Bekele NB, et al. Alterations in the mitochondrial displacement loop in lung cancers. *Clin Cancer Res* (2003) 9:5636–41. doi: 10.1038/nrm3997

73. Sazanov LA. A giant molecular proton pump: structure and mechanism of respiratory complex I. *Nat Rev Mol Cell Biol* (2015) 16:375–88. doi: 10.1038/nrm3997

74. Lapuente-Brun E, Moreno-Loshuertos R, Acín-Pérez R, Latorre-Pellicer A, Colás C, Balsa E, et al. Supercomplex assembly determines electron flux in the mitochondrial electron transport chain. *Sci (New York NY)* (2013) 340:1567–70. doi: 10.1126/science.1230381

75. Murphy MP. How mitochondria produce reactive oxygen species. *Biochem J* (2009) 417:1–13. doi: 10.1042/bj20081386

76. Dawson TM, Dawson VL. Molecular pathways of neurodegeneration in parkinson's disease. *Science* (2003) 302:819–22. doi: 10.1126/science.1087753

77. Balaban RS, Nemoto S, Finkel T. Mitochondria, oxidants, and aging. *Cell* (2005) 120:483–95. doi: 10.1016/j.cell.2005.02.001

78. Soini HK, Moilanen JS, Vilmi-Kerälä T, Finnilä S, Majamaa K. Mitochondrial DNA variant m.15218A > G in Finnish epilepsy patients who have maternal relatives with epilepsy, sensorineural hearing impairment or diabetes mellitus. *BMC Med Genet* (2013) 14:73. doi: 10.1186/1471-2350-14-73

79. Asahara H, Himeno H, Tamura K, Hasegawa T, Watanabe K, Shimizu M. Recognition nucleotides of escherichia coli tRNA(Leu) and its elements facilitating discrimination from tRNASer and tRNA(Tyr). *J Mol Biol* (1993) 231:219–29. doi: 10.1006/jmbi.1993.1277

80. Hudson G, Mowbray C, Elson JL, Jacob A, Boggild M, Torroni A, et al. Does mitochondrial DNA predispose to neuromyelitis optica (Devic's disease)? *Brain* (2008) 131:e93. doi: 10.1093/brain/awm224

81. Tanaka M, Cabrera VM, González AM, Larruga JM, Takeyasu T, Fuku N, et al. Mitochondrial genome variation in eastern Asia and the peopling of Japan. *Genome Res* (2004) 14:1832–50. doi: 10.1101/gr.2286304

82. Legros F, Chatzoglou E, Frachon P, Ogier De Baulny H, Laforêt P, Jardel C, et al. Functional characterization of novel mutations in the human cytochrome b gene. *Eur J Hum Genet* (2001) 9:510–8. doi: 10.1038/sj.ejhg.5200678

83. Forbes JM, Coughlan MT, Cooper ME. Oxidative stress as a major culprit in kidney disease in diabetes. *Diabetes* (2008) 57:1446–54. doi: 10.2337/db08-0057

84. Brownlee M. The pathobiology of diabetic complications: A unifying mechanism. *Diabetes* (2005) 54:1615–25. doi: 10.2337/diabetes.54.6.1615

85. Bonora BM, Avogaro A, Fadini GP. Extraglycemic effects of SGLT2 inhibitors: A review of the evidence. *Diab Metab syndrome Obes Targets Ther* (2020) 13:161–74. doi: 10.2147/dmso.S233538

86. Zheng SL, Roddick AJ, Aghar-Jaffar R, Shun-Shin MJ, Francis D, Oliver N, et al. Association between use of sodium-glucose cotransporter 2 inhibitors, glucagon-like peptide 1 agonists, and dipeptidyl peptidase 4 inhibitors with all-cause mortality in patients with type 2 diabetes: A systematic review and meta-analysis. *JAMA* (2018) 319:1580–91. doi: 10.1001/jama.2018.3024

frontiers | Frontiers in Endocrinology

TYPE Original Research
PUBLISHED 26 October 2022
DOI 10.3389/fendo.2022.1040014

OPEN ACCESS

EDITED BY
Carlos Guillén,
Department of Biochemistry and Molecular Biology, Complutense University, Spain

REVIEWED BY
Anne-Sophie Vercoutter-Edouart, Centre National de la Recherche Scientifique (CNRS), France
Edgar Zenteno,
National Autonomous University of Mexico, Mexico

*CORRESPONDENCE
Emilyn U. Alejandro
ealejand@umn.edu

†These authors share first authorship

SPECIALTY SECTION
This article was submitted to Diabetes: Molecular Mechanisms, a section of the journal Frontiers in Endocrinology

RECEIVED 08 September 2022
ACCEPTED 10 October 2022
PUBLISHED 26 October 2022

CITATION
Jo S, Pritchard S, Wong A, Avula N, Essawy A, Hanover J and Alejandro EU (2022) Pancreatic β-cell hyper-O-GlcNAcylation leads to impaired glucose homeostasis *in vivo*. *Front. Endocrinol.* 13:1040014. doi: 10.3389/fendo.2022.1040014

Pancreatic β-cell hyper-O-GlcNAcylation leads to impaired glucose homeostasis *in vivo*

Seokwon Jo[1†], Samantha Pritchard[1†], Alicia Wong[1,2], Nandini Avula[1], Ahmad Essawy[1], John Hanover[3] and Emilyn U. Alejandro[1*]

[1]Department of Integrative Biology & Physiology, University of Minnesota Medical School, Minneapolis, MN, United States, [2]Department of Genetics, Cell Biology & Development, University of Minnesota, Minneapolis, MN, United States, [3]Laboratory of Cell and Molecular Biology, National Institute of Diabetes and Digestive and Kidney Diseases (NIDDK), National Institutes of Health, Bethesda, MD, United States

Protein O-GlcNAcylation is a nutrient and stress-sensitive protein post-translational modification (PTM). The addition of an O-GlcNAc molecule to proteins is catalyzed by O-GlcNAc transferase (OGT), whereas O-GlcNAcase (OGA) enzyme is responsible for removal of this PTM. Previous work showed that OGT is highly expressed in the pancreas, and we demonstrated that hypo-O-GlcNAcylation in β-cells cause severe diabetes in mice. These studies show a direct link between nutrient-sensitive OGT and β-cell health and function. In the current study, we hypothesized that hyper-O-GlcNAcylation may confer protection from β-cell failure in high-fat diet (HFD)-induced obesity. To test this hypothesis, we generated a mouse model with constitutive β-cell OGA ablation (βOGAKO) to specifically increase O-GlcNAcylation in β-cells. Under normal chow diet, young male and female βOGAKO mice exhibited normal glucose tolerance but developed glucose intolerance with aging, relative to littermate controls. No alteration in β-cell mass was observed between βOGAKO and littermate controls. Total insulin content was reduced despite an increase in pro-insulin to insulin ratio in βOGAKO islets. βOGAKO mice showed deficit in insulin secretion *in vivo and in vitro.* When young animals were subjected to HFD, both male and female βOGAKO mice displayed normal body weight gain and insulin tolerance but developed glucose intolerance that worsened with longer exposure to HFD. Comparable β-cell mass was found between βOGAKO and littermate controls. Taken together, these data demonstrate that the loss of OGA in β-cells reduces β-cell function, thereby perturbing glucose homeostasis. The findings reinforce the rheostat model of intracellular O-GlcNAcylation where too much (OGA loss) or too little (OGT loss) O-GlcNAcylation are both detrimental to the β-cell.

KEYWORDS

O-linked N-acetylglucosamine (O-GlcNAc), O-GlcNAcylation, O-GlcNAcase (OGA), beta cell (β-cell), insulin, insulin secretion, high fat diet (HFD), Streptozocin (STZ)

Introduction

Protein O-GlcNAcylation is a nutrient and stress-sensitive protein post-translational modification (PTM). The addition of an O-GlcNAc molecule onto proteins is catalyzed by O-GlcNAc transferase (OGT), whereas O-GlcNAcase (OGA) enzymes are responsible for removal of this PTM. O-GlcNAcylation occurs in intracellular proteins in the cytosol, mitochondria, and nucleus of the cell (1). The substrate, UDP-N-acetylglucosamine (UDP-GlcNAc) is synthesized from the hexosamine biosynthetic pathway that incorporates major components of macronutrients (glucose, amino acids, lipid and nucleotides), integrating the nutrient status of the cell into intracellular response to regulate key cellular functions (2). Dysregulation of O-GlcNAc cycling has been associated with various pathophysiologies (3, 4), in particular, metabolic disorders such as diabetes (5).

OGT is highly expressed in the pancreas (6) and has distinctive effects in the pancreas, compared to other insulin-sensitive metabolic tissues (7). O-GlcNAcylation has been detected in embryonic pancreas (8) and has shown to be critical to maintain both endocrine and exocrine health and function. OGT loss or hypo-O-GlcNAcylation in pancreatic progenitors causes pancreatic hypoplasia (8). OGT deletion in β-cells or in α-cells reduces cell survival and function (7, 9, 10), thereby dysregulating glucose homeostasis *in vivo*. Islet O-GlcNAcylation is increased in early obesity and is required for β-cell adaptation to enhance insulin secretion in early states of obesity (11). More importantly, we showed that OGT expression and activity are reduced in human islets from donors with chronic obesity, and lower OGT expression is associated with reduced β-cell function (11). These studies show a direct link between nutrient-sensitive OGT and β-cell health and function.

O-GlcNAcylation has been implicated in the regulation of β-cell health and function by fine-tuning signaling pathways relevant to cell survival such as the UPR ER stress and mitochondrial function (12). In β-cells, OGT loss increases ER (10) and mitochondrial stress (12). Several OGT protein targets in β-cells have been identified including the master regulator Pdx1 (13, 14) (8), and others such as p53 (8), NeuroD1 (15), TxNIP (16) and eIF4G1 (17). The cycling of O-GlcNAcylation on these target proteins is balanced by the enzyme OGA. SNP in OGA gene is a type 2 diabetes susceptibility gene in humans (18). Currently, there are no known studies that aim to study the O-GlcNAc cycling specifically in the pancreatic β-cell and its subsequent effect on glucose homeostasis *in vivo*.

The perturbations in *O*-GlcNAc cycling have been studied *in vivo* using whole body and conditional deletion of OGA (19, 20). These studies revealed that complete deletion of OGA led to perinatal lethality, whereas heterozygosity of OGA deletion led to viable mice with perturbed metabolic phenotypes. Whole body heterozygosity of OGA in male mice led to lower body weight with improved glucose tolerance and these mice resisted high fat diet (HFD) induced weight gain associated with increased energy expenditure through brown adipose enhancement. In a separate study of conditional deletion of OGA through MMTV-Cre recombinase, the authors reported sexual dimorphism phenotypes: Males displayed normal body weight, glucose tolerance (GTT) and insulin secretion *in vivo*, while female mice exhibited greater body weight gain (increase in both lean and fat mass), normal GTT, and increased insulin secretion *in vivo* (19). Under metabolic stress (HFD), OGA deletion led to improved GTT and normal insulin secretion in male mice, and glucose intolerance in females despite improved insulin secretion *in vivo*. In this study, however, insulin sensitivity was not tested.

Previous reports investigating the requirements of OGA provided important information about the metabolic effects of altered *O*-GlcNAc cycling in the whole animal (19). However, these studies are limited due to deletion of OGA in various tissues with possible conflicting effects in different tissues. To study the effect of blunted O-GlcNAc cycling in β-cell health and function and its impact on whole body glucose homeostasis, we characterized the mouse model of pancreatic β-cell specific OGA deletion. We reveal age-dependent impairment in glucose tolerance in both male and female in βOGAKO mice under normal chow diet, and that glucose intolerance in these mice was associated with defects in insulin content and insulin secretion. In response to a high-fat diet, male and female βOGAKO mice developed worse glucose intolerance. Under the diabetogenic stressor, streptozocin, βOGAKO mice developed hyperglycemia like littermate controls. The present study highlights the importance of O-GlcNAcylation cycling in both male and female animals and its implication in β-cell failure in diabetes.

Results

Generation of pancreatic β-cell specific OGA deletion in mice

OGA, a key enzyme responsible for the removal of post-translational modification of O-GlcNAcylation, is a T2D susceptible gene in humans (21). To assess the role of OGA in the pancreatic β-cells and its subsequent contribution to glucose homeostasis, we generated a mouse model with β-cell specific ablation of OGA using the Rat-Insulin-Promoter driven Cre-recombinase and OGA floxed gene (RIP-cre; OGA flox/flox, herein referred to as βOGAKO). We confirmed that the isolated islets (containing β-cells and other endocrine cells) from βOGAKO mice show significantly lower OGA mRNA transcript and protein levels and increased protein O-GlcNAcylation levels than control islets (Figures 1A-D). Interestingly, we show reduced protein levels of OGT, without alterations to its transcript levels in βOGAKO

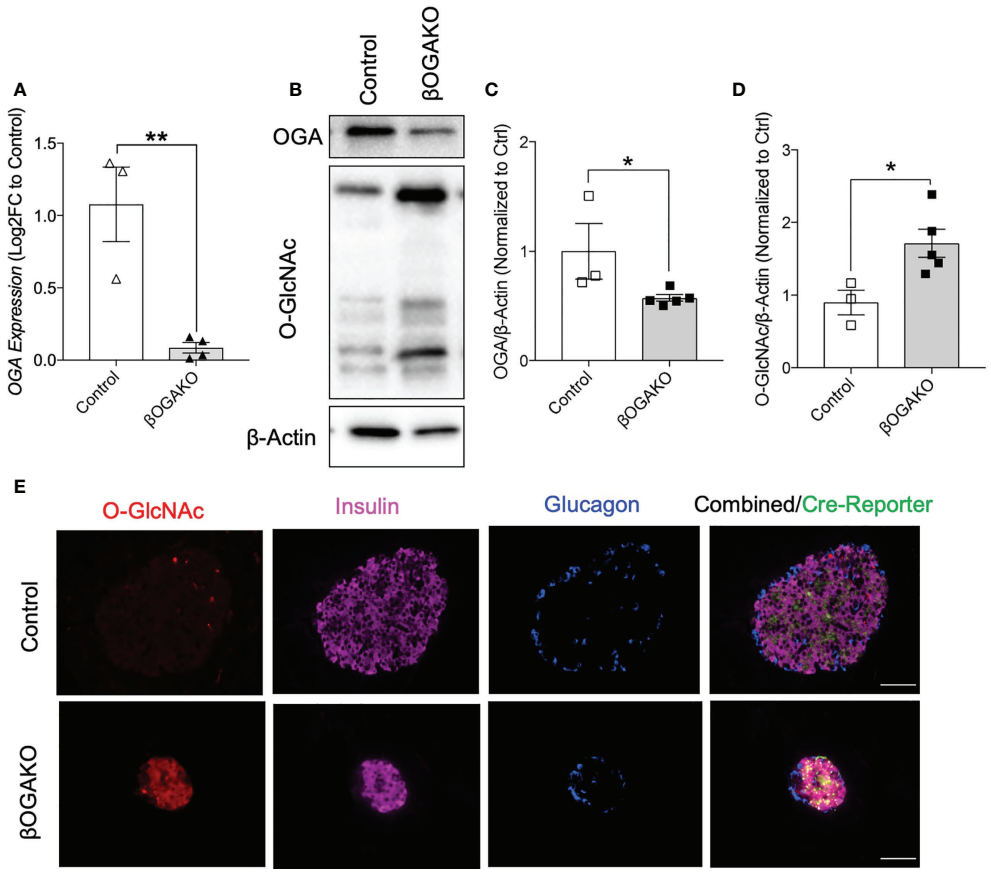

FIGURE 1
Validation of the β-Cell Specific Deletion of OGA. OGA mRNA level from pancreatic islets of control and βOGAKO mice **(A)**, normalized to beta-Actin mRNA (n=3-4). Representative western blot **(B)** and quantification of OGA **(C)** and pan O-GlcNAcylation **(D)**, normalized to beta-Actin (n=3-5). Immunofluorescence image of pancreatic islets showing O-GlcNAcylation (Red), Insulin (Purple), Glucagon (Blue) and Cre Reporter (Green) in Control and βOGAKO pancreas **(E)**. 40x magnification. Scale bar = 50 μm. Statistical analyses were conducted using unpaired, 2-way student t-test with significance *p<0.05, **p<0.001.

islets (Supplemental Figures 1A, B), suggesting that O-GlcNAc cycling enzyme expression is sensitive to overall O-GlcNAc status of the cell. Since pancreatic islets consist of other endocrine cell types that express OGA and the O-GlcNAc-modified proteins (e.g., α-cells), we validated the specificity of the deletion using immunofluorescence imaging. Here, we observed an increase in O-GlcNAcylation specifically in insulin producing β-cells (Figure 1E), validating the specificity of OGA deletion in βOGAKO mice.

OGA deletion in pancreatic β-cell perturbs glucose homeostasis under standard chow in age-dependent manner

To test the requirement of β-cell OGA in regulating whole body glucose homeostasis, we monitored the following parameters over time: body weight, blood glucose, and glucose and insulin tolerance *in vivo*. βOGAKO exhibited no differences in body weights and non-fasted blood glucose in both males (Supplemental Figures 1C, E) and females (Supplemental Figures 1D, F) compared to control mice. At 8-10-wks of age, male and female βOGAKO mice exhibited normal glucose and insulin tolerance when compared to control mice (Figures 2A-D). However, at 26wks of age, male and female βOGAKO mice exhibited glucose intolerance (Figures 2E, F), without gross alterations to insulin tolerance (Figure 2G). Consistently, in response to bolus of glucose treatment, βOGAKO mice failed to significantly increase insulin secretion, compared to control mice (Figure 2H), suggesting insulin secretion deficit as the driver of glucose intolerance at this age. Altogether, these data suggest that OGA deletion significantly alters basal β-cell function in both male and female mice under normal chow diet in an age-dependent manner.

10.3389/fendo.2022.1040014

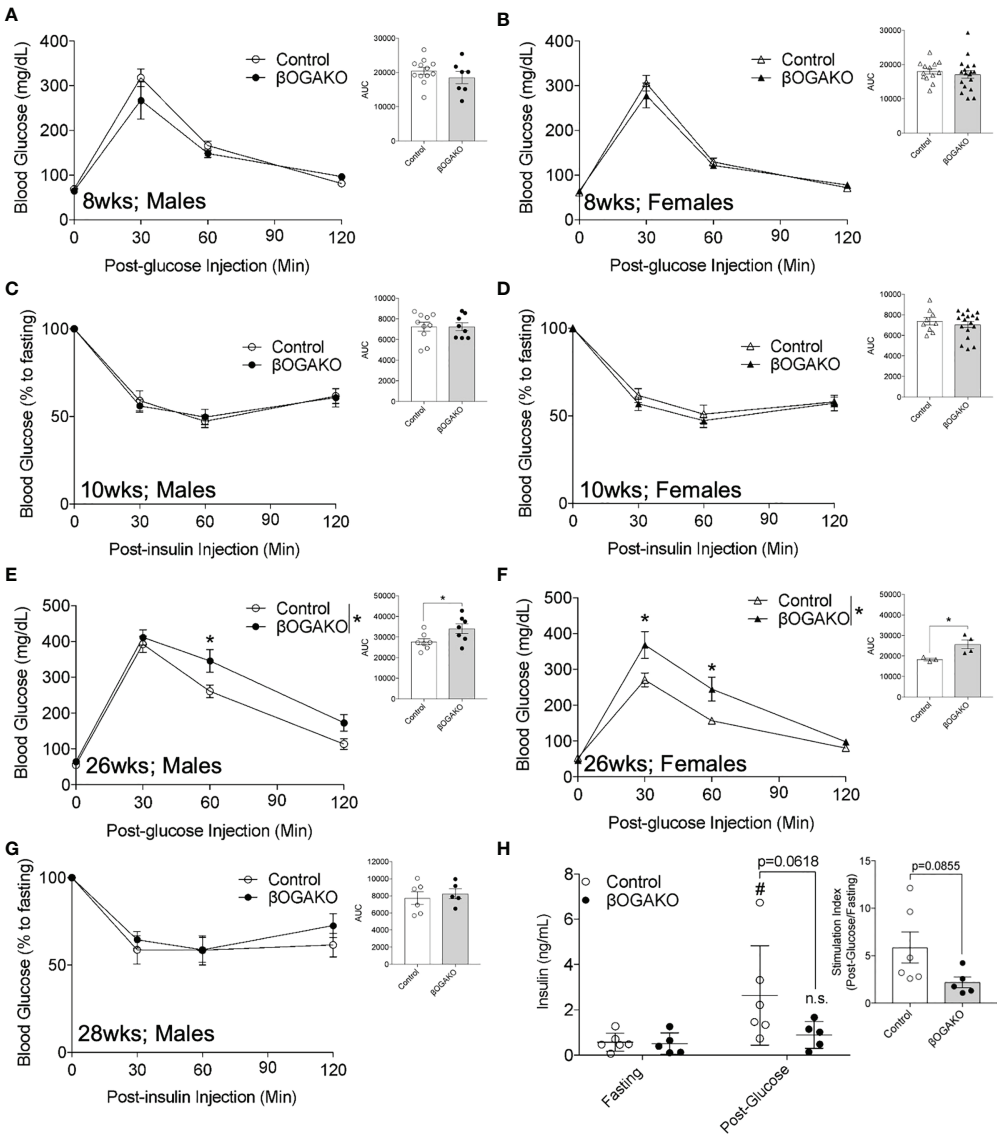

FIGURE 2
Loss of OGA in β-Cells Leads to Glucose Intolerance in Age-Dependent Manner in normal chow diet. *In vivo* glucose tolerance (2 g/kg glucose, i.p.) test of 8-wks (**A**, Male, n=7-12; **B**, Female, n=13-17) and insulin sensitivity (0.75 U/kg insulin, i.p.) of 10-wks (**C**, Male, n=8-10; **D**, Female, n=9-15). Glucose tolerance test of 26-wks (**E**, Male, n=7; **F**, Female, n=3-4) old mice and insulin of 28-wks old male (**G**, n=5-6) mice. *In vivo* glucose stimulated insulin secretion of male (**H**, n=5-6) with calculated stimulation index. Area under curve (AUC) of the blood glucose curves are presented for each figure. Statistical analyses were conducted using two-way ANOVA and unpaired, 2-way student t-test with significance *p < 0.05, #p<0.05 relative to fasting control. ns, non-statistical significance.

Normal β-cell mass but insulin secretion deficits in male and female βOGAKO mice

To further investigate the observed insulin secretion response *in vivo*, we assessed β-cell mass and function *ex vivo*. βOGAKO mice showed no alterations to pancreas mass, β-cell ratio, or β-cell mass (Figure 3A; Supplemental Figures 1G, H). Subsequently, we assessed the secretory function. βOGAKO islets secreted less insulin in response to glucose stimuli than the control islets (Figure 3B), and this was in part due to loss in insulin content in these islets (Figure 3C). With further analysis, we observed that proinsulin content and proinsulin to insulin ratio was decreased in βOGAKO islets, suggesting reduced proinsulin synthesis or enhanced processing in these islets (Figures 3D-F). In our previous study using the βOGTKO model, we showed that the expression of carboxypeptidase E (CPE), a proinsulin cleaving enzyme, was reduced and regulated indirectly by the

10.3389/fendo.2022.1040014

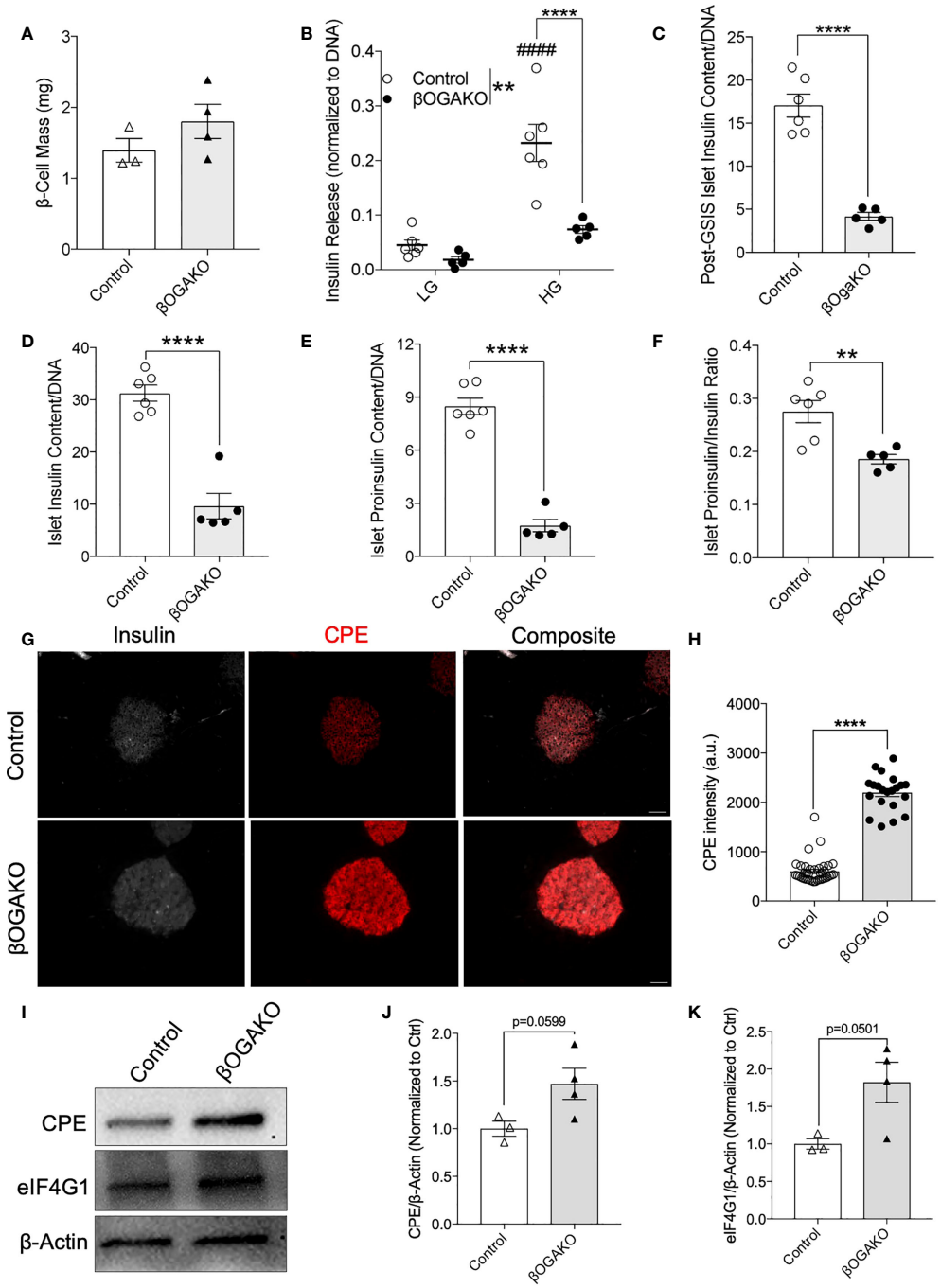

FIGURE 3
Impaired insulin secretion and processing in β-cell OGA deficient islets. β-cell mass of Control and βOGAKO female mice at 30-wks of age (**A**, n=3-4). *In Vitro* glucose stimulated insulin secretion assay with isolated primary islets from control and βOGAKO mice at 30-wks of age **(B)** with post-assay insulin content normalized to DNA **(C)** (n=5-6). Primary islet insulin **(D)** and proinsulin€) content normalized to DNA with proinsulin to insulin content ratio **(F)** (5-6). Immunofluorescence image of pancreatic islets showing CPE (red) and insulin (white) from Control and βOGAKO pancreas **(G)** and intensity quantification of CPE in insulin positive cells **(H)**. Islet analysis from n=2-3 animals. 40x magnification. Scale bar = 50 µm. Representative western blot **(I)** and quantification of CPE **(J)** and eIF4G1 **(K)**, normalized to beta-Actin (n=3-4). Statistical analyses were conducted using two-way ANOVA and unpaired, 2-way student t-test with significance *p<0.05, ** p<0.001, ****p<0.0001, $^{####}$pp<0.0001 relative to control fasting.

O-GlcNAcylation of a translational factor, eIF4G1 (17). Consistent with the βOGTKO model, we show that increased O-GlcNAcylation in βOGAKO islets led to increased CPE protein levels (Figures 3G-J), concomitantly with increased eIF4G1 protein expression (Figures 3I, K). Alterations to CPE and eIF4G1 protein expressions were observed without any significant changes to the transcript levels of CPE and eIF4G1 (Supplemental Figures 1I, J), highlighting the O-GlcNAcylation impact of these targets at the post-transcriptional level. Altogether, our data suggests that OGA deletion impacts insulin biosynthesis, processing, and secretory pathways, but not β-cell mass.

Male and female βOGAKO mice develop glucose intolerance in high fat diet feeding

To test their propensity to metabolic stress, male and female βOGAKO and littermate control mice were placed on a high-fat diet (HFD; 60% kcal) feed. We detected comparable body weight gain between the genotypes in both male and female mice (Figures 4A, B). Echo-MRI imaging performed at 30-wks post-HFD feeding corroborates this data, showing no alterations in fat or lean mass in either male or female βOGAKO mice (Supplemental Figures 2A-D). In early HFD feeding (4-wks), no alterations in glucose tolerance were observed in either male or female βOGAKO mice (Figures 4C, D). In contrast to normal glucose handling in early HFD, male βOGAKO mice developed significant glucose intolerance with female mice showing strong trends towards intolerance at 20-wks post-HFD feeding (Figures 4E, F). The development of glucose intolerance in βOGAKO mice became more severe by the effect of HFD feeding, when compared to normal chow diet (Supplemental Figures 2H). No differences were observed in insulin tolerance between control and βOGAKO mice fed a HFD regardless of sex (Supplemental Figures 2E, F). Subsequently, we assessed β-cell function *in vivo*. In early HFD feeding (6-wks), we found no significant differences in insulin secretion between control and βOGAKO mice (Supplemental Figure 2G). The deficit in insulin secretion in both male and female βOGAKO mice became apparent in longer HFD feeding (30-wks) (Figures 4G, H). However, there were no alterations to β-cell mass of βOGAKO mice post-32wk HFD feeding (Figures 4I, J), suggesting a defect in insulin secretory capacity. Altogether, these data suggest that hyper-O-GlcNAcylation in β-cells exacerbates the dysfunction in glucose homeostasis and insulin secretion under a diet stressor.

βOGAKO and littermate control mice display similar response to streptozocin stress

Streptozocin (STZ) is a common diabetogenic drug to induce hyperglycemia through death of pancreatic β-cells. One mechanism of action by STZ is the inhibition of OGA (17). We hypothesized that deletion of OGA may predispose these mice to diabetes by STZ treatment. To test this hypothesis, 8-10 wk old mice were treated with low-dose STZ injection for 5 days. Body weight, blood glucose and serum insulin were assessed for 2-wks post injection. In both sex, body weight remained normal across control and βOGAKO mice (Figures 5A, B). In male mice, control and βOGAKO mice developed hyperglycemia at an equal rate as the controls (Figure 5C). As expected, with low dose STZ treatment, the female mice maintained relatively normal blood glucose with no differences between the genotypes (Figure 5D). Consistent with the blood glucose levels, the serum insulin level between control and βOGAKO mice remained similar (Figures 5E, F). These data suggest that OGA deletion did not alter the mice's response to low dose STZ stressor relative to littermate controls.

Discussion

Previous studies have established that O-GlcNAcylation is required for proper β-cell function and metabolic regulation (17). However, it is not known whether dysregulated O-GlcNAc cycling through perturbation of OGA leads to alterations to insulin synthesis and secretion in pancreatic β-cells. To assess the relevance of OGA in β-cell function, we generated β-cell specific OGA knock-out mice. Hyper-O-GlcNAcylation appeared to have no impact on glucose tolerance until 28wks of age, where the animals develop glucose intolerance in part due to reduced glucose stimulated insulin secretion. This deficit in circulating insulin was in part due to dysfunction in β-cell function, but not in mass. The reduction in insulin secretion was associated with decreased total insulin content. To test the loss of OGA against metabolic challenge, we placed these mice in HFD for 25-wks. Body weight did not change for the duration of the metabolic challenge, but glucose intolerance worsened, with insulin secretion deficit, compared to mice fed normal chow diet. In response to the diabetogenic stressor, STZ, we detected no difference in susceptibility to diabetes in either male or female βOGAKO compared to controls, suggesting that HFD, but not STZ, heightened metabolic dysfunction in these mice.

Diabetes and hyperglycemia are often associated with increased O-GlcNAcylation and subsequent tissue dysfunction (1, 22). For example, increased O-GlcNAc modification in islets from diabetic Goto-Kakizaki rats is associated with loss of insulin secretion (23). Genetic deletion of OGA in tissues (such as liver and kidney using MMTV-Cre; OGA flox/+) led to sex-dependent differential metabolic phenotypes in both normal chow and high-fat diet (HFD) feeding (19). While this model is not a conditional deletion of OGA in pancreatic β-cells (24), a sexual-dimorphism in glucose homeostasis dysfunction under metabolic stress was apparent (increased body weight and increased insulin secretion in normal chow diet, and glucose

10.3389/fendo.2022.1040014

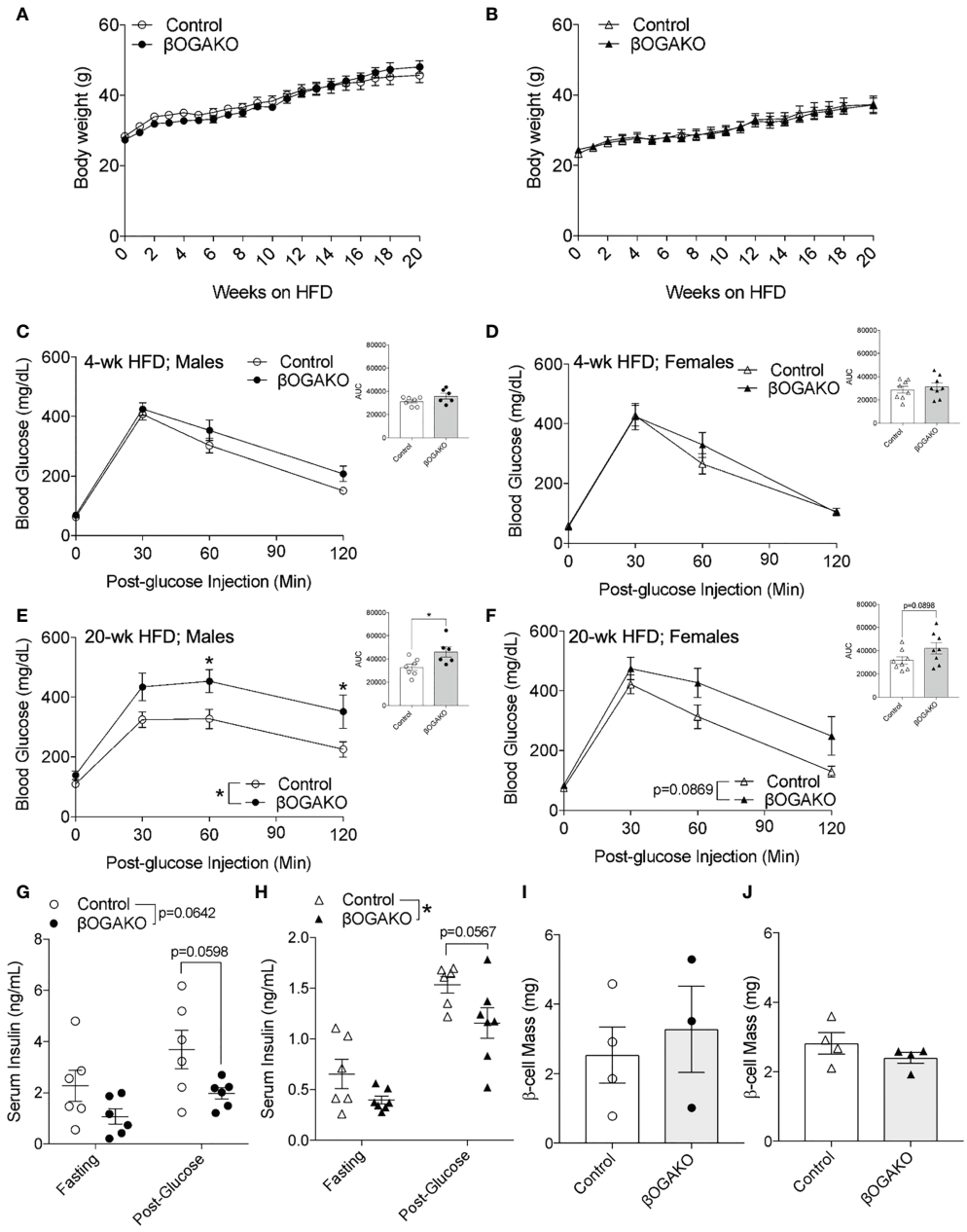

FIGURE 4
Perturbed glucose homeostasis in βOGAKO mice under high fat diet feeding. Body weight over 20-wks of high-fat-diet (HFD) feeding between control and βOGAKO male (**A**, n=6-7) and female (**B**, n=8) mice. *In vivo* glucose tolerance (2 g/kg glucose, i.p.) test on 4-wks (**C**; Male, **D**; Female) and 20-wks (**E**; Male, **F**; Female) post-HFD (n=6-7 for males and n=8 for females). *In vivo* glucose stimulated insulin secretion of male (**G**, n=6) and female mice 30-wk post-HFD (**H**, n=6-7). β-cell mass, assessed at 32-wk post-HFD in male (**I**, n=3-4) and female mice (**J**, n=4). Statistical analyses were conducted using two-way ANOVA and unpaired, 2-way student t-test with significance *p < 0.05.

intolerance in HFD despite increased insulin secretion in female, whereas, improved glucose tolerance without changes in insulin secretion in male fed HFD). Interestingly, in our model where OGA is genetically ablated specifically in β-cells, we detected similar metabolic phenotypes in both male and female βOGAKO mice in normal chow and HFD. In males, βOGAKO mice exhibited impaired glucose tolerance with deficit in insulin secretion in either chow diets, unlike normal and impaired glucose tolerance observed in the whole-body deletion model in normal chow or HFD, respectively. In females, βOGAKO consistently showed impairment in insulin secretion; yet whole-body deletion of OGA has led to increased

10.3389/fendo.2022.1040014

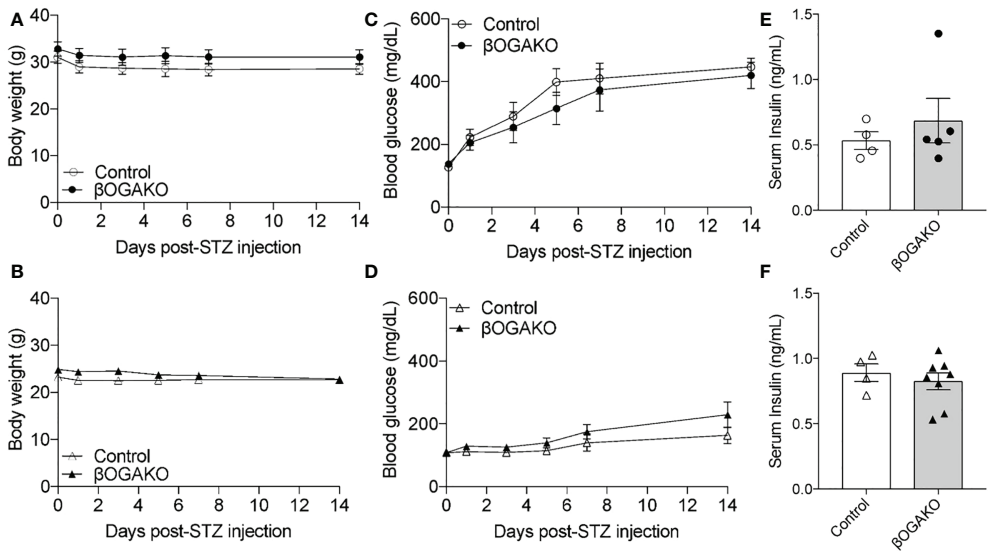

FIGURE 5
Normal response to diabetogenic STZ treatment in βOGAKO mice. Body weight (**A**, Male; **B**, Female) and blood glucose (**C**, Male; **D**, Female) tracked over 2-wks post-STZ injection (n=5-6 for Males, n=5-8 for Females). Serum insulin (**E**, Male; **F**, Female) at 2-wks post-STZ injection (n=4-5 for Males, n=4-8 for Females). Statistical analyses were conducted using two-way ANOVA and unpaired, 2-way student t-test with significance *p < 0.05.

insulin secretion in response to glucose. These data suggest that glucose tolerance and insulin secretion phenotypes in the whole body OGA deletion arises from non-β-cell OGA deficits. Consistent with this idea of differential effects of tissue specific perturbation of O-GlcNAc cycling, specific deletion of OGA in the brain leads to higher insulin in circulation (25). These data highlight the complexity of the glucose homeostasis and maintenance of circulating insulin *in vivo*.

In pancreatic β-cells, deletion of OGT, a model of hypo-O-GlcNacylation, led to the development of diabetes in mice with deficits in both β-cell mass and function (10). In the current model, deletion of OGA in β-cells led to glucose intolerance and insulin secretion deficits in older mice, though animals did not develop hyperglycemia or overt diabetes. These data suggest that perturbed cycling of O-GlcNAcylation on target proteins, whether it be too much or too little, is detrimental for β-cell function. In response to high glucose stimulation, βOGAKO mice failed to respond with adequate insulin secretion. We determined that this defect is in part due to reduced insulin content. In βOGAKO islets, pro-insulin levels and pro-insulin to insulin ratio was reduced, and this is associated with increased expression of prohormone processing enzyme carboxypeptidase E (CPE), suggesting increased pro-insulin processing with possible reduction in pro-insulin transcription or translation. In our previous work in βOGTKO islets, a model of hypo-O-GlcNAcylation, we found that reduced insulin content occurred in part due to disruption in insulin transcription (decrease *Ins1/2* mRNA and Pdx1 protein) as well as proinsulin processing, through dysregulation of CPE *via* O-GlcNAcylation of eIF4G1 (26). These data suggest that insulin processing in part through CPE and eIF4G1 is dependent on the presence of O-GlcNAcylation, where absence leads to reduced processing, while an increase in this PTM leads to enhanced proinsulin processing. However, given that insulin content is reduced in both βOGTKO and βOGAKO islets, overall insulin biosynthesis may be more dependent on O-GlcNAc cycling where either too little or too much O-GlcNAcylation inhibits this process and subsequent insulin secretion.

In addition to a HFD metabolic stressor, we utilized a diabetogenic stressor, streptozocin (STZ) to study the susceptibility of β-cell death under the condition of perturbed O-GlcNAc cycling. STZ is a GlcNAc analog that is selectively toxic to β-cells and one mechanism of action is the inhibition of OGA (27). STZ treatment increase O-GlcNAcylation in β-cells and is associated with β-cell death as transgenic mice with blunted glucosamine synthesis are resistant to STZ effects (28). In our previous study, we showed that transgenic overexpression of OGT in β-cells, a model of hyper-O-GlcNAcylation, led to protection against STZ in female mice (29). However, in the current of model of increasing O-GlcNAcylation *via* deletion of OGA in β-cells, mice exhibited typical diabetogenic effects from STZ, suggesting that STZ can induce β-cell dysfunction independent of its effect on OGA. Other molecular mechanisms of STZ-induced β-cell death include methylation of DNA, nitric oxide production and oxidative stress (30). Also, it is possible that persistent O-GlcNAcylation of a target proteins

require regulated cycling to impact their response to stress (in the case of OGT overexpression), rather than completely blunted PTM cycling (as in βOGAKO mice), highlighting the importance of enzyme kinetics in cellular response and function.

In summary, we demonstrate that ablation of OGA in β-cells causes a defect in insulin secretion but not β-cell mass. Mice lacking OGA in their β-cells develop glucose intolerance with age but not overt diabetes. These mild phenotypes are distinct to that of mice lacking OGT in their β-cells, where they develop severe hyperglycemia and over diabetes in early adulthood in part by decreased β-cell mass and insulin secretion failure. These studies highlight importance of O-GlcNAcylation cycling but also the distinct non-enzymatic actions of OGT and OGA in these cells.

Experimental procedures

Animal models and *in vivo* mouse procedures

The following mice were used as breeders for the study: OGA flox/flox (provided by Dr. John Hanover (NIH)), and mice harboring one allele of Cre-recombinase under the rat insulin 2 promoter [Rip-Cre; provided by Dr. Pedro Herrera (University of Geneva)], CAG-GFP Cre-recombinase reporter (Jackson Laboratories). All mice were group housed on a 14:10 light-dark cycle. High-fat diet (HFD; 60% Kcal of fat, D12492) was purchased from Research Diets, Inc. Glucose and insulin tolerance tests and *in vivo* glucose stimulated insulin secretion assays were performed as previously described (10), with littermate (OGA flox/flox, referred to as Control) mice. Low dose streptozocin (50 mg STZ/kg bw) was injected for 5-consecutive days and the mice were studied for 2-wks to assess metabolic parameters. All procedures were performed in accordance with the University of Minnesota Animal Studies Committee (IACUC #1806A36072).

Islet isolation and insulin secretion assay

We have previously described our islet isolation and insulin secretion assay technique (10). In brief, islets were isolated following ductal perfusion of collagenase and handpicked into RPMI media (10% FBS, 5 mM glucose) for overnight culture before experimental use. For the secretion assay, 3x10 islet aliquots per mouse were sequentially incubated in Krebs buffer at low glucose (2 mM, LG, 30 min), HG (high glucose, 16.7 mM, 30 min) and 30 mM KCl (15 min). Islet were collected into RIPA buffer (CST) with protease inhibitor cocktail (CST). Insulin secretion is presented as % of post-secretion islet insulin content. Total islet insulin content was calculated as the sum of secreted insulin + insulin content of the remaining islets, normalized to DNA.

Insulin ELISA

Insulin and proinsulin levels from random-fed serum, lysed isolated islets and islet secretion solutions were measured using Mouse Ultrasensitive Insulin ELISA kit (Alpco; 80-INSMSU-E01) per kit instruction. Content data was normalized to DNA, as determined by Quant-iT Pico Green dsDNA Assay (Molecular Probes).

Western blot

Primary pancreatic islets were lysed by sonication in 1x RIPA buffer, supplemented with protease and phosphatase inhibitor cocktails (CST). Upon BCA protein analysis, protein lysates were resolved by SDS-PAGE, followed by transfer to PVDF membrane. Membrane was blocked with 5% non-fat dry milk and probed with following antibodies: RL2 (Abcam; ab2739), OGA (Sigma; SAB4200311), OGT (CST; 24083), CPE (BDScience; 610759), eIF4G1 (Proteintech; 15704-1-AP), Actin (CST; 4967).

qPCR analysis

RNA was isolated from pancreatic islets, using RNeasy plus micro kit, following manufacturer's protocol. For qPCR, cDNA was synthesized from islet RNA, using high-capacity cDNA reverse-transcription kit (Applied Biosystems). Relative gene expression was assessed with Sybr Green (Applied Biosystems) on QuantStudio 6 Flex Real-Time PCR systems and calculated with ΔΔ cycle threshold (ΔΔCT) normalized to loading control. Primer sequences are: OGA Forward (TACCTGGGA GAGCCAGAAAC), OGA Rev (TGGATAACAGAAAGTG CCACA), CPE Forward (GCTCAGGTAATTGAAGTCTT), CPE Rev (TACTGCTCACGAATACAGTT), OGT Forward (ACTGTGTTCGCAGTGACCTG), OGT Rev (TCAAATAAC ATGCCTTGGCT), eIF4G1 Forward (TGGGAGGCTGATTCT CTACC), eIF4G1 Rev (GGAGACCTTCTAGATGCCA), Actin Forward (GCCCTGAGGCTCTTTTCCAG), and Actin Rev (TGCCACAGGATTCCATACCC).

Immunofluorescence & β-cell mass analysis

5 μm sections were generated at intervals of 200 μm from 5 different regions of each formalin-fixed and paraffin-embedded adult pancreas. Tissue sections were then selected from each region for staining. Following deparaffinization, antigens were retrieved by microwaving tissues in 0.01 M sodium citrate/citric acid for 12 minutes at 95C. Sections were then permeabilized with 0.01% Triton and blocked with Roche blocking buffer. Tissues were incubated overnight at 4°C in primary antibodies

against guinea pig insulin, mouse glucagon, and DAPI. Tissues were then washed with PBS-0.01% Tween and incubated with FITC, Cy3, and AMCA-conjugated secondary antibodies for 2 hours at 37°C. DAPI staining was also performed according to instructions provided by the manufacturer. β-cell mass was performed as previously described (10). For intensity analysis, all slides were imaged at the same time under equal channel exposure conditions. Using ImageJ (v1.53q), each image was thresholded such that only the islets were selected, and absolute average intensity was measured for each islet.

Statistical analysis

Data are presented as mean ± SEM and were analyzed using 2-tailed unpaired Student t-test. Multiple outcome data were assessed using repeated measures 2-way ANOVA. Statistical analyses were performed in GraphPad Prism version7 with a significance threshold of $p<0.05$.

Data availability statement

The original contributions presented in the study are included in the article/Supplementary Material.

Ethics statement

The animal study was reviewed and approved by IACUC at UMN.

Author contributions

Developed the study, SJ and SP. Designed experiments, generated and analyzed data, assisted with manuscript preparation, and approved the final version, SJ, SP, NA, AW, AE, JH, and EA. Interpreted the data and wrote and edited the manuscript, SJ and EA. Conceived the study and in charge of overall direction of this work, EA. All authors contributed to the article and approved the submitted version.

Funding

This work was supported by National Institutes of Health Grant NIDDK (R21DK112144 and R01DK115720 to EUA; F31DK131860 to SJ, T32 DK007203 for SP; and T32GM140936 for AW). This work was also supported by the Department of Integrative Biology and Physiology Accelerator Program.

Acknowledgments

We acknowledge Dr. Amber Lockridge, Ms. Grace Chung, and Mr. Nicholas Esch for technical support. We thank Dr. Thomas Pengo for his assistance in Fiji and the University of Minnesota Imaging Center for technical support. We thank Dr. Pilar Ariza Guzman for MRI in IBP phenotyping core at University of Minnesota. The tissue processing and embedding was performed at the laboratory of Dr. Jop van Berlo.

Conflict of interest

The authors declare that the research was conducted in the absence of any commercial or financial relationships that could be construed as a potential conflict of interest.

Publisher's note

Supplementary material

The Supplementary Material for this article can be found online at: https://www.frontiersin.org/articles/10.3389/fendo.2022.1040014/full#supplementary-material

SUPPLEMENTARY FIGURE 1
Normal Chow Diet Phenotype. OGT mRNA level from pancreatic islets of control and βOGAKO mice **(A)**, normalized to beta-Actin mRNA (n=3-4). Representative western blot and quantification of OGT **(B)**, normalized to beta-Actin (n=3-4). Body weight from 5- to 15-wks of age in male **(C)** and female **(D)** mice under normal chow diet (n=5-6 for males, n=8-11 for females). Non-fasted blood glucose at 15-16 wks of age in male **(E)** and female **(F)** mice (n=6-7 for males, n=4 females). Pancreas mass **(G)** and β-cell area to pancreas area ratio **(H)** from control and βOGAKO mice (n=3-4). CPE **(I)** and eIF4G1 **(J)** mRNA level from pancreatic islets of control and βOGAKO mice, normalized to beta-Actin mRNA (n=3-4). Statistical analyses were conducted using two-way ANOVA and unpaired, 2-way student t-test with significance *p<0.05

SUPPLEMENTARY FIGURE 2
High Fat Diet Phenotype. Echo-MRI analysis of fat mass and lean mass for male **(A, B)** and female **(C, D)** mice (n=6-7 for males and n=8 for females). Insulin sensitivity (0.75 U/kg insulin, i.p.) on 24-wks post-HFD for male **(E)** and female **(F)** mice. (n=6-7 for males and n=8 for females). *In vivo* GSIS of mice on 6-wks HFD (**G**) (n=4-7). IPGTT AUC from and comparing normal chow and HFD conditions **(H)**.

References

1. Bond MR, Hanover JA. A little sugar goes a long way: The cell biology of O-GlcNAc. *J Cell Biol* (2015) 208:869–80. doi: 10.1083/jcb.201501101

2. Akella NM, Ciraku L, Reginato MJ. Fueling the fire: Emerging role of the hexosamine biosynthetic pathway in cancer. *BMC Biol* (2019) 17:52. doi: 10.1186/s12915-019-0671-3

3. Ferrer CM, Sodi VL, Reginato MJ. O-GlcNAcylation in cancer biology: Linking metabolism and signaling. *J Mol Biol* (2016) 428:3282–94. doi: 10.1016/j.jmb.2016.05.028

4. Wright JN, Collins HE, Wende AR, Chatham JC. O-GlcNAcylation and cardiovascular disease. *Biochem Soc Trans* (2017) 45:545–53. doi: 10.1042/BST20160164

5. Ruan HB, Singh JP, Li MD, Wu J, Yang X. Cracking the O-GlcNAc code in metabolism. *Trends Endocrinol Metab* (2013) 24:301–9. doi: 10.1016/j.tem.2013.02.002

6. Lubas WA, Frank DW, Krause M, Hanover JA. O-Linked GlcNAc transferase is a conserved nucleocytoplasmic protein containing tetratricopeptide repeats. *J Biol Chem* (1997) 272:9316–24. doi: 10.1074/jbc.272.14.9316

7. Ida S, Morino K, Sekine O, Ohashi N, Kume S, Chano T, et al. Diverse metabolic effects of O-GlcNAcylation in the pancreas but limited effects in insulin-sensitive organs in mice. *Diabetologia* (2017) 60:1761–9. doi: 10.1007/s00125-017-4327-y

8. Baumann D, Wong A, Akhaphong B, Jo S, Pritchard S, Mohan R, et al. Role of nutrient-driven O-GlcNAc-posttranslational modification in pancreatic exocrine and endocrine islet development. *Development* (2020) 147(7): dev186643. doi: 10.1242/dev.186643

9. Essawy A, Jo S, Beetch M, Lockridge A, Gustafson E, Alejandro EU, et al. O-Linked n-acetylglucosamine transferase (OGT) regulates pancreatic alpha-cell function in mice. *J Biol Chem* (2021) 296:100297. doi: 10.1016/j.jbc.2021.100297

10. Alejandro EU, Bozadjieva N, Kumusoglu D, Abdulhamid S, Levine H, Haataja L, et al. Disruption of O-linked n-acetylglucosamine signaling induces ER stress and beta cell failure. *Cell Rep* (2015) 13:2527–38. doi: 10.1016/j.celrep.2015.11.020

11. Lockridge A, Jo S, Gustafson E, Damberg N, Mohan R, Olson M, et al. Islet O-GlcNAcylation is required for lipid potentiation of insulin secretion through SERCA2. *Cell Rep* (2020) 31:107609. doi: 10.1016/j.celrep.2020.107609

12. Mohan R, Jo S, Lockridge A, Ferrington DA, Murray K, Eschenlauer A, et al. OGT regulates mitochondrial biogenesis and function *via* diabetes susceptibility gene Pdx1. *Diabetes* (2021) 70:2608–25. doi: 10.2337/db21-0468

13. Kebede M, Ferdaoussi M, Mancini A, Alquier T, Kulkarni RN, Walker MD, et al. Glucose activates free fatty acid receptor 1 gene transcription *via* phosphatidylinositol-3-kinase-dependent O-GlcNAcylation of pancreas-duodenum homeobox-1. *Proc Natl Acad Sci USA* (2012) 109:2376–81. doi: 10.1073/pnas.1114350109

14. Gao Y, Miyazaki J, Hart GW. The transcription factor PDX-1 is post-translationally modified by O-linked n-acetylglucosamine and this modification is correlated with its DNA binding activity and insulin secretion in min6 beta-cells. *Arch Biochem Biophys* (2003) 415:155–63. doi: 10.1016/S0003-9861(03)00234-0

15. Andrali SS, Qian Q, Ozcan S. Glucose mediates the translocation of NeuroD1 by O-linked glycosylation. *J Biol Chem* (2007) 282:15589–96. doi: 10.1074/jbc.M701762200

16. Filhoulaud G, Benhamed F, Pagesy P, Bonner C, Fardini Y, Ilias A, et al. O-GlcNacylation links TxNIP to inflammasome activation in pancreatic beta cells. *Front Endocrinol (Lausanne)* (2019) 10:291. doi: 10.3389/fendo.2019.00291

17. Jo S, Lockridge A, Alejandro EU. eIF4G1 and carboxypeptidase e axis dysregulation in O-GlcNAc transferase-deficient pancreatic beta cells contributes to hyperproinsulinemia in mice. *J Biol Chem* (2019) 294(35):13040–50. doi: 10.1074/jbc.RA119.008670

18. Lehman DM, Fu DJ, Freeman AB, Hunt KJ, Leach RJ, Johnson-Pais T, et al. A single nucleotide polymorphism in MGEA5 encoding O-GlcNAc-selective n-acetyl-beta-D glucosaminidase is associated with type 2 diabetes in Mexican americans. *Diabetes* (2005) 54:1214–21. doi: 10.2337/diabetes.54.4.1214

19. Keembiyehetty C, Love DC, Harwood KR, Gavrilova O, Comly ME, Hanover JA, et al. Conditional knock-out reveals a requirement for O-linked n-acetylglucosaminase (O-GlcNAcase) in metabolic homeostasis. *J Biol Chem* (2015) 290:7097–113. doi: 10.1074/jbc.M114.617779

20. Yang YR, Jang HJ, Choi SS, Lee YH, Lee GH, Seo YK, et al. Obesity resistance and increased energy expenditure by white adipose tissue browning in oga(+/-) mice. *Diabetologia* (2015) 58:2867–76. doi: 10.1007/s00125-015-3736-z

21. Cameron EA, Martinez-Marignac VL, Chan A, Valladares A, Simmonds LV, Wacher N, et al, et al. MGEA5-14 polymorphism and type 2 diabetes in Mexico city. *Am J Hum Biol* (2007) 19:593–6. doi: 10.1002/ajhb.20639

22. Ma J, Hart GW. Protein O-GlcNAcylation in diabetes and diabetic complications. *Expert Rev Proteomics* (2013) 10:365–80. doi: 10.1586/14789450.2013.820536

23. Akimoto Y, Hart GW, Wells L, Vosseller K, Yamamoto K, Munetomo E, et al. Elevation of the post-translational modification of proteins by O-linked n-acetylglucosamine leads to deterioration of the glucose-stimulated insulin secretion in the pancreas of diabetic goto-kakizaki rats. *Glycobiology* (2007) 17:127–40. doi: 10.1093/glycob/cwl067

24. Wagner KU, McAllister K, Ward T, Davis B, Wiseman R, Hennighausen L, et al. Spatial and temporal expression of the cre gene under the control of the MMTV-LTR in different lines of transgenic mice. *Transgenic Res* (2001) 10:545–53. doi: 10.1023/a:1013063514007

25. Olivier-Van Stichelen S, Wang P, Comly M, Love DC, Hanover JA. Nutrient-driven O-linked n-acetylglucosamine (O-GlcNAc) cycling impacts neurodevelopmental timing and metabolism. *J Biol Chem* (2017) 292:6076–85. doi: 10.1074/jbc.M116.774042

26. Jo S, Lockridge A, Mohan R, Esch N, Schlichting R, Panigrahy N, et al. Translational factor eIF4G1 regulates glucose homeostasis and pancreatic beta-cell function. *Diabetes* (2020) 70(1):155–70. doi: 10.2337/db20-0057

27. Pathak S, Dorfmueller HC, Borodkin VS, van Aalten DM. Chemical dissection of the link between streptozotocin, O-GlcNAc, and pancreatic cell death. *Chem Biol* (2008) 15:799–807. doi: 10.1016/j.chembiol.2008.06.010

28. Liu K, Paterson AJ, Chin E, Kudlow JE. Glucose stimulates protein modification by O-linked GlcNAc in pancreatic beta cells: linkage of O-linked GlcNAc to beta cell death. *Proc Natl Acad Sci USA* (2000) 97:2820–5. doi: 10.1073/pnas.97.6.2820

29. Mohan R, Jo S, Chung EDS, Oribamise E, Lockridge A, Abrahante-Lloréns JE, et al. Pancreatic beta-cell O-GlcNAc transferase overexpression increases susceptibility to metabolic stressors in female mice. *Cells* (2021) 10:2801. doi: 10.3390/cells10102801

30. Eleazu CO, Eleazu KC, Chukwuma S, Essien UN. Review of the mechanism of cell death resulting from streptozotocin challenge in experimental animals, its practical use and potential risk to humans. *J Diabetes Metab Disord* (2013) 12:60. doi: 10.1186/2251-6581-12-60

frontiers | Frontiers in Endocrinology

TYPE Mini Review
PUBLISHED 17 November 2022
DOI 10.3389/fendo.2022.1052317

OPEN ACCESS

EDITED BY
S.R. Murthy Madiraju,
University of Montreal Hospital Centre (CRCHUM), Canada

REVIEWED BY
Shangang Zhao,
University of Texas Southwestern Medical Center, United States

*CORRESPONDENCE
Carlos Guillén
cguillen@ucm.es

SPECIALTY SECTION
This article was submitted to Diabetes: Molecular Mechanisms, a section of the journal Frontiers in Endocrinology

RECEIVED 23 September 2022
ACCEPTED 01 November 2022
PUBLISHED 17 November 2022

CITATION
García-Aguilar A and Guillén C (2022) Targeting pancreatic beta cell death in type 2 diabetes by polyphenols. *Front. Endocrinol.* 13:1052317. doi: 10.3389/fendo.2022.1052317

Targeting pancreatic beta cell death in type 2 diabetes by polyphenols

Ana García-Aguilar[1,2] and Carlos Guillén[2,3]*

[1]Department of Pharmacology, Pharmacognosy and Botany, Faculty of Pharmacy, Complutense University of Madrid, Madrid, Spain, [2]Diabetes and Associated Metabolic Diseases Networking Biomedical Research Centre Centro de Investigación Biomédica en Red. Diabetes y Enfermedades Metabólicas asociadas (CIBERDEM), Instituto de Salud Carlos III, Madrid, Spain, [3]Department of Biochemistry and Molecular Biology, Faculty of Pharmacy, Complutense University of Madrid, Madrid, Spain

Diabetes is a very complex disease which is characterized by the appearance of insulin resistance that is primarily compensated by an increase in pancreatic beta cell mass, generating hyperinsulinemia. After time, pancreatic beta cells die by apoptosis appearing in the second phase of the disease, and characterized by hypoinsulinemia. There are multiple conditions that can alter pancreatic beta cell homeostasis and viability, being the most relevant ones; ER stress, cytotoxicity by amylin, mTORC1 hyperactivity, oxidative stress, mitochondrial dysfunction, inflammation and alterations in autophagy/mitophagy flux. In addition, the possible effects that different polyphenols could exert in the modulation of these mechanisms and regulating pancreatic beta cell viability are analyzed. It is necessary a profound analysis and understanding of all the possible mechanisms involved in the control and maintenance of pancreatic beta cell viability to develop more accurate and target treatments for controlling beta cell homeostasis and preventing or even reversing type 2 diabetes mellitus.

KEYWORDS

diabetes, pancreatic beta cells, ER stress, autophagy, amylin, polyphenols

Introduction

Type 2 diabetes mellitus (T2DM) is a very complex metabolic disease characterized by insulin resistance as well as pancreatic β cell dysfunction, and it is considered a worldwide epidemic (1). The pathogenesis of T2DM is multifactorial and a subject of continuous intense investigation. β cells are a type of cells existing in the pancreatic islets of Langerhans that secrete insulin and amylin in response to increasing glycemia. Glucose stimulates transcription, translation and exocytosis of insulin in β cells to maintain

systemic glucose homeostasis. In this sense, β cells sense glucose which leads to an increase in the intracellular ATP/ADP ratio through its metabolism, thus, closing ATP-dependent potassium channels, depolarizing cellular membrane, stimulating calcium influx, and finally promoting insulin secretion.

Effects of gluco-, lipo- and glucolipotoxicity in insulin secretion

Plasma free fatty acids (FFAs) and glucose exert both positive and negative effects on pancreatic beta cell survival and insulin secretory function, depending on their concentration and duration.

In the presence of chronic hyperglycemia (glucotoxicity), the uncoupling protein 2 (UCP2) expression in beta cells is increased, and this event is associated with a reduction in the ratio of ATP to ADP, thus inhibiting glucose-stimulated insulin secretion (GSIS), which contributes to the development of T2DM (2–4). In this regard, it was described that UCP2 upregulation, by the deletion of the deacetylase SIRT1, contributes to diminish GSIS (5). More recently, other authors demonstrated that ROS and GSIS were increased in a β-cell–specific UCP2 knockout (βUCP2KO) model, highlighting that UCP2 negatively regulates GSIS by reducing mitochondrial ROS production, and not through a defect in ATP production (6).

In the same way, a chronically exposure of β cells to elevated concentration of FFAs, referred as lipotoxicity, results in disturbances in lipid metabolism regulation, impairs GSIS by an induction in UCP2 expression, increases beta-cell apoptosis and consequently induces T2DM (7, 8).

Regarding the effects of a combined and long-term exposure to elevated glucose and FFAs (glucolipotoxicity) on pancreatic beta-cell function and survival, recently it has been demonstrated that it leads to decreased GSIS and impaired insulin gene expression, contributing to β-cell failure and T2DM (9).

Dysfunctional mechanisms leading to beta cell dysfunction and T2DM progression

Different molecular mechanisms trigger beta cell dysfunction in a glucolipotoxic scenario and includes cytotoxicity of amylin, mTORC1 hyperactivation, ER and oxidative stress, mitochondrial dysfunction, autophagy impairment and islet inflammation. The main scope of this review is to shed light on the molecular mechanisms produced in pancreatic beta cells that lead to beta cell dysfunction, contributing to T2DM.

ER stress

The endoplasmic reticulum (ER) of beta cells has a high capacity of protein synthesis and folding. However, in the context of insulin resistance, beta cells need to synthesize insulin beyond their capacity for protein folding and secretion, and thereby activate the unfolded protein response (UPR). UPR is an adaptive signaling pathway to promote cellular survival upon accumulation of misfolded proteins in the ER. UPR signaling sensors are inositol-requiring enzyme 1 (IRE1); PKR-like ER kinase (PERK) and the activating transcription factor 6 (ATF6). However, if UPR is chronically activated, and protein-folding demand in the ER exceeds capacity, unfolded proteins start to accumulate within the ER leading to ER stress and cell death (10, 11).

In β-cells, chronic hyperglycemia and hyperlipidemia, especially the exposure to saturated long-chain free fatty acids, known as important causative factors of T2DM, enhanced ER calcium depletion, induce ER stress and thereby cause β-cell failure (11–13).

The relationship between ER stress-induced β-cell dysfunction and death has been extensively studied (14–17) and it was first evidenced in a rare autosomal recessive form of juvenile diabetes, the Wolcott-Rallison syndrome (18). In this syndrome, mutations have been identified in the EIF2AK3 gene encoding PERK, causing a loss-of-function of this protein and promoting ER stress-mediated β-cell death (19).

Furthermore, the pathogenesis of Wolfram syndrome, an autosomal recessive neurodegenerative disorder associated with juvenile-onset diabetes mellitus, involves chronic ER stress in β-cells. This syndrome is caused by a loss-of-function of the wolfram syndrome gene 1 (WFS1), a component of the UPR that participates in maintaining ER homeostasis in β-cells (20, 21).

Cytotoxicity of amylin

Amylin, or islet amyloid polypeptide (IAPP), is a 37-amino acid peptide hormone co-secreted with insulin by pancreatic islet β-cells in response to nutrients, including glucose, lipids or amino acids. It is a regulatory peptide that inhibits insulin and glucagon secretion in the islets, but also acts in the brain modulating satiety and inhibition of gastric emptying (22).

In human β cells, the precursor and the intermediate forms of IAPP were increased after prolonged exposure to high glucose (11). Furthermore, it is also hypothesized that amyloid aggregates composed of amylin were accumulated in the β cell of patients with T2DM, causing disruption of cell membrane (11), inflammasome activation (23), mitochondrial damage and ER-induced apoptosis (24, 25). More recently, it has been also demonstrated that overexpression of human amylin (hIAPP) in

INS-1 β-cells increases the fission of mitochondria, activates mTORC1 and inhibits mitophagy, contributing to β cell death (26).

mTORC1 hyperactivation

During the progression to T2DM, there are two phases. The first one is the insulin resistant prediabetic stage, in which the main event is the insulin resistance with normoglycemia. At this phase, β cells increase their mass by two mechanisms, to cope with an increased insulin demand: hyperplasia (cell number increase) and hypertrophy (cell size increase), with concomitant insulin and amylin secretion (27). This increase in β cell mass is accomplished by an hyperactivation of the mammalian target of rapamycin complex 1 (mTORC1) signaling, which is a key effector for the growth and survival of pancreatic β cells (28). The duration of this phase depends on the patient and, at a final stage, if mTORC1 remains chronically overactivated, pancreatic β cells fail, causing a significant reduction in β-cell mass, and thus, hypoinsulinemia appears triggering hyperglycemia. These two phases have been described in a mouse model with a chronic mTORC1 hyperactivation caused by a specific deletion of Tsc2 in β-cells (β-TSC2-/-). These mice showed an early phase with an increase in β-cell mass and an enhanced GSIS, but finally leading to β-cell failure and hyperglycemia in older mice (29). All these data pointed to mTORC1 signaling as a double-edged sword in the progression to T2DM (30).

Altered autophagy and mitophagy

Macroautophagy, referred to here as autophagy, is a conserved and a physiological defense mechanism against acute stress that maintains cellular quality control by removing protein aggregates and damaged organelles, and acts as an essential process for maintaining cellular homeostasis in eukaryotes alternatively to the ubiquitin-proteasome system (UPS) (31, 32). Currently, there are three main types of autophagy in mammalian cells: macroautophagy, chaperone-mediated autophagy and microautophagy. Multiple signaling pathways regulate this process, but one of most important is the mTORC1 pathway, which activation induces aging and inhibits autophagy (33). Importantly, autophagy deregulation is believed to cause or contribute to aging, as well as a number of age-related diseases, including T2DM (34, 35).

It has been extensively demonstrated that autophagy protects pancreatic β cells under chronic hyperglycemia or after exposure to high fat-diet, increasing β cell survival in the progression to T2DM. In fact, specific deletion of the autophagy gene Atg7 specifically in pancreatic β cells of mice leads to impaired glucose tolerance and GSIS caused by an increase in polyubiquitinated proteins and apoptosis (36, 37). Moreover, blocking autophagy by upregulating mTORC1 signaling using β-TSC2-/- mice, increased pancreatic β cell death as a consequence of an impairment of autophagy activation as well as an induction of ER stress (29). Thus, the concept that autophagy plays a protective role in β cells is based in its capacity to alleviate oxidative (38) and ER-stress (29, 39–41), as well as to clearance hIAPP and polyubiquitin protein aggregates formed in pancreatic islets, reducing their toxicity (42, 43), and consequently, preventing pancreatic β cell failure (29, 44).

Mitophagy is a specialized type of autophagy that eliminates damaged and dysfunctional mitochondria and serves to maintain energy balance, mitochondrial quality control and cellular protection against oxidative stress. The PTEN-induced kinase 1 (PINK1)-Parkin pathway plays a major role in mediating mitophagy. PINK1 protein is a sensor of mitochondrial depolarization because it accumulates specifically on the outer mitochondrial membrane (OMM) of damaged mitochondria, and from there, it recruits Parkin to mitochondria and activates it. Furthermore, Parkin protein is an E3 ubiquitin ligase that induces ubiquitination of several OMM proteins, and consequently, activates mitophagy (45). The role of Parkin in the mitophagy of β cells has been assessed in *Parkin*-/- streptozotocin-treated mice, which showed an impairment of glucose tolerance, and a reduction in ATP content as well as in GSIS (46). Moreover, mitophagy is activated under stressful conditions, such as an exposure to proinflammatory cytokines that induce mitochondrial damage. Thus, mitophagy-deficient β cells are more vulnerable to inflammatory stress, leading to the accumulation of dysfunctional and fragmented mitochondria, increasing β-cell death and exacerbating hyperglycemia (47).

In addition, prohibitin 2 (PHB2) is an inner mitochondrial membrane (IMM) protein, very important in development and cell proliferation, but it also has a functional role as a mitophagy receptor (48, 49) as well as in maintaining mitochondrial integrity and function. Indeed, *in vivo* ablation of Phb2 specifically in β-cells (β-*Phb2*-/-) resulted in an impairment of mitochondrial function, which leads to a loss of β-cell mass and GSIS, attributed to an increased apoptosis of β-cells (50).

Interestingly, the pancreatic duodenal homeobox factor 1 (PDX1), similar to other genes that cause monogenic diabetes of the young and T2DM, is a transcription factor essential for the development of the pancreas (51–53), and was also implicated in the control of mitophagy in pancreatic β-cells (54). Indeed, PDX1 deficiency has been associated with impaired mitochondrial function and mitophagy as well as a reduced GSIS by inhibition of the nuclear encoded mitochondrial factor A (TFAM) (55). In this sense, a high expression of microRNA-765 which targets and reduces the expression of PDX1, was founded in T2DM patients and it was correlated with an inhibition of both mitochondrial respiration and β-cell function (56).

Furthermore, mitochondrial dynamics (fission/fusion) are essential to maintain a balance between mitochondrial biogenesis and mitochondrial turnover. Recently, there is an increasing interest in understanding the role of mitochondrial dynamics in the development of T2DM. Regarding this, an imbalance between these processes leads to a reduction in mitophagy and an accumulation of dysfunctional mitochondria (57–59). Mitochondrial fusion is mainly coordinated by three GTPases, the homologous mitofusins 1 and 2 (MFN1, MFN2) localized in the OMM, and the optic atrophy 1 (OPA1) protein, which resides in the IMM. In contrast, fission is regulated by the soluble GTPase dynamin-related protein 1 (Drp1) and the mitochondrial fission 1 protein (FIS1). Herein, it is interesting to note that both FIS1 overexpression and FIS1 knockdown lead to a decrease in GSIS (60, 61), suggesting that GSIS in beta cells requires a precise expression level of this fission protein (62). Accordingly, a downregulation of Drp1 in the pancreatic β cell line INS-1E as well as in spread mouse islets significantly reduced the expression of mitochondrial fusion proteins (MFN1, MFN2 and OPA1), downregulated ATP content and GSIS (63). Additionally, an increase in the mRNA and protein expression of MFN2 and several mitophagy-related proteins (NIX, PINK1, and PARKIN) has been reported in prediabetic subjects, whereas patients with T2DM showed a decreased expression of these proteins (64), demonstrating the important role of mitophagy and mitochondrial dynamic in the pathogenesis of T2DM.

ROS and oxidative stress

The role of reactive oxygen species (ROS) in β cell function depends on the timing and strength of the signal. Moreover, β cells are more vulnerable to oxidative stress because of their minor capacity of scavenging oxidants when compared to other types of cells (65). Herein, a transient and moderate production of mitochondrial reactive oxygen species (mROS) is an important signaling to promote β cell function and GSIS, mimicking the glucose effect (6, 66). However, a chronic and persistent elevation of ROS, as a result from inflammation or excessive glucose and fatty acid concentrations, impairs β-cell function by repressing the ROS signal and/or inducing mitochondrial damage that also results in an increase in ROS production (67, 68). This increase in mitochondrial superoxide production activates UCPs *via* peroxidation of mitochondrial phospholipids. In agreement with this, morphology studies showed that β-cells from patients with T2D and from non-diabetic donors had similar numbers of mitochondria, but the mitochondrial density volume was significantly higher in diabetic islets, which has been associated with an increase in ROS production. In line with this, an upregulation of UCP2 protein levels was observed in type 2 diabetic islets when compared to non-diabetic ones (3).

Furthermore, ROS are able to oxidize cardiolipin (CL) and other mitochondrial inner membrane phospholipids, initiating the permeabilization of the outer mitochondrial membrane and subsequent release of cytochrome c into the cytosol, triggering apoptosis and β-cell mass reduction (69, 70).

Also, the group VIA Ca^{2+}-independent phospholipase A2 ($iPLA_2\beta$) proteins is attracting increasing interest as a central participant in CL remodeling and protects β cell mitochondria from oxidative damage (71). In fact, mutations in tafazzin (TAZ), a mitochondrial phospholipid-lysophospholipid transacylase that participates in CL remodeling, are implicated in Barth syndrome, in which patients lacking functional TAZ present with cardiomyopathy and skeletal dysfunction due to a total CL deficiency. Very recently, it has been demonstrated a reduced *ex vivo* insulin secretion under non-stimulatory low-glucose concentrations in islets isolated from TAZ KD mice, highlighting the importance of TAZ in regulating normal β-cell function (72).

Mitochondrial dysfunction

Mitochondrial DNA (mtDNA) mutations and chronic metabolic changes, such as glucotoxicity, are the main mechanisms that contribute to β cell mitochondrial dysfunction that results in an enhanced β cell apoptosis in T2DM (73).

Among mtDNA mutations, a reduced expression in the mitochondrial transcription factor B1 (TFB1M) of pancreatic islets founded in a β-cell specific KO of TFB1M (β-*Tfb1m*-/-) or caused by a variant of the *TFB1M* gene (rs950994), displayed mitochondrial dysfunction, reduced ATP production and, consequently, impaired GSIS (74, 75). Furthermore, there were an increase in the percentage of mitochondria with vesicular and swollen morphology, as long as an impairment of autophagy and mitophagy flux in β cells from β-*Tfb1m*-/- mice when compared to control islets (76). Together, these results highlighted the important role of TFB1M in mitochondrial and cellular function in pancreatic β cells. According to this, mitochondrial fragmentation occurs in β cells exposed to high-fat diet (HFD) (77).

In view of metabolic changes, hyperglycemia, a hallmark of T2DM, promotes the transfer of reducing equivalents to the respiratory chain in mitochondria of pancreatic β cells, resulting in the hyperpolarization of the mitochondrial membrane potential ($\Delta\Psi M$) and generation of ATP. Compared to control islets, diabetic islets display a decreased expression of several proteins involved in oxidative metabolism, including several components of the mitochondrial respiratory chain (78).

Moreover, diabetic islets showed reduced hyperpolarization of the ΔΨM, lower ATP levels at high glucose, impaired Ca2+ signaling and lowered GSIS (78–80). In this sense, it has been determined very recently that a reduction in the activity of the cytochrome C oxidase (complex IV) in islets could be a primary inborn defect that underlies β cell dysfunction (81).

Islet inflammation

Inflammatory stress plays a crucial role in the pathogenesis of T2DM. In fact, a mild inflammation inside islets can be detected in T2DM patients. In this regard, the administration of anti-inflammatory drugs generates a mild glucose decrease, suggesting that inflammation is involved in T2DM, although it is still unknown whether the effect of these anti-inflammatory medications has a direct impact in pancreatic islets or it is through the effect in other relevant metabolic tissues. In fact, this inflammation could be derived from nutrient overload, proinflammatory cytokines, amylin accumulation or ER stress (82). One of the organelles that is found altered after inflammation is mitochondria, with a dysfunctional production of ATP and inducing the proapoptotic machinery. An important mechanism to combat the accumulation of altered mitochondria after an inflammatory process is mitophagy, which is the specific mitochondrial clearance by using the autophagic machinery. In this regard, any change in mitophagy sensitizes pancreatic beta cells to inflammation. Then, mitophagy is a survival mechanism in these cells in response to inflammation (47). Oxidative stress is able to affect mitochondria and generates a higher amount of ROS because of the impairment in the antioxidant defenses, leading to mitochondrial dysfunction and pancreatic beta cell failure (83).

Effects of toxic metabolites in β cell function and viability

Apart from all the mechanisms previously explained having a deleterious effect on pancreatic beta cells' viability, there are several toxic metabolites coming from the environment such as pollutants or certain treatments that lead to a decrease in beta cell survival. Among the most relevant metabolites are the following: bisphenol A (BPA), heavy metal exposure, glucocorticoids and dioxins. BPA is a common contaminant found in the environment and it has been related with both T1DM and T2DM because of its involvement in the reduction and impairment of pancreatic β cells (84, 85). BPA is known as an endocrine disruptor, affecting the hormonal system and, as it was mentioned before, modifying cellular metabolism. Very importantly, BPA not only affects pancreatic β-cells but can modify glucagon secretion produced by α cells because of a switch in β to α cell ratio transition. Then, BPA is considered to affect the endocrine pancreas (86, 87). BPA has a lipophilic nature and most of the receptors are intracellular including binding to specific hormonal receptors such as sex hormone receptors for estrogen (ER) and androgen (AR) as well as thyroid hormone receptor (TR) and glucocorticoid receptor (GR). However, BPA can bind to other receptors located in the membrane such as the membrane estrogen receptor (mER) and G protein-coupled receptor (GPR30) (88). Very importantly, pancreatic β cell function is mediated by ERα and ERβ in response to BPA altering the expression and function of different ion channel (89).

Another important group of toxic metabolites is the exposition to heavy metals including cadmium, zinc, inorganic arsenite, manganese affecting to glucose homeostasis increasing the risk to suffer diabetes (90). For instance, the effect of cadmium is through an accumulation of lipids and an increase in both inflammation and in insulin secretion (91) and inducing the activation of c-Jun N-terminal kinases (JNK) and apoptosis (92). Arsenite is another toxic metabolite that is even more toxic than cadmium or manganese, because of its capacity to regulate miR-146A, controlled by nuclear factor-kB (NF-kB). In addition, arsenite downregulates the calcium-dependent protein kinase (CAMK2a), which regulates insulin secretion (93). Glucocorticoids are a group of steroids which are secreted by the adrenal cortex in our body and it is involved in the degradation and mobilization of stored energy involved in tissue repair, metabolic processes and many other functions. Glucocorticoids facilitate the appearance of insulin resistance and diabetes (94, 95). Furthermore, dioxins are other group of pollutants generates pancreatic β cell dysfunction (96). There are several mechanisms involved in pancreatic β cell toxicity produced by dioxins that have been reviewed very recently (97).

Prevention of beta cell dysfunction by polyphenols

Although there are multiple types of natural products, polyphenols represent more than 8000 compounds found in plants, presenting high evidence of its protective role in different metabolic and neurodegenerative diseases (98, 99). Polyphenols are a group of natural products that exert their antidiabetic effects *via* a variety of mechanisms which have been extensively studied and include an improvement in mitochondrial function by scavenging ROS which reduces oxidative damage. These treatments have in common an increase in mitochondrial function and biogenesis by the modulation of several pathways, including AMPK, SIRT1 and NRF-1 targets. One of the mechanisms involved in the protection of these compounds is

the enhancement of autophagic activity, alleviating the ER stress and mitochondrial dysfunction provoked by the accumulation of misfolded proteins in these cells (100). Polyphenols represent a promising chemical group for the prevention and treatment of several metabolic diseases such as T2DM. But, these compounds have additional properties such as regenerative capacity. This is important since, apart from avoiding its disappearance, it is possible to mediate an increase in the number of cells, having supplemental beneficial consequences (101).

As it was mentioned before, mTORC1 hyperactivation is a key event in the progression to T2DM. There is abundant evidence that important mechanisms involved in the protective effects of these polyphenols against the decline of β-cells have also been linked to autophagy enhancement, related to mTORC1 inhibition, with or without implication of AMPK activation. Then, mTORC1 downregulation through AMPK-dependent and AMPK-independent mechanisms are essential in the survival of pancreatic β cells. Different natural products have been involved in its modulation and hence, regulating the protective effect of autophagy including resveratrol, curcumin, ECCG, punicalagin, oleuropein and many others. Although many compounds have been studied, one of the best characterized molecules is resveratrol by the use of a great variety of approaches and very recently reviewed in (98). Regarding *in vitro* studies, resveratrol inhibits mTORC1 signaling pathway by the modulation of the acetylation status of TSC2 (102). Very recently this mechanism has been corroborated *in vivo*, avoiding lipid accumulation in the liver combating obesity and complications of diabetes (103). Autophagy promotes β-cell survival by enabling adaptive responses to alleviate ER stress, mitochondrial dysfunction and oxidative stress. In fact, there are many papers suggesting that mitophagy enhancement is a potential mechanism to preserve β-cell function and delay the progression of T2DM (104). Another important molecule involved in pancreatic β cell failure in T2DM is human amylin (hIAPP). hIAPP is a protein co-secreted with insulin by pancreatic β cells and possesses a higher propensity to misfold and aggregate inside these cells. This propensity is especially higher when there is an increase in insulin synthesis demand, which occurs during the progression to T2DM, a long period of time with a characteristic insulin resistance and an mTORC1 hyperactivity (28). Under these conditions, autophagy activation has protective effects and inhibits pancreatic β cell death, being a natural defense (42, 43). Flavonoids have also been involved in the protection of the deleterious effects of hIAPP aggregates in these cells (105–109). Apart from the actions of flavonoids already explained, flavonoids have been also involved in an increase in antioxidant enzymes, as a protective mechanism (110, 111). Very importantly, flavonoids are also important regulators of the aging process theyself, affecting not only diabetes but different age-associated diseases (112).

Altogether, there are several molecular mechanisms involved in β cell dysfunction and apoptosis, being some of the most important those depicted in Figure 1. This figure also shows the beneficial effects of some polyphenols in pancreatic β cells,

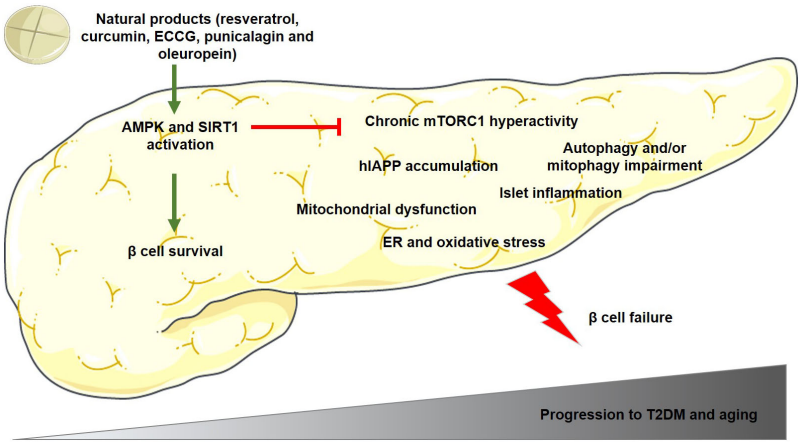

FIGURE 1
Main mechanisms involved in pancreatic β cell dysfunction and apoptosis during the progression to T2DM and/or aging. The polyphenols mentioned in this figure have been demonstrated to activate AMPK and SIRT1 proteins in β cells, which reduces mTORC1 hyperactivation and β cell failure, and as a consequence, preventing the onset and progression of T2DM. Green arrows indicate activation and red lines indicate inhibition of the activity of the target protein. AMPK, adenosine monophosphate (AMP)-activated protein kinase; ECCG, Epigallocatechin gallate; ER, endoplasmic reticulum; human amylin, hIAPP; mTORC1, mammalian/mechanistic target of rapamycin complex 1; SIRT1, sirtuin-1; T2DM, type 2 diabetes mellitus.

increasing cell survival and preventing the onset and progression of T2DM.

Conclusion

In this review, the main contributors to pancreatic beta cell failure as well as the key protective mechanisms of different polyphenols that interfere with the different mediators of pancreatic beta cell dysfunction in the progression to T2DM have been summarized. Although many distinct signaling pathways have been described, it is essential a better and more profound understanding of the pathophysiology of the disease in order to obtain better treatments to maintain and protect pancreatic beta cells for longer periods of time, prolonging its lifespan and avoiding the appearance of diabetes.

Author contributions

Both AG-A and CG have contributed to the writing as well as to the discussion of the manuscript. All authors contributed to the article and approved the submitted version.

Funding

This work was supported by grants PID2020-113361RB-I00 from Ministerio de Ciencia e Innovación and CIBER de Diabetes y Enfermedades Metabólicas Asociadas, Instituto de Salud Carlos III (Spain), to CG.

Conflict of interest

The authors declare that the research was conducted in the absence of any commercial or financial relationships that could be construed as a potential conflict of interest.

Publisher's note

All claims expressed in this article are solely those of the authors and do not necessarily represent those of their affiliated organizations, or those of the publisher, the editors and the reviewers. Any product that may be evaluated in this article, or claim that may be made by its manufacturer, is not guaranteed or endorsed by the publisher.

References

1. Ashcroft FM, Rorsman P. Diabetes mellitus and the beta cell: The last ten years. *Cell* (2012) 148(6):1160–71. doi: 10.1016/j.cell.2012.02.010

2. Chan CB, De Leo D, Joseph JW, McQuaid TS, Ha XF, Xu F, et al. Increased uncoupling protein-2 levels in beta-cells are associated with impaired glucose-stimulated insulin secretion: Mechanism of action. *Diabetes* (2001) 50(6):1302–10. doi: 10.2337/diabetes.50.6.1302

3. Anello M, Lupi R, Spampinato D, Piro S, Masini M, Boggi U, et al. Functional and morphological alterations of mitochondria in pancreatic beta cells from type 2 diabetic patients. *Diabetologia* (2005) 48(2):282–9. doi: 10.1007/s00125-004-1627-9

4. Henquin JC. Triggering and amplifying pathways of regulation of insulin secretion by glucose. *Diabetes* (2000) 49(11):1751–60. doi: 10.2337/diabetes.49.11.1751

5. Bordone L, Motta MC, Picard F, Robinson A, Jhala US, Apfeld J, et al. Sirt1 regulates insulin secretion by repressing Ucp2 in pancreatic beta cells. *PloS Biol* (2006) 4(2):e31. doi: 10.1371/journal.pbio.0040031

6. Robson-Doucette CA, Sultan S, Allister EM, Wikstrom JD, Koshkin V, Bhattacharjee A, et al. Beta-cell uncoupling protein 2 regulates reactive oxygen species production, which influences both insulin and glucagon secretion. *Diabetes* (2011) 60(11):2710–9. doi: 10.2337/db11-0132

7. Lameloise N, Muzzin P, Prentki M, Assimacopoulos-Jeannet F. Uncoupling protein 2: A possible link between fatty acid excess and impaired glucose-induced insulin secretion? *Diabetes* (2001) 50(4):803–9. doi: 10.2337/diabetes.50.4.803

8. Oh YS, Bae GD, Baek DJ, Park EY, Jun HS. Fatty acid-induced lipotoxicity in pancreatic beta-cells during development of type 2 diabetes. *Front Endocrinol (Lausanne)* (2018) 9:384. doi: 10.3389/fendo.2018.00384

9. Lytrivi M, Castell AL, Poitout V, Cnop M. Recent insights into mechanisms of beta-cell lipo- and glucolipotoxicity in type 2 diabetes. *J Mol Biol* (2020) 432 (5):1514–34. doi: 10.1016/j.jmb.2019.09.016

10. Fonseca SG, Gromada J, Urano F. Endoplasmic reticulum stress and pancreatic beta-cell death. *Trends Endocrinol Metab* (2011) 22(7):266–74. doi: 10.1016/j.tem.2011.02.008

11. Kanatsuka A, Kou S, Makino H. Iapp/Amylin and beta-cell failure: Implication of the risk factors of type 2 diabetes. *Diabetol Int* (2018) 9(3):143–57. doi: 10.1007/s13340-018-0347-1

12. Keane KN, Cruzat VF, Carlessi R, de Bittencourt PIJr., Newsholme P. Molecular events linking oxidative stress and inflammation to insulin resistance and beta-cell dysfunction. *Oxid Med Cell Longev* (2015) 2015:181643. doi: 10.1155/2015/181643

13. Hara T, Mahadevan J, Kanekura K, Hara M, Lu S, Urano F. Calcium efflux from the endoplasmic reticulum leads to beta-cell death. *Endocrinology* (2014) 155 (3):758–68. doi: 10.1210/en.2013-1519

14. QiNan W, XiaGuang G, XiaoTian L, WuQuan D, Ling Z, Bing C. Par-4/Nf-Kappab mediates the apoptosis of islet beta cells induced by glucolipotoxicity. *J Diabetes Res* (2016) 2016:4692478. doi: 10.1155/2016/4692478

15. Cnop M, Toivonen S, Igoillo-Esteve M, Salpea P. Endoplasmic reticulum stress and Eif2alpha phosphorylation: The Achilles heel of pancreatic beta cells. *Mol Metab* (2017) 6(9):1024–39. doi: 10.1016/j.molmet.2017.06.001

16. Zhang IX, Raghavan M, Satin LS. The endoplasmic reticulum and calcium homeostasis in pancreatic beta cells. *Endocrinology* (2020) 161(2):1–14. doi: 10.1210/endocr/bqz028

17. Cerf ME. Developmental programming and glucolipotoxicity: Insights on beta cell inflammation and diabetes. *Metabolites* (2020) 10(11):444. doi: 10.3390/metabo10110444

18. Delepine M, Nicolino M, Barrett T, Golamaully M, Lathrop GM, Julier C. Eif2ak3, encoding translation initiation factor 2-alpha kinase 3, is mutated in patients with Wolcott-rallison syndrome. *Nat Genet* (2000) 25(4):406–9. doi: 10.1038/78085

19. Wang R, Munoz EE, Zhu S, McGrath BC, Cavener DR. Perk gene dosage regulates glucose homeostasis by modulating pancreatic beta-cell functions. *PloS One* (2014) 9(6):e99684. doi: 10.1371/journal.pone.0099684

20. Fonseca SG, Fukuma M, Lipson KL, Nguyen LX, Allen JR, Oka Y, et al. Wfs1 is a novel component of the unfolded protein response and maintains homeostasis of the endoplasmic reticulum in pancreatic beta-cells. *J Biol Chem* (2005) 280 (47):39609–15. doi: 10.1074/jbc.M507426200

21. Morikawa S, Blacher L, Onwumere C, Urano F. Loss of function of Wfs1 causes er stress-mediated inflammation in pancreatic beta-cells. *Front Endocrinol (Lausanne)* (2022) 13:849204. doi: 10.3389/fendo.2022.849204

22. Westermark P, Andersson A, Westermark GT. Islet amyloid polypeptide, islet amyloid, and diabetes mellitus. *Physiol Rev* (2011) 91(3):795–826. doi: 10.1152/physrev.00042.2009

23. Morikawa S, Kaneko N, Okumura C, Taguchi H, Kurata M, Yamamoto T, et al. Iapp/Amylin deposition, which is correlated with expressions of asc and il-1beta in beta-cells of langerhans' islets, directly initiates Nlrp3 inflammasome activation. *Int J Immunopathol Pharmacol* (2018) 32:1–10. doi: 10.1177/2058738418788749

24. Lim YA, Rhein V, Baysang G, Meier F, Poljak A, Raftery MJ, et al. Abeta and human amylin share a common toxicity pathway *Via* mitochondrial dysfunction. *Proteomics* (2010) 10(8):1621–33. doi: 10.1002/pmic.200900651

25. Huang CJ, Lin CY, Haataja L, Gurlo T, Butler AE, Rizza RA, et al. High expression rates of human islet amyloid polypeptide induce endoplasmic reticulum stress mediated beta-cell apoptosis, a characteristic of humans with type 2 but not type 1 diabetes. *Diabetes* (2007) 56(8):2016–27. doi: 10.2337/db07-0197

26. Hernandez MG, Aguilar AG, Burillo J, Oca RG, Manca MA, Novials A, et al. Pancreatic beta cells overexpressing hiapp impaired mitophagy and unbalanced mitochondrial dynamics. *Cell Death Dis* (2018) 9(5):481. doi: 10.1038/s41419-018-0533-x

27. Cerf ME. Beta cell dysfunction and insulin resistance. *Front Endocrinol (Lausanne)* (2013) 4:37. doi: 10.3389/fendo.2013.00037

28. Guillen C, Benito M. Mtorc1 overactivation as a key aging factor in the progression to type 2 diabetes mellitus. *Front Endocrinol (Lausanne)* (2018) 9:621. doi: 10.3389/fendo.2018.00621

29. Bartolome A, Kimura-Koyanagi M, Asahara S, Guillen C, Inoue H, Teruyama K, et al. Pancreatic beta-cell failure mediated by Mtorc1 hyperactivity and autophagic impairment. *Diabetes* (2014) 63(9):2996–3008. doi: 10.2337/db13-0970

30. Ardestani A, Lupse B, Kido Y, Leibowitz G, Maedler K. Mtorc1 signaling: A double-edged sword in diabetic beta cells. *Cell Metab* (2018) 27(2):314–31. doi: 10.1016/j.cmet.2017.11.004

31. Murrow L, Debnath J. Autophagy as a stress-response and quality-control mechanism: Implications for cell injury and human disease. *Annu Rev Pathol* (2013) 8:105–37. doi: 10.1146/annurev-pathol-020712-163918

32. Kocaturk NM, Gozuacik D. Crosstalk between mammalian autophagy and the ubiquitin-proteasome system. *Front Cell Dev Biol* (2018) 6:128. doi: 10.3389/fcell.2018.00128

33. Abdrakhmanov A, Gogvadze V, Zhivotovsky B. To eat or to die: Deciphering selective forms of autophagy. *Trends Biochem Sci* (2020) 45(4):347–64. doi: 10.1016/j.tibs.2019.11.006

34. Horan MP, Pichaud N, Ballard JW. Review: Quantifying mitochondrial dysfunction in complex diseases of aging. *J Gerontol A Biol Sci Med Sci* (2012) 67 (10):1022–35. doi: 10.1093/gerona/glr263

35. Hubbard VM, Valdor R, Macian F, Cuervo AM. Selective autophagy in the maintenance of cellular homeostasis in aging organisms. *Biogerontology* (2012) 13 (1):21–35. doi: 10.1007/s10522-011-9331-x

36. Ebato C, Uchida T, Arakawa M, Komatsu M, Ueno T, Komiya K, et al. Autophagy is important in islet homeostasis and compensatory increase of beta cell mass in response to high-fat diet. *Cell Metab* (2008) 8(4):325–32. doi: 10.1016/j.cmet.2008.08.009

37. Sheng Q, Xiao X, Prasadan K, Chen C, Ming Y, Fusco J, et al. Autophagy protects pancreatic beta cell mass and function in the setting of a high-fat and high-glucose diet. *Sci Rep* (2017) 7(1):16348. doi: 10.1038/s41598-017-16485-0

38. Wu JJ, Quijano C, Chen E, Liu H, Cao L, Fergusson MM, et al. Mitochondrial dysfunction and oxidative stress mediate the physiological impairment induced by the disruption of autophagy. *Aging (Albany N Y)* (2009) 1(4):425–37. doi: 10.18632/aging.100038

39. Bartolome A, Guillen C, Benito M. Autophagy plays a protective role in endoplasmic reticulum stress-mediated pancreatic beta cell death. *Autophagy* (2012) 8(12):1757–68. doi: 10.4161/auto.21994

40. Marasco MR, Linnemann AK. Beta-cell autophagy in diabetes pathogenesis. *Endocrinology* (2018) 159(5):2127–41. doi: 10.1210/en.2017-03273

41. Lee YH, Kim J, Park K, Lee MS. Beta-cell autophagy: Mechanism and role in beta-cell dysfunction. *Mol Metab* (2019) 27S:S92–S103. doi: 10.1016/j.molmet.2019.06.014

42. Shigihara N, Fukunaka A, Hara A, Komiya K, Honda A, Uchida T, et al. Human iapp-induced pancreatic beta cell toxicity and its regulation by autophagy. *J Clin Invest* (2014) 124(8):3634–44. doi: 10.1172/JCI69866

43. Rivera JF, Costes S, Gurlo T, Glabe CG, Butler PC. Autophagy defends pancreatic beta cells from human islet amyloid polypeptide-induced toxicity. *J Clin Invest* (2014) 124(8):3489–500. doi: 10.1172/JCI71981

44. Kim J, Park K, Kim MJ, Lim H, Kim KH, Kim SW, et al. An autophagy enhancer ameliorates diabetes of human iapp-transgenic mice through clearance of amyloidogenic oligomer. *Nat Commun* (2021) 12(1):183. doi: 10.1038/s41467-020-20454-z

45. Pickrell AM, Youle RJ. The roles of Pink1, parkin, and mitochondrial fidelity in parkinson's disease. *Neuron* (2015) 85(2):257–73. doi: 10.1016/j.neuron.2014.12.007

46. Hoshino A, Ariyoshi M, Okawa Y, Kaimoto S, Uchihashi M, Fukai K, et al. Inhibition of P53 preserves parkin-mediated mitophagy and pancreatic beta-cell function in diabetes. *Proc Natl Acad Sci U.S.A.* (2014) 111(8):3116–21. doi: 10.1073/pnas.1318951111

47. Sidarala V, Pearson GL, Parekh VS, Thompson B, Christen L, Gingerich MA, et al. Mitophagy protects beta cells from inflammatory damage in diabetes. *JCI Insight* (2020) 5(24):e141138. doi: 10.1172/jci.insight.141138

48. Hernando-Rodriguez B, Artal-Sanz M. Mitochondrial quality control mechanisms and the phb (Prohibitin) complex. *Cells* (2018) 7(12):238. doi: 10.3390/cells7120238

49. Lahiri V, Klionsky DJ. Phb2/Prohibitin 2: An inner membrane mitophagy receptor. *Cell Res* (2017) 27(3):311–2. doi: 10.1038/cr.2017.23

50. Supale S, Thorel F, Merkwirth C, Gjinovci A, Herrera PL, Scorrano L, et al. Loss of prohibitin induces mitochondrial damages altering beta-cell function and survival and is responsible for gradual diabetes development. *Diabetes* (2013) 62 (10):3488–99. doi: 10.2337/db13-0152

51. Jennings RE, Berry AA, Kirkwood-Wilson R, Roberts NA, Hearn T, Salisbury RJ, et al. Development of the human pancreas from foregut to endocrine commitment. *Diabetes* (2013) 62(10):3514–22. doi: 10.2337/db12-1479

52. Zhu Y, Liu Q, Zhou Z, Ikeda Y. Pdx1, neurogenin-3, and mafa: Critical transcription regulators for beta cell development and regeneration. *Stem Cell Res Ther* (2017) 8(1):240. doi: 10.1186/s13287-017-0694-z

53. Zhu X, Oguh A, Gingerich MA, Soleimanpour SA, Stoffers DA, Gannon M. Cell cycle regulation of the Pdx1 transcription factor in developing pancreas and insulin-producing beta-cells. *Diabetes* (2021) 70(4):903–16. doi: 10.2337/db20-0599

54. Soleimanpour SA, Ferrari AM, Raum JC, Groff DN, Yang J, Kaufman BA, et al. Diabetes susceptibility genes Pdx1 and Clec16a function in a pathway regulating mitophagy in beta-cells. *Diabetes* (2015) 64(10):3475–84. doi: 10.2337/db15-0376

55. Gauthier BR, Wiederkehr A, Baquie M, Dai C, Powers AC, Kerr-Conte J, et al. Pdx1 deficiency causes mitochondrial dysfunction and defective insulin secretion through tfam suppression. *Cell Metab* (2009) 10(2):110–8. doi: 10.1016/j.cmet.2009.07.002

56. Zheng L, Wang Y, Li Y, Li L, Wang X, Li Y. Mir-765 targeting Pdx1 impairs pancreatic beta-cell function to induce type 2 diabetes. *Arch Physiol Biochem* (2021) 127:1–10. doi: 10.1080/13813455.2021.1946561

57. Meyer JN, Leuthner TC, Luz AL. Mitochondrial fusion, fission, and mitochondrial toxicity. *Toxicology* (2017) 391:42–53. doi: 10.1016/j.tox.2017.07.019

58. Bernhardt D, Muller M, Reichert AS, Osiewacz HD. Simultaneous impairment of mitochondrial fission and fusion reduces mitophagy and shortens replicative lifespan. *Sci Rep* (2015) 5:7885. doi: 10.1038/srep07885

59. Twig G, Elorza A, Molina AJ, Mohamed H, Wikstrom JD, Walzer G, et al. Fission and selective fusion govern mitochondrial segregation and elimination by autophagy. *EMBO J* (2008) 27(2):433–46. doi: 10.1038/sj.emboj.7601963

60. Park KS, Wiederkehr A, Kirkpatrick C, Mattenberger Y, Martinou JC, Marchetti P, et al. Selective actions of mitochondrial Fission/Fusion genes on metabolism-secretion coupling in insulin-releasing cells. *J Biol Chem* (2008) 283 (48):33347–56. doi: 10.1074/jbc.M806251200

61. Molina AJ, Wikstrom JD, Stiles L, Las G, Mohamed H, Elorza A, et al. Mitochondrial networking protects beta-cells from nutrient-induced apoptosis. *Diabetes* (2009) 58(10):2303–15. doi: 10.2337/db07-1781

62. Schultz J, Waterstradt R, Kantowski T, Rickmann A, Reinhardt F, Sharoyko V, et al. Precise expression of Fis1 is important for glucose responsiveness of beta cells. *J Endocrinol* (2016) 230(1):81–91. doi: 10.1530/JOE-16-0111

63. Reinhardt F, Schultz J, Waterstradt R, Baltrusch S. Drp1 guarding of the mitochondrial network is important for glucose-stimulated insulin secretion in pancreatic beta cells. *Biochem Biophys Res Commun* (2016) 474(4):646–51. doi: 10.1016/j.bbrc.2016.04.142

64. Bhansali S, Bhansali A, Walia R, Saikia UN, Dhawan V. Alterations in mitochondrial oxidative stress and mitophagy in subjects with prediabetes and type 2 diabetes mellitus. *Front Endocrinol (Lausanne)* (2017) 8:347. doi: 10.3389/fendo.2017.00347

65. Miki A, Ricordi C, Sakuma Y, Yamamoto T, Misawa R, Mita A, et al. Divergent antioxidant capacity of human islet cell subsets: A potential cause of beta-cell vulnerability in diabetes and islet transplantation. *PloS One* (2018) 13(5): e0196570. doi: 10.1371/journal.pone.0196570

66. Leloup C, Tourrel-Cuzin C, Magnan C, Karaca M, Castel J, Carneiro L, et al. Mitochondrial reactive oxygen species are obligatory signals for glucose-induced insulin secretion. *Diabetes* (2009) 58(3):673–81. doi: 10.2337/db07-1056

67. Pi J, Collins S. Reactive oxygen species and uncoupling protein 2 in pancreatic beta-cell function. *Diabetes Obes Metab* (2010) 12 Suppl 2:141–8. doi: 10.1111/j.1463-1326.2010.01269.x

68. Zorov DB, Juhaszova M, Sollott SJ. Mitochondrial reactive oxygen species (Ros) and ros-induced ros release. *Physiol Rev* (2014) 94(3):909–50. doi: 10.1152/physrev.00026.2013

69. Ma ZA. The role of peroxidation of mitochondrial membrane phospholipids in pancreatic beta -cell failure. *Curr Diabetes Rev* (2012) 8(1):69–75. doi: 10.2174/157339912798829232

70. Kagan VE, Tyurin VA, Jiang J, Tyurina YY, Ritov VB, Amoscato AA, et al. Cytochrome c acts as a cardiolipin oxygenase required for release of proapoptotic factors. *Nat Chem Biol* (2005) 1(4):223–32. doi: 10.1038/nchembio727

71. Zhao Z, Zhang X, Zhao C, Choi J, Shi J, Song K, et al. Protection of pancreatic beta-cells by group *Via* phospholipase a(2)-mediated repair of mitochondrial membrane peroxidation. *Endocrinology* (2010) 151(7):3038–48. doi: 10.1210/en.2010-0016

72. Cole LK, Agarwal P, Doucette CA, Fonseca M, Xiang B, Sparagna GC, et al. Tafazzin deficiency reduces basal insulin secretion and mitochondrial function in pancreatic islets from Male mice. *Endocrinology* (2021) 162(7):bqab102. doi: 10.1210/endocr/bqab102

73. Fex M, Nicholas LM, Vishnu N, Medina A, Sharoyko VV, Nicholls DG, et al. The pathogenetic role of beta-cell mitochondria in type 2 diabetes. *J Endocrinol* (2018) 236(3):R145–R59. doi: 10.1530/JOE-17-0367

74. Sharoyko VV, Abels M, Sun J, Nicholas LM, Mollet IG, Stamenkovic JA, et al. Loss of Tfb1m results in mitochondrial dysfunction that leads to impaired insulin secretion and diabetes. *Hum Mol Genet* (2014) 23(21):5733–49. doi: 10.1093/hmg/ddu288

75. Koeck T, Olsson AH, Nitert MD, Sharoyko VV, Ladenvall C, Kotova O, et al. A common variant in Tfb1m is associated with reduced insulin secretion and increased future risk of type 2 diabetes. *Cell Metab* (2011) 13(1):80–91. doi: 10.1016/j.cmet.2010.12.007

76. Nicholas LM, Valtat B, Medina A, Andersson L, Abels M, Mollet IG, et al. Mitochondrial transcription factor B2 is essential for mitochondrial and cellular function in pancreatic beta-cells. *Mol Metab* (2017) 6(7):651–63. doi: 10.1016/j.molmet.2017.05.005

77. Stiles L, Shirihai OS. Mitochondrial dynamics and morphology in beta-cells. *Best Pract Res Clin Endocrinol Metab* (2012) 26(6):725–38. doi: 10.1016/j.beem.2012.05.004

78. Lu H, Koshkin V, Allister EM, Gyulkhandanyan AV, Wheeler MB. Molecular and metabolic evidence for mitochondrial defects associated with beta-cell dysfunction in a mouse model of type 2 diabetes. *Diabetes* (2010) 59 (2):448–59. doi: 10.2337/db09-0129

79. Silva JP, Kohler M, Graff C, Oldfors A, Magnuson MA, Berggren PO, et al. Impaired insulin secretion and beta-cell loss in tissue-specific knockout mice with mitochondrial diabetes. *Nat Genet* (2000) 26(3):336–40. doi: 10.1038/81649

80. Gerencser AA. Bioenergetic analysis of single pancreatic beta-cells indicates an impaired metabolic signature in type 2 diabetic subjects. *Endocrinology* (2015) 156(10):3496–503. doi: 10.1210/en.2015-1552

81. Weksler-Zangen S. Is type 2 diabetes a primary mitochondrial disorder? *Cells* (2022) 11(10):1617. doi: 10.3390/cells11101617

82. Lytrivi M, Igoillo-Esteve M, Cnop M. Inflammatory stress in islet beta-cells: Therapeutic implications for type 2 diabetes? *Curr Opin Pharmacol* (2018) 43:40–5. doi: 10.1016/j.coph.2018.08.002

83. Sha W, Hu F, Bu S. Mitochondrial dysfunction and pancreatic islet beta-cell failure (Review). *Exp Ther Med* (2020) 20(6):266. doi: 10.3892/etm.2020.9396

84. Weldingh NM, Jorgensen-Kaur L, Becher R, Holme JA, Bodin J, Nygaard UC, et al. Bisphenol a is more potent than phthalate metabolites in reducing pancreatic beta-cell function. *BioMed Res Int* (2017) 2017:4614379. doi: 10.1155/2017/4614379

85. Howard SG. Developmental exposure to endocrine disrupting chemicals and type 1 diabetes mellitus. *Front Endocrinol (Lausanne)* (2018) 9:513. doi: 10.3389/fendo.2018.00513

86. Ropero AB, Alonso-Magdalena P, Garcia-Garcia E, Ripoll C, Fuentes E, Nadal A. Bisphenol-a disruption of the endocrine pancreas and blood glucose homeostasis. *Int J Androl* (2008) 31(2):194–200. doi: 10.1111/j.1365-2605.2007.00832.x

87. Banerjee O, Singh S, Saha I, Pal S, Banerjee M, Kundu S, et al. Molecular dissection of cellular response of pancreatic islet cells to bisphenol-a (Bpa): A comprehensive review. *Biochem Pharmacol* (2022) 201:115068. doi: 10.1016/j.bcp.2022.115068

88. Cimmino I, Fiory F, Perruolo G, Miele C, Beguinot F, Formisano P, et al. Potential mechanisms of bisphenol a (Bpa) contributing to human disease. *Int J Mol Sci* (2020) 21(16):5761. doi: 10.3390/ijms21165761

89. Martinez-Pinna J, Marroqui L, Hmadcha A, Lopez-Beas J, Soriano S, Villar-Pazos S, et al. Oestrogen receptor beta mediates the actions of bisphenol-a on ion channel expression in mouse pancreatic beta cells. *Diabetologia* (2019) 62(9):1667–80. doi: 10.1007/s00125-019-4925-y

90. Dover EN, Patel NY, Styblo M. Impact of *in vitro* heavy metal exposure on pancreatic beta-cell function. *Toxicol Lett* (2018) 299:137–44. doi: 10.1016/j.toxlet.2018.09.015

91. Hong H, Xu Y, Xu J, Zhang J, Xi Y, Pi H, et al. Cadmium exposure impairs pancreatic beta-cell function and exaggerates diabetes by disrupting lipid metabolism. *Environ Int* (2021) 149:106406. doi: 10.1016/j.envint.2021.106406

92. Huang CC, Kuo CY, Yang CY, Liu JM, Hsu RJ, Lee KI, et al. Cadmium exposure induces pancreatic beta-cell death *Via* a Ca(2+)-triggered Jnk/Chop-related apoptotic signaling pathway. *Toxicology* (2019) 425:152252. doi: 10.1016/j.tox.2019.152252

93. Beck R, Chandi M, Kanke M, Styblo M, Sethupathy P. Arsenic is more potent than cadmium or manganese in disrupting the ins-1 beta cell microrna landscape. *Arch Toxicol* (2019) 93(11):3099–109. doi: 10.1007/s00204-019-02574-8

94. Beaupere C, Liboz A, Feve B, Blondeau B, Guillemain G. Molecular mechanisms of glucocorticoid-induced insulin resistance. *Int J Mol Sci* (2021) 22 (2):623. doi: 10.3390/ijms22020623

95. Rafacho A, Ortsater H, Nadal A, Quesada I. Glucocorticoid treatment and endocrine pancreas function: Implications for glucose homeostasis, insulin resistance and diabetes. *J Endocrinol* (2014) 223(3):R49–62. doi: 10.1530/JOE-14-0373

96. De Tata V. Association of dioxin and other persistent organic pollutants (Pops) with diabetes: Epidemiological evidence and new mechanisms of beta cell dysfunction. *Int J Mol Sci* (2014) 15(5):7787–811. doi: 10.3390/ijms15057787

97. Hoyeck MP, Matteo G, MacFarlane EM, Perera I, Bruin JE. Persistent organic pollutants and beta-cell toxicity: A comprehensive review. *Am J Physiol Endocrinol Metab* (2022) 322(5):E383–413. doi: 10.1152/ajpendo.00358.2021

98. Garcia-Aguilar A, Palomino O, Benito M, Guillen C. Dietary polyphenols in metabolic and neurodegenerative diseases: Molecular targets in autophagy and biological effects. *Antioxid (Basel)* (2021) 10(2):142. doi: 10.3390/antiox10020142

99. Oh YS. Plant-derived compounds targeting pancreatic beta cells for the treatment of diabetes. *Evid Based Complement Alternat Med* (2015) 2015:629863. doi: 10.1155/2015/629863

100. Brimson JM, Prasanth MI, Malar DS, Thitilertdecha P, Kabra A, Tencomnao T, et al. Plant polyphenols for aging health: Implication from their autophagy modulating properties in age-associated diseases. *Pharm (Basel)* (2021) 14(10):982. doi: 10.3390/ph14100982

101. Semwal DK, Kumar A, Aswal S, Chauhan A, Semwal RB. Protective and therapeutic effects of natural products against diabetes mellitus *Via* regenerating pancreatic beta-cells and restoring their dysfunction. *Phytother Res* (2021) 35 (3):1218–29. doi: 10.1002/ptr.6885

102. Garcia-Aguilar A, Guillen C, Nellist M, Bartolome A, Benito M. Tsc2 n-terminal lysine acetylation status affects to its stability modulating Mtorc1 signaling and autophagy. *Biochim Biophys Acta* (2016) 1863(11):2658–67. doi: 10.1016/j.bbamcr.2016.08.006

103. Han HS, Kim SG, Kim YS, Jang SH, Kwon Y, Choi D, et al. A novel role of Crtc2 in promoting nonalcoholic fatty liver disease. *Mol Metab* (2022) 55:101402. doi: 10.1016/j.molmet.2021.101402

104. Shan Z, Fa WH, Tian CR, Yuan CS, Jie N. Mitophagy and mitochondrial dynamics in type 2 diabetes mellitus treatment. *Aging (Albany N Y)* (2022) 14 (6):2902–19. doi: 10.18632/aging.203969

105. Araujo AR, Reis RL, Pires RA. Natural polyphenols as modulators of the fibrillization of islet amyloid polypeptide. *Adv Exp Med Biol* (2020) 1250:159–76. doi: 10.1007/978-981-15-3262-7_11

106. Wang Y, Hu T, Wei J, Yin X, Gao Z, Li H. Inhibitory activities of flavonoids from scutellaria baicalensis georgi on amyloid aggregation related to type 2 diabetes and the possible structural requirements for polyphenol in inhibiting the

nucleation phase of hiapp aggregation. *Int J Biol Macromol* (2022) 215:531–40. doi: 10.1016/j.ijbiomac.2022.06.107

107. Nie T, Cooper GJS. Mechanisms underlying the antidiabetic activities of polyphenolic compounds: A review. *Front Pharmacol* (2021) 12:798329. doi: 10.3389/fphar.2021.798329

108. Abioye RO, Okagu OD, Udenigwe CC. Inhibition of islet amyloid polypeptide fibrillation by structurally diverse phenolic compounds and fibril disaggregation potential of rutin and quercetin. *J Agric Food Chem* (2022) 70 (1):392–402. doi: 10.1021/acs.jafc.1c06918

109. Alkahtane AA, Alghamdi HA, Almutairi B, Khan MM, Hasnain MS, Abdel-Daim MM, et al. Inhibition of human amylin aggregation by flavonoid chrysin: An *in-silico* and *in-vitro* approach. *Int J Med Sci* (2021) 18(1):199–206. doi: 10.7150/ijms.51382

110. Umeno A, Horie M, Murotomi K, Nakajima Y, Yoshida Y. Antioxidative and antidiabetic effects of natural polyphenols and isoflavones. *Molecules* (2016) 21 (6):708:112 (2176). doi: 10.3390/molecules21060708

111. Xiao JB, Hogger P. Dietary polyphenols and type 2 diabetes: Current insights and future perspectives. *Curr Med Chem* (2015) 22(1):23–38. doi: 10.2174/0929867321666140706130807

112. Fan X, Fan Z, Yang Z, Huang T, Tong Y, Yang D, et al. Flavonoids-natural gifts to promote health and longevity. *Int J Mol Sci* (2022) 23(4):2176. doi: 10.3390/ijms23042176

frontiers | Frontiers in Endocrinology

TYPE Original Research
PUBLISHED 28 November 2022
DOI 10.3389/fendo.2022.1058345

OPEN ACCESS

EDITED BY
Carlos Guillén,
Complutense University, Spain

REVIEWED BY
Mridusmita Saikia,
Cornell University, United States
Peter Thompson,
University of Manitoba, Canada

*CORRESPONDENCE
Arnaud Zaldumbide
a.zaldumbide@lumc.nl

†These authors have contributed equally to this work and share first authorship

‡These authors share senior authorship

SPECIALTY SECTION
This article was submitted to Diabetes: Molecular Mechanisms, a section of the journal Frontiers in Endocrinology

RECEIVED 30 September 2022
ACCEPTED 01 November 2022
PUBLISHED 28 November 2022

CITATION
Szymczak F, Cohen-Fultheim R, Thomaidou S, de Brachène AC, Castela A, Colli M, Marchetti P, Levanon E, Eizirik D and Zaldumbide A (2022) ADAR1-dependent editing regulates human β cell transcriptome diversity during inflammation. *Front. Endocrinol.* 13:1058345. doi: 10.3389/fendo.2022.1058345

ADAR1-dependent editing regulates human β cell transcriptome diversity during inflammation

Florian Szymczak[1†], Roni Cohen-Fultheim[2†], Sofia Thomaidou[3†], Alexandra Coomans de Brachène[1], Angela Castela[1], Maikel Colli[1], Piero Marchetti[4], Erez Levanon[2], Decio Eizirik[1‡] and Arnaud Zaldumbide[3*‡]

[1]ULB Center for Diabetes Research, Medical Faculty, Université Libre de Bruxelles, Brussels, Belgium, [2]Institute of Nanotechnology and Advanced Materials, Bar-Ilan University, Ramat Gan, Israel, [3]Department of Cell and Chemical Biology, Leiden University Medical Center, Leiden, Netherlands, [4]Department of Clinical and Experimental Medicine, University of Pisa, Pisa, Italy

Introduction: Enterovirus infection has long been suspected as a possible trigger for type 1 diabetes. Upon infection, viral double-stranded RNA (dsRNA) is recognized by membrane and cytosolic sensors that orchestrate type I interferon signaling and the recruitment of innate immune cells to the pancreatic islets. In this context, adenosine deaminase acting on RNA 1 (ADAR1) editing plays an important role in dampening the immune response by inducing adenosine mispairing, destabilizing the RNA duplexes and thus preventing excessive immune activation.

Methods: Using high-throughput RNA sequencing data from human islets and EndoC-βH1 cells exposed to IFNα or IFNγ/IL1β, we evaluated the role of ADAR1 in human pancreatic β cells and determined the impact of the type 1 diabetes pathophysiological environment on ADAR1-dependent RNA editing.

Results: We show that both IFNα and IFNγ/IL1β stimulation promote ADAR1 expression and increase the A-to-I RNA editing of Alu-Containing mRNAs in EndoC-βH1 cells as well as in primary human islets.

Discussion: We demonstrate that ADAR1 overexpression inhibits type I interferon response signaling, while ADAR1 silencing potentiates IFNα effects. In addition, ADAR1 overexpression triggers the generation of alternatively spliced mRNAs, highlighting a novel role for ADAR1 as a regulator of the β cell transcriptome under inflammatory conditions.

KEYWORDS

beta cell (β cell), inflammation, T1D (type 1 diabetes), transcriptome, RNA editing

Introduction

The type I interferon (IFN) response has recently been identified as a common signature for the development of autoimmunity (1). Induction of type I IFN (IFNα/β) following viral infection or endogenous release of mitochondrial genetic material is a highly regulated process in which pattern recognition receptors (PRR), such as MDA5, RIG-I and TLR3, act in concert to control inflammasome activation and the production of IFNα and IFNβ (2). In addition to this well-described sensing machinery, the adenosine-to-inosine conversion (A-to-I) catalyzed by the adenosine deaminase acting on RNA 1 (ADAR1) plays an important role in fine-tuning the innate immune response by destabilizing double-stranded RNA (dsRNA) duplexes and therefore reducing PRR substrate to limit further and potentially excessive inflammation (3).

ADAR1 exists as two isoforms that contain a central dsRNA binding domain and an enzymatic deaminase domain located in the C-terminal region. Both isoforms differ in localization (p110 remains mainly nuclear while p150 is expressed in the nucleus and cytosol) and by the presence of a nuclear export signal located in the N-terminus (4). ADAR1 has an essential role in modifying self-dsRNA formed by repetitive inverted elements, such as *Alu* short interspersed nuclear elements (SINE) elements, which inhibits the immune response triggered by the recognition of self-dsRNA by PRR.

Dysregulation of ADAR1 has been implicated in several interferonopathies, autoimmune diseases and tumor progression. Mutations within the RNA binding domain of ADAR1 alter both substrate affinity and specificity which affect RNA deamination and trigger the constitutive type I IFN response in Aicardi-Goutières syndrome (5). In contrast, high ADAR1 expression level has also been correlated with high tumor T-cell infiltrating lymphocytes (TIL) in breast cancer, and an increased amino acid substitution in the recognized antigens (a consequence of cytosine-to-uracil or adenosine-to-inosine editing at the RNA level) (6), demonstrating for the first time a role for RNA editing enzymes in the generation of tumor-specific neoantigens. Similarly, such processes have been proposed as a potential source of neoantigens involved in the development of autoimmune systemic lupus erythematosus (7).

In type 1 diabetes (T1D), increasing evidence indicate that local inflammation or other forms of stress combined with genetic predisposition leads to the generation and accumulation of aberrant or modified proteins to which central tolerance is lacking (8, 9). Examples of enzymatic deamidation or citrullination of self-antigens (e.g., proinsulin, C-peptide, GAD65, IA-2, GRP78, IAPP), as a consequence of activation of peptidyl arginine deiminase (PAD) or tissue transglutaminase (tTG) detected in pancreatic β cells in response to stress or primary islets from T1D patients, illustrate how the islet microenvironment can drive autoimmunity (10, 11).

RNA editing is a post-translational modification mediated by adenosine and cytosine deaminases which catalyzes the edition of a nucleotide into another in the context of an "editosome" (12). In addition to an amino acid change, RNA editing may enhance transcriptome complexity/diversity by directly changing splicing acceptor site motifs or altering splicing enhancer sequences with possible consequences for β cell immunogenicity (13, 14). In T1D, circulating T cells directed against alternative splice variants of GAD65, secretogranin V, CCNI-008, IAPP and Phogrin have been recently detected in patient blood samples and in the pancreatic islets (15).

To investigate the effect of the T1D pathophysiological inflammatory milieu on ADAR1 and the β cell transcriptome, we have analyzed high-throughput RNA sequencing data from human islets and EndoC-βH1 cells exposed to IFNα or IFNγ/IL1β, cytokines that contribute to the pathogenesis of T1D (16, 17). We demonstrate herein that inflammatory-mediated changes characteristic of early and late T1D development can trigger an increased A-to-I Alu editing rate. In addition, we demonstrate that ADAR1 not only dampens the innate immune response in β cells but also contributes to the transcriptome complexity with possible consequences for β cell function.

Materials and methods

Cell culture and treatment

EndoC-βH1 cells, kindly provided by Dr. Raphael Scharfmann (Paris Descartes University, France) (18), were maintained in low glucose DMEM supplemented with 5.5 µg/ml human transferrin, 10 mM Nicotinamide, 6.7 ng/ml Selenite, 50 µM β-mercaptoethanol, 2% human albumin, 100 units/ml penicillin and 100 µg/ml streptomycin. Cells were seeded in extracellular matrix, fibronectin pre-coated culture plates.

Preprocessing and alignment of RNA sequencing data for the editome analysis

Raw FASTQ quality was assessed using FastQC version 0.11.8 and PCR duplicates were removed with Super Deduper (19). Remaining reads were uniquely aligned to the reference genome (hg38 and mm10 assemblies) using STAR (20) version 2.7.3a with parameters –alignSJoverhangMin 8 –alignIntronMax 1000000 –alignMatesGapMax 600000 –outFilterMismatchNoverReadLmax 1 –outFilterMultimapNmax 1.

Alu editing index

RNA Editing Index (21) version 1.0 was used to assess the overall editing in *Alu* elements, respectively. This measure calculates the average editing level across all adenosines in repetitive elements weighted by their expression, thereby

quantifying the ratio of A-to-G mismatches over the total number of nucleotides aligned to repeats and comprising a global, robust measure of A-to-I RNA editing.

Quantification of expression

Abundance quantification was done using the quasi-mapping-based mode Salmon (21) (version 0.11.2) for human genome assembly hg38 with GENCODE version 24 and mouse genome assembly mm10 with GENCODE version 20. Gene expression analysis was later completed by using the tximport R package (version 1.12.3) to transfer Salmon's isoform-level abundances to gene-level abundances (22, 23).

RNA-sequencing and differential expression analysis

Total RNA was purified from EndoC-βH1 and EndoC-βH1/ADAR1 cells using the Nucleospin miRNA Kit (Bioke) according to the manufacturer's guidelines. RNA quality was determined by Experion RNA StdSens 1K Analysis Kit (Bio-Rad, product number 7007103) on a Experion Automated Electrophoresis System (Bio-Rad) following the manufacturer's protocol. Strand-specific bulk RNA sequencing was performed on a NovaSeq 6000 (2x150 paired-end with a depth of >150 million reads) by Eurofins Genomics Europe Sequencing GmbH (Konstanz, Germany). Reads were quality checked with fastp (24) to exclude reads of poor quality and remove remaining adapters. We used Salmon v1.3 (25) with additional parameters "–seqBias –gcBias –validateMappings" to quantify the gene and transcript expression. GENCODE was used as the reference genome and was indexed with default parameters. Differential Gene Expression (DGE) was performed with DESEq2 v.1.30.1 (26) with paired experiments included in the general linear model (i.e., ~ pairing + overexpression). For each gene, we obtained a $\log_2$ fold-change ($\log_2$FC), associated to an adjusted P value, which highlights the difference in gene expression between ADAR1-overexpressing cells and control cells. Gene Set Enrichment Analysis (GSEA) was performed using the above-generated DGE data with fGSEA (27). We pre-ranked genes according to the value of the Wald-test statistics provided by the DESeq2 output. Up- (enrichment) and down-regulated (depletion) pathways were considered significant when adj. P value < 0.05, regardless of their normalized enrichment score (Supplementary Data S1).

Gene-sets affected by alternative splicing were evaluated with clusterProfiler (28) with Gene Ontology as the reference (Supplementary Data S2).

RT-PCR

Total RNA was extracted from EndoC-βH1 using NucleoSpin Kit (#740609.50S, Bioke). Approximately 0.5ug of RNA was used for reverse transcription. Oligo (dT) primers were used in the reaction. For siRNA experiments, RNA was isolated using Dynabeads mRNA DIRECT purification kit (Invitrogen, Carlsbad, California, USA) and reverse transcribed using Reverse Transcriptase Core kit (Eurogentec, Liège, Belgium). Real-time PCR amplification was done with SsoAdvanced Universal SYBR Green Supermix (BIO-RAD, Hercules, California, USA) and amplicons were quantified using a standard curve. Expression of the transcript of interest was detected using the following primers: ADAR1-p150 Fw GAATCCGCGGCAGGGGTAT, ADAR1-p150 Rv: GCTTAA GCAGGAAACTACTGGG; ADAR1 endogenous Fw: CCGCACT GGCAGTCTCCGGGTG, ADAR1 endogenous Rv: CCTGGCCC AGGCTGCTGGTACC, INS Fw: AAGAGGCCATCAAGCAG ATCA, INS Rv: CAGGAGGCGCATCCACA, PDX1 Fw: CCATG GATGAAGTCTACCAAAGCT PDX1 Rv: CGTGAGATGTACTT GTTGAATAGGAACT, MAFA Fw: AGTCCTGCCGCTTCAAG, MAFA Rv: ACAGGTCCCGCTCTTTGG, NKX6.1 Fw: CTG GCCTGTACCCCTCATCA, NKX6.1 Rv: CTTCCCGTCTTT GTCCAACAA, GAPDH Fw: CCTGTTCGACAGTCAGCCG, GAPDH Rv: CGACCAAATCCGTTGACTCC; ACTIN Fw: CTG TACGCCAACACAGTGCT; ACTIN Rv: GCTCAGGAGGAGC AATGATC; STAT1 Fw: CACAAGGTGGCAGGATGTCT, STAT1 Rv: TCCCCGACTGAGCCTGATTA; MDA5 Fw: GTT GCTCACAGTGGTTCAGG; MDA5 Rv: GCTTGGCAATA TTTCTCTTGGT; IFNB Fw: AGGACAGGATGAACTTTGAC; IFNb Rv: TGATAGACATTAGCCAGGAG; IFIT1 fw: CAGAAT AGCCAGATCTCAGAGG; IFIT1 Rv: CCAGACTATCC TTGACCTGATG; CXCL10 Fw: AGTGGCATTCAAGGAGTA CC; CXCL10 Rv: TGATGGCCTTCGATTCTGGA

Western blot analyses

Cells were lysed in RIPA buffer supplemented with protease inhibitor cocktail (Roche). Protein quantification was performed with the BCA protein assay kit (Thermo Fisher Scientific). 25 µg protein extracts were loaded on 10% acrylamide/bis acrylamide SDS page gel. After electrophoresis, protein transfer was performed onto a nitrocellulose membrane (GE Healthcare). Membranes were stained with primary antibodies overnight at 4°C and secondary HRP conjugated antibodies (Santa Cruz Biotechnology) for 1 hour RT. Antibodies used were: anti-ADAR1 [#ab168809, Abcam (Figures 1, 2) and #14175, Cell Signaling Technology (Figure 3)], anti-STAT1 and anti-STAT2 (#14995 and #72604, Cell Signaling Technology) and as a loading control anti-actin (#0869100, MP Biomedicals) or anti-tubulin.

Lentiviruses production and transduction

The vectors were produced as described previously (29). Viral supernatants (MOI=2) were added to fresh medium

supplemented with 8 μg/mL Polybrene (Sigma-Aldrich), and the cells were incubated overnight. The next day, the medium was replaced with fresh medium. Transduction efficiency was analyzed 3–6 days after transduction.

RNA interference

EndoC-βH1 cells were transfected overnight with 30 nmol/L of siRNA and cells were kept in culture for 48 hours. Transfection was performed using siRNA targeting ADAR (5'-TTCCGTTACCGCAGGGATCTA-3'; 1027416, Qiagen, Venlo, The Netherlands) using Lipofectamine RNAiMax (Invitrogen, Carlsbad, CA, USA). Allstars Negative Control siRNA (siCTL; Qiagen) was used as a negative control.

Assessment of cell apoptosis

Cells were stained with the DNA-binding dyes propidium iodide (PI) and Hoechst 33342 (10 μg/ml, Sigma-Aldrich) to count apoptotic cells under a fluorescent microscope. In each experimental condition, a minimum of 500 cells were counted by two independent observers (one of them unaware of sample identity).

Data and materials availability

Bulk RNA-seq data that were generated by this study is available on the Gene Expression Omnibus (GEO) database under the accession number GSE214851. Other datasets mentioned are available on GEO using accession numbers GSE133218, GSE137136, GSE148058 and GSE108413.

Results

Cytokines trigger increased expression of ADAR1 in β cells

IFNα and IFNγ play important roles in T1D pathogenesis, from initiation of autoimmunity (IFNα) to the more advanced β cell destruction process (IFNɣ) (30, 31). To identify key pathways involved during T1D development, we used RNA-seq datasets from human islets and EndoC-βH1 cells exposed to IFNα (24h) or IFNγ/IL1β (48h), and searched for common differentially regulated genes (32, 33). This resulted in the identification of 623 common genes in EndoC-βH1 cells and 577 common genes in primary human islets. As expected, gene ontology pathway analysis identified IFN signaling and genes involved in HLA class I antigen peptide processing and presentation, highlighting the importance of the islet microenvironment in triggering cytotoxic T lymphocyte (CTL)-mediated β cell destruction (Figure 1A). In addition to immune-related genes, we observed that both IFNα and IFNγ/IL1β stimulation led to a significant increase in expression of ADAR1 in EndoC-βH1 cells and primary human islets suggesting an increased RNA deamination rate in β cells during inflammation (Figure 1B). We confirmed the effect of the different cytokines on *ADAR1* mRNA and protein expression in EndoC-βH1 cells using *STAT1* expression as a control for treatment effectiveness (Figures 1C, D). Of note, the expression of the isoform p150 of ADAR1 protein was undetectable in the absence of cytokine stimulation.

Enhanced A-to-I editing in β cells following IFNα and proinflammatory cytokine stimulation

To determine the consequences of the observed high ADAR1 expression following proinflammatory cytokine stimulation, and to decipher the RNA editome, we screened for A-to-G RNA mismatches (i.e., inosines present in the RNA are reverse transcribed into guanosines in cDNA and A-to-I editing is detected as A-to-G mismatches) by comparing reads in IFNα and IFNγ/IL1β-treated samples and non-treated samples against genomic reference (34, 35). Using the RNA editing index to measure the global rate of editing in *Alu* regions, we observed that IFNα and IFNγ/IL1β specifically triggered A-to-I RNA editing in β cells and primary human islet samples (Figures 2A, B).

ADAR overexpression inhibits the antiviral response while ADAR silencing exacerbates the effects of IFNα in β cells

To model the effect of ADAR1-p150 independently of the pleiotropic effects of cytokines, we generated a stable ADAR1-overexpressing human β cell line, by lentivirus transduction. In these cells, we detected an over 20-fold increase in ADAR1-p150 gene expression, and confirmed the corresponding increase in protein level by western blot analysis (Figure 3A). While ADAR1 overexpression had no major impact on endogenous ADAR1, PDX1 and MAFA gene expression, we observed a slight but significant increased NKX6.1 and a 50% decreased insulin gene expression suggesting that ADAR1 may interfere with β cell function (Supplementary Figure 1A). Differential gene expression analysis performed on high-depth RNA-seq revealed profound transcriptome changes following ADAR1 overexpression. In total, 2,851 genes were differentially expressed (1,477 up-regulated, 1,374 down-regulated - $|Log_2FC| > 0.58$; P adj. P value < 0.05) (Figure 3B and Supplementary Data S1). Among them, we observed regulation

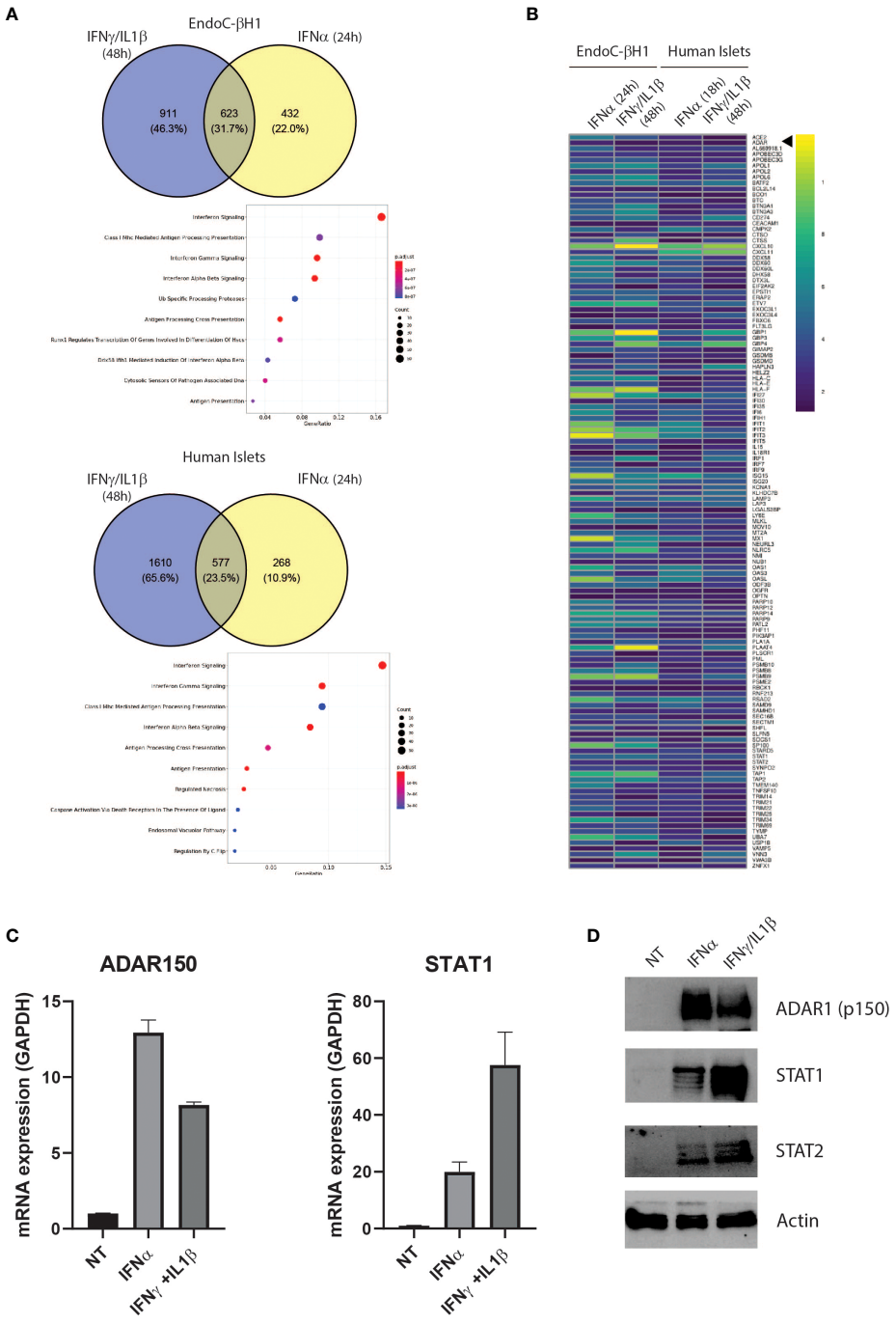

FIGURE 1
The proinflammatory cytokines IFNα and IFNɣ+IL-1β induce a partially shared gene signature in EndoC-βH1 and human islets Venn diagrams of up-regulated ($log_2FC > 0.58$ and adj. P value < 0.05) genes in EndoC-βH1 and human islets after exposure to IFNɣ+IL-1β **(A)**, top) and IFNα **(A)**, bottom). Common genes have been tested for enrichment – using REACTOME as the reference – and significantly enriched pathways are represented as a dot plot: the x-axis represents the gene ratio and the y-axis the enriched pathways. **(B)** Heatmap representing the log_2 fold change of the 128 up-regulated genes in all 4 datasets ($|log_2FC| > 0.58$ and adj. P value < 0.05). **(C)** ADAR1 p150 and STAT1 gene expression in EndoC-βH1 were assessed by qPCR after cytokine treatment. n=3 independent experiments **(D)** ADAR1 p150 ADAR1 (detected using Anti-ADAR1 #ab168809, Abcam), STAT1 and STAT2 protein expression determined by western blot. β-actin expression was used as loading control.

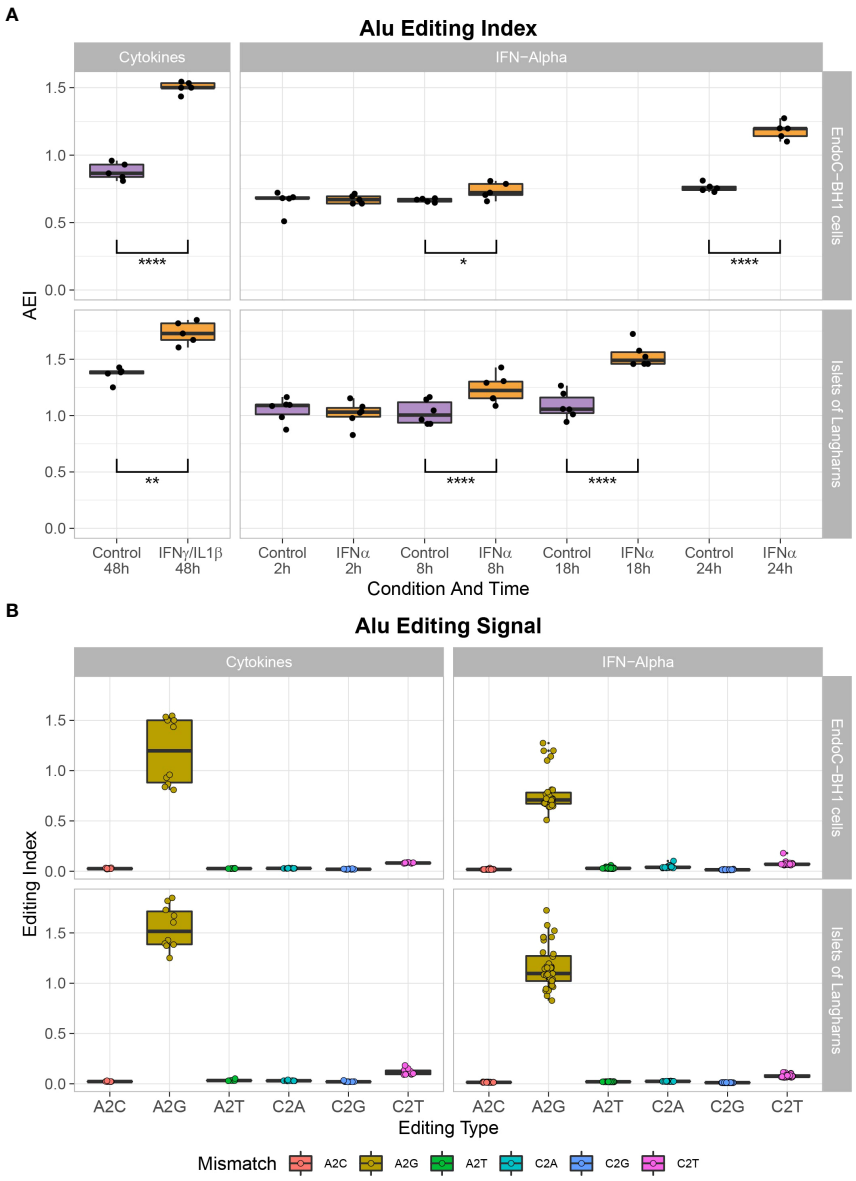

FIGURE 2
Cytokine treatment leads to A- to I- mutation in EndoC-βH1 and primary human islets. **(A)** Global A-to-I RNA editing index across *Alu* elements (short interspersed nuclear elements) in RNA-seq data demonstrates a higher A-to-I editing signal in IFNα or IFNɣ/IL1β stimulated samples after 8 hours and 48 hours, respectively. Student's paired two-tailed t-test; *P<0.05, **P<0.005, ****P<0.0001. **(B)** Noise levels (non-A-to-G mismatches) are notably lower than seen in the global editing index's biological signal (A-to-G mismatch).

of genes involved in immune system processes and defense to bacterium, confirming a role for ADAR1 in immune response (Figure 3C).

To validate this observation, we triggered the type I IFN response in β cells by mimicking viral infection *via* poly-I:C transfection (36). Poly-I:C transfection led to an increase in IFNβ expression and downstream IFN-stimulated genes (ISG) such as *MDA5*, *IFIT1*, *CXCL10* and *STAT1*, but ADAR1 overexpression completely abolished this antiviral response (Figure 3D).

To confirm these data using a reverse approach, we used an siRNA targeting *ADAR1* leading to 40-70% reduction in gene and protein expression (Figures 4A–D). Of note, ADAR silencing had no effect on β cell identity genes and insulin expression (Supplementary Figure 1B). As expected, while IFNα treatment induced the expression of several ISGs [e.g., *STAT1* (Figure 4E) *MDA5* (Figure 4F) and MX1 (Figure 4G)], ADAR1 silencing potentiated the effect of IFNα on the expression of these antiviral genes and sensitized EndoC-βH1 cells to IFNα-

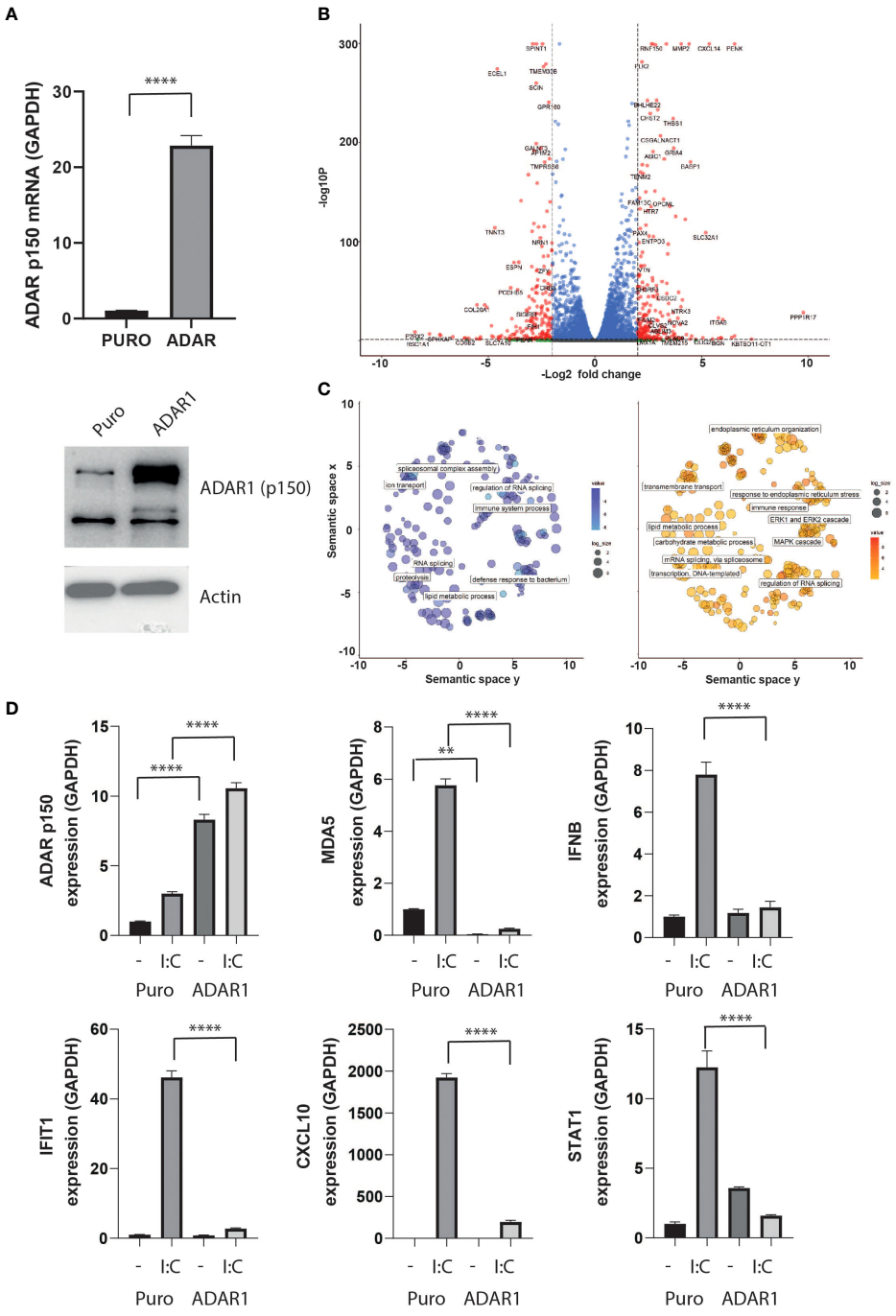

FIGURE 3
ADAR1 overexpression inhibits the type I IFN response. **(A)** ADAR1 p150 expression in EndoC-βH1 and EndoC- βH1 (ADAR1) cells determined by qPCR (upper panel) and western blot analysis using Anti-ADAR1 #ab168809, Abcam (lower panel). **(B)** Volcano plot on differential expressing genes after *ADAR1* overexpression. Dashed lines show $log_2FC \leq -2$ or $log_2FC \geq 2$ and adj. P value < 0.05. Plot was generated using Enhanced Volcano **(C)** Pathway analysis on downregulated (left, $log_2FC \leq -2$, adj. P value < 0.05) and upregulated (right, $log_2FC \geq 2$, adj. P value < 0.05) genes. Plots were generated using Revigo. **(D)** Gene expression of *ADAR1 p150, MDA5, IFNβ, IFITH1, CXCL10* and *STAT1* after ADAR1 overexpression in the presence or absence of polyI:C. N=3 independent experiments. Data are expressed as means of independent experiments ± SEM. Differences between groups were evaluated using one-way ANOVA or linear mixed model in case of missing values, followed by Bonferroni *post-hoc* test. ***P*<0.01 and *****P*<0.0001.

mediated cell death (Figure 4H). Altogether, these data unveil a role for ADAR1 in dampening the type I IFN response to prevent an excessive inflammatory response potentially leading to β cell death.

ADAR1 overexpression triggers alternative splicing events in β cells

Besides a role in immunity, gene ontology pathway analysis presented in Figure 2C revealed a possible role of ADAR1 in regulating alternative splicing. Considering the trend for an increased A-to-I *Alu* editing rate in ADAR1 overexpressing cells (Figure 5A), we studied the impact of adenosine deamination on the β cell coding transcriptome and searched for the presence of ADAR1-induced alternative splice variants. Of importance, in these cells, we observed an increased ADAR3 expression following ADAR1 transduction (Figure 5A).

After aligning the RNA sequencing reads to the reference genome, we identified a total of 323 alternatively spliced events (both known and *de novo*), modified by *ADAR1* overexpression (Figures 5B, C). These events derived mainly from spliced exons (SE, 70%), but also mutually exclusive exons (ME, 10%) and alternative 3' spliced sites (A3SS, 10%). Retained introns (RI, 7%) and alternative 5' spliced sites (A5SS, 3%) were less abundant. Genes affected by alternative splicing were analyzed for pathway enrichment analysis using the REACTOME platform and were found to be mainly related to β cell function (e.g., pre-synapse, regulation of neurotransmitter levels), vesicle location (e.g., synaptic vesicle, vesicle-mediated

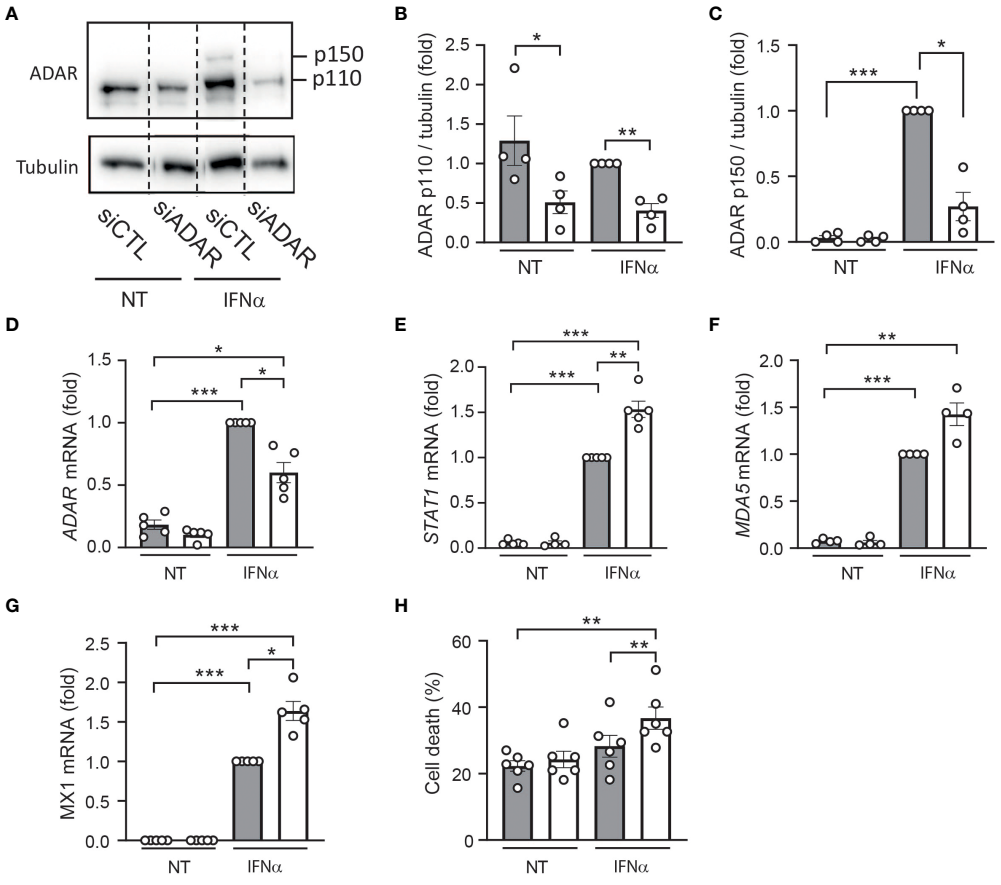

FIGURE 4
ADAR1 silencing exacerbates the effects of IFNα in human β cells. EndoC-βH1 cells were transfected with an siRNA control (siCTL: grey bars) or with an siRNA targeting ADAR (white bars) and left to recover for 48h. After this period, cells were left untreated (NT) or were treated with IFNα (2000 U/ml) for 24h. **(A)** Protein expression was measured by western blotting using Anti-ADAR1 antibody #14175 (Cell Signaling Technology) and representative images of 4 independent experiments are shown. Densitometry results are shown for ADAR p110 **(B)** and ADAR p150 **(C)**. mRNA expression of ADAR **(D)**, STAT1 **(E)**, MDA5 **(F)** and MX1 **(G)** was analyzed by RT-qPCR and normalized by β-actin. Values of siCTL + IFNα were considered as 1. **(H)** Cell death was evaluated using HO/PI staining. Data are expressed as means of independent experiments (shown as individual data points, n=4-6) ± SEM. Differences between groups were evaluated using one-way ANOVA or linear mixed model in case of missing values, followed by Bonferroni *post-hoc* test. *p<0.05, **p<0.01 and ****p<0.0001.

transport to the plasma membrane) and protein transport (Figure 5D).

Discussion

Our report positions ADAR1 as both an important player in dampening innate immunity in β cells and as a key editor of the β cell transcriptome. While exposure to inflammation, characteristic of the early or later stages of T1D development, is usually associated with deleterious effects, the data presented here recall earlier work on enhanced expression of Programmed death-ligand 1 PD-L1 detected in β cells from long-standing T1D individuals (37), suggesting that ADAR1, like PD-L1, is involved in the positive adaptive mechanisms to protect β cells from further destruction. During T1D, the induction of the unfolded protein response, following exposure to virus or inflammatory cytokines, participates in this adaptive phase to restore cellular homeostasis or to initiate apoptosis in the case of unresolved stress (38). At this decision point, the A-to-I editing induced by ADAR1 has been implicated in PERK activation and apoptosis induction *via* EIF2a/CHOP pathway (39). Other reports describe additional RNA-editing independent effects of ADAR1 *via* direct interaction with RIG-I, PKR or NF90 that could regulate cellular stress and the type I interferon response (3, 40, 41).

Supporting the concept that β cells are not passive victims in their destruction (8), our results show that the increased

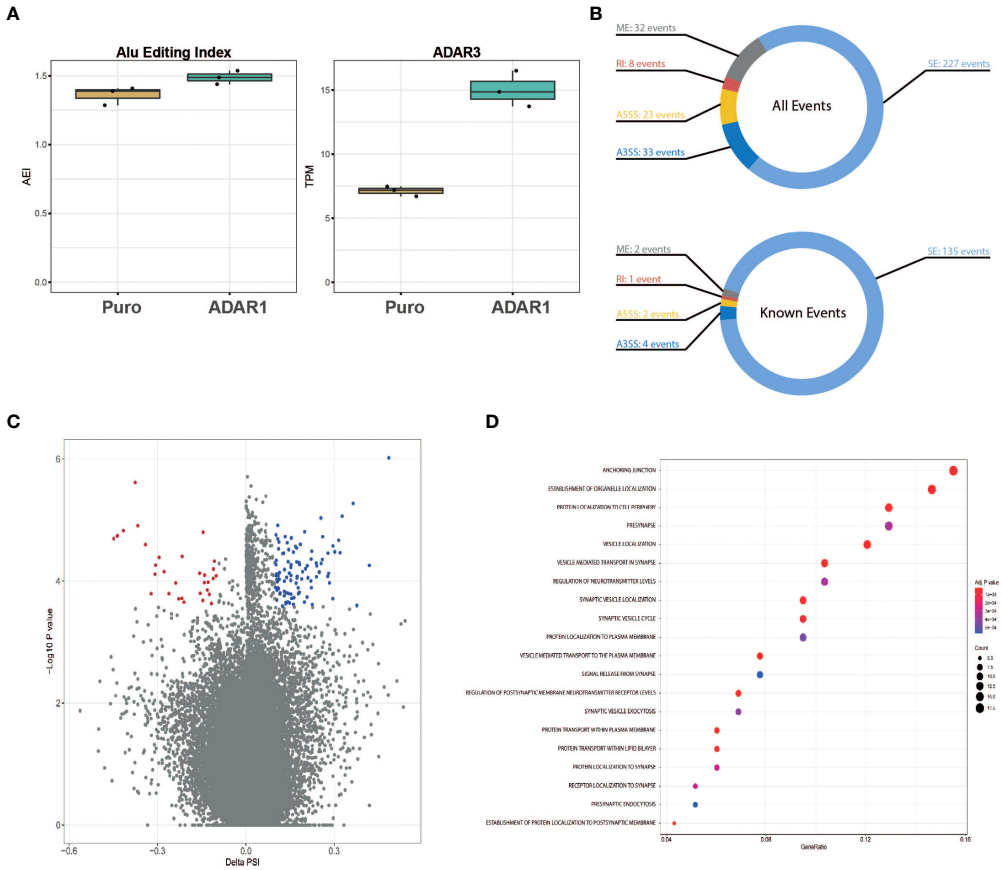

FIGURE 5
ADAR1 overexpression triggers alternative splicing in EndoC-βH1. **(A)** Global A-to-I RNA editing index across Alu elements (short interspersed nuclear elements) in Puro modified EndoC-βH1 and ADAR1 modified EndoC-βH1 cells (left panel), ADAR3 expression in Puro and ADAR1 modified EndoC-βH1. Data are shown as Transcript Per Million. **(B)** Donut charts representing the cumulated number of known and *de novo* alternative splicing events (top), and known events only (bottom). Events displayed have |ΔPSI| >0.10 and FDR <0.05. **(C)** Volcano plot of the inclusion and exclusion SE (skipped exon) events in EndoC-βh1 cells overexpressing ADAR1. Negative PSI indicates the inclusion of the event in ADAR1-overexpressing EndoC-βH1 cells whereas positive PSI indicates exclusion. Each dot represents an event with its ΔPSI (x-axis) associated to its *P*-value (y-axis). Colored dots (blue and red) represent genes with FDR<0.05. **(D)** Dot plot of the enrichment analysis, using Gene Ontology as reference, shows gene sets affected by known splicing events in cells overexpressing ADAR1. Gene ratio (x-axis) refers to the percentage of total genes input with alternative splicing events in selected GO terms (y-axis). SE, Spliced Exon; RI, Retain Intro; MXE, Mutually Exclusive Exon; A3SS, 3′ Alternative Splicing Site; A5SS, 5′ Alternative Splice Site.

RNA editing rate correlates also with the emergence of novel transcript variants, demonstrating that ADAR1 activity is not only limited to *Alu* sequences but also affects coding regions with possible consequences for gene regulation and cell function (42). Surprisingly, ADAR1 p150 overexpression in EndoC-β H1 cells led a to concomitant increase in ADAR3 expression, which has been reported to act as a negative regulator of ADAR1-mediated editing (43). The competition between the different ADAR proteins may explain the relatively low editing rate measured in our samples and add to the complexity of gene editing regulation.

Despite the higher editing rate observed in inflammatory conditions or following ADAR1 overexpression, it is unlikely that all of the detected alternative splicing results solely from a direct A-to-I RNA editing of the target genes. As described here, ADAR1 overexpression led to extensive regulation of the RNA processing machinery or of spliceosome formation suggesting that ADAR1 may affect the transcriptome by modulating the expression of *trans*-regulatory elements. Among them, the splicing regulators ELAVL4 and NOVA2, previously reported as important splicing-regulatory RNA binding proteins involved in modulating β cell survival (44), were upregulated in response to ADAR1 transduction. The increased cell death observed after ADAR1-specific inhibition (Figure 4) is in line with this observation. Another report describes that the loss of RNA editing activity may lead to non-apoptotic cell death induction directly mediated by MDA5 (45), indicating that ADAR1 inhibition may lead to different forms of cell death. Of note, ADAR1 expression in our dataset led to decreased expression of pseudokinase mixed lineage kinase domain-like protein (MLKL) that serves as an effector in necroptosis.

The present results illustrate a central role of ADAR1 in β cells during inflammation and shed light on a novel regulatory mechanism potentially used by β cells to cope with environmental changes after viral infection but also during the different phases of inflammation. Although ADAR1-dependent effects are mostly protective, the functional and immunological consequences of mutations induced by RNA editing, including the potential generation of neoantigens, remain to be investigated.

Data availability statement

The data presented in the study are deposited in the Gene Expression Omnibus (GEO) database under the accession number GSE214851. Other datasets mentioned are using accession numbers GSE133218, GSE137136, GSE148058 and GSE108413.

Author contributions

FS, RC-F, ST and MC analyzed the RNA sequencing datasets and wrote the manuscript. ST and AB performed the experiments. AC and PM provided additional data for the revised manuscript. EL, DE and AZ supervised the project and wrote the manuscript. All authors contributed to the article and approved the submitted version.

Funding

This research has been supported by the Israel Science Foundation (grant numbers 2039/20 and, 231/21 to EL), the DON Foundation and the Dutch Diabetes Research Foundation, JDRF and by IMI2-JU under grant agreement No 115797 (INNODIA) and No 945268 (INNODIA HARVEST). These joint undertakings receive support from the European Union's Horizon 2020 research and innovation programme and European Federation of Pharmaceutical Industries and Associations (EFPIA), JDRF, and the Leona M. and Harry B. Helmsley Charitable Trust. DE acknowledges the support of grants from the Welbio-FNRS (Fonds National de la Recherche Scientifique) (WELBIO-CR-2019C-04), Belgium; the JDRF (3-SRA-2022-1201-S-B); the National Institutes of Health Human Islet Research Network Consortium on Beta Cell Death and Survival from Pancreatic β-Cell Gene Networks to Therapy [HIRN-CBDS]) (grant U01 DK127786). F.S. is supported by a Research Fellow (Aspirant) fellowship from the Fonds National de la Recherche Scientifique (FNRS, Belgium).

Acknowledgments

The authors are grateful to Isabelle Millard, Anyishaï Musuaya, Nathalie Pachera and Cai Ying, (ULB Center for Diabetes Research), Steve Cramer and Martijn Rabelink (LUMC) for providing excellent technical support.

Conflict of interest

The authors declare that the research was conducted in the absence of any commercial or financial relationships that could be construed as a potential conflict of interest.

Publisher's note

Supplementary material

The Supplementary Material for this article can be found online at: https://www.frontiersin.org/articles/10.3389/fendo.2022.1058345/full#supplementary-material

SUPPLEMENTARY FIGURE 1
ADAR1 modulation and β cell identity and function. **(A)** ADARp150 and ADAR1 endogenous (upper panel), INS, PDX1, MAFA and NKX6.1 (lower panel) expression level following ADAR1 overexpression. **(B)** INS, PDX1, MAFA and NKX6.1 gene expression level upon ADAR1 specific inhibition by siRNA. Data are expressed as means of independent experiments (n=3) ± SD. Differences between groups were evaluated using unpaired t-test. $^{**}p<0.01$ and $^{****}p<0.0001$.

SUPPLEMENTARY DATA SHEET 1
Differential gene expression detected in EndoC-βH1 following ADAR1 overexpression.

SUPPLEMENTARY DATA SHEET 2
Gene-sets affected by alternative splicing in ADAR1 overexpressing cells.

References

1. Szymczak F, Colli ML, Mamula MJ, Evans-Molina C, Eizirik DL. Gene expression signatures of target tissues in type 1 diabetes, lupus erythematosus, multiple sclerosis, and rheumatoid arthritis. *Sci Adv* (2021) 7(2):1–11. doi: 10.1126/sciadv.abd7600

2. Dias Junior AG, Sampaio NG, Rehwinkel J. A balancing act: Mda5 in antiviral immunity and autoinflammation. *Trends Microbiol* (2019) 27(1):75–85. doi: 10.1016/j.tim.2018.08.007

3. Lamers MM, van den Hoogen BG, Haagmans BL. Adar1: "Editor-in-Chief" of cytoplasmic innate immunity. *Front Immunol* (2019) 10:1763. doi: 10.3389/fimmu.2019.01763

4. Heraud-Farlow JE, Walkley CR. The role of rna editing by Adar1 in prevention of innate immune sensing of self-rna. *J Mol Med (Berl)* (2016) 94 (10):1095–102. doi: 10.1007/s00109-016-1416-1

5. Rice GI, Kasher PR, Forte GM, Mannion NM, Greenwood SM, Szynkiewicz M, et al. Mutations in Adar1 cause aicardi-goutieres syndrome associated with a type I interferon signature. *Nat Genet* (2012) 44(11):1243–8. doi: 10.1038/ng.2414

6. Song IH, Kim YA, Heo SH, Park IA, Lee M, Bang WS, et al. Adar1 expression is associated with tumour-infiltrating lymphocytes in triple-negative breast cancer. *Tumour Biol* (2017) 39(10):1010428317734816. doi: 10.1177/1010428317734816

7. Roth SH, Danan-Gotthold M, Ben-Izhak M, Rechavi G, Cohen CJ, Louzoun Y, et al. Increased rna editing may provide a source for autoantigens in systemic lupus erythematosus. *Cell Rep* (2018) 23(1):50–7. doi: 10.1016/j.celrep.2018.03.036

8. Eizirik DL, Pasquali L, Cnop M. Pancreatic beta-cells in type 1 and type 2 diabetes mellitus: Different pathways to failure. *Nat Rev Endocrinol* (2020) 16 (7):349–62. doi: 10.1038/s41574-020-0355-7

9. Mallone R, Eizirik DL. Presumption of innocence for beta cells: Why are they vulnerable autoimmune targets in type 1 diabetes? *Diabetologia* (2020) 63 (10):1999–2006. doi: 10.1007/s00125-020-05176-7

10. Nguyen H, Guyer P, Ettinger RA, James EA. Non-genetically encoded epitopes are relevant targets in autoimmune diabetes. *Biomedicines* (2021) 9(2):1–13. doi: 10.3390/biomedicines9020202

11. Rodriguez-Calvo T, Johnson JD, Overbergh L, Dunne JL. Neoepitopes in type 1 diabetes: Etiological insights, biomarkers and therapeutic targets. *Front Immunol* (2021) 12:667989. doi: 10.3389/fimmu.2021.667989

12. Christofi T, Zaravinos A. Rna editing in the forefront of epitranscriptomics and human health. *J Transl Med* (2019) 17(1):319. doi: 10.1186/s12967-019-2071-4

13. Tang SJ, Shen H, An O, Hong H, Li J, Song Y, et al. Cis- and trans-regulations of pre-mrna splicing by rna editing enzymes influence cancer development. *Nat Commun* (2020) 11(1):799. doi: 10.1038/s41467-020-14621-5

14. Zhou C, Wei Z, Zhang L, Yang Z, Liu Q. Systematically characterizing a-to-I rna editing neoantigens in cancer. *Front Oncol* (2020) 10:593989. doi: 10.3389/fonc.2020.593989

15. Gonzalez-Duque S, Azoury ME, Colli ML, Afonso G, Turatsinze JV, Nigi L, et al. Conventional and neo-antigenic peptides presented by beta cells are targeted by circulating naive Cd8+ T cells in type 1 diabetic and healthy donors. *Cell Metab* (2018) 28(6):946–60.e6. doi: 10.1016/j.cmet.2018.07.007

16. Akhbari P, Richardson SJ, Morgan NG. Type 1 diabetes: Interferons and the aftermath of pancreatic beta-cell enteroviral infection. *Microorganisms* (2020) 8 (9):1–18. doi: 10.3390/microorganisms8091419

17. Colli ML, Szymczak F, Eizirik DL. Molecular footprints of the immune assault on pancreatic beta cells in type 1 diabetes. *Front Endocrinol (Lausanne)* (2020) 11:568446. doi: 10.3389/fendo.2020.568446

18. Ravassard P, Hazhouz Y, Pechberty S, Bricout-Neveu E, Armanet M, Czernichow P, et al. A genetically engineered human pancreatic beta cell line exhibiting glucose-inducible insulin secretion. *J Clin Invest* (2011) 121(9):3589–97. doi: 10.1172/JCI58447

19. Petersen KR, Streett DA, Gerritsen AT, Hunter SS, Settles ML. . super deduper, fast pcr duplicate detection in fastq files. In: *Proceedings of the 6th ACM conference on bioinformatics, computational biology and health informatics;*. Atlanta, Georgia: Association for Computing Machinery (2015). p. 491–2.

20. Dobin A, Davis CA, Schlesinger F, Drenkow J, Zaleski C, Jha S, et al. Star: Ultrafast universal rna-seq aligner. *Bioinformatics* (2013) 29(1):15–21. doi: 10.1093/bioinformatics/bts635

21. Roth SH, Levanon EY, Eisenberg E. Genome-wide quantification of adar adenosine-to-Inosine rna editing activity. *Nat Methods* (2019) 16(11):1131–8. doi: 10.1038/s41592-019-0610-9

22. Love MI, Anders S, Kim V, Huber W. Rna-seq workflow: Gene-level exploratory analysis and differential expression. *F1000Res* (2015) 4:1070. doi: 10.12688/f1000research.7035.1

23. Soneson C, Love MI, Robinson MD. Differential analyses for rna-seq: Transcript-level estimates improve gene-level inferences. *F1000Res* (2015) 4:1521. doi: 10.12688/f1000research.7563.2

24. Chen S, Zhou Y, Chen Y, Gu J. Fastp: An ultra-fast all-in-One fastq preprocessor. *Bioinformatics* (2018) 34(17):i884–i90. doi: 10.1093/bioinformatics/bty560

25. Patro R, Duggal G, Love MI, Irizarry RA, Kingsford C. Salmon provides fast and bias-aware quantification of transcript expression. *Nat Methods* (2017) 14 (4):417–9. doi: 10.1038/nmeth.4197

26. Love MI, Huber W, Anders S. Moderated estimation of fold change and dispersion for rna-seq data with Deseq2. *Genome Biol* (2014) 15(12):550. doi: 10.1186/s13059-014-0550-8

27. Korotkevich G, Sukhov V, Budin N, Shpak B, Artyomov MN, Sergushichev A. Fast gene set enrichment analysis. *bioRxiv* (2021), 060012. doi: 10.1101/060012

28. Yu G, Wang LG, Han Y, He QY. Clusterprofiler: An r package for comparing biological themes among gene clusters. *OMICS* (2012) 16(5):284–7. doi: 10.1089/omi.2011.0118

29. Carlotti F, Bazuine M, Kekarainen T, Seppen J, Pognonec P, Maassen JA, et al. Lentiviral vectors efficiently transduce quiescent mature 3t3-L1 adipocytes. *Mol Ther* (2004) 9(2):209–17. doi: 10.1016/j.ymthe.2003.11.021

30. Lombardi A, Tsomos E, Hammerstad SS, Tomer Y. Interferon alpha: The key trigger of type 1 diabetes. *J Autoimmun* (2018) 94:7–15. doi: 10.1016/j.jaut.2018.08.003

31. von Herrath MG, Oldstone MB. Interferon-gamma is essential for destruction of beta cells and development of insulin-dependent diabetes mellitus. *J Exp Med* (1997) 185(3):531–9. doi: 10.1084/jem.185.3.531

32. Colli ML, Ramos-Rodriguez M, Nakayasu ES, Alvelos MI, Lopes M, Hill JLE, et al. An integrated multi-omics approach identifies the landscape of interferon-Alpha-Mediated responses of human pancreatic beta cells. *Nat Commun* (2020) 11(1):2584. doi: 10.1038/s41467-020-16327-0

33. Ramos-Rodriguez M, Raurell-Vila H, Colli ML, Alvelos MI, Subirana-Granes M, Juan-Mateu J, et al. The impact of proinflammatory cytokines on the beta-cell regulatory landscape provides insights into the genetics of type 1 diabetes. *Nat Genet* (2019) 51(11):1588–95. doi: 10.1038/s41588-019-0524-6

34. Bazak L, Haviv A, Barak M, Jacob-Hirsch J, Deng P, Zhang R, et al. A-to-I rna editing occurs at over a hundred million genomic sites, located in a majority of human genes. *Genome Res* (2014) 24(3):365–76. doi: 10.1101/gr.164749.113

35. Porath HT, Carmi S, Levanon EY. A genome-wide map of hyper-edited rna reveals numerous new sites. *Nat Commun* (2014) 5:4726. doi: 10.1038/ncomms5726

36. Vig S, Lambooij JM, Dekkers MC, Otto F, Carlotti F, Guigas B, et al. Er stress promotes mitochondrial DNA mediated type-1 interferon response in beta-cells and interleukin-8 driven neutrophil chemotaxis. *Front Endocrinol* (2022) 13:991632. doi: 10.3389/fendo.2022.991632

37. Colli ML, Hill JLE, Marroqui L, Chaffey J, Dos Santos RS, Leete P, et al. Pdl1 is expressed in the islets of people with type 1 diabetes and is up-regulated by interferons-alpha and-gamma *Via* Irf1 induction. *EBioMedicine* (2018) 36:367–75. doi: 10.1016/j.ebiom.2018.09.040

38. Roep BO, Thomaidou S, van Tienhoven R, Zaldumbide A. Type 1 diabetes mellitus as a disease of the beta-cell (Do not blame the immune system)? *Nat Rev Endocrinol* (2021) 17(3):150–61. doi: 10.1038/s41574-020-00443-4

39. Guallar D, Fuentes-Iglesias A, Souto Y, Ameneiro C, Freire-Agulleiro O, Pardavila JA, et al. Adar1-dependent rna editing promotes met and ipsc reprogramming by alleviating er stress. *Cell Stem Cell* (2020) 27(2):300–14 e11. doi: 10.1016/j.stem.2020.04.016

40. Licht K, Jantsch MF. The other face of an Editor: Adar1 functions in editing-independent ways. *Bioessays* (2017) 39(11):1–6. doi: 10.1002/bies.201700129

41. Nie Y, Ding L, Kao PN, Braun R, Yang JH. Adar1 interacts with Nf90 through double-stranded rna and regulates Nf90-mediated gene expression independently of rna editing. *Mol Cell Biol* (2005) 25(16):6956–63. doi: 10.1128/MCB.25.16.6956-6963.2005

42. Nishikura K. A-to-I editing of coding and non-coding rnas by adars. *Nat Rev Mol Cell Biol* (2016) 17(2):83–96. doi: 10.1038/nrm.2015.4

43. Raghava Kurup R, Oakes EK, Manning AC, Mukherjee P, Vadlamani P, Hundley HA. Rna binding by Adar3 inhibits adenosine-to-Inosine editing and promotes expression of immune response protein mavs. *J Biol Chem* (2022) 298 (9):102267. doi: 10.1016/j.jbc.2022.102267

44. Juan-Mateu J, Rech TH, Villate O, Lizarraga-Mollinedo E, Wendt A, Turatsinze JV, et al. Neuron-enriched rna-binding proteins regulate pancreatic beta cell function and survival. *J Biol Chem* (2017) 292(8):3466–80. doi: 10.1074/jbc.M116.748335

45. Walkley CR, Kile BT. Cell death following the loss of Adar1 mediated a-to-I rna editing is not effected by the intrinsic apoptosis pathway. *Cell Death Dis* (2019) 10(12):913. doi: 10.1038/s41419-019-2160-6

frontiers | Frontiers in Endocrinology

TYPE Mini Review
PUBLISHED 30 November 2022
DOI 10.3389/fendo.2022.1019935

OPEN ACCESS

EDITED BY
Carlos Guillén,
Complutense University, Spain

REVIEWED BY
Vikrant Rai,
Western University of Health Sciences, United States

*CORRESPONDENCE
Guanwen Sun
ldr3012@163.com
Huhe Bao
BHH_orthopaedist@163.com

†These authors have contributed equally to this work and share first authorship

SPECIALTY SECTION
This article was submitted to Diabetes: Molecular Mechanisms, a section of the journal Frontiers in Endocrinology

RECEIVED 15 August 2022
ACCEPTED 14 November 2022
PUBLISHED 30 November 2022

CITATION
Li D, Guo J, Ni X, Sun G and Bao H (2022) The progress and challenges of circRNA for diabetic foot ulcers: A mini-review.
Front. Endocrinol. 13:1019935.
doi: 10.3389/fendo.2022.1019935

The progress and challenges of circRNA for diabetic foot ulcers: A mini-review

Deer Li[1,2†], Jiaxing Guo[3†], Xiyu Ni[1,2†], Guanwen Sun[2*] and Huhe Bao[2*]

[1]Graduate School, Inner Mongolia Medical University, Hohhot, China, [2]Department of Traumatology and Orthopedics, Inner Mongolia People's Hospital, Hohhot, China, [3]Department of Joint Surgery, The Second Affiliated Hospital, Inner Mongolia Medical University, Hohhot, China

Since the Human Genome Project was successfully completed, humanity has entered a post-genome era, and the second-generation sequencing technology has gradually progressed and become more accurate. Meanwhile, circRNAs plays a crucial role in the regulation of diseases and potential clinical applications has gradually attracted the attention of physicians. However, the mechanisms of circRNAs regulation at the cellular and molecular level of diabetic foot ulcer (DFU) is still not well-understood. With the deepening of research, there have been many recent studies conducted to explore the effect of circRNAs on DFU. In this mini-review, we discuss the potential role of circRNAs as therapeutic targets and diagnostic markers for DFU in order to gain a better understanding of the molecular mechanisms that underlie the development of DFU and to establish a theoretical basis for accurate treatment and effective prevention.

KEYWORDS

diabetic foot ulcers, circRNAs, differential expression, diagnostic markers, therapeutic targets

Introduction

Diabetic foot ulcer (DFU) is one of the most common lower limb complications of diabetes mellitus (DM) (1). According to relevant studies, the 5-year and 10-year mortality of DFU patients is 22% and 71% respectively, and the amputation rate is 29.3% (2). The etiology of DFU is attributed to a variety of causes, including chronic inflammation, diabetic peripheral neuropathy, and vascular endothelial damage of the distal arterial vasculature. However, the lack of typical signs and symptoms in the early stages of the disease makes misdiagnosis and under diagnosis a common occurrence in clinical work. Although there are many medical and surgical treatments in clinic, the risk of chronic ulcer or even amputation is easy to occur due to the lack of effective diagnostic

markers and treatment targets. Therefore, it is important to explore the etiological mechanism to provide theoretical basis for accurate treatment and diagnosis.

CircRNAs are important regulators in the cellular life cycle. It is a class of non-coding RNA formed by covalent cyclization, which is abundantly expressed in eukaryotic organisms and has high stability. Studies have shown that circRNAs play an important role in cell proliferation, apoptosis, metabolism, inflammation and other biological processes (3). In addition, circRNAs are closely related to the development of many diseases, such as DM and cancer (4). Therefore, this mini-review provides a comprehensive review of the biological role of circRNAs in DFU and explores the possibility of circRNAs as a therapeutic target and diagnostic marker for DFU by reviewing the literature and related materials.

Pathophysiology of DFU

Normally, wound healing undergoes several phases, including hemostasis, inflammation, proliferation, migration, re-epithelization and remodeling (5). However, there are several factors that contribute to the non-healing of DFU. Hyperglycemia, chronic inflammation, dysfunction of microcirculation and macrocirculation, hypoxia, sensory neuropathy and neuropeptide signal damage are the main factors that lead to the difficulty of wound healing (6). However, hyperglycemia may be the most critical point of non-healing of wounds. It has been reported that hyperglycemia can promote vascular endothelial cell (ECs) dysfunction and induce apoptosis (7). ECs dysfunction leads to a decrease in various angiogenic and vasoactive factors secreted by it, as well as a decrease in new blood vessel formation (8–10). Studies have shown that endothelial dysfunction is the intrinsic cause of impaired wound healing (11–13). In addition, hyperglycemia directly affects the activity of keratinocytes (HEKs) and fibroblasts (FBs), leading to changes in protein synthesis, proliferation, and migration (14). It will seriously affect the re-epithelization and remodeling of the wounds, which in turn leads to non-healing of wounds. Recently, there is increasing evidence that hyperglycemia leads to impaired cell response to hypoxia (15). Hypoxia can prolong the damage by increasing the level of free oxygen radicals. Meanwhile, inflammation caused by chronic hyperglycemia will further increase oxidative stress and pro-inflammatory chemokines to reduce cell proliferation and migration then ultimately delay wound healing (16, 17). Studies have shown that diabetic peripheral neuropathy is one of the main causes of foot ulcers (18). It is believed that glial cell apoptosis and autophagy in the peripheral nervous system caused by hyperglycemia stimulation are the main causes for the occurrence and development of peripheral neuropathy (19–21). In brief, the main characteristics of diabetic wound non-healing are decreased angiogenesis, decreased recruitment of bone marrow-derived endothelial progenitor cells (EPC), decreased proliferation and migration of FBs and HEKs, and apoptosis of nerve cells (22). Interestingly, recent studies have shown that circRNAs play an important role in the pathophysiology of DFU wound healing. This may provide a novel idea for finding diagnostic marks and therapeutic targets of DFU.

CircRNA

Overview of circRNA molecules

CircRNAs is a class of non-linear RNA molecule, which is not easily degraded by nucleic acid exonucleases and is formed by covalent cyclization. circRNAs are mainly produced by covalent connection of upstream and downstream sites during back-splicing. Most of the circRNAs were earlier undetected in RNA sequence due to the lack of 3 ‘ poly tails, and as the technology has evolved, over 183,000 have been identified now (23). Broadly, circRNAs can be classified into 4 types, EcircRNA composed of exons and mainly located in the cytoplasm; EIcircRNA with the combination of introns and exons and mainly located in the nucleus; CiRNA composed of introns, mainly located in the nucleus (24–27); circRNA produced by cyclization of viral RNA gene, tRNA, rRNA or snRNA (Figure 1).

The main biological functions of circRNA

Understanding the ways which circRNAs participates in regulating biological processes further broadens our horizons. circRNAs has various biological functions, such as affecting the splicing of linear RNA and regulating transcription. ① Acting as a transcriptional regulator; CircRNAs can interact with U1 snRNA to form circRNA-U1 snRNP complex, and then further interact with RNA Pol II transcription complex at the promoter of parent gene to alter gene transcription and expression (28). For example, circ_ANKRD52, generated from gene ANKRD52, is capable of accumulating to its transcription sites and regulates elongation Pol II machinery acting as a positive regulator for transcription (29). ② Acting as miRNA sponges; MiRNA can bind directly to target mRNA in a base-pair fashion and trigger cleavage of mRNA or inhibit translation of mRNA (30). CircRNAs located in cytoplasm also contain complementary miRNA binding sites, and thus serve as competitive inhibitors for miRNA. In human cells, circ_ASAP1 can act as a sponge of miR_326 and miR_532_5p to promote hepatocellular carcinoma under hypoxic conditions (31). In addition, new circRNA sponges are continually being discovered in various disciplines. Circ_ITCH sponges miR-7,

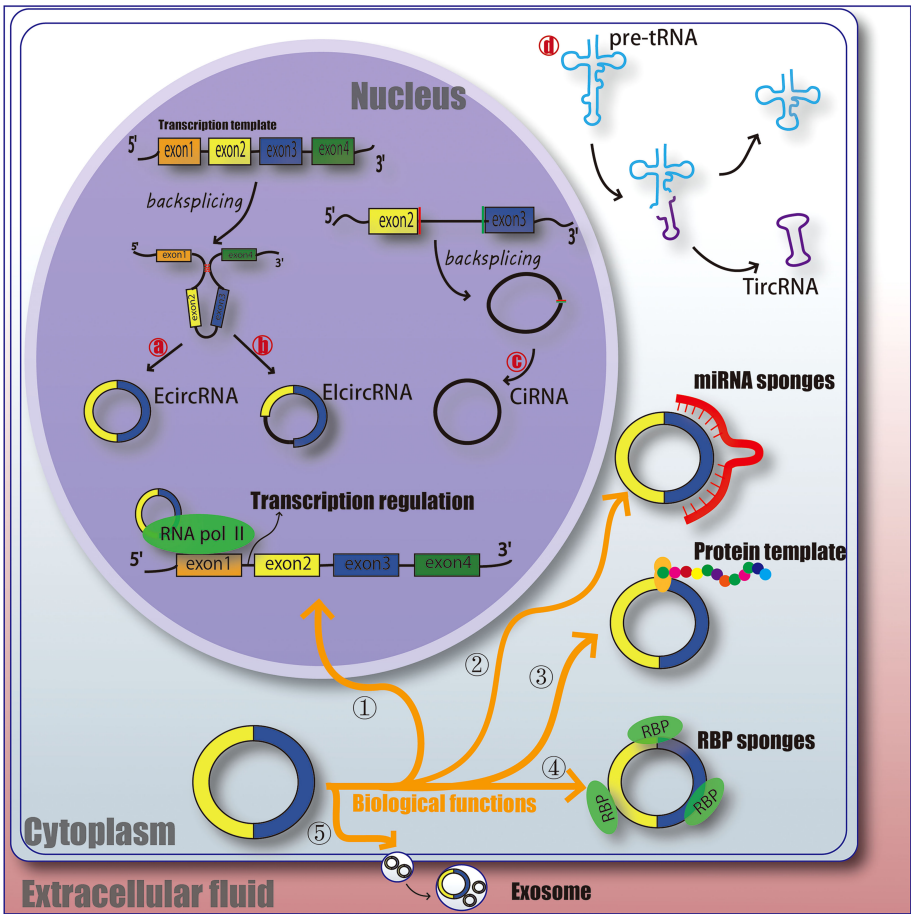

FIGURE 1
The function and classification of circRNA. EcircRNA, exonic circRNA. EIcircRNA, exon - intron circRNA. CiRNA, intronic circRNA. TircRNA, tRNA intronic circRNA. RNA pol II, RNA polymerase II. RBP, RNA-binding protein. miRNA, microRNA.

miR-17 and miR-214 in esophageal squamous cell carcinoma (ESCs) and inhibits tumor proliferation (32). CiRS-7 acts as a miR-7 sponge in many pathophysiological processes, including myocardial infarction, hepatocellular carcinoma (HCC) and gastric cancer (GC) (32–34). These results suggest that circRNAs as miRNA sponges might be a common function of circRNAs. ③ Protein templates; At first, people thought that circRNAs was a non-coding RNA (24, 35). However, recent studies have found that extensive N6-methyladenosine (m6A) modification is enough to drive circRNAs to translate in a cap-independent manner, as well as m6A reader YTHDF3 and translation initiation factors eIF4G2 and eIF3A (36). And further analysis indicates that translatable circRNAs may be common in human transcriptome (37). However, the translation ability and efficiency of circRNA are still remains controversial. ④ Binding with RBP (RNA-binding protein); CircRNAs have also been reported to act as sponges for proteins to alter pathophysiological progress. For example, circ_ZFR can promote the proliferation of hepatocellular carcinoma by binding with MAP2K1 (38). Circ_Foxo3 has high binding affinity with anti-aging ID-1, transcription factor E2F1, and anti-stress proteins FAK and HIF1A, and keeps them in the cytoplasm, leading to the aggravation of cell aging (39). ⑤ Act as a biomarker for clinical diagnosis or treatment; It is mainly due to the highly conservative nature and unique molecular structure of circRNAs, and researchers are still studying whether it can be a mature marker for the treatment and diagnosis of diseases. Therefore, the physiological characteristics of circRNAs may provide some idea for us to explore the etiology, treatment and diagnosis of DFU (Figure 1).

Correlation between DFU and circRNAs

With the rapid development of the circRNA field, circRNAs in the wound tissues or blood of DFU patients has been detected by RNA-sequencing or gene microarray analysis, and the potential correlation between DFU and circRNAs expression

levels has been detected. For example, Zhao et al. (40) detected circRNAs in the serum of 3 patients with DFU and 9 patients with DM, and found that compared with DM patients, the serum of DFU patients showed 10 upregulated and 23 downregulated circRNAs. Tian et al. (41) analyzed a set of microarray data and found 65 differentially expressed circRNAs, including 25 upregulated and 40 downregulated circRNAs, in 8 non-DM patients' (normal group) tissues and 9 DFU patients' (DFU group) tissues. Liao et al. (42) analyzed 5 non-DM patients' tissues and 5 DFU patients wound tissues by using a set of microarray data, and found 8 differentially expressed circRNAs. All evidence indicated that circRNAs are differentially expressed in DFU and may be involved in certain academic biological processes and signaling pathways to the healing process of DFU by regulating some target genes.

The role of circRNAs in ulcer tissue

We comprehensively summarized all circRNAs related to DFU, and found that circRNAs can regulate various cells involved in DFU wound healing, and regulate its downstream substances through some specific signaling pathways, thus acting as biological regulators (Table 1).

Effect of circRNAs on human epidermal keratinocytes

Human Epidermal Keratinocytes (HEKs) are a class of epithelial cells that synthesize keratin and gradually proliferate and differentiate from deeper layers to form keratinized HEKs that act as barrier. Re-epithelization is the process of wound healing and restoration of intact epidermis, which is closely regulated by the migration and proliferation of HEKs (65, 66). Evidence suggests that migration of HEKs plays a vital role in covering the wound surface during wound re-epithelization (67, 68). Therefore, elucidating the mechanism of HEKs driving from the wound edge to the wound bed may provide crucial novel insights for the treatment of DFU. Wang et al. (43) showed that circ_0084443 was significantly expressed in DFU patients' wound tissues and was found to be most highly expressed in HEKs, followed by FBs, ECs, and silencing circ_0084443 increased migration of HEKs, while over-expression of circ_0084443 promoted proliferation of HEKs. In addition, they found that hsa_circ_0084443 in HEKs can mediate the biological effects of PI3K, EGFR and ERK signaling pathways, but blocking these signaling pathways can inhibit the migration of HEKs (43). PI3K, EGFR and ERK signaling pathways are relatively mature and well-recognized effective pathways in the DFU healing process (69–71), which also laterally proves that circ_0084443 may play a key role in ulcer healing. SRTING database is a powerful online website for analyzing protein interactions (PPI network). Wang et al. (43) found HBEGF and HIFA in PPI network regulated by circ_0084443. Previous studies have also shown that HBEGF and HIF1A can regulate the migration and proliferation of HEKs (72–74). Furthermore, the downstream targets of circ_0084443 may not be limited to a specific one or several. For example, circ_0084443 also can inactivate TGF-β signaling pathway through miR-17-3p/FOXO4 axis, and then promote migration of HEKs (44). Han et al. (45) found that knocking down circ_PRKDC (also called circ_0084443 based on the circRNA ID of circRNA database) changes the expression of two main extracellular matrix proteins (MMP2 and MMP9) related to cell migration through miR-31/FBN1 axis, and then promotes wound healing. Jiang et al. (46) found that circ_PRKDC can directly target miR-20a-3p to regulate the expression of RASA1 and promote the migration of HEKs. This may provide strong evidence that circ_0084443 promotes the migration of HEKs. Re-epithelization requires not only the migration but also the proliferation and differentiation of HEKs. However, some studies have shown that circRNA has the biological function of regulating proliferation and differentiation. Chen et al. (47) found that circ_0008450 could activate TGF-β/Smad signaling pathway by down-regulating Runx3 expression while promoting proliferation, migration and epithelial-mesenchymal transformation of HEKs. In addition, the increase of hypoxia conditions and the damage of cells' response to hypoxia are important reasons for the delay of wound healing (15). Yu et al. (48) found that circ_Ttc3 alleviated hypoxic injury and activated NF-κB and PI3K/AKT signaling pathways by downregulating miR-449a in HEKs. Although a small amount of circRNAs has been found in wounds today, these targets provide us with great value in the treatment of chronic wounds or in the exploration of etiological mechanisms.

Effect of circRNAs on vascular endothelial cells

Endothelial cell (ECs) dysfunction is the initial stage of DFU. The cause of endothelial dysfunction may be due to prolonged hyperglycemia (75). Due to hyperglycemia, impaired chemotaxis, cell proliferation, and migration, the healing process is badly disturbed (14). Therefore, ameliorating endothelial dysfunction is essential for the healing of chronic wounds. It has been found that various kinds of circRNAs can regulate endothelial dysfunction. For example, Zhang et al. (49) found that high glucose (HG)-induced upregulation of circ_BPTF in ECs, and circ_BPTF regulated endothelial dysfunctions, including cell apoptosis, inflammatory responses and oxidative stress, by mediating the miR-384/LIN28B axis. Shan et al. (50) found high expression of circ_HIPK3 in HG-induced ECs, and circHIPK3 acts as an endogenous miR-30a-3p sponge to inhibit miR-30a-3p activity, thereby leading to

TABLE 1 Regulatory effects of different circRNAs on key genes and signaling pathways.

Authors	circRNAs	miRNAs	Targets	Signaling pathways	Function
Wang et al. (43)	circ_0084443↓	–	HBEGF/ HIF1A↓	PI3K、 EGFR and ERK Signaling Pathway	Promoting proliferation and inducing migration of HEKs
He et al. (44)	circ_0084443↓	miR17-3p↑	FOXO4↓	TGFβ Signaling Pathway	Inducing migration of HEKs
Han et al. (45)	circ_PRKDC ↓	miR-31↑	FBN1/MMP2/ MMP9↑	–	Inducing migration of HEKs
Jiang et al. (46)	circ_PRKDC↓	miR-20a-3p↑	RASA1↓	–	Inducing migration of HEKs
Chen et al. (47)	circ_0008450↓	–	Runx3 ↑	TGF-β/Smad signaling pathway	Inhibiting proliferation, migration and epithelial-mesenchymal transformation of HEKs
Yu et al. (48)	circ_Ttc3↑	miR-449a↓		NF-κB、PI3K-AKT signaling pathway	Raising viability and reducing apoptosis of HEKs
Zhang et al. (49)	circ_BPTF↑	miR-384↓	LIN28B↓	–	Inducing endothelial dysfunction, including apoptosis, inflammatory responses, oxidative stress
Shan et al. (50)	circ_HIPK3↑	miR-30a-3p↓	VEGFC/FZD4/ WNT2↑	–	Increasing acellular capillary number
Cao et al. (51)	circ_HIPK3↓	miR-124↑	–	–	Promoting apoptosis, inhibiting migration and tube formation of ECs
Cheng et al. (52)	circ_0068087↓	miR-197↑	TLR4/NF-κB/ NLRP3↓	–	Ameliorating the inflammatory response and endothelial dysfunction of ECs
Yang et al. (53)	circ_101238↑	miR-138-5p↓	CDK6↑	–	Promoting the proliferation of FBs
Liu et al. (54)	circ_0043688↑	miR-145-5p↓	FGF2↑	–	Promoting the proliferation, migration, invasion and ECM production of FBs
Wu et al. (55)	circ_PDE7B↑	miR-661↓	FGF2↑	–	Promote the proliferation, migration and invasion of FB, and inhibit apoptosis.
Zhang et al. (56)	circ_0008259↑	–	COL1A1/ COL3A1↓	–	Inhibiting collagen (II and III) synthesis
Lv et al. (57)	circ_COL5A1↑	miR-7-5p↓	Epac1↑	PI3K-AKT signaling pathway	Promote the proliferation, migration and invasion of FBs
Su et al. (58)	circ_AMD1↑	miR-27a-3p↓	COL1A1↑	–	Promoting the proliferation and collagen synthesis of FBs
Bai et al. (59)	circ_LRP6↑	miR545-3p↓	HMGA1↑	–	Promoting the proliferation, migration and invasion of VSMCs
Shi et al. (60)	circ_0008028↑	miR-182-5p↓	TRIB3↑	–	Induce proliferation, calcification and autophagy of VSMCs
Wang et al. (61)	circ_0077930 ↓	miR_622↓	KARS↑	–	Promoting senescence of VSMCs and keeps them in G1 phase for a long time
Chen et al. (62)	circ_WDR77 (circ_0013509) ↑	miR-124↓	FGF-2↑	–	Promoting the proliferation and migration of VSMCs
Liu et al. (63)	circ_ACR↓	miR-145-3p↑	–	PI3K/AKT/mTOR signaling pathway	Leading to apoptosis, autophagy, oxidative stress in SCs
Liu et al. (64)	circ_0002538 ↑	miR-138-5p↓	PLLP↑	–	Promoting the migration and myelin formation of SCs

Symbols ↑ means "Increase expression". Symbols ↓ means “Decrease expression”.

increased expression of vascular endothelial growth factor-C (VEGFC), FZD4, and WNT2. Further study has also found that silencing circ_HIPK3 resulted in the accumulation of miR-124 and eventually endothelial dysfunction, including promotion of apoptosis, delay of the migration of ECs and inhibition of tubulation (51). A sustained HG environment promotes oxidative stress, apoptosis, and inflammatory factor expression, which result in the dysfunction of ECs (76–78). Furthermore, enhanced proinflammatory chemokines disturb wound healing, leading to diabetic ulcers (17). Cheng et al. (52) found that the down-regulation of circ_0068087 ameliorated the HG-induced TLR4/NF-κB/NLRP3 inflammasome-mediated inflammation and dysfunction of ECs by sponging miR-197. Previous studies have also shown that suppression of the NF-κB and NLRP3 inflammasome pathways ameliorate HG-induced inflammatory responses and endothelial dysfunction (79–81). This indicates that some circRNAs have regulatory effects on the well-known targets for alleviating endothelial dysfunction and inflammatory

response. However, due to the lack of exploration of circRNAs, we still can't fully know its regulatory role in ECs.

Effect of circRNAs on fibroblasts

Fibroblasts (FBs) play an important role in wound tissue repair. They move to the wound area during wound formation and synthesize collagen and fibronectin with other extracellular matrix (ECM) to generate the forces needed to shrink the wound. Studies have shown that differential expression of extracellular matrix produced, assembled and reshaped by FBs also leads to poor wound healing in DFU (82). The latest studies have shown that circRNAs can regulate the proliferation, migration and apoptosis of FBs. Yang et al. (53) found that high expression of circ_101238 promoted the FBs proliferation *via* miR-138-5p/CDK6. FBs are the primary factors of wound healing through which they respond to the proliferation, migration, and myofibroblast differentiation capabilities of specific cytokines such as fibroblasts growth factor (FGF) (83). Liu et al. (54) found that circ_0043688 can regulate the proliferation, migration, invasion and ECM production of FBs by targeting miR- 145- 5p/FGF2 axis. Another study also showed that the circ_PDE7B/mir-661 axis accelerated the proliferation, migration and invasion of FBs by up-regulating FGF2 (55). Collagen can promote the migration of FBs to the wound area, thus accelerating wound healing and enhancing re-epithelization (84–86). Zhang et al. (56) found that over expression of circ_0008259 in FBs inhibited the production of collagen (I and III). Lv et al. (57) found that circ_COL5A1 regulates the proliferation, migration and invasion of FBs through the circ_COL5A1/miR-7-5p/Epac1 axis. In addition, circ_AMD1 can regulate p63 mutation *via* miR-27a-3p, which in turn promotes proliferation and collagen synthesis of FBs (58). Although research on circRNAs in FBs is still in its infancy, these circRNAs may still be important targets for DFU wound healing. At the same time, the above-mentioned FBs-related circRNAs were not found in DFU wounds, but their value in wound healing studies is indisputable.

Effect of circRNAs on vascular smooth muscle cells

Vascular Smooth Muscle Cells (VSMCs), the main cells that constitute the middle membrane of blood vessels, and play an important role in various pathophysiological processes. VSMCs are known for their plasticity, which can change their morphology and growth state to exert contraction and synthesis functions (87). VSMCs exhibit a contractile phenotype under physiological conditions, and they can switch to a proliferative phenotype under extracellular stimulation (88). Studies have shown that HG may induce the excessive proliferation and migration of VSMCs, leading to vascular occlusion (89). Therefore, preventing abnormal proliferation and migration of VSMCs and promoting vascular recanalization may be a valuable direction for the treatment of DFU. It was found that circRNAs can regulate VSMCs. Bai et al. (59) found that circ_LRP6 was upregulated in HG-induced VSMCs, which promoted the proliferation, migration and invasion of VSMCs, whereas knocking down circ_LRP6 eliminated the capability of proliferation, migration and invasion *via* miR545-3p/HMGA1.Shi et al. (60) found that cic_0008028 induces proliferation, calcification and autophagy of HG-induced VSMCs *via* miR-1825P/TRIB3. In addition, Wang et al. (61) found that circ_0077930 caused senescence of VSMCs *via* miR_622-KARS and kept VSMCs in G1 phase for a long time. Chen et al. (62) found that circ_WDR77 (circ_0013509) targeted FGF-2 through miR-124 to regulate the proliferation and migration of VSMCs, while silencing circ_WDR77 played an inhibitory role.

Effect of circRNAs on Schwann cells

Schwann cells (SCs), also known as nerve sheath cells, are myelin cells surrounding neuronal axons in the peripheral nervous system and secrete a variety of neurotrophic factors, which are closely related to peripheral neuropathy in DFU. HG-induced apoptosis and autophagy in neuroglial cells of the peripheral nervous system are considered to be the main causes for the occurrence and development of DFU neuropathy (19, 20). Liu et al. (63) observed *in vitro* that circ_ACR reduced apoptosis, autophagy and oxidative stress in HG induced SCs by downregulating miR-145-3p. And has effect on PI3K/AKT/mTOR signaling pathway. In addition, Liu et al. (64) found that downregulation of circ_0002538 expression in DFU peripheral neuropathy regulates migration and myelin formation of SCs through miR-138-5p/PLLP axis, which in turn improves symptoms. Although it provides new ideas in the pathogenesis and treatment of DFU. However, it is still necessary to conduct a comprehensive and holistic studies.

Prospective applications of circRNAs in the diagnosis and treatment of DFU

circRNAs as a diagnostic marker

The diagnosis of DFU is still mainly based on the clinical manifestations of patients and other auxiliary examinations, but due to the lack of typical symptoms and signs in the early stage of

DFU, it is easy to be missed and misdiagnosed the disease. In recent years, with the development of gene sequencing technology, circRNA has gradually become a new exploration direction, and its potential as a diagnostic marker of DFU has been discovered. For example, the level of circ_102958 in gastric cancer tissues positively correlated with TNM staging (p= 0.032) and the area under ROC curve (AUC) was 0.74 (90). Compared with obtaining tissues, blood samples collected from DFU patients may more ethical and more acceptable. Exosomes are vesicles containing a variety of RNAs and proteins, which naturally exist in extracellular fluid and act as information exchange and substance transfer vector between cells (91). In addition, with the development of technology, it has been found that exosomes play an indispensable role in the early diagnosis, treatment and prognosis of some diseases, such as cancer and metabolic diseases (92). Chen et al. (93) analyzed a set of microarray data (GSE114248) with circ_0000907 and circ_0057362 as candidate markers and found that the AUC values of circ_0000907 and circ_0057362 in serum exosomes for the diagnosis of early stage and DM were 0.7564 and 0.8327, respectively. Meanwhile, expression of circ_0000907 and circ_0057362 was negatively correlated with ankle-brachial index (ABI) and percutaneous partial pressure of oxygen (TcPO2) (93). Based on the above research, circ_0000907 and circ_0057362 showed specificity in distinguishing DFU from diabetes in serum. Secondly, circ_0000907 and circ_0057362 in serum positively correlated with the severity of DFU, which may provide important clinical significance for Wagner stage for DFU patients in early stage. It may also be necessary to have stability and a long half-life as diagnostic markers. Han et al. (45) found that circ_PRKDC was significantly resistant to RNase R compared with PRKDC mRNA, and its half-life was longer. Zhang et al. (49) also found that RNase R hardly changed the expression of circ_BPTF, but significantly weakened the expression of linear mRNA BPTF. Although circRNA has been shown to be valuable as a diagnostic marker in DFU, it still requires strict clinical studies to detect circRNA in serum as an accurate and effective diagnostic marker of DFU. There are still some problems need to be solved, such as (a) how to select the most effective therapeutic targets; (b) evaluating the specificity and sensitivity of the screened targets; (c) specific regulatory mechanisms of targets.

circRNA as a DFU therapeutic target

Recent studies have shown that circRNA plays an important role in DFU, and some drugs have potential binding sites with circRNA, which provides a basis for exploring drugs with circRNA as a therapeutic target. For example, Xiang et al. (94) found that circ_Krt13 and circ_Krt14 down regulated Ltga3 and Mylk4 expression through downstream miR-665-3p and miR-706 in traditional Chinese medicine (Sheng-ji Hua-yu formula) for the treatment of DFU. At the same time, this plays a key role in the inflammatory phase as well as in the maturation phase to improve the wound healing rate of DFU.

In addition, the difficulty in wound healing for DFU may be due to abnormal expression of some circRNAs, and supplementation or inhibition of some circRNAs or their downstream targets by exogenous sources may be a therapeutic method for DFU. For example, Shang et al. (95) transplanted the overexpressed circ_Klhl8 into a wound of DFU patient using ECs as a vector and found that it promoted angiogenesis by miR-212-3p/SIRT5. In addition, Cheng et al. (96) found that the expression of circ_0058092 was decreased in ECs under HG conditions, and transfection of plasmids overexpressing circ_0058092 inhibited the release of inflammatory cytokine and restored the proliferation and migration capacity of ECs *via* miR-217/FOXO3. Feng et al. (97) used PLCDH-circ_ACR-carrying lentivirus to transfect wound of DFU and found that it alleviated apoptosis, autophagy and oxidative stress in SCs by reducing miR-144-3p and thus promoting activation of PI3K/AKT/mTOR pathway.

Finally, circRNA can also be used as a key point of stem cell therapy to regulate the DFU healing process. Zhang et al. (98) found that circ_0075932 in adipocyte-derived exosome mediates AuroraA/NF-kB pathway activation by directly binding to PUM2, thereby inducing inflammation and apoptosis of HEK. However, silencing PUM2, AuroraA, or blocking NF-kB has the opposite effect. Shi et al. (99) found that exosomes derived from mmu_circ_0000250 modified adipose derived mesenchymal stem cells ADSCs promoted wound healing in DFU by inducing miR-128-3p/SIRT1-mediated autophagy. In addition, Wang et al. (100) found that circ_Gcap14 regulated miR-18a-5p/HIF-1α to enhance the expression of vascular growth factor (VEGF) in DFU (Table 2).

Challenges of circRNAs in clinical applications

CircRNA may play different roles at different stages of DFU wound healing. For example, Han et al. (45) found that the expression level of circ_PRKDC did not decrease immediately after skin injury, but decreased by about 1.2 times on the first day after injury (inflammatory phase) and rapidly decreased about 3.4 times on the seventh day after injury (proliferative phase). This indicates that circ_PRKDC is dynamic and not static, and its role in inflammatory phase may be limited, but it plays an important role in the proliferation phase. However, many studies are still committed to studying the regulatory mechanism of circRNA as sponge of miRNA in DFU rather than studying its dynamics at various stages of wound healing. This may be due to the fact that the study of circRNAs in DFU is just beginning. The expression of circRNAs at each stage of DFU wound healing is dynamic, and there is a large number of

TABLE 2 Regulatory effects of different circRNAs in the treatment of DFU.

Authors	Drugs/ Vectors	circRNAs	miRNAs	Targets	Signaling pathways	Function
Xiang et al. (94)	Sheng-ji Hua-yu formula	circ_Krt13↓ circ_Krt14↓	miR-665-3p↑ miR-706↑	Ltga3↓ Mylk4↑	–	Shorten inflammation period and accelerating maturation period of DFU wound
Shang et al. (95)	ECs	circ_Klhl8 (circ_0001373) ↑	miR-212-3p↓	SIRT5↑	–	Promoting angiogenesis
Cheng et al. (96)	Plasmid	circ_0058092↑	miR−217↓	FOXO3↑	–	Restore the proliferation and migration capabilities of ECs
Feng et al. (97)	Lentivirus	circ_ACR↑	miR-144-3p↓	–	PI3K/AKT/mTOR signaling pathway	Inhibiting apoptosis of SCs
Zhang et al. (98)	Exosome	circ_0075932↑	–	PUM2↑	AuroraA/NF-kB signaling pathway	Inducing inflammation and apoptosis of HEKs
Shi et al. (99)	Exosome	mmu_circ_0000250↑	miR-128-3p↓	SIRT1↑	–	Promote wound angiogenesis and inhibiting apoptosis of ECs
Wang et al. (100)	Exosome	circ_Gcap14↑	miR-18a-5p↓	HIF-1α/ VEGF↓	–	Promoting angiogenesis

circRNAs during DFU wound healing. It may affect specificity of circRNAs as diagnostic markers. This indicates that although the diagnostic potential of circRNA for DFU is well known, it is difficult to apply clinically due to its dynamics and instability in DFU healing process. In addition, the activities of circRNAs may overlap and the interactions are complex. CircRNAs have multiple downstream targets, regulate multiple signaling pathways, and participate in multiple physiological processes in different cells and tissues, so their functions may be different depending on the cells, tissues and target sites (43). For example, Wanni Zhao et al. (101) found that compared with the DM patients, the DFU patients had 33 circRNAs differentially expressed, of which circ_FBXO7, ATM and LMBRD1 were the most significant, and signalling pathway enrichment analysis revealed that multiple pathways such as lysosomal pathway, Chagas disease pathway, herpes simplex virus infection pathway, and methane metabolism played important roles in the development of DFU. It reveals that the expression level of circRNAs in DFU was significantly changed and a complex interaction network was formed with its downstream target gene and signaling pathway. Therefore, it is possible to act in various cells by interacting with or overlapping with different signaling pathways. For this reason, it is a great challenge to sort out the most critical circRNAs for clinical application. Although our mini review has been discussed the role of circRNAs in different cells, the current research is still not enough to clarify its role in different cells. Therefore, as the study progresses, it is necessary to conduct an objective and reasonable comprehensive analysis of the expression differences of these circRNAs in the next step.

In terms of accurate therapy, the selection of circRNAs as a therapeutic target for DFU requires an appropriate method. For example, the use of gene modification techniques or methylation enzyme modifications to alter expression level of circRNAs for therapeutic purposes, but there is a lack of reliable gene modification techniques in clinic (102). Another method is to change the expression of circRNAs in DFU tissues using circRNA mimics or viral vectors, but due to biosafety concerns, it is not suitable for clinical treatment at this stage (103). Although circRNAs are more conservative and stable than other non-coding RNAs, circRNAs are easily hydrolyzed in the wound microenvironment and enters the cell membrane in a free state with difficulty (104). This may have had little or no effect on the treatment of DFU wound healing. Therefore, if circRNAs are to be used clinically, they must be delivered in a safe, reliable, effective, and less side-effect delivery system. Unfortunately, such an effective delivery system is still lacking at this stage. Recently, several studies have shown that exosomes have the potential to become new effective delivery vectors because they can protect payloads from chemical and enzymatic degradation and escape recognition by the immune system (98, 99, 105). However, the difficulty of exosome extraction and high cost limit its clinical application and there is a lack of techniques for transferring circRNAs to exosomes at present (106, 107). Therefore, research on circRNAs is still in the basic research stage, and it is still a long way from clinical application.

Conclusion

With the advancement of technology and deepening of study, circRNAs are expected to be accurate and effective biomarkers and targets for the diagnosis and treatment of DFU. However, the study of circRNAs is still in its infancy and is mostly based on basic research, so preclinical or clinical studies are needed to validate its future clinical application. In addition, it requires

researchers to identify more specific circRNAs, and provide more evidence for diagnostic markers and therapeutic targets of DFU.

Author contributions

DL and JG wrote the manuscript. DL, HB and XN performed the literature review and revised the manuscript. GS provided ideas and developed the protocol for the review. All authors contributed to the article and approved the submitted version.

Funding

This study was supported by the Inner Mongolia Autonomous Region Academician Expert Workstation Construction Project (2019); Inner Mongolia People's Hospital Doctor Research Start-up Foundation (2020BS01).

Conflict of interest

The authors declare that the research was conducted in the absence of any commercial or financial relationships that could be construed as a potential conflict of interest.

Publisher's note

References

1. Djibril AM, Mossi EK, Djagadou AK, Balaka A, Tchamdja T, Moukaila R. Epidemiological, diagnostic, therapeutic and evolutionary features of diabetic foot: a study conducted at the medico-surgical clinic, university hospital sylvanus olympio in lomé. *Pan Afr Med J* (2018) 30:4. doi: 10.11604/pamj.2018.30.4.14765

2. Rastogi A, Goyal G, Kesavan R, Bal A, Kumar H, Mangalanadanam, et al. Long term outcomes after incident diabetic foot ulcer: Multicenter large cohort prospective study (EDI-FOCUS investigators) epidemiology of diabetic foot complications study: epidemiology of diabetic foot complications study. *Diabetes Res Clin Pract* (2020) 162:108113. doi: 10.1016/j.diabres.2020.108113

3. Wang Z, Huang K, Xu J, Liu J, Zheng Y. Insights from dysregulated mRNA expression profile of β-cells in response to proinflammatory cytokines. *J Immunol Res* (2022) 2022:4542487. doi: 10.1155/2022/4542487

4. Shang FF, Luo S, Liang X, Xia Y. Alterations of circular RNAs in hyperglycemic human endothelial cells. *Biochem Biophys Res Commun* (2018) 499(3):551–5. doi: 10.1016/j.bbrc

5. Schultz GS, Davidson JM, Kirsner RS, Bornstein P, Herman IM. Dynamic reciprocity in the wound microenvironment. *Wound Repair Regener* (2011) 19 (2):134–48. doi: 10.1111/j.1524-475X.2011.00673.x

6. Baltzis D, Eleftheriadou I, Veves A. Pathogenesis and treatment of impaired wound healing in diabetes mellitus: new insights. *Adv Ther* (2014) 8):817–36. doi: 10.1007/s12325-014-0140-x

7. Rosso A, Balsamo A, Gambino R, Dentelli P, Falcioni R, Cassader M, et al. p53 mediates the accelerated onset of senescence of endothelial progenitor cells in diabetes. *J Biol Chem* (2006) 281(7):4339–4347. doi: 10.1074/jbc.M509293200

8. Dvorin EL, Wylie–Sears J, Kaushal S, Martin DP, Bischoff J. Quantitative evaluation of endothelial progenitors and cardiac valve endothelial cells: Proliferation and differentiation on poly–glycolic acid/poly–4 –hydroxybutyrate scaffold in response to vascular endothelial growth factor and transforming growth factor beta1. *Tissue Eng* (2004) 9(3):487–493. doi: 10.1089/107632703322066660

9. Rethineswaran VK, Kim YJ, Jang WB, Ji ST, Kang S, Kim DY, et al. Enzyme –aided extraction of fucoidan by AMG augments the functionality of EPCs through regulation of the AKT/Rheb signaling pathway. *Mar Drugs* (2019) 17(7):392. doi: 10.3390/md17070392

10. Jin H, Zhang Z, Wang C, Tang Q, Wang J, Bai X, et al. Melatonin protects endothelial progenitor cells against AGE–induced apoptosis *via* autophagy flux stimulation and promotes wound healing in diabetic mice. *Exp Mol Med* (2018) 50 (11):1–15. doi: 10.1038/s12276-018-0177-z

11. Gao J, Zhao G, Li W, Zhang J, Che Y, Song M, et al. MiR–155 targets PTCH1 to mediate endothelial progenitor cell dysfunction caused by high glucose. *Exp Cell Res* (2018) 366:55–62. doi: 10.1016/j.yexcr.2018.03.012

12. Okonkwo UA, DiPietro LA. Diabetes and wound angiogenesis. *Int J Mol Sci* (2017) 18(7):1419. doi: 10.3390/ijms18071419

13. Wang M, Wang C, Chen M, Xi Y, Cheng W, Mao C, et al. Efficient angiogenesis-based diabetic wound healing/skin reconstruction through bioactive antibacterial adhesive ultraviolet shielding nanodressing with exosome release. *ACS Nano* (2019) 13(9):10279–93. doi: 10.1021/acsnano.9b03656

14. Blakytny R, Jude EB. Altered molecular mechanisms of diabetic foot ulcers. *Int J Low Extremity Wounds* (2009) 8(2):95–104. doi: 10.1177/1534734609337151

15. Catrina SB. Impaired hypoxia-inducible factor (HIF) regulation by hyperglycemia. *J Mol Med (Berl)* (2014) 92(10):1025–34. doi: 10.1007/s00109-014-1166-x

16. Blakytny R, Jude E. The molecular biology of chronic wounds and delayed healing in diabetes. *Diabetes Med* (2006) 23(6):594–608. doi: 10.1111/j.1464-5491.2006.01773.x

17. Falanga V. Wound healing and its impairment in the diabetic foot. *Lancet* (2005) 366(9498):1736–43. doi: 10.1016/S0140-6736(05)67700-8

18. Shaw JE, Boulton AJM. The pathogenesis of diabetic foot problems. *overview Diabetes* (1997) 46(suppl.):S58–61. doi: 10.2337/diab.46.2.s58

19. Goncalves NP, Vaegter CB, Andersen H, Ostergaard L, Calcutt NA, Jensen TS. Schwann cell interactions with axons and microvessels in diabetic neuropathy. *Nat Rev Neurol* (2017) 13:135–47. doi: 10.1038/nrneurol.2016.201

20. Tsuda M. Microglia in the spinal cord and neuropathic pain. *J Diabetes Investig* (2016) 7(1):17–26. doi: 10.1111/jdi.12379

21. Zochodone DW. Diabetic polyneuropathy: An update. *Curr Opin Neurol* (2008) 21:527–33. doi: 10.1097/WCO.0b013e32830b84cb

22. Brem H, Tomic-Canic M. Cellular and molecular basis of wound healing in diabetes. *J Clin Invest* (2007) 117(5):1219–22. doi: 10.1172/JCI32169

23. Dong R, Ma XK, Li GW, Yang L. CIRCpedia v2: an updated database for comprehensive circular RNA annotation and expression comparison. *Genomics Proteomics Bioinf* (2018) 16(4):226–33. doi: 10.1016/j.gpb.2018.08.001

24. Salzman J, Gawad C, Wang PL, Lacayo N, Brown PO. Circular RNAs are the predominant transcript isoform from hundreds of human genes in diverse cell types. *PloS One* (2012) 7(2):e30733. doi: 10.1371/journal.pone.0030733

25. Memczak S, Jens M, Elefsinioti A, Torti F, Krueger J, Rybak A, et al. Circular RNAs are a large class of animal RNAs with regulatory potency. *Nature* (2013) 495 (7441):333–8. doi: 10.1038/nature11928

26. Zhang M, Huang N, Yang X, Luo J, Yan S, Xiao F, et al. A novel protein encoded by the circular form of the SHPRH gene suppresses glioma tumorigenesis. *Oncogene* (2018) 37(13):1805–14. doi: 10.1038/s41388-017-0019-9

27. Lu Z, Filonov GS, Noto JJ, Schmidt CA, Hatkevich TL, Wen Y, et al. Metazoan tRNA introns generate stable circular RNAs in vivo. *RNA* (2015) 21 (9):1554–65. doi: 10.1261/rna.052944.115

28. Li Z, Huang C, Bao C, Chen L, Lin M, Wang X, et al. Exon-intron circular RNAs regulate transcription in the nucleus. *Nat Struct Mol Biol* (2015) 22(3):256–64. doi: 10.1038/nsmb.2959

29. Zhang Y, Zhang XO, Chen T, Xiang JF, Yin QF, Xing YH, et al. Circular intronic long noncoding RNAs. *Mol Cell* (2013) 51(6):792–806. doi: 10.1016/j.molcel.2013.08.017

30. Ambros V. The functions of animal microRNAs. *Nature* (2004) 431 (7006):350–5. doi: 10.1038/nature02871

31. Hu ZQ, Zhou SL, Li J, Zhou ZJ, Wang PC, Xin HY, et al. Circular RNA sequencing identifies circASAP1 as a key regulator in hepatocellular carcinoma metastasis. *Hepatology* (2020) 72(3):906–22. doi: 10.1002/hep.31068

32. Yu L, Gong X, Sun L, Zhou Q, Lu B, Zhu L. The circular RNA Cdr1as act as an oncogene in hepatocellular carcinoma through targeting miR-7 expression. *PloS One* (2016) 11(7):e0158347. doi: 10.1371/journal.pone.0158347

33. Geng HH, Rui L, Su YM, Jie X, Min P, Cai XX, et al. The circular RNA Cdr1as promotes myocardial infarction by mediating the regulation of miR-7a on its target genes expression. *PloS One* (2016) 11(3):e0151753. doi: 10.1371/journal.pone.0151753

34. Pan H, Li T, Jiang Y, Pan C, Ding Y, Huang Z, et al. Overexpression of circular RNA ciRS-7 abrogates the tumor suppressive effect of miR-7 on gastric cancer *via* PTEN/PI3K/AKT signaling pathway. *J Cell Biochem* (2018) 119(1):440–6. doi: 10.1002/jcb.26201

35. Jeck WR, Sorrentino JA, Wang K, Slevin MK, Burd CE, Liu J, et al. Circular RNAs are abundant, conserved, and associated with ALU repeats. *RNA* (2013) 19 (2):141–57. doi: 10.1261/rna.035667.112

36. Yang Y, Fan X, Mao M, Song X, Wu P, Zhang Y, et al. Extensive translation of circular RNAs driven by N6-methyladenosine. *Cell Res* (2017) 27(5):626–41. doi: 10.1038/cr.2017.31

37. Pamudurti NR, Bartok O, Jens M, Ashwalfluss R, Stottmeister C, Ruhe L, et al. Translation of circRNAs. *Mol Cell* (2017) 66(1):9–21. doi: 10.1016/j.molcel.2017.02.021

38. Cedric BC, Souraka TDM, Feng YL, Kisembo P, Tu JC. CircRNA ZFR stimulates the proliferation of hepatocellular carcinoma through upregulating MAP2K1. *Eur Rev Med Pharmacol Sci* (2020) 24(19):9924–31. doi: 10.26355/eurrev_202010_23203

39. Du WW, Yang W, Chen Y, Wu ZK, Foster FS, Yang Z, et al. Foxo3 circular RNA promotes cardiac senescence by modulating multiple factors associated with stress and senescence responses. *Eur Heart J* (2016) 38(18):1402–12. doi: 10.1093/eurheartj/ehw001

40. Zhao W, Liang J, Chen Z, Diao Y, Miao G. Combined analysis of circRNA and mRNA profiles and interactions in patients with diabetic foot and diabetes mellitus. *Int Wound J* (2020) 17(5):1183–93. doi: 10.1111/iwj.13420

41. Tian M, Dong J, Yuan B, Jia H. Identification of potential circRNAs and circRNA-miRNA-mRNA regulatory network in the development of diabetic foot ulcers by integrated bioinformatics analysis. *Int Wound J* (2021) 18(3):323–31. doi: 10.1111/iwj

42. Liao S, Lin X, Mo C. Integrated analysis of circRNA-miRNA-mRNA regulatory network identifies potential diagnostic biomarkers in diabetic foot ulcer. *Noncoding RNA Res* (2020) 5(3):116–24. doi: 10.1016/j.ncrna.2020.07.001

43. Wang A, Toma MA, Ma J, Li D, Vij M, Chu T, et al. Circular RNA hsa_circ_0084443 is upregulated in diabetic foot ulcer and modulates keratinocyte migration and proliferation. *Adv Wound Care (New Rochelle)* (2020) 9(4):145–60. doi: 10.1089/wound.2019.0956

44. He Z, Xu X. Circ_0084443 inhibits wound healing *via* repressing keratinocyte migration through targeting the miR-17-3p/FOXO4 axis. *Biochem Genet* (2022) 60(4):1236–52. doi: 10.1007/s10528-021-10157-5

45. Han D, Liu W, Li G, Liu L. Circ_PRKDC knockdown promotes skin wound healing by enhancing keratinocyte migration *via* miR-31/FBN1 axis. *J Mol Histol* (2021) 52(4):681–91. doi: 10.1007/s10735-021-09996-8

46. Jiang LN, Ji X, Liu W, Qi C, Zhai X. Identification of the circ_PRKDC/miR-20a-3p/RASA1 axis in regulating HaCaT keratinocyte migration. *Wound Repair Regener* (2022) 30(2):282–91. doi: 10.1111/wrr.12988

47. Chen H, Xu X, Lai L, Huo R, Chen M. Circ_0008450 downregulates Runx3 to promote the proliferation and epithelial-mesenchymal transition of human keratinized epithelial cells. *Cell Cycle* (2020) 19(23):3303–16. doi: 10.1080/15384101.2020.1842665

48. Yu L, Wang Q, Liu N, Zhao J, Yu J, Tao S. Circular RNA circ-Ttc3 protects HaCaT cells from hypoxic injury by downregulation of miR-449a. *IUBMB Life* (2020) 72(3):505–14. doi: 10.1002/iub.2236

49. Zhang W, Sui Y. CircBPTF knockdown ameliorates high glucose-induced inflammatory injuries and oxidative stress by targeting the miR-384/LIN28B axis in human umbilical vein endothelial cells. *Mol Cell Biochem* (2020) 471(1):101–11. doi: 10.1007/s11010-020-03770-2

50. Shan K, Liu C, Liu BH, Chen X, Dong R, Liu X, et al. Circular noncoding RNA HIPK3 mediates retinal vascular dysfunction in diabetes mellitus. *Circulation* (2017) 136(17):1629–42. doi: 10.1161/CIRCULATIONAHA.117.029004

51. Cao Y, Yuan G, Zhang Y, Lu R. High glucose-induced circHIPK3 downregulation mediates endothelial cell injury. *Biochem Biophys Res Commun* (2018) 507(1-4):362–8. doi: 10.1016/j.bbrc.2018.11.041

52. Cheng J, Liu Q, Hu N, Zheng F, Zhang X, Ni Y, et al. Downregulation of hsa_circ_0068087 ameliorates TLR4/NF-κB/NLRP3 inflammasome-mediated inflammation and endothelial cell dysfunction in high glucose conditioned by sponging miR-197. *Gene* (2019) 709:1–7. doi: 10.1016/j.gene.2019.05.012

53. Yang D, Li M, Du N. Effects of the circ_101238/miR-138-5p/CDK6 axis on proliferation and apoptosis keloid fibroblasts. *Exp Ther Med* (2020) 20(3):1995–2002. doi: 10.3892/etm.2020.8917

54. Liu Y, Wang X, Ni Z, Li Y, Song J, Zhu F, et al. Circular RNA hsa_circ_0043688 serves as a competing endogenous RNA for microRNA-145-5p to promote the progression of keloids *via* fibroblast growth factor-2. *J Clin Lab Anal* (2022) 36(8):e24528. doi: 10.1002/jcla.24528

55. Wu F, He H, Chen Y, Zhu D, Jiang T, Wang J. CircPDE7B/miR-661 axis accelerates the progression of human keloid fibroblasts by upregulating fibroblast growth factor 2 (FGF2). *Mol Cell Biochem* (2022) 477(4):1113–26. doi: 10.1007/s11010-021-04345-5

56. Zhang Z, Yu K, Liu O, Xiong Y, Yang X, Wang S, et al. Expression profile and bioinformatics analyses of circular RNAs in keloid and normal dermal fibroblasts. *Exp Cell Res* (2020) 388(1):111799. doi: 10.1016/j.yexcr.2019.111799-111808

57. Lv W, Liu S, Zhang Q, Hu W, Wu Y, Ren Y. Circular RNA circCOL5A1 sponges the miR-7-5p/Epac1 axis to promote the progression of keloids through regulating PI3K/Akt signaling pathway. *Front Cell Dev Biol* (2021) 9:626027. doi: 10.3389/fcell.2021.626027

58. Su P, Qiao Q, Ji G, Zhang Z. CircAMD1 regulates proliferation and collagen synthesis *via* sponging miR-27a-3p in P63-mutant human dermal fibroblasts. *Differentiation* (2021) 119:10–8. doi: 10.1016/j.diff.2021.04.002

59. Bai Y, Liu F, Yang Z. CircRNA LRP6 promotes high-glucose induced proliferation and migration of vascular smooth muscle cells through regulating miR-545-3p/HMGA1 signaling axis. *Am J Transl Res* (2021) 13(8):8909–20.

60. Shi L, Li Y, Shi M, Li X, Li G, Cen J, et al. Hsa_circRNA_0008028 deficiency ameliorates high glucose-induced proliferation, calcification, and autophagy of vascular smooth muscle cells *via* miR-182-5p/TRIB3 axis. *Oxid Med Cell Longev* (2022) 2022:5142381. doi: 10.1155/2022/5142381

61. Wang S, Zhan J, Lin X, Wang YJ, Wang Y, Liu Y. CircRNA-0077930 from hyperglycaemia-stimulated vascular endothelial cell exosomes regulates senescence in vascular smooth muscle cells. *Cell Biochem Funct* (2020) 38(8):1056–68. doi: 10.1002/cbf.3543

62. Chen J, Cui L, Yuan J, Zhang Y, Sang H. Circular RNA WDR77 target FGF-2 to regulate vascular smooth muscle cells proliferation and migration by sponging miR-124. *Biochem Biophys Res Commun* (2017) 494(1-2):126–32. doi: 10.1016/j.bbrc.2017.10.068

63. Liu Y, Chen X, Yao J, Kang J. Circular RNA ACR relieves high glucose-aroused RSC96 cell apoptosis and autophagy *via* declining microRNA-145-3p. *J Cell Biochem* (2019). doi: 10.1002/jcb.29568

64. Liu Y, Xu Z, Liu W, Ren S, Xiong H,T, et al. The circ_0002538/miR-138-5p/PLLP axis regulates Schwann cell migration and myelination in diabetic peripheral neuropathy. *bioRxiv* (2022). doi: 10.1101/2022.02.24.481714

65. Lewis CJ, Mardaryev AN, Poterlowicz K, Sharova TY, Aziz A, Sharpe DT, et al. Bone morphogenetic protein signaling suppresses wound-induced skin repair by inhibiting keratinocyte proliferation and migration. *J Invest Dermatol* (2014) 134(3):827–37. doi: 10.1038/jid.2013.419

66. Lan CC, Liu IH, Fang AH, Wen CH, Wu CS. Hyperglycaemic conditions decrease cultured keratinocyte mobility: Implications for impaired wound healing in patients with diabetes. *Br J Dermatol* (2008) 159(5):1103–15. doi: 10.1111/j.1365-2133.2008.08789.x

67. Redd MJ, Cooper L, Wood W, Stramer B, Martin P. Wound healing and inflammation: embryos reveal the way to perfect repair. *Philos Trans R Soc Lond B Biol Sci* (2004) 359(1445):777–84. doi: 10.1098/rstb.2004.1466

68. Krishnaswamy VR, Korrapati PS. Role of dermatopontin in re-epithelialization: Implications on keratinocyte migration and proliferation. *Sci Rep* (2014) 4:7385. doi: 10.1038/srep07385

69. Wei F, Wang A, Wang Q, Han W, Rong R, Wang L, et al. Plasma endothelial cells-derived extracellular vesicles promote wound healing in diabetes through YAP and the PI3K/Akt/mTOR pathway. *Aging (Albany NY)* (2020) 12(12):12002–18. doi: 10.18632/aging.103366

70. Zhong H, Qian J, Xiao Z, Chen Y, He X, Sun C, et al. MicroRNA-133b inhibition restores EGFR expression and accelerates diabetes-impaired wound healing. *Oxid Med Cell Longev* (2021) 2021:9306760. doi: 10.1155/2021/9306760

71. Yang SL, Han R, Liu Y, Hu LY, Li XL, Zhu LY. Negative pressure wound therapy is associated with up-regulation of bFGF and ERK1/2 in human diabetic foot wounds. *Wound Repair Regener* (2014) 22(4):548–54. doi: 10.1111/wrr.12195

72. Poumay Y, De Rouvroit CL. HB-EGF, the growth factor that accelerates keratinocyte migration, but slows proliferation. *J Invest Dermatol* (2012) 132:2129–30. doi: 10.1038/jid.2012.225

73. Shirakata Y. Heparin-binding EGF-like growth factor accelerates keratinocyte migration and skin wound healing. *J Cell Sci* (2005) 118:2363–70. doi: 10.1242/jcs.02346

74. Fitsialos G, Bourget I, Augier S, Ginouvès A, Rezzonico R, Odorisio T, et al. HIF1 transcription factor regulates laminin-332 expression and keratinocyte migration. *J Cell Sci* (2008) 121:2992–3001. doi: 10.1242/jcs.029256

75. Versari D, Daghini E, Virdis A, Ghiadoni L, Taddei S. Endothelial dysfunction as a target for prevention of cardiovascular disease. *Diabetes Care* (2009) Suppl 2):S314–321. doi: 10.2337/dc09-S330

76. Gu TT, Song L, Chen TY, Wang X, Zhao XJ, Ding XQ, et al. Fructose downregulates miR-330 to induce renal inflammatory response and insulin signaling impairment: attenuation by morin. *Mol Nutr Food Res* (2017) 61 (8):1600760. doi: 10.1002/mnfr.201600760

77. Zhang J, Jin J, Liu J, He Y, Zhang P, Ye W, et al. A study of the correlation of insulin resistance and leptin with inflammatory factors and vascular endothelial injury in T2DM patients with CHD. *Exp Ther Med* (2018) 16(1):265–9. doi: 10.3892/etm.2018.6170

78. Saberi Firouzi S, Namazi Sarvestani N, Bakhtiarian A, Ghazi Khansari M, Karimi MY, Ranjbar A, et al. Sildenafil protective effects on high glucose-induced neurotoxicity in PC12 cells: the role of oxidative stress, apoptosis, and inflammation pathways in an *in vitro* cellular model for diabetic neuropathy. *Neurol Res* (2018) 40(8):624–36. doi: 10.1080/01616412.2018.1458813

79. Bruder-Nascimento T, Ferreira NS, Zanotto CZ, Ramalho F, Pequeno IO, Olivon VC, et al. NLRP3 inflammasome mediates aldosterone-induced vascular damage. *Circulation* (2016) 134(23):1866–80. doi: 10.1161/CIRCULATIONAHA.116.024369

80. Li Y, Liu M, Zuo Z, Liu J, Yu X, Guan Y, et al. TLR9 regulates the NF-κB-NLRP3-IL-1β pathway negatively in salmonella-induced NKG2D-mediated intestinal inflammation. *J Immunol* (2017) 199(2):761–73. doi: 10.4049/jimmunol.1601416

81. Zhang X, Du Q, Yang Y, Wang J, Dou S, Liu C, et al. The protective effect of luteolin on myocardial ischemia/reperfusion (I/R) injury through TLR4/NF-κB/NLRP3 inflammasome pathway. *BioMed Pharmacother* (2017) 91:1042–52. doi: 10.1016/j.biopha.2017.05.033

82. Maione AG, Smith A, Kashpur O, Yanez V, Knight E, Mooney DJ, et al. Altered ECM deposition by diabetic foot ulcer-derived fibroblasts implicates fibronectin in chronic wound repair. *Wound Repair Regene* (2016) 24(4):630–43. doi: 10.1111/wrr.12437

83. Watarai A, Schirmer L, Thönes S, Freudenberg U, Werner C, Simon JC, et al. TGFβ functionalized starPEG-heparin hydrogels modulate human dermal fibroblast growth and differentiation. *Acta Biomater* (2015) 25:65–75. doi: 10.1016/j.actbio.2015.07.036

84. Munish T, Ramneesh G, Sanjeev S, Jasdeep S, Jaspal S, Nikhil G. Comparative study of collagen based dressing and standard dressing in diabetic foot ulcer. *J Evol Med Dent Sci* (2015) 4(21):3614–22. doi: 10.14260/jemds/2015/521

85. Chalimidi KR, Kumar Y, Kini UA. Efficacy of collagen particles in chronic non healing ulcers. *J Clin Diagn Res* (2015) 9(6):PC01–3. doi: 10.7860/JCDR/2015/11782.6001

86. Lullove EJ, Liden B, Winters C, McEneaney P, Raphael A, Lantis Ii JC. A multicenter, blinded, randomized controlled clinical trial evaluating the effect of omega-3-rich fish skin in the treatment of chronic, nonresponsive diabetic foot ulcers. *Wounds* (2021) 33(7):169–77. doi: 10.25270/wnds/2021.169177

87. Wang G, Jacquet L, Karamariti E, Xu Q. Origin and differentiation of vascular smooth muscle cells. *J Physiol* (2015) 593(14):3013–30. doi: 10.1113/JP270033

88. Shi J, Yang Y, Cheng A, Xu G, He F. Metabolism of vascular smooth muscle cells in vascular diseases. *Am J Physiol Heart Circ Physiol* (2020) 319(3):H613–31. doi: 10.1152/ajpheart.00220.2020

89. Majesky MW, Dong XR, Regan JN, Hoglund VJ. Vascular smooth muscle progenitor cells: building and repairing blood vessels. *Circ Res* (2011) 108(3):365–77. doi: 10.1161/CIRCRESAHA.110.223800

90. Wei J, Wei W, Xu H, Wang Z, Gao W, Wang T, et al. Circular RNA hsa_circRNA_102958 may serve as a diagnostic marker for gastric cancer. *Cancer biomark* (2020) 27(2):139–45. doi: 10.3233/CBM-182029

91. Pegtel DM, Gould SJ. Exosomes. *Annu Rev Biochem* (2019) 88:487–514. doi: 10.1146/annurev-biochem-013118-111902

92. Santasusagna S, Moreno I, Navarro A, Rodenas FM, Hernández R, Castellano JJ, et al. Prognostic impact of miR-200 family members in plasma and exosomes from tumor-draining versus peripheral veins of colon cancer patients. *Oncology* (2018) 95(5):309–18. doi: 10.1159/000490726

93. Chen ZJ, Shi XJ, Fu LJ, Liu J, Shi K, Su PK, et al. Serum and exosomal hsa_circ_0000907 and hsa_circ_0057362 as novel biomarkers in the early diagnosis of diabetic foot ulcer. *Eur Rev Med Pharmacol Sci* (2020) 24:8117–26. doi: 10.26355/eurrev_202008_22498

94. Xiang Y, Kuai L, Ru Y, Jiang J, Li X, Li F, et al. Transcriptional profiling and circRNA-miRNA-mRNA network analysis identify the biomarkers in sheng-ji hua-yu formula treated diabetic wound healing. *J Ethnopharmacol* (2021) 268:113643. doi: 10.1016/j.jep.2020.113643

95. Shang B, Xu T, Hu N, Mao Y, Du X. Circ-Klhl8 overexpression increased the therapeutic effect of EPCs in diabetic wound healing *via* the miR-212-3p/SIRT5 axis. *J Diabetes Complications* (2021) 35(11):108020. doi: 10.1016/j.jdiacomp.2021.108020

96. Cheng J, Hu W, Zheng F, Wu Y, Li M. hsa_circ_0058092 protects against hyperglycemia-induced endothelial progenitor cell damage *via* miR-217/FOXO3. *Int J Mol Med* (2020) 46(3):1146–54. doi: 10.3892/ijmm.2020.4664

97. Feng C, Lv X, Tan H, Deng Q, Zheng E. Apoptosis and autophagy inhibited by autophagy-related circular RNA in schwann cells *via* miR-144-3p/PI3K/AKT/mTOR pathway. *RNA Dis* (2020) 7:e461. doi: 10.14800/rd.461

98. Zhang X, Chen L, Xiao B, Liu H, Su J. Circ_0075932 in adipocyte-derived exosomes induces inflammation and apoptosis in human dermal keratinocytes by directly binding with PUM2 and promoting PUM2-mediated activation of AuroraA/NF-κB pathway. *Biochem Biophys Res Commun* (2019) 511(3):551–8. doi: 10.1016/j.bbrc.2019.02.082

99. Shi R, Jin Y, Hu W, Lian W, Cao C, Han S, et al. Exosomes derived from mmu_circ_0000250-modified adipose-derived mesenchymal stem cells promote wound healing in diabetic mice by inducing miR-128-3p/SIRT1-mediated autophagy. *Am J Physiol Cell Physiol* (2020) 318(5):C848–56. doi: 10.1152/ajpcell.00041.2020

100. Wang Z, Feng C, Liu H, Meng T, Huang W, Long X, et al. Hypoxic pretreatment of adipose-derived stem cells accelerates diabetic wound healing *via* circ-Gcap14 and HIF-1α/VEGF mediated angiopoiesis. *Int J Stem Cells* (2021) 14 (4):447–54. doi: 10.15283/ijsc21050

101. Zhao W, Meng X, Liang J. Analysis of circRNA-mRNA expression profiles and functional enrichment in diabetes mellitus based on high throughput sequencing. *Int Wound J* (2022) 19(5):1253–62. doi: 10.1111/iwj.13838

102. Xiao S, Zhang D, Liu Z, Jin W, Huang G, Wei Z, et al. Diabetes-induced glucolipotoxicity impairs wound healing ability of adipose-derived stem cells-through the miR-1248/CITED2/HIF-1α pathway. *Aging (Albany NY)* (2020) 12 (8):6947–65. doi: 10.18632/aging.103053

103. Cornetta K, Duffy L, Turtle CJ, Jensen M, Forman S, Binder-Scholl G, et al. Absence of replication competent lentivirus in the clinic: Analysis of infused T cell products. *Mol Ther* (2018) 26(1):280–8. doi: 10.1016/j.ymthe.2017.09.008

104. Lv Q, Deng J, Chen Y, Wang Y, Liu B, Liu J. Engineered human adipose stem-cell-derived exosomes loaded with miR-21-5p to promote diabetic cutaneous wound healing. *Mol Pharm* (2020) . 17(5):1723–33. doi: 10.1002/smll.201904044

105. Xiong Y, Chen L, Yan C, Zhou W, Endo Y, Liu J, et al. Circulating exosomal miR-20b-5p inhibition restores wnt9b signaling and reverses diabetes-associated impaired wound healing. *Small* (2020) 16(3):e1904044. doi: 10.1002/smll.201904044

106. He C, Zheng S, Luo Y, Wang B. Exosome theranostics: Biology and translational medicine. *Theranostics* (2018) 8(1):237–55. doi: 10.7150/thno.21945

107. Qiu H, Liu S, Wu K, Zhao R, Cao L, Wang H. Prospective application of exosomes derived from adipose-derived stem cells in skin wound healing: A review. *J Cosmet Dermatol* (2020) 19(3):574–81. doi: 10.1111/jocd.13215

frontiers | Frontiers in Endocrinology

TYPE Systematic Review
PUBLISHED 10 January 2023
DOI 10.3389/fendo.2022.971354

OPEN ACCESS

EDITED BY
Carlos Guillén,
Department of Biochemistry and Molecular Biology, Complutense University, Spain

REVIEWED BY
Jacopo Sabbatinelli,
Università Politecnica delle Marche, Italy
Alessandro Rolfo,
University of Turin, Italy
Vernon Dolinsky,
University of Manitoba, Canada

*CORRESPONDENCE
Kimberly A. Lewis
kimberly.lewis@ucsf.edu

SPECIALTY SECTION
This article was submitted to Diabetes: Molecular Mechanisms, a section of the journal Frontiers in Endocrinology

RECEIVED 17 June 2022
ACCEPTED 20 December 2022
PUBLISHED 10 January 2023

CITATION
Lewis KA, Chang L, Cheung J, Aouizerat BE, Jelliffe-Pawlowski LL, McLemore MR, Piening B, Rand L, Ryckman KK and Flowers E (2023) Systematic review of transcriptome and microRNAome associations with gestational diabetes mellitus. *Front. Endocrinol.* 13:971354. doi: 10.3389/fendo.2022.971354

Systematic review of transcriptome and microRNAome associations with gestational diabetes mellitus

Kimberly A. Lewis[1*], Lisa Chang[1], Julinna Cheung[2], Bradley E. Aouizerat[3], Laura L. Jelliffe-Pawlowski[4], Monica R. McLemore[5], Brian Piening[6], Larry Rand[7], Kelli K. Ryckman[8] and Elena Flowers[1]

[1]School of Nursing, Department of Physiological Nursing, University of California, San Francisco, San Francisco, CA, United States, [2]College of Biological Sciences, University of California at Davis, Davis, CA, United States, [3]College of Dentistry, New York University, New York, NY, United States, [4]Department of Epidemiology and Biostatistics, School of Medicine, University of California at San Francisco, San Francisco, CA, United States, [5]School of Nursing, Department of Family Health Care Nursing, University of California, San Francisco, San Francisco, CA, United States, [6]Earle A. Chiles Research Institute, Providence St Joseph Health, Portland, OR, United States, [7]Obstetrics and Gynecology, Reproductive Sciences, School of Medicine, University of California at San Francisco, San Francisco, CA, United States, [8]Department of Epidemiology, College of Public Health, University of Iowa, Iowa City, IA, United States

Purpose: Gestational diabetes (GDM) is associated with increased risk for preterm birth and related complications for both the pregnant person and newborn. Changes in gene expression have the potential to characterize complex interactions between genetic and behavioral/environmental risk factors for GDM. Our goal was to summarize the state of the science about changes in gene expression and GDM.

Design: The systematic review was conducted using the Preferred Reporting Items for Systematic Reviews and Meta-Analyses guidelines.

Methods: PubMed articles about humans, in English, from any date were included if they described mRNA transcriptome or microRNA findings from blood samples in adults with GDM compared with adults without GDM.

Results: Sixteen articles were found representing 1355 adults (n=674 with GDM, n=681 controls) from 12 countries. Three studies reported transcriptome results and thirteen reported microRNA findings. Identified pathways described various aspects of diabetes pathogenesis, including glucose and insulin signaling, regulation, and transport; natural killer cell mediated cytotoxicity; and fatty acid biosynthesis and metabolism. Studies described 135 unique miRNAs that were associated with GDM, of which eight (miR-16-5p, miR-17-5p, miR-20a-5p, miR-29a-3p, miR-195-5p, miR-222-3p, miR-210-3p, and miR-342-3p) were described in 2 or more studies. Findings suggest that miRNA levels vary based on the time in pregnancy when GDM develops, the time point at which they were measured, sex assigned at birth of the offspring,

and both the pre-pregnancy and gestational body mass index of the pregnant person.

Conclusions: The mRNA, miRNA, gene targets, and pathways identified in this review contribute to our understanding of GDM pathogenesis; however, further research is warranted to validate previous findings. In particular, longitudinal repeated-measures designs are needed that control for participant characteristics (e.g., weight), use standardized data collection methods and analysis tools, and are sufficiently powered to detect differences between subgroups. Findings may be used to improve early diagnosis, prevention, medication choice and/or clinical treatment of patients with GDM.

KEYWORDS

mRNA, miRNA, transcriptome, miRNAome, microRNA (miR), gestational diabetes (GDM), differential gene expression (DGE), metabolic pathways

1 Introduction

Gestational diabetes (GDM) is associated with an increased risk for preterm birth and related complications for both the pregnant person and newborn (1). GDM is defined as chronic hyperglycemia that begins in the second or third trimester of pregnancy (1). The prevalence of GDM is increasing, and ranges from 1.7-11.6% internationally and from 2.5-7.6% in North America (2). GDM is often associated with pancreatic β-cell dysfunction that may lead to onset of diabetes after pregnancy (1, 3). Additionally, the offspring of pregnant people affected by GDM are more likely to develop attention deficit hyperactivity disorder, autism spectrum disorder, diabetes, and obesity (4–6). The pathogenesis of GDM is unclear, but evidence supports links between obesity, adipokines (the signaling molecules secreted by adipose tissue), or disruptions in oxidative stress mechanisms and GDM incidence (7, 8).

Changes in gene expression have the potential to characterize complex interactions between genetic and behavioral/environmental risk factors for GDM (8–10). Messenger ribonucleic acid (mRNA) are single stranded RNAs that translate genetic information into biologically active molecules. Given that mRNAs characterize, affect, and/or are associated with the expression of genes within an individual's environment and context, they may be useful biomarkers of risk for GDM and potentially provide insights about the underlying mechanisms of risk (11). A previous review of the literature summarized genes that were differently expressed in GDM compared to other types of diabetes (8, 12). Differently expressed genes were influenced by GDM disease duration, obesity, number of gestations, glucose serum levels and the use of medications (12). However, prior studies have reported discrepant findings and it remains unclear how mRNA expression differs between blood samples from pregnant individuals with GDM relative to healthy individuals without GDM.

MicroRNAs, or miRNAs, are small, non-coding RNAs that interfere with mRNA translation to alter the expression levels of gene products (13, 14). Current biomarkers for GDM do not provide early detection of who is at greatest risk, do not characterize differences in the specific risk profile, and do not always predict resulting complications (15, 16). Circulating miRNAs are promising diagnostic biomarkers that represent environmental or behavioral influences on gene expression, potentially providing a more comprehensive measure of risk (15–19). A prior literature review summarized miRNA expression in the blood of pregnant people with GDM compared with healthy controls and found initial evidence that select miRNAs may be promising biomarkers for early detection of GDM risk, but concluded that there was insufficient overall evidence, particularly from samples of diverse individuals, to draw definitive conclusions (10).The purpose of this systematic review was to summarize the research about differences in circulating transcriptome (mRNA) and miRNA levels of adults with GDM compared with healthy controls. This paper updates previous literature reviews by incorporating both mRNA and miRNA studies in the synthesized analysis for a more robust understanding of the pathogenesis of GDM and associated complications.

2 Materials and methods

The systematic review was conducted using the Preferred Reporting Items for Systematic Reviews and Meta-Analyses (PRISMA) guidelines (19). The research question was formulated using the acronym PICOS, which stands for population,

intervention/exposure, comparators, outcomes, and study designs. The study population is pregnant adults with GDM or adults with a history of GDM. The intervention/exposure in this case is an exposure to GDM during pregnancy. The comparator is adults without GDM. The study designs of interest were observational, cohort, quasi experimental, or experimental designs. The literature was searched by two independent reviewers (KL, JC) in PubMed for primary research articles about humans available in English from any date. The search terms, defined by a medical librarian experienced with systematic reviews, were as follows: "diabetes, gestational" [MeSH Terms] AND ("transcriptome" [MeSH Terms] OR "gene expression" [MeSH Terms] OR "micrornas" [MeSH Terms] OR "epigenomics"[MeSH Terms] or "Gene Expression Profiling"[Mesh]) AND ((humans[Filter]) AND (English[Filter])) AND ((humans[Filter]) AND (English[Filter])).

Included articles described the full transcriptome, the miRNAome, or a panel of at least three or more miRNAs in blood samples from adults with GDM compared with adults without GDM. Studies were excluded if they did not include a healthy control group for comparison, or if they were exclusively mechanistic studies conducted *in vitro* using a pregnant person's blood samples.

Data were extracted about study and sample characteristics, study methods, instrumentation and data acquisition, validation, key findings, and limitations. This systematic review extracted the data based on the terminology reported by the authors of the studies included, including for race/ethnicity, sex/gender, and trimester in which the blood was drawn. A weighted mean and standard deviation were calculated using Excel software for the participant's age, body mass index (BMI), and gestational age at the time of the blood draw, grouped by GDM or healthy controls. A formal risk of bias analysis was conducted using the Cochrane criteria for observational studies (20, 21).

3 Results

The PRISMA flow diagram provides an overview of the search strategy (Figure 1). After eliminating duplicates and applying inclusion and exclusion criteria, 16 articles were found representing 1375 adults (n=684 with GDM, n=691 controls) from 12 countries. Three studies reported transcriptome results and 13 reported miRNA-ome findings. An overview of the included studies and their key findings are presented in Tables 1–4.

3.1 Sample characteristics

Data were extracted from the included studies about participants' age, race, ethnicity, nationality, BMI, and gestational age at the time of blood sampling (Tables 1, 2). Overall, participants with GDM were slightly older than participants in the healthy control groups ($t(1256) = 4.36$ years, $p<0.0001$). The weighted mean age of the GDM group was 31.9 ± 3.0 years. The weighted mean age of the control group was 31.1 ± 3.5 years.

In the transcriptome studies, the participants' nationality was reported in two studies, ethnicity was reported in one study, and race was reported in one study. The sample of participants from the transcriptome studies was 75% Greek nationality (22), 14% South African nationality and Black race (23), and 11% Chinese ethnicity (24). The articles did not define how race, ethnicity, or nationality were measured (i.e., self-identified, reference criteria, or other method). Seven of the 13 miRNA studies, representing 48.4% of miRNA participants, did not report race, ethnicity, or nationality of their participants (25–31). Of the miRNA studies that did, two reported nationalities, described as 12% South African; 10% Canadian; and 1% Other. Four studies reported race (12% Black, 55% White, 28% Other). One study reported ethnicity as European (15%) or Non-European (3%). Wander et al. (2017) included Hispanic ethnicity as a category in their race demographic, but they did not report the findings (32).

The time point in which BMI was measured varied by study. Five studies measured pre-pregnancy BMI (23, 29, 30, 32, 33). Ten studies measured BMI at the time of the blood sampling (23–25, 27–29, 31, 33–35). Five studies also measured gestational weight gain (22, 23, 30, 32, 33). The BMI ranges of included participants also varied by study. Overall, the BMI of the GDM group was significantly higher than the control group ($t(1256) = 11.26$ kg/m^2, $p<0.0001$). The weighted mean BMI of the GDM group was 26.2 ± 3.2 kg/m^2 and the control group was 24.2 ± 3.1 kg/m^2. The participants in two of the three transcriptome studies

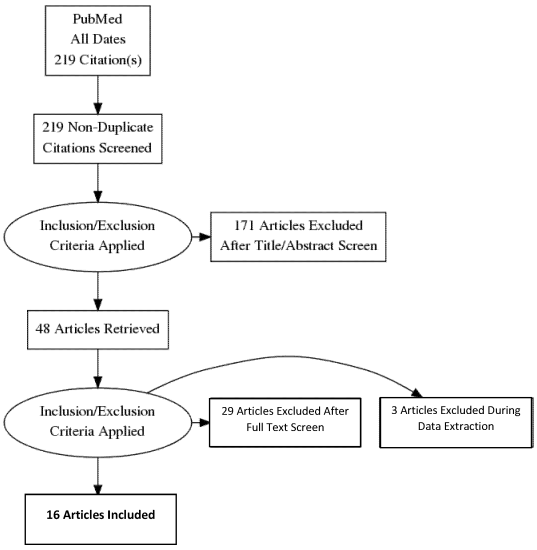

FIGURE 1
Preferred reporting Items for systematic reviews and meta-analyses flow diagram of the search strategy.

TABLE 1 Summary of transcriptome studies included in the final sample.

Author (Year)	Study Purpose, Design, Setting	Sample	Instrumentation/Methods	Key Findings
Pappa et al. (2013)	**Purpose:** To investigate expression patterns of 10 major clock-related genes in the peripheral blood leucocytes of GDM women **Design:** Observational **Setting:** NR **Location:** Athens, Greece	**Sample:** *N* = 64 n = 40 GDM (20 GDM-Insulin; 20 GDM-Diet) n = 20 Controls n = 4 pregnant with T2D **Age (years)**: Range & Standard Deviation NR; 29.41 ± 4.07 (GDM-Insulin) 31.25 ± 4.42 (GDM-Diet) 29.09 ± 6.93 (Control) **BMI (kg/m^2):** Range & Standard Deviation NR; 22.77 ± 3.39 (GDM-Insulin) 21.83 ± 2.43 (GDM-Diet) 23.99 ± 4.34 (Control) **Gestational Age at Sampling (weeks):** NR, all blood draws done in 3rd trimester **Race:** NR **Ethnicity:** NR **Nationality:** Greek, 100%	**Methods:** AllPrep DNA/RNA/Protein mini kit (Qiagen); RT-PCR mRNA transcript levels of 10 clock genes (*CLOCK1*, *BMAL1*, *PER1*, *PER2*, *PER3*, *PPARA*, *PPARD*, *PPARG*, *CRY1*, and *CRY2*) were compared **Validation**: NR **Tissue:** Peripheral leukocytes	No significant differences in mRNA levels between the subgroups of GDM-Insulin and GDM-Diet mRNA levels of *BMAL1*, *PER3*, *PPARD* and *CRY2* genes were significantly ↓ in both GDM subgroups compared to healthy controls *PER3* was significantly negatively correlated with HgbA1C Significant positive correlation between the expression of *BMAL1* versus *CRY2*, and between *BMAL1* versus *PPARD*
Steyn et al. (2019)	**Purpose:** To investigate potential GDM effect on gene regulation in fetal placental tissue and blood samples from mothers with GDM **Design:** Observational **Setting:** Chris Hani Baragwanath Academic Hospital **Location:** Soweto, South Africa	**Sample:** *N* = 12 n = 6 GDM n = 6 Control **Age (years)**: Range & Standard Deviation NR; 31.3 (GDM) 26.7 (Controls) **BMI (kg/m^2)**: Range & Standard Deviation NR; 37.9 (GDM) 30.8 (Controls) **Gestational Age at Sampling (weeks)**: Range 29-33; Mean & Standard Deviation by group NR **Race**: Black, 100% **Ethnicity**: NR **Nationality**: South African, 100%	**Methods:** Tempus™ Spin RNA Isolation Kit Protocol; RNA-Seq **Validation**: Q-RT-PCR, using *RPLPO, ACTB* and *HPRT1* housekeeping genes and 20 selected genes **Tissue:** Whole blood	1088 differentially expressed genes, reduced to 60 candidate genes; top gene ontology terms were binding activity and catalytic activity. Pathways most enriched were carbohydrate and NADP metabolism. Five genes (*G6PD, TKT, ALDOA, PGLS, DCXR*) clustered together with those pathways and code for enzymes in the pentose phosphate pathway. Negative correlations: * *G6PD* mRNA expression with maternal glucose at fasting, 1 hour, and 2 hours post-glucose load. *TKT* mRNA expression and maternal glucose levels at fasting and at 1-hour post-glucose load.*IGFBP-1* maternal glucose levels at fasting, 1- and 2 hours post-glucose load; and for *IGFBP-2* at fasting and 1-hour post-glucose load. There was a significant positive correlation of *IGFBP-1* mRNA expression in maternal blood with birthweight.
Zhao et al. (2011)*	**Purpose:** To determine what genes and/or pathways are associated with GDM in Chinese ethnicity patients **Design:** Observational **Setting:** Beijing Obstetrics and Gynecology Hospital **Location**: Beijing, China	**Sample**: *N* = 9 n = 5 GDM n = 4 Control **Age (years)**: Range 25-37; 30.0 ± 3.7 (GDM) 33.0 ± 3.6 (Control) **BMI (kg/m^2)**: Range: 23.4-31.9; 29.6 ± 2.1 (GDM) 26.0 ± 2.3 (Control) **Gestational Age at Sampling (weeks)**	**Methods:** QIAamp RNA Blood Mini Kit and RNase-Free DNAse; Illumina Sentrix Human-6 v2 Expression Bead-Chips **Validation:** Q-RT-PCR for 4 genes found in the blood samples (*VAV3, TNF, PTPN6, CD48*); *ACTB* for internal control; strong agreement was observed in all genes Used FDR to adjust for multiple comparisons **Tissue:** Peripheral leukocytes	5197 genes in blood were differently expressed in GDM patients after adjustment for multiple comparisons. 52% ↑ GDM vs Control; 48% ↓ GDM vs Control. Genes relevant to GDM pathogenesis: *KLRK1* (NKG2D) *HCST* (DAP10) *IFNG* *TNF* *IL1B*

(Continued)

TABLE 1 Continued

Author (Year)	Study Purpose, Design, Setting	Sample	Instrumentation/Methods	Key Findings
		Range 23-41; 33.8 ± 7.3 (GDM) 37.5 ± 0.7 (Control) **Race**: NR **Ethnicity**: Chinese, 100% **Nationality**: NR		*LEP* *HLA-G* *VAV3* *PTPN6* *CD48* *IL15* 32 enriched pathways; 8 pathways (25% of total) were related to immunity and inflammation. Others included cancer-related pathways, infectious diseases, cell growth and death, metabolic disorders, endocrine system and signal transduction. Top 6 enriched KEGG pathways: natural killer cell mediated cytotoxicity, epithelial cell signaling in Helicobacter pylori infection, apoptosis, toll-like receptor signaling pathway, proteasome, and antigen processing and presentation.

NR=not reported; GDM=gestational diabetes; T2D=type 2 diabetes; NK=natural killer cells; RNA=ribonucleic acid; DNA=deoxyribonucleic acid; PCR=polymerase chain reaction; RT-PCR=Reverse transcription polymerase chain reaction; Q-RT-PCR=quantitative reverse transcription polymerase chain reaction; mRNA=messenger ribonucleic acid; HgbA1c=hemoglobin A1c; RNA-Seq=ribonucleic acid sequencing; RPLP0= Ribosomal Protein Lateral Stalk Subunit P0 gene; ACTB=Actin Beta; HPRT1= hypoxanthine phosphoribosyltransferase 1; G6PD= Glucose-6-phosphate dehydrogenase; TKT=Transketolase; ALDOA= Aldolase, Fructose-Bisphosphate A; PGLS= 6-Phosphogluconolactonase; DCXR= Dicarbonyl And L-Xylulose Reductase; IGFBP=Insulin-Like Growth Factor Binding Protein; VAV3=Vav Guanine Nucleotide Exchange Factor 3; TNF=tumor necrosis factor; PTPN6= Protein Tyrosine Phosphatase Non-Receptor Type 6; CD48=CD48 Molecule; FDR=False Discovery Rate; KLRK1= killer cell lectin like receptor K1; NKG2D=Natural Killer Group 2D; HCST=Hematopoietic Cell Signal Transducer; DAP10= deoxyribonucleic acid polymerase III-activating protein of 10KDa; ITAM=Immunoreceptor Tyrosine-Based Activation Motif; INFG=Interferon Gamma; IL1B=Interleukin 1-Beta; LEP=Leptin; HLA-G=Human Leukocyte Antigen G; IL15=Interleukin 15; KEGG= Kyoto Encyclopedia of Genes and Genomes

*The validation genes and gene findings as reported in the abstract do not match the text of the manuscript; Findings from the body of the manuscript were reported because the narrative matches the table of results. See further discussion in risk of bias analysis and limitations sections.

The up arrow means upregulated and the down arrow means downregulated.

had BMIs in the overweight and obese ranges. In ten of the miRNA studies, the BMI of the GDM group was significantly higher than control groups at the time of the blood draw. Two of the miRNA studies differentiated results unique to the lean participants in their samples (30, 32).

Figure 2 provides an overview of the gestational age at the time of the blood sample collection for mRNA and miRNA analysis. Although the gestational age at time of blood draw varied by study, there was no difference in the weighted mean gestational age of participants with GDM compared to controls for the overall sample.

3.2 Study characteristics

Data were extracted about the study design, GDM definition and diagnostic criteria used, exclusion criteria, tissue type, blood sample collection time points, and trimester represented for all included studies (Tables 1, 2). All studies were observational and cross-sectional, except for two studies which measured the miRNAs at three time points each (25, 26).

The criteria used to define and diagnose GDM varied by study. Eight of the studies cited the International Association of Diabetes and Pregnancy Study Groups' criteria (23, 25, 28, 29, 33, 35–37), six cited the ADA (22, 25–27, 31, 32), two cited the National Diabetes Data Group (24, 30), one cited Society of Obstetricians and Gynaecologists of Canada (34), and one referenced the World Health Organization (37). The exclusion criteria were also unstandardized. Self-reported measures or prior clinic records were used most often to exclude pre-gestational diabetes. Some studies excluded participants with specific conditions, fetal abnormalities, and/or complicated pregnancies from both groups (23, 25–27, 30, 31, 34–37) while another excluded complicated pregnancies only in the control group (32), and still others did not specify if there were exclusions except prior history of diabetes and carbohydrate metabolism disorders (22, 24, 28, 29, 33). Six of the studies included only singleton pregnancies (23, 27, 31, 32, 36, 37); the others did not specify whether the pregnancies reflected by the study results were singletons or multiple gestation.

The point in the pregnancy in which mRNAs and miRNAs were assessed was disparate across the studies, as detailed in Figure 2. In addition, the definition of a particular trimester by gestational age in weeks was unstandardized and inconsistently reported. For example, two studies measured only participants in their first trimester (29, 34), but they used different weeks to

TABLE 2 Summary of micro-RNA (miRNA) studies included in the final sample.

Author (Year)	Study Purpose, Design, Setting	Sample	Instrumentation/Methods	Key Findings
Cao et al. (2017)	**Purpose:** To determine if miR-16-5p, miR-17-5p, and miR-20a-5p can serve as diagnostic markers for GDM and what their relationship is to different GDM factors (BMI, insulin resistance, and tumor necrosis) **Design:** Observational **Setting:** Tianjin Central Hospital of Gynaecology Obstetrics **Location:** Tianjin, China	**Sample:** *N* = 157 n = 85 GDM n = 72 Control **Age (years)**: Range & Standard Deviation NR; 26.8 ± 3.5 (GDM) 26.4 ± 3.6 (Control) **BMI**: Range & Standard Deviation NR; 25.1 ± 2.8 (GDM) 23.4 ± 2.3 (Control) **Gestational Age at Sampling (weeks)**: Range 24-28; 25.8 ± 2.5 (GDM) 26.1 ± 1.2 (Control) **Race:** NR **Ethnicity:** NR **Nationality:** NR	**Methods:** 3 time points - q4 weeks until GDM diagnosis. RNeasy plus mini kit qRT-PCR was used to quantify miRNAs (miR-16-5p, miR-17-5p, miR-19a-3p, miR-19b-3p, miR-20a-5p) from plasma. **Validation**: NR **Tissue:** Plasma	↑: miR-16-5p, miR-17-5p, miR-20a-5p in pregnant people with GDM compared with controls at each time point. Positive correlation between these miRNAs and insulin resistance, but not with TNF-α or BMI.
Gillet et al. (2019)	**Purpose:** To determine if there is differential expression of 17 miRNAs in circulating extracellular vesicles (EVs) in GDM and Control pregnant women. **Design:** Observational **Setting:** Centre Hospitalier Universitaire **Location:** Sherbrooke, QC, Canada	**Sample:** *N* = 69 n = 23 GDM n = 46 Control **Age (years):** Range & Standard Deviation NR; 29.8 ± 5.3 (GDM) 27.9 ± 4.4 (Control) **BMI (kg/m^2):** Range & Standard Deviation NR; 28.2 ± 7.2 (GDM) 24.5 ± 4.7 (Control) **Gestational Age at Sampling (weeks):** Range 6-15 weeks; 10.5 ± 2.5 (GDM) 10.6 ± 2.4 (Control) **Race**: NR **Ethnicity**: NR **Nationality**: Canadian (92.8%); Other (7.2%)	**Methods:** Q-RT- PCR EV presence confirmed as early as 8 weeks gestation. 4335 initial targets narrowed to 58 targets involved in 257 pathways. 3 pathways selected for this analysis: the type 2 diabetes mellitus signaling pathway, the insulin receptor signaling pathway, and the AMP-activated protein kinase (AMPK) signaling pathway. **Validation**: Internal validation per Brosseau et al. **Tissue:** Serum extracellular vesicles	10 of the 17 miRNAs (miR-122-5p, miR-132-3p, miR-1323, miR-136-5p, miR-182-3p, miR-210-3p, miR-29a, miR-29b-3p, miR-342-3p, and miR-520h) were ↑ in GDM vs control. Enriched pathways: insulin receptor signaling pathway, AMPK signaling pathway, and epidermal growth factor receptor-phosphatidylinositol 3-kinase-Akt pathway–involved in placental development, fetal growth, and insulin and glucose regulation.
Hromadnikova et al. (2020)	**Purpose:** To conduct risk assessments for developing diabetes mellitus, cardiovascular and cerebrovascular diseases in patients who have had GDM 3-11 years post-delivery using epigenetic modifications of miRNA. **Design:** Observational **Setting:** NR **Location**: Czech Republic	**Sample:** *N* = 200 n = 111 GDM (93 GDM on diet; 18 GDM on diet & therapy) n = 89 Control **Age (years):** Range & Standard Deviation NR; 38.70 ± 0.37 (GDM on diet) 38.61 ± 0.80 (GDM on diet & therapy) 38.33 ± 0.38 (Control) **BMI (kg/m^2):** Range & Standard Deviation NR; 23.85 ± 0.37 (GDM on diet) 27.21± 0.83 (GDM on diet & therapy) 23.15 ± 0.38 (Control) **Gestational Age at Sampling (weeks):** Not Applicable (data collected 3-11 years post-delivery) **Race:** Caucasian, 100%	**Methods:** RT-PCR **Validation**: NR **Tissue:** Whole blood	The expression of 26 miRNAs (miR-1-3p, miR-16-5p, miR-17-5p, miR-20a-5p, miR-20b-5p, miR-21-5p, miR-23a-3p, miR-24-3p, miR-26a-5p, miR-29a-3p, miR-100-5p, miR-103a-3p, miR-125b-5p, miR-126-3p, miR-130b-3p, miR-133a-3p, miR-143-3p, miR-145-5p, miR-146a-5p, miR-181a-5p, miR-195-5p, miR-199a-5p, miR-221-3p, miR-342-3p, miR-499a-5p, and miR-574-3p) ↑ in women previously affected with GDM compared to controls, even on average 5 years postpartum. Combined screening of 16 of those miRNAs (miR-1-3p, miR-16-5p, miR-17-5p, miR-20b-5p, miR-21-5p, miR-23a-3p, miR-26a-5p, miR-29a-3p, miR-103a-3p, miR-133a-3p,

(Continued)

TABLE 2 Continued

Author (Year)	Study Purpose, Design, Setting	Sample	Instrumentation/Methods	Key Findings
		Ethnicity: NR **Nationality:** NR		miR-146a-5p, miR-181a-5p, miR-195-5p, miR-199a-5p, miR-221-3p, and miR-499a-5p) showed the highest accuracy to detect mothers with a prior exposure to GDM (AUC 0.900, p < 0.001, sensitivity 77.48%, specificity 93.26%, cut o_ >0.611270413). It was able to identify 77.48% of mothers with an ↑ cardiovascular risk at 10.0% false positive rate. No difference in miRNA expression profiles between GDM on diet only and GDM on the combination of diet + therapy Predicted miRNA targets reflect pathways related to insulin signaling, type 1 diabetes mellitus, and type 2 diabetes mellitus
Lamadrid-Romero et al. (2018)	**Purpose:** To determine if 12 neural development miRNAs are altered in GDM **Design:** Observational **Setting:** Instituto Nacional de Perinatología **Location:** Mexico City, Mexico	**Sample:** *N* = 151 n = 67 GDM 1st Trimester: 27 2nd Trimester: 26 3rd Trimester: 21 n = 74 Control 1st Trimester: 14 2nd Trimester: 26 3rd Trimester: 27 **Age (years)**: NR (Range 18 -35) **BMI (kg/m^2)**: NR (below 29 as inclusion criteria) **Gestational Age at Sampling (weeks)**: NR **Race**: NR **Ethnicity**: NR **Nationality**: NR	**Methods:** TRIzol reagent; qRT-PCR Different sample sizes were analyzed for different miRNAs. **Validation**: NR **Tissue:** Serum	↑ miR-183-5p, miR-200b-3p, miR-125-5p, and miR-1290 were detected during the first trimester for GDM group. ↑ miR-183-5p, miR-200b-3p, miR-125-5p and miR-137 were detected in the second and third trimester, respectively.
Pfeiffer et al. (2020)	**Purpose:** To determine if there is a signature in 4 circulating miRNAs of interest in lean women with GDM who have no insulin resistance risk factors **Design:** Observational **Setting:** Endocrinology and Pregnancy Clinic, Puerta del Mar University Hospital, Cadiz **Location:** Cadiz, Spain	**Sample:** *N* = 60 n = 31 GDM n = 29 Matched Control **Age (years):** Range & Standard Deviation NR; 31.9 ± 1.8 (GDM) 31.0 ± 3.6 (Control) **BMI (kg/m^2):** Range & Standard Deviation NR; 22.5 ± 1.8 (GDM) 22.3 ± 1.8 (Control) **Gestational Age at Sampling (weeks):** Range 26-30; NR (GDM) NR (Control) **Race**: NR **Ethnicity**: NR **Nationality**: NR	**Methods:** miRNeasy Serum/Plasma kit (Qiagen) Q-RT-PCR 4 miRNAs measured: miR-224, miR-103-3p, miR-206, and miR-330-3p Multivariable logistic regression model included age, pregestational BMI, weight gain, triglycerides, and the 4 miRNAs measured in this study. **Validation**: NR **Tissue:** Serum	miR-330-3p was 5.2-fold ↑ in the GDM group compared to control. ↑ levels of miR-330-3p in GDM group compared with control were associated with: 1. a ↑ proportion of spontaneous deliveries than cesarean section in GDM 2. ↑ levels in GDM with spontaneous deliveries 3. ↑ levels in GDM patients treated with diet, but not GDM treated with insulin 1031 gene targets of miR-330-3p predicted; insulin signaling pathway was one of 12 pathways overrepresented. miR-330-3p was significant independent predictor of GDM in the final model.
Pheiffer et al. (2018)	**Purpose:** To determine if serum miRNAs are	**Sample:** N = 81 n = 28 GDM	**Methods:** miRNeasy Serum/Plasma kit (Qiagen); MiScript miRNA PCR (miR-16-5p, miR-17-5p, miR-19a-3p,	miR-20a-5p, miR-222-3p significantly ↓ in South African women with GDM compared to

(Continued)

TABLE 2 Continued

Author (Year)	Study Purpose, Design, Setting	Sample	Instrumentation/Methods	Key Findings
	regulated in South African women with GDM in a similar manner to other populations. **Design:** Observational **Setting**: Primary clinic **Location**: Johannesburg, South Africa	n = 53 Control **Age (years)**: Range & Standard Deviation NR; 29.5 ± 6.2 (GDM) 28.6 ± 6.4 (Control) **BMI (kg/m^2):** Range & Standard Deviation NR; 28.1 (23.9-31.3) (GDM) 26.2 (21.9-29.8) (Control) **Gestational Age at Sampling (weeks)**: Range 24-28; 26.0 (24.0-28.0) (GDM) 27.0 (25.0-28) (Control) **Race:** Black, 100% **Ethnicity:** NR **Nationality:** South African	miR-19b-3p, miR-20a-5p, miR-29a-3p, miR-132-3p, and miR-222-3p) **Validation**: NR **Tissue:** Serum	healthy pregnant controls using an FDR cutoff of 0.15. miR-20a-5p and the presence of 1 or more risk factors was significant independent predictor for GDM Risk factors: advanced maternal age (age ≥ 35 years), obesity (body mass index ≥ 30 kg/m2), family history of diabetes mellitus, delivery of a previous baby >4 kg, glucosuria, recurrent pregnancy loss, stillbirth, or birth of a baby with congenital abnormalities. Age, BMI, and miR-222-3p were not significantly, independently associated with GDM. 53 KEGG pathways for regulation, various cancers, and insulin signaling were enriched by miR-20a-5p gene targets
Sorensen et al. (2021)	**Purpose**: To determine if a panel of 8 miRNAs at baseline could be used in the GDM prediction for obese pregnant women **Design:** Observation (nested case-control study) **Setting:** DALI Lifestyle Study of 9 European Countries **Location**: Austria	**Sample:** *N* = 123 n = 41 Control n = 41 early-GDM n = 41 late-GDM **Age (years):** Range & Standard Deviation NR; 33.2 ± 3.8 (Control) 33.7 ± 4 (early-GDM) 32.7 ± 4 (late-GDM) **BMI (kg/m^2)**: Range & Standard Deviation NR; 33.3 (32.2–35.4) (Control) 33.3 (31.7–36.0) (early-GDM) 33.3 (31.7–35.9) (late-GDM) **Gestational Age at Sampling (weeks):** Range <20 weeks (early-GDM); 24-28 (late-GDM); 15.2 ± 2.4 (Control) 14.9 ± 2.4 (early-GDM) 15.3 ± 2.5 (late-GDM) **Race**: NR **Ethnicity**: 90% European (Control) 80% European (early-GDM) 78% European (late-GDM) **Nationality**: NR	**Methods:** MultiScribe™ Reverse Transcription kit; RT-PCR PCR. **Validation**: NR **Tissue:** Serum	3 out of 8 miRNA (miR-16-5p, miR-29a-3p, and miR-134-5p) levels were ↑ at baseline in women who went on to develop GDM. Women with late-onset GDM had ↑ miR-16-5p and miR-122-5p than women with early-onset GDM. The 3 miRNAs combined differentiated between late GDM cases and healthy controls (AUC = 71.7%). Adding fasting plasma glucose increased AUC to 81.0%. Adding maternal heart rate, neck size, or maternal height individually to the combined 3 miRNAs increased AUC to 72.7%. 1890 unique targets identified; most linked to miR-29a-3p; 148 targets common between 2 or more miRNAs. Vascular endothelial growth factor (VEGF)-, fibroblast growth factor (FGF)-, phosphoinositide (PI)-3 kinase-, Notch- and insulin signaling pathways were found to be overrepresented of predicted targets of the miRNAs. miR-29a-3p, miR-134-5p and miR-16-5p positively correlated with 2-h fasting glucose levels measured at 24–28 weeks of gestation after adjustment for maternal age and BMI, gestational age, and offspring sex. miR-16-5p positively correlated with HgbA1C; miR-122-5p negatively correlated with insulin sensitivity, HDL cholesterol, and leptin; and miR-122-5p positively correlated with birthweight

(Continued)

TABLE 2 Continued

Author (Year)	Study Purpose, Design, Setting	Sample	Instrumentation/Methods	Key Findings
Stirm et al. (2018)	**Purpose:** To determine if non-coding RNA in white blood cells play a role in patients with GDM compared to controls **Design:** Observational **Setting:** NR **Location:** Germany	**Sample:** Screening: *N* = 16 n = 8 GDM n = 8 Control Validation: *N* = 60 n = 30 GDM n = 30 NGT **Age (years):** Range & Standard Deviation NR; Screening 33 ± 5 (Control) 32 ± 3 (GDM) Validation 32 ± 4 (Control) 31 ± 4 (GDM) **BMI (kg/m^2):** Range & Standard Deviation NR; Screening 28.1 ± 5.4 (Control) 29.1 ± 6.1 (GDM) Validation 29.5 ± 5.6 (Control) 29.8± 4.07 (GDM) **Gestational Age at Sampling (weeks):** Range 24-32; Screening 23 ± 9.5 (Control) 25.9 ± 1.7 (GDM) Validation 27.6 ± 2.37 (Control) 27 ± 2.3 (GDM) **Race**: Caucasian, 100% **Ethnicity**: NR **Nationality**: NR	**Methods:** RT-q-PCR **Validation**: Internal and external validation methods used **Tissue:** Whole blood	29 miRNAs ↑ in GDM patients compared to controls miR-19a, miR-142, miR-143, miR-340, miR-7g, and miR-19b were selected for external q-PCR validation. miR-340 was found at ↑ levels in GDM *PAIP1*, a downstream target was significantly ↓ in GDM. The 4 miRNAs positively associated with BMI were unrelated to GDM. ↑ insulin or ↓ glucose reduced miR-340 expression.
Tagoma et al. (2018)	**Purpose:** To determine and compare the expression profiles of plasma miRNA in GDM and Control pregnant women. **Design:** Observational **Setting:** Tartu University Hospital Women's Clinic **Location:** Estonia	**Sample**: *N* = 22 n = 13 GDM n = 9 Control **Age (years):** Range & Standard Deviation NR; 31.1 ± 4.2 (GDM) 28.1 ± 4.5 (Control) **BMI (kg/m^2):** Range & Standard Deviation NR; 28.4 ± 6.8 (GDM) 21.3 ± 1.7 (Control) **Gestation Age at Sampling (weeks)**: Range 23-31; 27.5 ± 1.9 (GDM) 25.3 ± 1.9 (Control) **Race:** NR **Ethnicity:** NR **Nationality:** NR	**Methods:** miRNeasy Serum/Plasma Kit (Qiagen); qRT-PCR using the miScript II RT Kit (Qiagen). **Validation**: Internal validation of 3 upregulated miRNAs using RT-PCR (miR-195-5p, miR-30d-5p, and miR-92a-3p) **Tissue:** Plasma	15 miRNAs were ↑ in GDM group, 41 significantly enriched pathways. The 15 miRNAs were miR-7e-5p, miR-7g-5p, miR-100-5p, miR-101-3p, miR-146a-5p, miR-18a-5p, miR-195-5p, miR-222-3p, miR-23b-3p, miR-30b-5p, miR-30c-5p, miR-30d-5p, miR-342-3p, miR-423-5p, and miR-92a-3p. miR-195-5p had highest fold upregulation out of top 3 validated miRNA (miR-195-5p, miR-30d-5p, and miR-92a-3p). Fatty acid biosynthesis and fatty acid metabolism pathways were overrepresented miR-195-5p targeted highest number of genes important in the fatty acid metabolism pathway.
Wander et al. (2017)	**Purpose:** To determine if levels of circulating candidate miRNAs during 7-23 weeks of pregnancy	**Sample:** *N* = 116 n = 36 GDM n = 80 Control **Age (years):** Range & Standard	**Methods:** Exiqon miRCURY™ RNA Biofluids Isolation Kit; qRT-PCR for candidate miRNAs (miR-126-3p, miR-155-5p, miR-21-3p, miR-146b-5p, miR-210-3p, miR-222-3p, miR-	After adjusting for gestational age at blood draw, ↑ miR-155-5p and miR-21-3p levels were associated with ↑ odds for GDM, while miR-146b-5p and miR-517-5p odds of

(Continued)

TABLE 2 Continued

Author (Year)	Study Purpose, Design, Setting	Sample	Instrumentation/Methods	Key Findings
	are related to GDM development **Design:** Observational **Setting:** Center for Perinatal Studies at Swedish Medical Center **Location:** Seattle, Washington, USA	Deviation NR; 34.3 ± 3.6 (GDM) 32.9 ± 4.4 (Control) **BMI (kg/m^2):** Range & Standard Deviation NR; 25.5 ± 6.7 (GDM) 21.7 ± 4.1 (Control) **Gestational Age at Sampling (weeks):** Range 7.0-22.9; 15.1 ± 2.9 (GDM) 16.5 ± 2.3 (Control) **Race:** 67% White (GDM) 80% White (Control) **Ethnicity:** Hispanic ethnicity was included as a category of race, but details NR **Nationality:** NR	223-3p, miR-517-5p, miR-518a-3p, and miR-29a-3p) **Validation**: NR **Tissue:** Plasma	GDM were borderline. After adjusting for gestational age at blood draw, maternal age, and pre-pregnancy BMI, only miR-21-3p remained significantly associated with ↑ odds of GDM. miR-21-3p and miR-210-3p were detected in GDM overweight/obese but not lean women. Six miRNAs (miR-155-5p, -21-3p, -146b-5p, -223-3p, -517-5p, and -29a-3p) were detected in GDM patients carrying male fetuses.
Yoffe et al. (2019)	**Purpose:** To determine which miRNAs measured during the first trimester are best for early GDM detection and differentiation. **Design:** Observational **Setting:** Careggi University Hospital (Italy); August Pi i Sunyer Biomedical Research Institute (Spain) **Location:** Italy and Spain	**Sample:** Initial Cohort: *N* = 43 n = 23 GDM n = 20 Control Validation Cohort: *N* = 20 n = 10 GDM n = 10 Control **Age (years)**: Range & Standard Deviation NR; 34 (32.5-37.5) (GDM) 34.5 (32.0-37.2) (Control) **BMI (kg/m^2):** Range & Standard Deviation NR; 28.6 (20.4-31.1) (GDM) 22.2 (20.1-31) (Control) **Gestational Age at Sampling (weeks):** Range 9-11 weeks; 10 (10.0-10.6) (GDM) 10 (10.0-10.2) (Control) **Race**: NR **Ethnicity**: NR **Nationality**: NR	**Methods:** miRNeasy Serum/Plasma Kit of collected blood samples; Nanostring ncounter profiled 798 human miRNAs GDM detection – machine learning models with leave-one-out cross validation (LOOCV) procedure **Validation**: External validation of the two upregulated miRNAs in a separate cohort using RT-qPCR; Internal validation using RT-qPCR **Tissue:** Plasma	22 samples from the initial cohort (51%) were removed from downstream analysis after quantifying miRNAs and prior to evaluating differently expressed miRNAs. In the remaining samples, miR-223 and miR-23a were found to be ↑ in GDM patients. When both miRNAs are used with a logistic regression model, this resulted in an AUC score of 0.91.
Zhao et al. (2011)	**Purpose:** To determine if serum miRNA and GDM have any associations; To determine if serum miRNA profiles could predict GDM before blood glucose changes **Design:** Observational (retrospective nested case-control study with multiple sites) **Setting:** Hospital system **Location:** Changzhou, China; Wuxi, China	*N*=152 *N*=48 (discovery stage) n=24 GDM n=24 Control Internal Validation Stage (n=36 per group) External Validation Stage (n=16 per group) **Age (years)**: Range & Standard Deviation NR; 28.8 ± 2.2 (GDM) 29.5 ± 1.9 (Control) **BMI (kg/m^2)**: Range & Standard Deviation NR; 21.4 ± 1.7 (GDM) 21.9 ± 1.8 (Control) **Gestational Age at Sampling (weeks)**: Range 16-19;	**Methods:** Qiagen miRNeasy Mini kit; TLDA Chips; Q-RT-PCR **Validation**: Internal and external validation methods used **Tissue:** Serum	10 miRNAs selected out of 73 total. miR-132, miR-29a, and miR-22 were found to be significantly ↓ in GDM. The AUC for the three miRNAs combined was greater (66.9%) than for individual miRNAs. miR-29a is inferred to be a negative regulator of glucose serum as knockdown of miR-29a led to ↑ *PCK2* expression. ↑ *PCK2* could then lead to an increase in glucose levels.

(Continued)

TABLE 2 Continued

Author (Year)	Study Purpose, Design, Setting	Sample	Instrumentation/Methods	Key Findings
		17.4 ± 0.7 (GDM) 17.2 ± 0.8 (Control) **Race**: NR **Ethnicity**: NR **Nationality**: NR		
Zhu et al. (2015)	**Purpose:** To profile plasma miRNA that are differentially expressed in GDM patients compared to controls **Design:** Observational **Setting:** Zhongda Hospital, Southeast University, Nanjing, China **Location:** Nanjing, China	**Sample:** *N* = 20 n = 10 GDM n = 10 Control **Age (years):** Range & Standard Deviation NR; 30.03 ± 3.56 (GDM) 26.67 ± 4.59 (Control) **BMI (kg/m^2):** Range & Standard Deviation NR; 23.94 ± 2.98 (GDM) 19.24 ± 1.07 (Control) **Gestational Age at Sampling: (weeks):** Range 16-19; 17.66 ± 0.85 (GDM) 18.17 ± 0.93 (Control) Race: NR Ethnicity: NR Nationality: NR	**Methods:** miRNeasy Serum/Plasma Kit; RNA-seq **Validation**: Internal qRT-PCR used to validate 5 of the differentially expressed miRNAs using the Applied Biosystems 7500 Real-Time PCR System. **Tissue:** Plasma	32 miRNAs were differentially expressed in GDM with 20 being ↓ and 12 being ↑. 5 of the ↑ miRNAs (hsa-miR-16-5p, hsa-miR-17-5p, hsa-miR-19a-3p, hsa-miR-19b-3p, hsa-miR-20a-5p) were validated. 18 enriched pathways identified: endocytosis, mitogen-activated protein kinase (MAPK) signaling, insulin signaling, mTOR signaling, type 2 diabetes, Wnt signaling, proteoglycans in cancer, and transforming growth factor-β (TGF-β) signaling. Pathways suggest associations to insulin resistance and abnormal pregnancies.

NR=not reported; GDM=gestational diabetes; T2D=type 2 diabetes; RNA=ribonucleic acid; PCR=polymerase chain reaction; RT-PCR=reverse transcription polymerase chain reaction; Q-RT-PCR=quantitative reverse transcription polymerase chain reaction; HgbA1c=hemoglobin A1c; RNA-Seq=ribonucleic acid sequencing; TNF=tumor necrosis factor; FDR=false discovery rate; KEGG= Kyoto Encyclopedia of Genes and Genomes; BMI=body mass index; EV=extracellular vesicle; AMPK=adenosine monophosphate-activated protein kinase; AUC=area under the curve; HDL=high-density lipoprotein; PAIP1= polyadenylate-binding protein-interacting protein 1; PCK2= phosphoenolpyruvate carboxykinase 2, mitochondrial; MAPK=mitogen-activated protein kinase.
The up arrow means upregulated and the down arrow means downregulated.

define the end of the first trimester (i.e., <12 weeks or <14 weeks). Four studies reported miRNA results discretely within the second trimester, which was defined as weeks 13-26 (25–27, 31), and three studies were discretely within the third trimester, defined as weeks 27 through the end of pregnancy (22, 23, 26). Two studies reported findings from the time period that corresponds with the standard of care for assessing for gestational diabetes (weeks 24-28), although this range spans late second trimester to early third trimester (25, 36). Others' ranges spanned two or more trimesters (28, 31–33, 37).

3.3 Instrumentation, data acquisition, and data analysis

Instrumentation, data acquisition, and analysis methods were disparate across studies (Tables 1–3). The three transcriptome studies each used different methods for mRNA quantitation (22–24). One study used RNA-Sequencing methods (23), and another used microarray methods (24). Pappa et al. (2013) used real time quantitative polymerase chain reaction (qPCR) for quantitation since they evaluated a panel of ten "clock genes" associated with diurnal rhythms. Both Steyn et al. (2019) and Zhao et al. (2011) used reverse transcription qPCR (RT-qPCR) for internal validation (23, 24). Twelve out of the 13 miRNA studies (92%) used real time qPCR methods for miRNA quantitation (Table 2). The other study (8%) used the Nanostring ncounter platform (29). Internal and external validation methods were included in 54% and 23% of miRNA studies, respectively. Table 3 provides an overview of the bioinformatics tools used in each of the studies where applicable.

3.4 Transcriptome studies

The transcriptome studies collectively identified 6,289 differentially expressed genes (DEGs). Overall, 2,702 DEGs (43.0%) were described as upregulated in participants with GDM compared to controls, while 2,499 DEGs (39.7%) were described as downregulated in GDM compared to controls. The candidate genes and target pathway findings are detailed in Table 1. The transcriptome pathways identified described various aspects of diabetes pathogenesis, including insulin and glucose signaling, regulation, and transport; natural killer cell mediated cytotoxicity; NADP and carbohydrate metabolism;

TABLE 3 Tools utilized by included studies for mRNA and miRNA gene targets and pathway analyses.

First Author (Year)	TargetScan*	DIANA v. 3 miRPath	Tarbase 7.0	PANTHER*	DAVID*	None/Not Applicable	Other Tools	Other: Explained
Sorensen et al. (2021)	X			X				
Pfeiffer et al. (2020)	X			X			X	EnrichR; Interpro Domains 2019; Pfamdomains
Zhu et al. (2015)	X				X		X	PicTar; miRanda
Stirm et al. (2018)	X						X	miRlastic R approach
Steyn et al. (2019)				X	X			
Pheiffer et al. (2018)		X	X					
Lamadrid-Romero et al. (2018)		X	X					
Tagoma et al. (2018)		X	X					
Gillet et al. (2019)							X	Qiagen Ingenuity Pathway Analysis
Hromadnikova et al. (2020)							X	miRwalk 2.0
Yoffe et al. (2019)							X	Gene Ontology Enrichment Analysis Software Toolkit (GOEAST)
Zhao et al. (2011)							X	Pathway Express (part of Onto-Tools) Cytoscape Software
Cao et al. (2017)						X		
Pappa et al. (2013)						X		
Wander et al. (2017)						X		
Zhao (2) et al. (2011)						X		

*Various versions. The shading/X means that the referenced study used that tool.

immunity and inflammation; fatty acid biosynthesis and metabolism; and circadian clock rhythms.

The transcriptome studies analyzed correlations between mRNA levels and outcomes like glucose levels in the pregnant person, insulin resistance/insulin sensitivity, hemoglobin A1c (HbA1c), and birth weight. Glucose-6-phosphate dehydrogenase (*G6PD)*, insulin-like growth factor binding protein (*IGFBP-1)*, *IGFBP-2*, and transketolase (*TKT)* were inversely correlated with glucose levels in the pregnant person, measured at one or more time points. No significant correlation was found between *IGFBP-6* and glucose levels. Period circadian level 3 (*PER3)* was inversely correlated with HbA1c. *IGFBP-1* was positively correlated with the infants' birthweight, while *IGFBP-2 and IGFBP-6* were not significantly correlated with birthweight.

3.5 miRNA studies

In the thirteen miRNA studies, 135 unique miRNAs were associated with GDM. Eight (miR-16-5p, miR-17-5p, miR-20a-5p, miR-29a-3p, miR-195-5p, miR-222-3p, miR-210-3p, and miR-342-3p) were described in two or more studies. See

TABLE 4 miRNAs described in two or more studies.

miRNA	Studies in Which miRNA was Described (*n*)	Upregulated *n* (%)	Downregulated *n* (%)	No Difference *n* (%)
miR-16-5p	5	4 (80%)	–	1 (20%)
miR-17-5p	4	3 (75%)	–	1 (25%)
miR-195-5p	2	2 (100%)	–	–
miR-20a-5p	4	3 (75%)	1 (25%)	–
miR-210-3p*	2	2 (100%)	–	–
miR-222-3p	3	1 (33%)	1 (33%)	1 (33%)
miR-29a	6	3 (50%)	1 (17%)	2 (33%)**
miR-342-3p	3	3 (100%)	–	–

*Associated with GDM in obese but not lean pregnant people
**Found only in pregnant people carrying fetuses assigned the sex of male at birth
miRNA – microRNA

Table 4 for details about the number of studies that described each miRNA, and whether or not it was found to be upregulated, downregulated, or no difference from healthy controls.

Within the studies, miRNA levels varied based on the time in pregnancy when GDM develops, the trimester or time period at which miRNAs were measured, sex of the fetus, obesity in the pregnant person, and treatment type (diet vs. pharmaceutical).

3.5.1 Time in pregnancy

Two studies measured the miRNAs at multiple time points from the same participants (25, 26). In those studies, expression levels of miR-16-5p, miR-17-5p, and miR-20a-5p increased in each trimester as compared with the first trimester in the GDM group but remained constant in the control group (25). In contrast, miR-125b-5p increased over time from the first

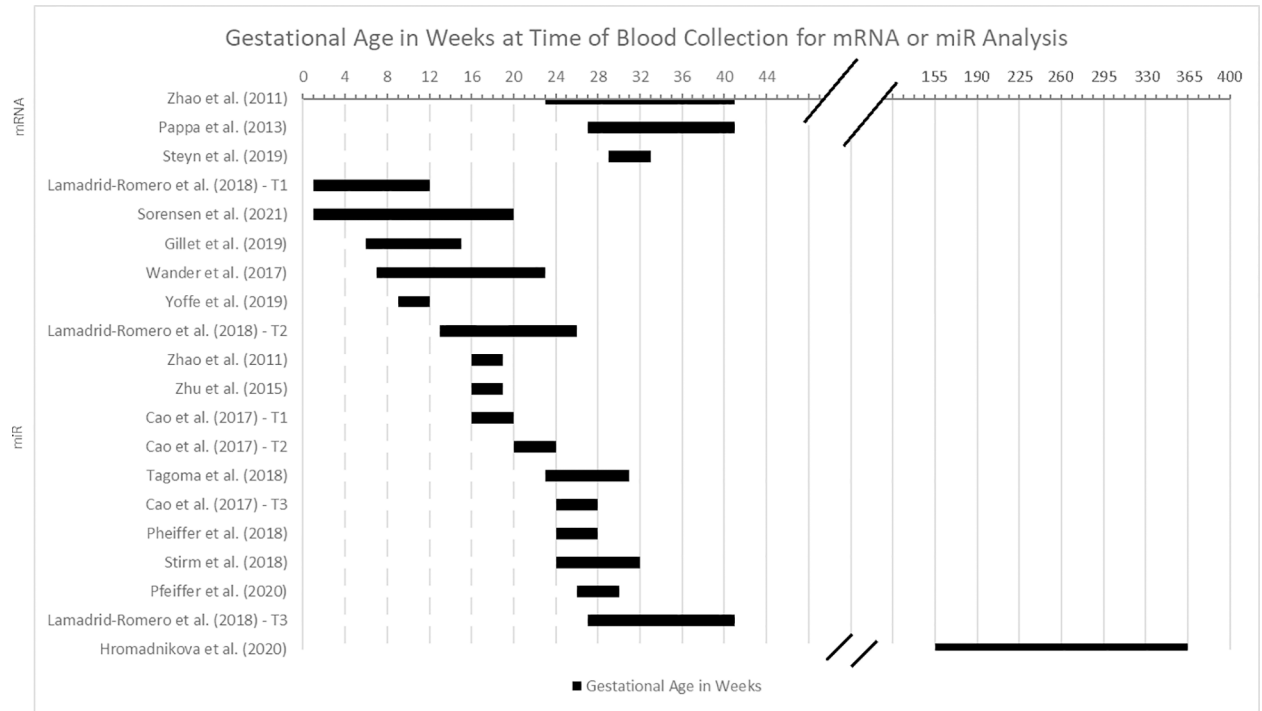

FIGURE 2
Gestational age in weeks at time of blood collection for miRNA or mRNA analysis.

trimester to the third for the control group (26). Expression of miR-125b-5p was significantly higher in the GDM group compared to healthy controls in the first trimester, but then levels decreased 10-fold below those of the control group in the second trimester GDM samples (26). In control samples, expression levels of miR-183-5p, miR-200b-3p, and miR-125b-5p were the highest in the second trimester, whereas the highest level of miR-137 was observed in the third trimester (26).

When comparing first trimester GDM expression levels to controls, miR-183-5p, miR-200b-3p, miR-125b-5p, miR-1290 (26), miR-223, and miR-23a (29) were higher in the GDM group. During the second trimester, in the GDM group, the expression levels of miR-183-5p (26), miR-16-5p, miR-17-5p, miR-19a-3p, miR-19b-3p, miR-20a-5p (25, 27), were higher and miR-128-5p (26), miR-132, miR-29a, and miR-22 (31) were lower as compared with the control group. Finally, during the third trimester, in the GDM group, studies reported a higher level of miR-137 and lower levels of miR-183-5p and miR-200b-3p relative to the control group (26).

Four studies measured miRNA expression at the time of GDM diagnosis, between 24-28 weeks gestation and collectively identified 35 miRNAs that were significantly different in the GDM group compared to controls (25, 30, 33, 36). MiR-222-3p was significantly lower in South African pregnant people with GDM relative to controls (36). MiR-16-5p, miR-17-5p (25), miR-340 (33), and miR-330-3p (30) were significantly upregulated in the GDM group. Stirm et al. (2018) identified an additional 29 miRNAs that were significantly upregulated in the GDM group (false discovery rate <0.1) compared to controls, although miR-340 was the only one that was validated in their study (33). MiR-20a-5p was reported in two studies with mixed results. In one study conducted in China, miR-20a-5p was significantly higher in the GDM group, whereas in another study of South African pregnant people, miR-20a-5p was significantly lower.

One study measured miRNA levels in the formerly pregnant person an average of 5 years after birth of the baby (35). They found 26 miRNAs that were significantly higher in participants with a history of GDM compared to controls. A composite of 16 of the 26 miRNAs was identified as the best predictor of GDM exposure during pregnancy in their participants.

3.5.2 Sex assigned at birth of the offspring

Two studies considered sex assigned at birth of the offspring in their analyses. Wander et al. (2017) differentiated results by sex of the offspring which was determined using retrospective chart review after delivery (32). They detected six miRNAs (miR-155-5p, miR-21-3p, miR-146b-5p, miR-223-3p, miR-517-5p, and miR-29a-3p) that were significantly different in the blood samples of participants with GDM carrying male fetuses. Conversely, Sorensen et al. (2021) found no sex-dependent differences in expression of miR-29a-3p and miR134-5p (37).

3.5.3 Associations with BMI

In most studies, the GDM group had a significantly higher BMI at the time of the blood draw compared to the control group. Three studies reported findings for lean (i.e., pre-pregnancy BMI <25 kg/m^2), overweight/obese (i.e., pre-pregnancy BMI ≥ 25 kg/m^2), or obese (i.e., pre-pregnancy BMI ≥ 29 kg/m^2) pregnant people (30, 32, 37). Sorensen et al. (2021) identified three miRNAs (miR-16-5p, miR-29a-3p, miR-134-5p) that were higher at baseline in obese women who went on to develop GDM (37). These three miRNAs combined differentiated those women who developed GDM earlier in pregnancy from those who developed GDM later in pregnancy, with the highest levels at baseline in women who developed GDM late in pregnancy. In the other two studies, miR-21-3p, miR-210-3p (32), and miR-330-3p (30) were significantly increased in obese but not lean women.

3.5.4 Differences by treatment type

Two studies analyzed miRNA findings based on GDM treatment type (30, 35). Higher levels of miR-330-3p were associated with patients with GDM treated with diet, but not GDM treated with insulin, compared to controls (30). Hromadnikova et al. (2020) found no difference in miRNA expression profiles between GDM on diet only and GDM on the combination of diet plus pharmacologic therapy, however the pharmacologic group included 17 participants on insulin and 1 participant on metformin (35). Another study by Pheiffer et al. (2018) reported that their participants with GDM were treated with either metformin, insulin, and/or diet, but did not specify any details to characterize the sample or to differentiate results by treatment type (36).

3.5.5 miRNA and health outcome correlations

Three studies described the relationships between miRNAs and related health outcomes (25, 33, 37). MiR-16-5p was positively correlated with insulin resistance (25), 2-hour fasting glucose levels at 24-28 weeks of gestation, and HbA1c (37). There was a positive correlation between miR-17-5p, and miR-20a-5p and insulin resistance, but not with tumor necrosis factor- α (TNF-α) or BMI (25). MiR-29a-3p and miR-134-5p were positively correlated with 2-h fasting glucose levels measured at 24–28 weeks of gestation after adjustment for maternal age and BMI, gestational age, and offspring sex (37). MiR-122-5p was negatively correlated with insulin sensitivity, high density lipoprotein (HDL) cholesterol, and leptin; and positively correlated with birthweight (37). Four miRNAs (miR-4473, miR-199-5a, miR-339-5p, and miR-3653-5p) were positively associated with BMI but were unrelated to GDM (33).

3.6 Risk of bias findings

Risk of bias was assessed in terms of recruitment and sampling methods, confidence in the assessment of exposure, confidence in assessment of the outcomes, matching between cases and controls, potential confounders, and missing data. Most studies described sample recruitment from eligible patients who were seen in a particular clinic. In most studies, the cases and controls were recruited during the same time. However, it is unknown to what extent these cases and controls were drawn from same population, and unknown how representative the samples are of the general population since sample characteristics were described inconsistently.

Confidence in assessment of exposure was assessed by considering the method of diagnosis of GDM and comorbidities. Variations in the GDM definition, diagnostic criteria referenced, and methods of GDM diagnosis were found across studies, although most were assessed between 24-28 weeks gestation. For example, the American Diabetes Association (ADA) recommends that pregnant people who test positive for diabetes during the first trimester be diagnosed with type 2 diabetes (T2D) (1). However, Lamadrid-Romero et al. (2018) classified those participants as having GDM because they had no prior risk factors for T2D (26). It is unknown to what extent undiagnosed T2D prior to pregnancy affected the results, due to the nature of the GDM diagnostic process.

Confidence in the individual studies' assessment of the molecular markers was mixed. Most studies provided detailed descriptions of their analysis methods, but across the studies, instrumentation and analysis tools were unstandardized. One transcriptome study reported different results in the abstract versus the body of the manuscript. For the review of literature described in this paper, findings were reported from the body of the manuscript because the text in the results section matched the figures and discussion. Finally, validation of the mRNA and miRNA measurements was used only in a subset of studies and was not consistently applied in all studies.

Matching of exposed and unexposed participants for potential confounders affecting the outcome was done in a minority of studies. As expected, in most studies that measured fasting glucose and HbA1c, those levels were higher in the GDM group than the control group at the time of mRNA or miRNA analysis. BMI was also significantly higher in the GDM group in a majority of studies at the time of the blood draw. Other potential confounders such as pre-pregnancy BMI, weight gain during pregnancy, age of the pregnant person, gestational age at time of blood draw, singleton pregnancy, primiparous, behaviors during pregnancy such as smoking, and other sociocultural factors were recorded or adjusted for inconsistently across studies. It is also unknown if behavioral and environmental exposures were consistent among cases and controls because of limited sample characteristics reported. For example, it is unknown to what extent behaviors like physical activity, diet, smoking, exercise or psychosocial factors like stress, environmental factors, access to resources and prenatal care, health literacy, low socioeconomic status (SES), education, or structural racism resulting from being a member of racial ethnic minority groups, may be affecting results.

Missing data were described in some studies. For example, some studies analyzed different sample sizes for different time points (26), some had missing sample characteristics like age, BMI, or gestational age (24, 32), and some had missing blood samples and analyzed a smaller subset for the mRNA or miRNA results (32).

4 Discussion

This systematic review of the literature identified 16 articles that measured the transcriptome or miRNA expression in blood specimens of 684 adults with GDM compared to 691 healthy controls. Most studies applied an observational, cross-sectional design. Collectively, findings span the entire pregnancy from the first to the third trimester. Additional repeated measures studies are needed to compare mRNA or miRNA levels across gestational ages in the same participants.

The studies represent participants residing in 12 countries, with most set in China and South Africa. There is emerging evidence that differences in geographic location and ethnicity may be reflected in circulating miRNA levels (38, 39). Overall, most of the studies included in our review did not cite standardized definitions of race, ethnicity, and nationality to characterize the samples. To ensure high-quality precision healthcare that is equitable and representative, accurate sample descriptions are needed. Samples of diverse individuals should be recruited to ensure that the findings can be generalizable.

Overall, participants with GDM were slightly older with a significantly higher BMI at the time of the blood draw compared to controls. Few studies utilized either matching in their study design or controlled for confounders in their analyses. As age and weight may influence mRNA and miRNA levels, further research is needed to isolate the influence of GDM from other potentially confounding factors.

Three transcriptome studies were found that assessed circulating mRNA levels in pregnant people with GDM compared with healthy controls (22–24). All three studies represent mRNA levels in the third trimester. The transcriptome studies collectively identified 6,289 DEGs, of which 2,702 (43.0%) were described as upregulated in participants with GDM compared to controls, while 2,499 (39.7%) were described as downregulated in GDM compared to controls.

Expression levels of four mRNAs related to circadian clock rhythms were found to be significantly lower in pregnant people with GDM and were significantly correlated with HbA1c levels in one study (22). These four mRNAs were brain and muscle aryl hydrocarbon receptor nuclear translocator-like protein 1

(*BMAL1*), *PER3*, peroxisome proliferator activated receptor delta (*PPARD*), and cryptochrome circadian regulator 2 (*CRY2*). However, none of the ten circadian clock genes measured by Pappa et al. (2013) were reported in the supplementary results tables of the other two transcriptome studies (22–24). Differentially expressed clock genes are consistent with other studies that showed associations between sleep disruptions/night shift work and GDM (40). Specifically, sleep disruptions in GDM are associated with higher morning blood cortisol and glucose levels, increasing the need for long-acting insulin at night for patients with GDM. Previous studies about the role of circadian genes in T2D have indicated that *BMAL1* works in coordination with *CLOCK* as transcriptional activators of the circadian clock's self-sustained transcriptional-translational feedback loops (41). These activators function as positive elements driving transcription of *PER*s, *CRY*s, and numerous other downstream elements involved in glucose metabolism and postprandial glycemia (41).

We extracted data from the transcriptome articles about the target pathways implicated by their findings and the tools they used to analyze them. Studies used different databases to determine the biological pathways related to their results. For example, Steyn et al. (2019) used the protein analysis through evolutionary relationships (PANTHER) and the database for annotation, visualization and integrated discovery (DAVID) tools (23), while Zhao et al. (2011) used Pathway Express (23, 24).

Collectively, the target pathways identified using these tools described various aspects of diabetes pathogenesis, including insulin and glucose signaling, regulation, and transport; natural killer cell mediated cytotoxicity; NADP and carbohydrate metabolism; immunity and inflammation; fatty acid biosynthesis and metabolism. The transcriptome pathways identified by the findings reflect the multi-system, complex nature of the disease (42). A prior study conducted by Flowers et al. (2022) assessed pathways targeted by differentially expressed miRNAs in people at risk for T2D and identified three themes (i.e., metabolism and inflammation, endocrine, and hormone) (43). Many of the implicated pathways identified by the studies included in this review also fit within these themes. Additional research is needed to validate transcriptome findings related to GDM in larger samples and additional settings and to determine how the pathophysiology of GDM may relate to the pathophysiology that underlies risk for T2D. Standardization is needed for data acquisition and analysis tools.

The miRNA study designs, participant characteristics, gestational age at the time of the miRNA blood analysis, and data analysis tools were disparate. Our analysis revealed that miRNA levels varied based on the time in pregnancy when GDM develops, the trimester or time period at which miRNAs were measured, sex of the fetus, obesity in the pregnant person, and treatment type (diet versus pharmaceutical). We delineated the miRNAs that were found to be significantly different in pregnant people with GDM by first trimester, second trimester, and the gestational age corresponding with GDM diagnosis (24-28 weeks gestation).

In the thirteen miRNA studies, 135 unique miRNAs were associated with GDM. Eight of these circulating miRNAs (miR-16-5p, miR-17-5p, miR-20a-5p, miR-29a-3p, miR-195-5p, miR-222-3p, miR-210-3p, and miR-342-3p) were the most validated for GDM. This list is updated from the previous review by Ibarra et al. (2018) by adding three miRNAs to the list (miR-195-5p, miR-210-3p, and miR-342-3p) and integrating any new findings about the five most-validated miRNAs previously identified (miR-16-5p, miR-17-5p, miR-20a-5p, miR-29a-3p, and miR-222-3p) (44). What is known from previous literature about each of these miRNAs in relation to GDM, other types of diabetes, obesity and weight change, or relevant pregnancy-related outcomes are discussed in more detail below. Animal model study findings are included in those cases where human study findings are unavailable.

4.1 miR-16-5p

MiR-16-5p is a powerful regulator of the insulin signaling pathway, pancreatic β-cell proliferation and apoptosis, and branched chain amino acids involved in insulin dysregulation (45–48). Target genes of miR-16-5p in mouse model and *in vitro* mechanistic studies include those that encode for insulin receptor substrate (IRS) proteins 1 and 2, the insulin receptor (INSR), and at least 24 other targets in the insulin signaling pathway like ak strain transforming (AKT) protein 1 and 3 (45–48). Other targets include genes encoding for the mammalian target of rapamycin (mTOR) protein and b-cell leukemia/lymphoma 2 protein (BCL-2) expression (45, 48), among others.

Our review found that miR-16-5p was upregulated compared to the control group in 80% (4 out of 5) of the included studies that reported it in their findings (Table 4). It was upregulated prior to onset of GDM in the first trimester (weeks 9-12) (48), during weeks 16-19 (27, 37), and in weeks 24-28 (25, 37, 48). Elevated gestational miR-16-5p may persist beyond pregnancy and may be permanently altered in women with GDM (35). However, in other studies conducted in Turkey, South Africa, and Poland, no significant difference was found in women with GDM compared with controls (36, 48–50). These mixed results may reflect regional environmental or cultural differences in miRNA expression levels, or instrumentation and study design differences, but further research is necessary to validate findings.

MiR-16-5p has been associated with traditional clinical indicators and long- and short-term outcomes. For example, elevated miR-16-5p is correlated with homeostatic model assessment of insulin resistance (HOMA-IR) (47, 48), insulin resistance (25), and cardiovascular disease risk (35), but not with preeclampsia (51). MiR-16-5p may also be associated with pre-pregnancy weight, because it has been reported to be elevated in

overweight and obese women before week 20 gestation (37, 48). Further, it is consistently downregulated after surgical weight loss interventions in obese human and animal studies (46). Notably, in our sample of studies, miR-16-5p was not correlated with BMI in women with GDM (25). Future studies may seek to control for pre-pregnancy weight, weight category at the time of the blood draw, or gestational weight changes in their analyses for miR-16-5p to differentiate the effects of obesity from GDM pathology on miR-16-5p levels.

The findings from our review suggest that elevated baseline and first trimester miR-16-5p may be a predictor of late-onset GDM, particularly when combined with other miRNAs associated with GDM (37). These findings suggest that therapies that lower miR-16-5p prior to or early in pregnancy may help to prevent or decreased risk for GDM. However, more studies are needed to validate these findings, to understand regional or cultural differences, and to differentiate the contribution of obesity from pathology unique to GDM.

4.2 miR-17-5p

MiR-17-5p is involved in cell proliferation, inflammation, mitochondrial function, and diabetes-related vascular damage (48, 52). High glucose induction of human trophoblast cells *in vitro* led to upregulation of miR-17-5p in a simulated diabetic environment (52). There is some evidence that two enzymes associated with mitochondrial function, mitofusins 1 and 2, are targets of miR-17-5p (52).

In our sample, miR-17-5p was upregulated in 75% (3/4) of the studies (25, 27, 35). MiR-17-5p levels were upregulated compared with controls in weeks 16-19 (27) and 3-5 years post-pregnancy (35). During weeks 24-28 at the typical time of GDM diagnosis, expression levels were mixed. One study conducted in a sample of pregnant people in China found miR-17-5p levels to be upregulated (25), while two other studies of samples of South African and Turkish pregnant people, respectively, found no difference (36, 49). These mixed results may reflect cultural and environmental differences between the samples. Like miR-16-5p, miR-17-5p was positively correlated with insulin resistance but not TNF-α or BMI in one study (25). Also, like miR-16-5p, miR-17-5p has been linked to obesity, except that in the obese and coronary artery disease phenotypes the miR-17-5p levels were downregulated compared with healthy controls instead of upregulated as we found in our review (53). Further research is warranted to understand to what extent differences in miRNA expression levels are due to GDM pathology or obesity, and to describe how gestational miR-17-5p levels may change with weight changes.

4.3 miR-195-5p

In mouse and *in vitro* models, placental miR-195-5p targeted vascular endothelial growth factor A (*VEGFA*) in placental cells (54), and was an enhancer of zeste homolog 2 (*EZH2*) in umbilical cells (54), both of which may contribute to endothelial cell dysfunction and GDM progression. In the two studies that were included in our review, miR-195-5p was upregulated in pregnant people with GDM compared with controls in weeks 23-31 (28) and 3-5 years post pregnancy (35). This finding is consistent with previous work by Wang et al. (2020), who also found miR-195-5p to be upregulated at 25 weeks gestation in pregnant people with GDM compared with controls. MiR-195-5p targeted several of the genes important in the fatty acid metabolism pathway, including fatty acid desaturase 2 (*FADS2*), elongase of very long fatty acid 5, acetyl co-A carboxylase α *(ELOVL5)*, acetyl co-A synthetase 3 and 4 *(ACSL3, ACSL4)*, hydroxyacyl-CoA dehydrogenase trifunctional multienzyme complex subunit α *(HADHA)*, and carnitine palmitoyltransferase 1A genes *(CPT1A)* (28). This suggests that alterations in lipid metabolism, associated with changes in miR-195-5p expression, may be an important aspect of GDM pathogenesis and an area of focus for future study.

Mechanistic mouse model and *in vitro* studies about the role of miR-195-5p in GDM suggests that high levels of miR-195-5p inhibits cell proliferation and angiogenesis in human placental microvascular and umbilical endothelial cells treated with a high glucose condition (54, 55). The direction of the effect on cell apoptosis may vary by tissue, as high miR-195-5p inhibited apoptosis in umbilical endothelial cells (55) and increased apoptosis in the placental endothelial cells (54), both of which were undesirable effects contributing to cellular dysfunction. Additional studies are warranted to fully understand the mechanism of miR-195-5p in GDM pathogenesis. Two studies have measured associations between miR-195-5p and body mass and reported no association (35, 56), suggesting that obesity and gestational weight changes may not play a significant role in miR-195-5p levels in GDM. However, due to the connection between miR-195-5p and altered lipid metabolism, further validation of these results is warranted.

4.4 miR-20a-5p

The mechanism of miR-20a-5p's involvement in GDM is unknown, but miR-20a-5p has been linked to cardiovascular disease, T2D, and pregnancy-related birth outcomes like small for gestational age and fetal growth restriction (57). In a study of participants undergoing coronary angiography, miR-20a-5p was associated with kidney function and estimated glomerular filtration rate after controlling for several confounders including T2D (58). In another study comparing participants with abdominal aortic aneurism with and without T2D, miR-20a-5p was associated with fructosamine concentration (59). MiR-20a-5p levels were significantly upregulated in the group with T2D compared with controls (59).

We found that miR-20a-5p was upregulated in pregnant people with GDM compared with controls in 75% of studies (3/4) in the final sample in this review (25, 27, 35). Levels were downregulated in the other 25% (36). For the studies that showed upregulated expression in pregnant people with GDM compared to controls, two of the studies were done in China (25, 27) and the other from the Czech Republic (35). Expression levels of miR-20a-5p were upregulated compared with controls across gestational periods and beyond—in weeks 16-19 (27), weeks 24-28 (25), and 3-7 years post-pregnancy (35). The average BMI for most study groups (pregnant people with GDM or control) in the three studies that reported upregulation had BMIs in the normal range. In contrast, in a study of South African pregnant people, miR-20a-5p was significantly lower in participants with GDM than participants in the control group in weeks 24-28 (36). The difference in findings may reflect regional or ethnic differences between the samples, but notably, the South African participants were more obese than participants in the other three studies. Previous mouse model studies have linked miR-20a-5p with induction of adipogenesis and lipogenesis *via* a novel regulatory circuit called CCAAT/enhancer-binding protein α/miR-20a-5p/Transducer Of ERBB2, 2 or TOB2 (60). Yet in the one study in our review that tested correlations between the miRNAs and clinical measures, miR-20a-3p was not correlated with BMI, but it was positively correlated with insulin resistance (25). Further research is warranted to validate previous findings, to understand the relationships between pre-gestational BMI, gestational weight gain or loss, and miR-20a-5p, and to distinguish the influence of obesity versus GDM pathology on miR-20a-5p expression levels.

4.5 miR-210-3p

MiR-210-3p is involved in hypoxia, insulin resistance, and anti-angiogenesis (34). Overexpression of miR-210-3p is predicted to inhibit insulin binding to the insulin receptor protein, the function of AMPK, and ultimately, β-oxidation and glucose transport (34). MiR-210-3p in late pregnancy has been positively associated with gestational age at birth (61). We found that results for miR-210-3p were mixed. Gillet et al. found it to be upregulated in pregnant people with GDM compared with controls (34), while Wander et al. found no difference (32). In one sample, miR-210-3p was associated with GDM in pregnant people with overweight or obesity but not those participants who were lean (32).

4.6 miR-222-3p

The role of miR-222-3p in GDM is unknown, but previous mechanistic studies implicate circulating miR-222-3p levels in both obesity and T2D (62–65). MiR-222-3p targets at least three experimentally validated genes of which low levels have been associated with T2D pathology: O-6-Methylguanine-DNA Methyltransferase (*MGMT*), Serine/threonine-protein phosphatase 2A 55 kDa regulatory subunit B-α isoform (*PPP2R2A*), and Reversion Inducing Cysteine Rich Protein With Kazal Motifs (*RECK*) (62, 63). In a mouse model mechanistic study, miR-222-3p also mediated the therapeutic effects pioglitazone, an oral hypoglycemic drug used for T2D, on skeletal muscle tissue, independent of the PPARγ mechanism-of-action of the drug (66).

In mouse models of obesity, overexpression of miR-222-3p was associated with increased adiposity by targeting DNA damage inducible transcript 4 (*Ddit4*) in adipocyte specific miR-221/222 knockout, which was associated with the suppression of the tuberous sclerosis complex 2 (TSC2)/mTOR complex 1 (mTORC1)/ribosomal protein S6 kinase (S6K) pathway (65). Circulating levels of miR-222-3p have been downregulated post-bariatric surgery induced weight loss in at least two studies (67). Paradoxically, however, circulating levels of miR-222-3p increased rather than decreased in overweight and obese human participants after a diet-induced weight loss intervention (68).

In our systematic review, results for miR-222-3p in pregnant people with GDM compared with controls were mixed, with one each downregulated during weeks 24-28 gestation (36), upregulated between weeks 23-21 gestation (28), and no difference during weeks 7-22.9 gestation (32). These three studies took place in different countries (South Africa, Estonia, and the United States, respectively). Although the difference was significant between the pregnant people with GDM and controls, miR-222-3p was not significantly, independently associated with GDM in a logistic regression model by Pheiffer et al. (36). While these three studies (28, 32, 36) did not describe correlations between miR-222-3p and any clinical parameters or outcomes, a validation study by Filardi et al. (2022) found that miR-222-3p was positively correlated with fasting blood glucose and birth weight in the third trimester in pregnant people with GDM (62). Overall, the highly disparate findings in studies about T2D, obesity, weight loss, and GDM suggest a complex mechanism that warrants further research.

4.7 miR-29a-3p

In our review, miR-29a-3p was the most validated because it was reported in 46% of the articles in our final sample, but results were mixed. MiR-29a-3p was upregulated compared with controls in 50% (3/5 studies) (34, 35, 37) and downregulated in 17% (1/5 studies) (31). Two studies (33%) found no difference (32, 36). Zhao et al. (2011) inferred miR-29a-3p to be a negative regulator of serum glucose because knockdown of miR-29a led to increased mitochondrial phosphoenolpyruvate carboxykinase

2 (*PCK2)* expression (31). Increased *PCK2* could then lead to an increase in glucose levels. However, their study was the only one in our sample in which the levels of miR-29a-3p were lower in pregnant people with GDM than controls, so the collective evidence does not yet support this inference. Further research is warranted to fully understand the mechanism and how it may vary by region or ethnicity.

4.8 miR-342-3p

The synthesized evidence from our review suggest that not only is miR-342-3p linked to complications of diabetes as previously proposed (18, 69), but it also may be an early indicator of risk. In the three studies in our review that described miR-342-3p levels, the miRNA was upregulated in 100% of them, spanning early to mid-pregnancy and several years post-pregnancy in diverse geographic locations (28, 34, 35). These three study samples were comparable in mean BMI by study group. In type 2 diabetes, miR-342-3p is predicted to inhibit *GLUT2* and trigger impaired insulin secretion in pancreatic β islet cells (34). It is one of the miRNAs that has been shown to be dysregulated across types of diabetes, including GDM, T1D, T2D (18, 70), and in people with obesity (71, 72). For people with metabolic syndrome at risk for diabetes, miR-324-3p is one of at least 49 miRNAs associated with insulin resistance in at least three studies (73). MiR-342-3p may also operate as a novel epigenetic integrator linking adipogenic homeostasis and angiogenesis (69). As such, it may be a useful early marker of metabolic risk. In mouse models of obesity, *SNAP25* was identified as a major target gene of miR-342-3p and the reduced expression of *SNAP25* may link to functional impairment hypothalamic neurons and excess of food intake (74). The inhibition of miR-342-3p may be a potential candidate for miRNA-based therapy for obesity (74). Due to miR-342-3p's strong associations with obesity in animal studies, GDM studies should consider controlling for baseline obesity and gestational weight changes, or to consider differentiating from metabolically healthy people with obesity any potential mechanisms that are unique to GDM pathology.

4.9 Other subgroup analyses and overlap with T1D and T2D

Other subgroup analyses included differences in miRNAs by sex of the fetus or by GDM treatment type. Findings suggest that the sex of the fetus may affect maternal circulating miRNAs, however the two studies in our final sample that measured sex reported mixed results (32, 37). Further studies are warranted to better understand if or how sex of the offspring may influence GDM.

Only two studies in our final sample differentiated findings by GDM treatment type (diet versus diet with pharmacologic therapy) with mixed results. These results are complicated by mixing treatment types (i.e., insulin, metformin) within the group of participants with GDM, such as in Hromadnikova et al. (2020) included one participant on metformin with the 17 other participants who were treated with insulin (35). MiR-330-3p was the only miRNA found in our systematic review to vary by treatment group, with levels significantly higher in the GDM group treated with diet alone rather than diet plus insulin (30). Additional studies are needed to understand how miRNAs may vary within treatment groups, because metformin has been associated with the expression of miRNA levels in people undergoing treatment for insulin-resistant diseases (75). More research is needed to fully understand how metformin influences the expression of miRNAs in pregnant people with GDM.

The gene targets and miRNAs identified in this review mostly differ from those that have been previously emphasized for T1D and T2D, suggesting a distinct pathophysiology for GDM (76–78). Some exceptions are miR-16-5p (43), miR-29a-3p, miR-146a, miR-182, and miR-342-3p as previously mentioned in section 4.7 (18, 31–34, 36, 37, 43, 70, 76, 77, 79, 80). MiR-29a-3p was reported with mixed results in both GDM and T2D studies, with one or more study showing it to be upregulated and one or more showing it to be downregulated compared with controls. MiR-146a was significantly upregulated in both GDM and T2D studies. MiR-182 was reported to have significantly higher levels in GDM studies but was significantly downregulated in studies of T1D and T2D.

4.10 Risk of bias and limitations

The studies in the final sample are at moderate risk of bias due to several reasons, including the cross-sectional design, differences in sample characteristics between groups at the time of the analysis, inconsistencies in the standards used for GDM diagnosis, varying molecular quantitation methods and data analysis tools, and the handling of missing data. An international consensus is needed for GDM definitions and diagnostic criteria. More rigorous methods are needed to ensure that participants did not have pre-existing diabetes prior to pregnancy. We found that exclusion criteria were unstandardized, which adds additional complexity while synthesizing results across studies.

Replication and validation studies are needed before any of the mRNA or miRNA targets can be useful as clinical biomarkers or therapeutic targets. As this field of science continues to develop, efforts to standardize sample characterization, diagnostic guidelines, validation, and data acquisition and analysis tools and methods would strengthen the synthesis of results. Nonetheless, these studies represent the best available knowledge about transcriptional differences in the

blood samples of adults with GDM compared to controls. This review was limited in that the search was conducted in only one database and only articles available in English were included in this analysis. Our ability to integrate the transcriptome studies with the miRNAome studies was limited by the findings available within each of the individual articles.

Many of the studies presented truncated findings or made available partial datasets. This limited our ability to search for overlapping gene targets and pathways between the miRNA and mRNA studies. Journals are increasingly requiring authors to make available full datasets with their publications. If applied consistently, this practice will allow for improved synthesis and validation of findings across multiple omics studies in the future.

4.11 Conclusions

Findings from this systematic review contribute new insights into the state of the science on transcriptomics and miRNA expression in blood from adults with GDM compared with healthy controls. Differences in expression of mRNA and miRNA levels were identified by gestational age at the time of the study, sex of the fetus, BMI of the pregnant person, and GDM treatment type. Metabolic pathways identified in these studies reflect the multi-system, complex pathophysiology of GDM. Eight miRNAs were found to be the most validated in the current literature: miR-16-5p, miR-17-5p, miR-20a-5p, miR-29a-3p, miR-195-5p, miR-222-3p, miR-210-3p, and miR-342-3p. With the exception of miR-222-3p, the most-validated miRs were upregulated in adults with GDM compared with controls in a majority of the studies that reported about them. The reasons for differences in the direction of change in the results (upregulated, downregulated, no difference) across studies are unknown, but may be related to confounding effects like maternal obesity, gestational weight changes, geographic or ethnic differences, instrumentation and data analysis differences, and study designs. Additional research, particularly with repeated measurement designs, is warranted to validate and refine the evidence, with an emphasis on standardization of research methods and recruiting diverse samples with sufficient power for subgroup analyses.

Data availability statement

The original contributions presented in the study are included in the article/supplementary material. Further inquiries can be directed to the corresponding author.

Author contributions

All authors reviewed and approved the final version of the manuscript. EF, KL, JC, BA, LJ-P, MM, BP, LR, and KR contributed to the conceptualization of the work and critically revised the manuscript. KL and JC completed the search, data extraction, and data analysis. KL was lead author. KL and LC wrote and formatted the data tables and figures.

Acknowledgments

The authors would like to acknowledge the contributions of Lena Noya who helped with the search.

Conflict of interest

The authors declare that the research was conducted in the absence of any commercial or financial relationships that could be construed as a potential conflict of interest.

Publisher's note

All claims expressed in this article are solely those of the authors and do not necessarily represent those of their affiliated organizations, or those of the publisher, the editors and the reviewers. Any product that may be evaluated in this article, or claim that may be made by its manufacturer, is not guaranteed or endorsed by the publisher.

References

1. American Diabetes Association. 2. classification and diagnosis of diabetes: *Standards of medical care in diabetes-2020. Diabetes Care* (2020) 43(Suppl 1):S14–31. doi: 10.2337/dc20-S002

2. Schneider S, Bock C, Wetzel M, Maul H, Loerbroks A. The prevalence of gestational diabetes in advanced economies. *J Perinat Med* (2012) 40(5):511–20. doi: 10.1515/jpm-2012-0015

3. Järvelä IY, Juutinen J, Koskela P, Hartikainen AL, Kulmala P, Knip M, et al. Gestational diabetes identifies women at risk for permanent type 1 and type 2 diabetes in fertile age: Predictive role of autoantibodies. *Diabetes Care* (2006) 29 (3):607–12. doi: 10.2337/diacare.29.03.06.dc05-1118

4. Atègbo JM, Grissa O, Yessoufou A, Hichami A, Dramane KL, Moutairou K, et al. Modulation of adipokines and cytokines in gestational diabetes and macrosomia. *J Clin Endocrinol Metab* (2006) 91(10):4137–43. doi: 10.1210/jc.2006-0980

5. Kong L, Nilsson IAK, Gissler M, Lavebratt C. Associations of maternal diabetes and body mass index with offspring birth weight and prematurity. *JAMA Pediatr* (2019) 173:371–8. doi: 10.1001/jamapediatrics.2018.5541

6. Ornoy A, Becker M, Weinstein-Fudim L, Ergaz Z. Diabetes during pregnancy: a maternal disease complicating the course of pregnancy with long-term deleterious effects on the offspring. a clinical review. *Int J Mol Sci* (2021) 22 (6):2965. doi: 10.3390/ijms22062965

7. Robitaille J, Grant AM. The genetics of gestational diabetes mellitus: evidence for relationship with type 2 diabetes mellitus. *Genet Med* (2008) 10(4):240–50. doi: 10.1097/GIM.0b013e31816b8710

8. Evangelista AF, Collares CV, Xavier DJ, Macedo C, Manoel-Caetano FS, Rassi DM, et al. Integrative analysis of the transcriptome profiles observed in type 1, type 2 and gestational diabetes mellitus reveals the role of inflammation. *BMC Med Genomics* (2014) 7:28. doi: 10.1186/1755-8794-7-28

9. Zhao S, Liu M-F. Mechanisms of microRNA-mediated gene regulation. *Sci China Ser C: Life Sci* (2009) 52:1111–6. doi: 10.1007/s11427-009-0152-y

10. Moen GH, Sommer C, Prasad RB, Sletner L, Groop L, Qvigstad E, et al. Mechanisms in endocrinology: epigenetic modifications and gestational diabetes: a systematic review of published literature. *Eur J Endocrinol* (2017) 176(5):R247–67. doi: 10.1530/EJE-16-1017

11. Destefanis E, Avşar G, Groza P, Romitelli A, Torrini S, Pir P, et al. A mark of disease: how mRNA modifications shape genetic and acquired pathologies. *RNA* (2021) 27(4):367–89. doi: 10.1261/rna.077271.120

12. Vasu S, Kumano K, Darden CM, Rahman I, Lawrence MC, Naziruddin B, et al. MicroRNA Signatures as Future Biomarkers for Diagnosis of Diabetes States. *Cells* (2019) 8(12):1533. doi: 10.3390/cells8121533

13. O'Brien J, Hayder H, Zayed Y, Peng C. Overview of microRNA biogenesis, mechanisms of actions, and circulation. *Front Endocrinol* (2018) 9:402. doi: 10.3389/fendo.2018.00402

14. Soifer HS, Rossi JJ, Saetrom P. MicroRNAs in disease and potential therapeutic applications. *Mol Ther* (2007) 15(12):2070–9. doi: 10.1038/sj.mt.6300311

15. Vaishya S, Sarwade RD, Seshadri V. MicroRNA, proteins, and metabolites as novel biomarkers for prediabetes, diabetes, and related complications. *Front Endocrinol* (2018) 9:180. doi: 10.3389/fendo.2018.00180

16. Yang X, Wu N. MicroRNAs and exosomal microRNAs may be possible targets to investigate in gestational diabetes mellitus. *Diabetes Metab Syndr Obes* (2022) 15:321–30. doi: 10.2147/DMSO.S330323

17. Flowers E, Kanaya AM, Fukuoka Y, Allen IE, Cooper B, Aouizerat BE. Preliminary evidence supports circulating microRNAs as prognostic biomarkers for type 2 diabetes. *Obes Sci Pract* (2017) 3(4):446–52. doi: 10.1002/osp4.134

18. Flowers E, Allen IE, Kanaya AM, Aouizerat BE. Circulating MicroRNAs predict glycemic improvement and response to a behavioral intervention. *biomark Res* (2021) 9(1):65. doi: 10.1186/s40364-021-00317-5

19. Page MJ, McKenzie JE, Bossuyt PM, Boutron I, Hoffmann TC, Mulrow CD, et al. The PRISMA 2020 statement: an updated guideline for reporting systematic reviews. *BMJ* (2021) 372:n71. doi: 10.1136/bmj.n71

20. Igelström E, Campbell M, Craig P, Katikireddi SV. Cochrane's risk of bias tool for non-randomized studies (ROBINS-I) is frequently misapplied: A methodological systematic review. *J Clin Epidemiol* (2021) 140:22–32. doi: 10.1016/j.jclinepi.2021.08.022

21. Sterne JAC, Hernán MA, Reeves BC, Savović J, Berkman ND, Viswanathan M, et al. ROBINS-I: a tool for assessing risk of bias in non-randomized studies of interventions. *BMJ* (2016) 355:i4919. doi: 10.1136/bmj.i4919

22. Pappa KI, Gazouli M, Anastasiou E, Iliodromiti Z, Antsaklis A, Anagnou NP. Circadian clock gene expression is impaired in gestational diabetes mellitus. *Gynecol Endocrinol* (2013) 29(4):331–5. doi: 10.3109/09513590.2012.743018

23. Steyn A, Crowther NJ, Norris SA, Rabionet R, Estivill X, Ramsay M. Epigenetic modification of the pentose phosphate pathway and the IGF-axis in women with gestational diabetes mellitus. *Epigenomics* (2019) 11(12):1371–85. doi: 10.2217/epi-2018-0206

24. Zhao YH, Wang DP, Zhang LL, Zhang F, Wang DM, Zhang WY. Genomic expression profiles of blood and placenta reveal significant immune-related pathways and categories in Chinese women with gestational diabetes mellitus. *Diabetes Med* (2011) 28(2):237–46. doi: 10.1111/j.1464-5491.2010.03140.x

25. Cao YL, Jia YJ, Xing BH, Shi DD, Dong XJ. Plasma microRNA-16-5p, -17-5p and -20a-5p: Novel diagnostic biomarkers for gestational diabetes mellitus. *J Obstet Gynaecol* (2017) 6:974–81. doi: 10.1111/jog.13317

26. Lamadrid-Romero M, Solís KH, Cruz-Reséndiz MS, Pérez JE, Díaz NF, Flores-Herrera H, et al. Central nervous system development-related microRNAs levels increase in the serum of gestational diabetic women during the first trimester of pregnancy. *J Neurosci Res* (2018) 130:8–22. doi: 10.1016/j.neures.2017.08.003

27. Zhu Y, Tian F, Li H, Zhou Y, Lu J, Ge Q. Profiling maternal plasma microRNA expression in early pregnancy to predict gestational diabetes mellitus. *Int J Gynaecol Obstet* (2015) 130(1):49–53. doi: 10.1016/j.ijgo.2015.01.010

28. Tagoma A, Alnek K, Kirss A, Uibo R, Haller-Kikkatalo K. MicroRNA profiling of second trimester maternal plasma shows upregulation of miR-195-5p in patients with gestational diabetes. *Gene* (2018) 672:137–42. doi: 10.1016/j.gene.2018.06.004

29. Yoffe L, Polsky A, Gilam A, Raff C, Mecacci F, Ognibene A, et al. Early diagnosis of gestational diabetes mellitus using circulating microRNAs. *Eur J Endocrinol* (2019) 181(5):565–77. doi: 10.1530/EJE-19-0206

30. Pfeiffer S, Sánchez-Lechuga B, Donovan P, Halang L, Prehn J, Campos-Caro A, et al. Circulating miR-330-3p in late pregnancy is associated with pregnancy outcomes among lean women with GDM. *Sci Rep* (2020) 10(1):908. doi: 10.1038/s41598-020-57838-6

31. Zhao C, Dong J, Jiang T, Shi Z, Yu B, Zhu Y, et al. Early second-trimester serum miRNA profiling predicts gestational diabetes mellitus. *PloS One* (2011) 6 (8):e23925. doi: 10.1371/journal.pone.0023925

32. Wander PL, Boyko EJ, Hevner K, Parikh VJ, Tadesse MG, Sorensen TK, et al. Circulating early- and mid-pregnancy microRNAs and risk of gestational diabetes. *Diabetes Res Clin Pract* (2017) 132:1–9. doi: 10.1016/j.diabres.2017.07.024

33. Stirm L, Kovárová M, Perschbacher S, Michlmaier R, Fritsche L, Siegel-Axel D, et al. BMI-independent effects of gestational diabetes on human placenta. *J Clin Endocrinol Metab* (2018) 103(9):3299–309. doi: 10.1210/jc.2018-00397

34. Gillet V, Ouellet A, Stepanov Y, Rodosthenous RS, Croft EK, Brennan K, et al. miRNA profiles in extracellular vesicles from serum early in pregnancies complicated by gestational diabetes mellitus. *J Clin Endocrinol Metab* (2019) 104 (11):5157–69. doi: 10.1210/jc.2018-02693

35. Hromadnikova I, Kotlabova K, Dvorakova L, Krofta L. Evaluation of vascular endothelial function in young and middle-aged women with respect to a history of pregnancy, pregnancy-related complications, classical cardiovascular risk factors, and epigenetics. *Int J Mol Sci* (2020) 21(2):430. doi: 10.3390/ijms21020430

36. Pheiffer C, Dias S, Rheeder P, Adam S. Decreased expression of circulating miR-20a-5p in south African women with gestational diabetes mellitus. *Mol Diagn* (2018) 22(3):345–52. doi: 10.1007/s40291-018-0325-0

37. Sørensen AE, van Poppel MNM, Desoye G, Damm P, Simmons D, Jensen DM, et al. The DALI core investigator group. the predictive value of miR-16, -29a and -134 for early identification of gestational diabetes: A nested analysis of the DALI cohort. *Cells* (2021) 10(1):170. doi: 10.3390/cells10010170

38. Flowers E, Ramírez-Mares JD, Velazquez-Villafaña M, Rangel-Salazar R, Sucher A, Kanaya AM, et al. Circulating microRNAs associated with prediabetes and geographic location in latinos. *Int J Diabetes Dev Ctries* (2021) 41(4):570–8. doi: 10.1007/s13410-020-00917-1

39. Flowers E, Kanaya AM, Zhang L, Aouizerat BE. The role of racial and ethnic factors in microRNA expression and risk for type 2 diabetes. *Front Genet* (2022) 13:853633. doi: 10.3389/fgene.2022.853633

40. Weschenfelder F, Lohse K, Lehmann T, Schleußner E, Groten T. Circadian rhythm and gestational diabetes: working conditions, sleeping habits and lifestyle influence insulin dependency during pregnancy. *Acta Diabetol* (2021) 58(9):1177–86. doi: 10.1007/s00592-021-01708-8

41. Jakubowicz D, Wainstein J, Tsameret S, Landau Z. Role of high energy breakfast "big breakfast diet" in clock gene regulation of postprandial hyperglycemia and weight loss in type 2 diabetes. *Nutrients* (2021) 13(5):1558. doi: 10.3390/nu13051558

42. Alejandro EU, Mamerto TP, Chung G, Villavieja A, Gaus NL, Morgan E, et al. Gestational diabetes mellitus: A harbinger of the vicious cycle of diabetes. *Int J Mol Sci* (2020) 21(14):5003. doi: 10.3390/ijms21145003

43. Flowers E, Asam K, Allen IE, Kanaya AM, Aouizerat BE. Co-expressed microRNAs, target genes and pathways related to metabolism, inflammation and endocrine function in individuals at risk for type 2 diabetes. *Mol Med Rep* (2022) 25 (5):156. doi: 10.3892/mmr.2022.12672

44. Ibarra A, Vega-Guedes B, Brito-Casillas Y, Wägner AM. Diabetes in pregnancy and microRNAs: promises and limitations in their clinical application. *Noncoding RNA* (2018) 4(4):32. doi: 10.3390/ncrna4040032

45. Calimlioglu B, Karagoz K, Sevimoglu T, Kilic E, Gov E, Arga KY. Tissue-specific molecular biomarker signatures of type 2 diabetes: an integrative analysis of transcriptomics and protein-protein interaction data. *OMICS* (2015) 19(9):563–73. doi: 10.1089/omi.2015.0088

46. Catanzaro G, Filardi T, Sabato C, Vacca A, Migliaccio S, Morano S, et al. Tissue and circulating microRNAs as biomarkers of response to obesity treatment strategies. *J Endocrinol Invest* (2021) 44(6):1159–74. doi: 10.1007/s40618-020-01453-9

47. Hubal MJ, Nadler EP, Ferrante SC, Barberio MD, Suh JH, Wang J, et al. Circulating adipocyte-derived exosomal microRNAs associated with decreased insulin resistance after gastric bypass. *Obes* (2017) 25(1):102–10. doi: 10.1002/oby.21709

48. Juchnicka I, Kuźmicki M, Niemira M, Bielska A, Sidorkiewicz I, Zbucka-Krętowska M, et al. miRNAs as predictive factors in early diagnosis of gestational diabetes mellitus. *Front Endocrinol* (2022) 13:839344. doi: 10.3389/fendo.2022.839344

49. Balci S, Gorur A, Derici Yıldırım D, Cayan F, Tamer L. Expression level of miRNAS in patients with gestational diabetes. *Turkish J Biochem* (2020) 45(6):825–31. doi: 10.1515/tjb-2019-0157

50. Hocaoglu M, Demirer S, Loclar Karaalp I, Kaynak E, Attar E, Turgut A, et al. Identification of miR-16-5p and miR-155-5p microRNAs differentially expressed in circulating leukocytes of pregnant women with polycystic ovary syndrome and gestational diabetes. *Gynecol Endocrinol* (2021) 37(3):216–20. doi: 10.1080/09513590.2020.1843620

51. Hocaoglu M, Demirer S, Senturk H, Turgut A, Komurcu-Bayrak E. Differential expression of candidate circulating microRNAs in maternal blood leukocytes of the patients with preeclampsia and gestational diabetes mellitus. *Pregnancy Hypertens* (2019), 17:5–11. doi: 10.1016/j.preghy.2019.04.004

52. Li J, Liu Z, Wu T, Li S, Sun Y. MicroRNA-17-5p acts as a biomarker and regulates mitochondrial dynamics in trophoblasts and endothelial cells by targeting the mitofusins Mfn1/Mfn2 in gestational diabetes mellitus. *Arch Med Sci* (2022) . doi: 10.5114/aoms/145778

53. Deiuliis JA. MicroRNAs as regulators of metabolic disease: pathophysiologic significance and emerging role as biomarkers and therapeutics. *Int J Obes* (2016) 40 (1):88–101. doi: 10.1038/ijo.2015.170

54. Zheng H, Yu Z, Wang H, Liu H, Chen X. MicroRNA-195-5p facilitates endothelial dysfunction by inhibiting vascular endothelial growth factor a in gestational diabetes mellitus. *Reprod Biol* (2022) 22(1):100605. doi: 10.1016/j.repbio.2022.100605

55. Liao X, Zhou Z, Zhang X. Effects of miR−195−5p on cell proliferation and apoptosis in gestational diabetes mellitus *via* targeting EZH2. *Mol Med Rep* (2020), 22(2):803–9. doi: 10.3892/mmr.2020.11142

56. Peña-Cano MI, Saucedo R, Morales-Avila E, Valencia J, Zavala-Moha JA, López A. Deregulated microRNAs and adiponectin in postmenopausal women with breast cancer. *Gynecol Obstet Invest* (2019) 84(4):369–77. doi: 10.1159/000496340

57. Hromadnikova I, Kotlabova K, Krofta L. First-trimester screening for fetal growth restriction and small-for-Gestational-Age pregnancies without preeclampsia using cardiovascular disease-associated MicroRNA biomarkers. *Biomedicines* (2022) 10(3):718. doi: 10.3390/biomedicines10030718

58. Muendlein A, Geiger K, Leiherer A, Saely CH, Fraunberger P, Drexel H. Evaluation of the associations between circulating microRNAs and kidney function in coronary angiography patients. *Am J Physiol Renal Physiol* (2020) 318(2):F315–21. doi: 10.1152/ajprenal.00429.2019

59. Lareyre F, Clément M, Moratal C, Loyer X, Jean-Baptiste E, Hassen-Khodja R, et al. Differential micro-RNA expression in diabetic patients with abdominal aortic aneurysm. *Biochimie* (2020), 162:1–7. doi: 10.1016/j.biochi.2019.03.012

60. Zhou J, Yang J, Wang X, Li M, Li F, Zhu E, et al. A novel regulatory circuit "C/EBPα/miR-20a-5p/TOB2" regulates adipogenesis and lipogenesis. *Front Endocrinol* (2020) 10:894. doi: 10.3389/fendo.2019.00894

61. Howe CG, Foley HB, Kennedy EM, Eckel SP, Chavez TA, Faham D, et al. Extracellular vesicle microRNA in early versus late pregnancy with birth outcomes in the MADRES study. *Epigenetics* (2022) 17(3):269–85. doi: 10.1080/15592294.2021.1899887

62. Filardi T, Catanzaro G, Grieco GE, Splendiani E, Trocchianesi S, Santangelo C, et al. Identification and validation of miR-222-3p and miR-409-3p as plasma biomarkers in gestational diabetes mellitus sharing validated target genes involved in metabolic homeostasis. *Int J Mol Sci* (2022) 23(8):4276. doi: 10.3390/ijms23084276

63. Goldsworthy M, Bai Y, Li CM, Ge H, Lamas E, Hilton H, et al. Haploinsufficiency of the insulin receptor in the presence of a splice-site mutation in ppp2r2a results in a novel digenic mouse model of type 2 diabetes. *Diabetes* (2016), 65(5):1434–46. doi: 10.2337/db15-1276

64. Villard A, Marchand L, Thivolet C, Rome S. Diagnostic value of cell-free circulating microRNAs for obesity and type 2 diabetes: A meta-analysis. *J Mol biomark Diagn* (2015) 6(6):251. doi: 10.4172/2155-9929.1000251

65. Yamaguchi S, Zhang D, Katayama A, Kurooka N, Sugawara R, Albuayjan HHH, et al. Adipocyte-specific inhibition of mir221/222 ameliorates diet-induced obesity through targeting ddit4. *Front Endocrinol* (2022) 12:750261. doi: 10.3389/fendo.2021.750261

66. de Mendonça M, de Sousa É, da Paixão AO, Araújo Dos Santos B, Roveratti Spagnol A, Murata GM, et al. MicroRNA miR-222 mediates pioglitazone beneficial effects on skeletal muscle of diet-induced obese mice. *Mol Cell Endocrinol* (2020) 501:110661. doi: 10.1016/j.mce.2019.110661

67. Langi G, Szczerbinski L, Kretowski A. Meta-analysis of differential miRNA expression after bariatric surgery. *J Clin Med* (2019), 8(8):1220. doi: 10.3390/jcm8081220

68. Hess AL, Larsen LH, Udesen PB, Sanz Y, Larsen TM, Dalgaard LT. Levels of circulating miR-122 are associated with weight loss and metabolic syndrome. *Obesity* (2020), 28(3):493–501. doi: 10.1002/oby.22704

69. Cheng S, Cui Y, Fan L, Mu X, Hua Y. T2DM inhibition of endothelial miR-342-3p facilitates angiogenic dysfunction *via* repression of FGF11 signaling. *Biochem Biophys Res Commun* (2018) 503(1):71–8. doi: 10.1016/j.bbrc.2018.05.179

70. Collares CV, Evangelista AF, Xavier DJ, Rassi DM, Arns T, Foss-Freitas MC, et al. Identifying common and specific microRNAs expressed in peripheral blood mononuclear cell of type 1, type 2, and gestational diabetes mellitus patients. *BMC Res Notes* (2013) 6:491. doi: 10.1186/1756-0500-6-491

71. Chartoumpekis DV, Zaravinos A, Ziros PG, Iskrenova RP, Psyrogiannis AI, Kyriazopoulou VE, et al. Differential expression of microRNAs in adipose tissue after long-term high-fat diet-induced obesity in mice. *PloS One* (2012) 7(4):e34872. doi: 10.1371/journal.pone.0034872

72. Wang L, Xu L, Xu M, Liu G, Xing J, Sun C, et al. Obesity-associated miR-342-3p promotes adipogenesis of mesenchymal stem cells by suppressing CtBP2 and releasing C/EBPα from CtBP2 binding. *Cell Physiol Biochem* (2015) 35 (6):2285–98. doi: 10.1159/000374032

73. Solís-Toro D, Mosquera Escudero M, García-Perdomo HA. Association between circulating microRNAs and the metabolic syndrome in adult populations: A systematic review. *Diabetes Metab Syndr* (2022) 16(1):102376. doi: 10.1016/j.dsx.2021.102376

74. Zhang D, Yamaguchi S, Zhang X, Yang B, Kurooka N, Sugawara R, et al. Upregulation of *mir342* in diet-induced obesity mouse and the hypothalamic appetite control. *Front Endocrinol* (2021) 12:727915. doi: 10.3389/fendo.2021.727915

75. Alimoradi N, Firouzabadi N, Fatehi R. Metformin and insulin-resistant related diseases: Emphasis on the role of microRNAs. *BioMed Pharmacother* (2021) 139:111662. doi: 10.1016/j.biopha.2021.111662

76. Mao Y, Mohan R, Zhang S, Tang X. MicroRNAs as pharmacological targets in diabetes. *Pharmacol Res* (2013) 75:37–47. doi: 10.1016/j.phrs.2013.06.005

77. Mononen N, Lyytikäinen LP, Seppälä I, Mishra PP, Juonala M, Waldenberger M, et al. Whole blood microRNA levels associate with glycemic status and correlate with target mRNAs in pathways important to type 2 diabetes. *Sci Rep* (2019) 9(1):8887. doi: 10.1038/s41598-019-43793-4

78. Pordzik J, Jakubik D, Jarosz-Popek J, Wicik Z, Eyileten C, De Rosa S, et al. Significance of circulating microRNAs in diabetes mellitus type 2 and platelet reactivity: bioinformatic analysis and review. *Cardiovasc Diabetol* (2019) 18:113. doi: 10.1186/s12933-019-0918-x

79. Karolina DS, Armugam A, Tavintharan S, Wong MT, Lim SC, Sum CF, et al. MicroRNA 144 impairs insulin signaling by inhibiting the expression of insulin receptor substrate 1 in type 2 diabetes mellitus. *PloS One* (2011) 6(8):e22839. doi: 10.1371/journal.pone.0022839

80. Wang J, Pan Y, Dai F, Wang F, Qiu H, Huang X. Serum miR-195-5p is upregulated in gestational diabetes mellitus. *J Clin Lab Anal* (2020) 34(8):e23325. doi: 10.1002/jcla.23325

frontiers | Frontiers in Endocrinology

TYPE Original Research
PUBLISHED 13 January 2023
DOI 10.3389/fendo.2022.1043543

OPEN ACCESS

EDITED BY
Carlos Guillén,
Complutense University, Spain

REVIEWED BY
Silvana Bordin,
University of São Paulo, Brazil
Laia Tolosa,
Instituto Investigación Sanitaria La Fe, Spain

*CORRESPONDENCE
Joana Paiva Miranda
jmiranda@ff.ulisboa.pt

SPECIALTY SECTION
This article was submitted to Diabetes: Molecular Mechanisms, a section of the journal Frontiers in Endocrinology

RECEIVED 13 September 2022
ACCEPTED 24 November 2022
PUBLISHED 13 January 2023

CITATION
Rodrigues JS, Faria-Pereira A, Camões SP, Serras AS, Morais VA, Ruas JL and Miranda JP (2023) Improving human mesenchymal stem cell-derived hepatic cell energy metabolism by manipulating glucose homeostasis and glucocorticoid signaling. *Front. Endocrinol.* 13:1043543. doi: 10.3389/fendo.2022.1043543

Improving human mesenchymal stem cell-derived hepatic cell energy metabolism by manipulating glucose homeostasis and glucocorticoid signaling

Joana Saraiva Rodrigues[1], Andreia Faria-Pereira[2], Sérgio Póvoas Camões[1], Ana Sofia Serras[1], Vanessa Alexandra Morais[2], Jorge Lira Ruas[3] and Joana Paiva Miranda[1*]

[1]Research Institute for Medicines (imed.ULisboa), Faculty of Pharmacy, Universidade de Lisboa, Lisbon, Portugal, [2]Instituto de Medicina Molecular João Lobo Antunes, Faculdade de Medicina, Universidade de Lisboa, Lisbon, Portugal, [3]Department of Physiology and Pharmacology, Biomedicum, Karolinska Institutet, Stockholm, Sweden

Introduction: The development of reliable hepatic *in vitro* models may provide insights into disease mechanisms, linking hepatocyte dysmetabolism and related pathologies. However, several of the existing models depend on using high concentrations of hepatocyte differentiation-promoting compounds, namely glucose, insulin, and dexamethasone, which is among the reasons that have hampered their use for modeling metabolism-related diseases. This work focused on modulating glucose homeostasis and glucocorticoid concentration to improve the suitability of a mesenchymal stem-cell (MSC)-derived hepatocyte-like cell (HLC) human model for studying hepatic insulin action and disease modeling.

Methods: We have investigated the role of insulin, glucose and dexamethasone on mitochondrial function, insulin signaling and carbohydrate metabolism, namely AKT phosphorylation, glycogen storage ability, glycolysis and gluconeogenesis, as well as fatty acid oxidation and bile acid metabolism gene expression in HLCs. In addition, we evaluated cell morphological features, albumin and urea production, the presence of hepatic-specific markers, biotransformation ability and mitochondrial function.

Results: Using glucose, insulin and dexamethasone levels close to physiological concentrations improved insulin responsiveness in HLCs, as demonstrated by AKT phosphorylation, upregulation of glycolysis and downregulation of *Irs2* and gluconeogenesis and fatty acid oxidation pathways. Ammonia detoxification, EROD and UGT activities and sensitivity to paracetamol cytotoxicity were also enhanced under more physiologically relevant conditions.

Conclusion: HLCs kept under reduced concentrations of glucose, insulin and dexamethasone presented an improved hepatic phenotype and insulin sensitivity demonstrating superior potential as an *in vitro* platform for modeling energy metabolism-related disorders, namely for the investigation of the insulin signaling pathway.

KEYWORDS

alternative hepatic *in vitro* models, mesenchymal stem cells, hepatocyte-like cells, insulin, glucose, dexamethasone, metabolism

Introduction

Obesity, considered a global epidemic and a major cause of death, is closely related to insulin resistance (IR) that may lead to non-alcoholic fatty liver disease (NAFLD) and type 2 diabetes (T2D). Playing a key role in the control of systemic glucose and lipid metabolism, the liver is a crucial insulin target organ. It is the main source of endogenous glucose, produced *via* gluconeogenesis, and thus has a key part in IR and associated disorders. Moreover, insulin has a direct action on the control of glucose metabolism in hepatocytes (1). Therefore, identifying the specific role of insulin on hepatocyte metabolism in physiological and in IR conditions is crucial to unravel the link between IR and related pathological conditions. However, for this field to progress there is a need for human-based physiologically relevant hepatic culture models that enable investigating insulin action in the hepatocyte and its role in metabolic homeostasis and disease progression.

The well-described drawbacks associated to the use of human primary hepatocytes (hpHeps) have promoted a growing interest within the scientific community for developing reliable human physiological hepatic models, namely by deriving hepatocyte-like cells (HLCs) from induced pluripotent stem cells (iPSCs), mesenchymal stem cells (MSCs) or other stem cells (2–6). In particular, our group has previously characterized and validated the use of MSC-derived HLCs, namely in comparison with other cell lines, which support the use of these HLCs for other applications, namely as an *in vitro* platform for disease modeling (4, 5). Still, a fully mature and stable hepatic phenotype has not been reached yet. Strategies to counteract the loss of hepatocyte function, viability and the differentiated phenotype in culture rely deeply on the use of differentiation-promoting compounds, such as glucose, dexamethasone and insulin (7–11).

Although it is appreciated that dexamethasone and other glucocorticoids can differentially regulate some drug-detoxifying enzymes, such as cytochrome P450 (CYP) enzymes, it is not clear what their role is in hepatic differentiation. In fact, dexamethasone selectively induces or inhibits some CYP isoforms while hyper- and hypo-glycemic conditions also cause differences in the functionality of different CYP isoforms (12–14). Moreover, the involvement of glucose or insulin in hepatic differentiation is also not fully understood, and the concentrations used are often far from human physiological values (within the millimolar range for glucose and nanomolar range for insulin). This ultimately interferes with energy homeostasis and eventually causes IR *in vitro*, compromising the use of these models for studying metabolic disease development or progression (13). As for the insulin signaling pathway in *in vitro* hepatic models, this remains largely uncharacterized. A recent study has directly compared insulin action in several hepatic cell lines, showing that none of them resemble pHeps in terms of energy metabolism (1). The authors attributed the inadequacy of the different cell lines for metabolism studies or disease modeling to defective levels of gluconeogenic enzymes and glucose production or insulin unresponsiveness.

Here, we investigated the effects of reducing insulin and dexamethasone levels in glucose metabolism, biotransformation ability, mitochondrial activity, as well as ammonia detoxification and albumin secretion. We further analyzed the expression of genes involved in glycolysis, gluconeogenesis, fatty acid (FA) and bile acid metabolism, and mitochondrial function and if it correlates with an improvement in the metabolic profile of cells.

Materials and methods

All culture media and supplements, solvents (all analytical grade) and other chemicals were acquired from Sigma-Aldrich (Madrid, Spain) unless specified.

Cell culture

The isolation of human neonatal mesenchymal stem cells (hnMSCs) was approved by the Ethics Committee of the Cascais Hospital Dr. José de Almeida. hnMSCs isolated from human umbilical cord stroma were fully characterized (15) and cultured as described by Santos et al. (16). For generating HLCs, a three-step differentiation protocol was applied to hnMSCs as detailed previously (4). From D21 onwards, HLCs seeded in collagen-

coated culture plates were maintained in one of four media formulations comprehending different glucose, insulin, and dexamethasone concentrations supplemented with 1% of DMSO, 8 ng/mL of oncostatin M (OSM), 1% of penicillin-streptomycin (PS) and 0.01% of amphotericin B (Ampho): (i) Diff, as detailed previously (4), with Iscove's modified Dulbecco's medium (IMDM) containing 25 mM of glucose, 1.72 µM of insulin and 1 µM of dexamethasone; (ii) Diff $^{-glu}$, with Dulbecco's modified Eagle's medium (DMEM), supplemented with L-glutamic acid, L-proline, HEPES and alanine to match IMDM concentrations, containing 5 mM of glucose, 1.72 µM of insulin and 1 µM of dexamethasone; (iii) Physiol $^{+glu}$, with IMDM supplemented with 1 nM of insulin, 100 nM of dexamethasone and 0.2% of bovine serum albumin (BSA); and (iv) Physiol, with DMEM supplemented with 1 nM of insulin, 100 nM of dexamethasone and 0.2% BSA (Table 1).

HepG2 cells (ATCC, MD, USA) and cryopreserved hpHeps (pool of 10 donors; Invitrogen, CA, USA) were cultured as described previously (4, 5).

Collagen coating

The protocol for rat-tail extraction was performed as described by Rajan et al. (17). The extracted rat-tail collagen was dissolved in 0.1% acetic acid to a stock concentration of 1 mg/mL. The stock solution was diluted in PBS to 0.2 mg/mL in a volume that assures total culture surface coverage. After 1h-incubation at 37 °C, cell culture surfaces were washed with PBS before inoculation. The differentiation process occurred using this collagen coating until D17 in T-flasks and onwards for cultures in well plates.

Urea and albumin production

Urea and albumin were quantified in cell culture supernatants using a colorimetric urea kit (QuantiChrom™ Urea Assay Kit, BioAssay Systems, Hayward, CA, USA) and an enzyme-linked immunosorbent assay (ELISA) kit (Bethyl Laboratories, Montgomery, TX, USA), respectively. The absorbance was measured at 520 nm for urea and 450 nm for albumin in a microplate reader (SPECTROStar Omega, BMG Labtech, Stuttgart, Germany), according to manufacturer's instructions. Data is presented as the rate of production: µg/10^6 cells.h (for urea) and pg/10^6 cells.h (for albumin).

TABLE 1 Concentrations of glucose, insulin and dexamethasone present in Diff and Physiol media.

	Diff	Physiol
Concentrations	25 mM of glucose 1.72 µM of insulin 1 µM of dexamethasone	5 mM of glucose 1 nM of insulin 100 nM of dexamethasone

Biotransformation activity

EROD assay covers CYP1A1 and CYP1A2 activity (12, 18–25). The protocol herein used was adapted from Donato et al. (26) and consisted in a 90-minute cell incubation with 8 µM of 7-ethoxyresorufin followed by a 2-hour enzymatic digestion with β-glucuronidase/arylsulfatase. The concentration of the product (7-hydroxyresorufin) was measured at an excitation wavelength of 530 nm and an emission of 590 nm.

UGTs' activity was determined by quantification of 4-methylumbelliferone (4-MU) before and after cell incubation to evaluate the extent of substrate conversion, as described by Miranda et al. (27, 28).

Protein quantification was performed as detailed in Cipriano et al. (4). EROD and UGT activities were normalized to incubation time (h) and cell number (10^6 cells).

Mitochondrial function

HLC mitochondrial function was assessed by direct measurement of the oxygen consumption rate (OCR) using extracellular flux analysis (XF24, Seahorse Biosciences, North Billerica, MA, USA). HLCs were inoculated in pre-coated Seahorse XF cell culture plates as described in section Cell culture' methods section. The Mitochondrial Stress Test assay was performed in XF Base medium (Agilent Technologies, Santa Clara, CA, USA) with 1 mM of pyruvate, 2 mM of L-glutamine (ThermoFisher Scientific, Waltham, MA, USA) and 10 mM of glucose. Baseline OCR were measured every 7 minutes. Following baseline measurements, oligomycin (1.5 µM), Carbonyl cyanide-4-(trifluoromethoxy)phenylhydrazone (FCCP) (1.25 µM), and rotenone (2 µM) and antimycin A (2 µM) were sequentially injected to measure OCR. From the obtained OCR profile, basal respiration, ATP production, maximal respiration and spare respiratory capacity could be calculated. Protein extraction from the HLCs was performed with RIPA lysis buffer supplemented with protease inhibitors 1x (Roche, Basel, Switzerland). Protein concentration (µg/µL) was determined using the bicinchoninic acid (BCA) protein assay kit (Pierce) according to manufacturer instructions. Mitochondrial function was normalized to the protein concentration (µg/µL) of each well.

HLC viability assessment upon paracetamol exposure

Paracetamol cytotoxicity was evaluated using the MTS reduction assay (Promega, Madison, WI, USA). At D34, cells were exposed to concentrations of paracetamol of 0, 5, 10, 15, 20, 25, 50 and 75 mM. Cell viability was measured upon a 24-hour incubation, according to manufacturer's instructions. IC_{50} was calculated with a nonlinear regression fit for the Log_{10}

transformation of the concentration values using GraphPad Prism (GraphPad Software, La Jolla, CA, USA). The percentage of viable cells was calculated relative to non-treated HLCs.

Periodic acid Schiff's staining

PAS staining was performed as described previously (4, 5). The wells were rinsed with distilled water and were observed under light microscope (Olympus CK30 inverted microscope, Tokyo, Japan).

Insulin stimuli

The hormone stimuli assays were performed at D34, exposing cells to 80 nM of insulin for 8 hours for gene expression analysis and for 30 minutes for AKT phosphorylation analysis. Before the insulin stimuli, cells culture medium was changed to starvation medium (DMEM, 1% of PS, 4 mM of glutamine, 1% of DMSO, 8 ng/mL of OSM and 0.2% of BSA), for an incubation period of 2 hours, to enhance the response to insulin incubation, as described in Correia et al. (29).

Gene expression

Total RNA of 6.0×10^5 cells was isolated using TRIzol (Life Technologies, Carlsbad, CA, USA) and extracted according to the manufacturer's instructions. RNA concentration was determined by measuring the absorbance at 260 nm using LVis plate mode (SPECTROstar Omega, BMG Labtech). cDNA was synthesized from 1 µg of RNA using NZY First-Strand cDNA Synthesis Kit (NZYTech, Lisbon, Portugal), according to the manufacturer's instructions. Quantitative real-time polymerase chain reaction (RT-qPCR) was performed using PowerUp SYBR Green Master Mix (Life Technologies) for a final reaction volume of 15 µL, using 2 µL of template cDNA and 0.333 µM of forward and reverse primers. Primer sequences are provided in Table 2. Reaction was performed on QuantStudio™ 7 Flex Real-Time PCR System (Applied Biosystems, Foster City, CA, USA) according to the described by Cipriano et al. (4, 5). The comparative Ct method ($2^{-\Delta\Delta Ct}$) was used to quantify gene expression, which was normalized to a reference gene (β-actin).

Western blot analysis

Western blot analysis was performed on HLC lysates. 30 µg of protein, quantified by Bradford protein assay kit according to manufacturer instructions, were separated by 12% SDS-PAGE and were transferred to PVDF membrane. Rabbit monoclonal antibody against human AKT (1:1000; Cell Signaling Technology, Danvers, MA, USA) and rabbit monoclonal antibody against human p-AKT (1:1000; Cell Signaling Technology) were used as primary antibodies. All blots were probed overnight at 4°C. Anti-rabbit horseradish peroxidase-conjugated antibody was used as secondary (1:20 000; Jackson ImmunoResearch, Ely, Cambridgeshire, UK). Immunoreacted proteins were detected by using Immobilon Western Blotting Kit (Merck Millipore, Burlington, MA, USA).

Statistical analysis

The results are presented as Average ± SEM unless stated otherwise. Data was analyzed with two-way ANOVA with

TABLE 2 Primers used for RT-qPCR characterization of HLCs, undifferentiated hnMSCs and hpHeps.

Gene	Forward sequence (5'-3')	Reverse sequence (5'-3')
β-actin	CATGTACGTTGCTATCCAGGC	CTCCTTAATGTCACGCACGAT
Ck-19	ATGGCCGAGCAGAACCGGAA	CCATGAGCCGCTGGTACTCC
Cyp3a4	ATTCAGCAAGAAGAACAAGGACA	TGGTGTTCTCAGGCACAGAT
Hnf-4a	ATTGACAACCTGTTGCAGGA	CGTTGGTTCCCATATGTTCC
Alb	TGCTTGAATGTGCTGATGACAGGG	AAGGCAAGTCAGCAGGCATCTCATC
Ck-18	TGGTACTCTCCTCAATCTGCTG	CTCTGGATTGACTGTGGAAGT
Pdk4	TCTGAGGCTGATGACTGGTG	GGAGGAAACAAGGGTTCACA
Pepck	GCTTTTCAGCATCTCCAAGGA	GCTTCAAGGCAAGGATCTCTC
G6pase	CAGAGCAATCACCACCAAGC	ACATTCATTCCTTCCTCCATCC
Ppara	CTGTCATTCAAGCCCATCTTC	TTATTTGCCACAACCCTTCC
Cpt1a	TCCAGTTGGCTTATCGTGGTG	TCCAGAGTCCGATTGATTTTTGC
Acox1	ACTCGCAGCCAGCGTTATG	AGGGTCAGCGATGCCAAAC
Fxr	AGAACCTGGAAGTGGAACC	CTCTGCTACCTCAGTTTCTCC
Ppargc1a	GCTGAAGAGGCAAGAGACAGA	AAGCACACACACCACACACA
Irs2	CGGTGAGTTCTACGGGTACAT	TCAGGGTGTATTCATCCAGCG

GraphPad Prism. A threshold of $p < 0.05$ was considered statistically significant.

Results

Reducing glucose, insulin and dexamethasone concentrations enhances the hepatic phenotype and biotransformation competence of HLCs

Ideally, *in vitro* hepatic models should retain most, if not all, of the characteristic biochemical machinery and molecular pathways that allow for a normal phenotype. We evaluated the effect of glucose, insulin and dexamethasone levels on HLC maturation by analyzing hepatic morphological features, albumin and urea production, as well as the presence of hepatic-specific markers and the biotransformation ability of HLCs at day 27 (D27) and day 34 (D34), corresponding to 1 and 2 weeks in culture post differentiation, respectively. As such, a comparative analysis of glucose, insulin and dexamethasone at physiological levels, corresponding to the plasmatic levels observed *in vivo* (Physiol), and the levels routinely used in hepatic *in vitro* cultures (Diff) (4) was performed to better understand their effect on hepatocyte biology and phenotype (Table 1). HepG2 and hpHeps and undifferentiated cells (hnMSCs) were used as positive and negative controls, respectively.

Under Physiol conditions, cells displayed a typical polygonal hepatocyte-like shape with one or more nuclei with prominent nucleoli in both days (Figure 1A). The expression levels of the hepatic-specific genes *Alb*, *Cyp3a4 and Hnf4a* in HLCs were higher in Diff ($p < 0.001$, $p < 0.001$ and $p < 0.01$, respectively) and in Physiol ($p < 0.01$, $p < 0.001$ and $p > 0.05$, respectively) at D34 relative to hnMSCs (Figure 1B). *Ck-18* expression, on the other hand, was similar to that of hnMSCs, whereas the cholangiocyte marker *Ck-19* was not detected in both media. These observations were further supported by identical albumin production in both conditions (Figure 2A) and higher levels of urea synthesis at D27 in HLCs maintained in Physiol when compared to Diff ($p < 0.05$) (Figure 2B). Curiously, overall, intermediate concentrations of glucose, dexamethasone and insulin (Diff $^{-glu}$ and Physiol $^{+glu}$) did not result in an improvement of the HLC phenotype when compared to Physiol (Supplementary Figures 1, 2).

The hepatic phenotype was further assessed by measuring phase I and II enzyme activity. EROD activity, covering CYP1A1 and CYP1A2 activity (12, 18–25), at D34, was higher in HLCs maintained in Physiol than cells in Diff ($p < 0.01$) and HepG2 ($p < 0.001$) (Figure 3A). Concerning phase II of biotransformation, UGT activity in HLCs kept in Physiol at D34 was superior to all other conditions, including hpHeps ($p < 0.001$) (Figure 3B). These results indicate that HLCs maintained in Physiol were metabolic competent, which was further confirmed by the cells' ability to metabolize the model drug, paracetamol (Figure 4). Cell viability was evaluated by MTS reduction assay and the IC_{50} for HLCs kept in Physiol and in Diff were 21.04 mM and 30.00 mM, respectively, suggesting that HLCs kept in Physiol were more sensitive to paracetamol exposure than in Diff.

HLCs cultured in a more physiological medium display increased ATP production and maximal mitochondrial functional capacity

To evaluate mitochondrial function in the different cells we used an extracellular flux analyzer (Seahorse XFp). Real time oxygen consumption rates (OCR) in hnMSCs and HLCs were measured using Seahorse XFp Cell Mito Stress Test (Figure 5A). Basal respiration (Figure 5B) shows the cellular energetic demands under baseline conditions. At D27, HLCs in both media displayed higher basal respiration, being significantly higher than in cells at the hepatoblast phase (D17) ($p < 0.01$) or undifferentiated ($p < 0.05$); whereas at D34 there was a decrease in basal respiration in both conditions (Diff, $p < 0.01$). ATP production (Figure 5C) refers to the reduction in OCR upon inhibition of ATP synthase activity. HLCs in Physiol at D27 had a significantly higher ATP production than cells at D17 and hnMSCs ($p < 0.001$ and $p < 0.05$, respectively). Maximal respiration (Figure 5D), on the other hand, demonstrates the maximum rate of respiration that the cell can achieve by stimulating the respiratory chain to operate at maximum capacity and it was significantly higher in HLCs in Physiol at D27 when compared to hnMSCs ($p < 0.01$) and cells at D17 ($p < 0.05$). Finally, spare respiration (Figure 5E) indicates cell fitness or flexibility to respond to an energetic demand as well as how closely the cell is to respire at its maximum capacity. Herein, HLCs in both Physiol and Diff at D27 displayed enhanced cell fitness when compared to undifferentiated cells ($p < 0.05$). Importantly, neither of the intermediate conditions tested presented improved mitochondrial activity when compared to Physiol (Supplementary Figure 4). These data support the higher differentiation degree of HLCs in Physiol throughout time, which is known to be associated with higher rates of mitochondria respiration when compared to undifferentiated cells.

HLCs under more physiological conditions display insulin-responsive glucose metabolism

To evaluate HLC insulin signaling we measured glycogen storage ability (Figure 6A), AKT phosphorylation (Figure 6B) and insulin receptor substrate 2 (*Irs2*) expression (Figure 6C). Moreover, the effects of insulin stimuli on the expression of genes involved in glycolysis (*Pdk4*), gluconeogenesis (*Pepck* and

10.3389/fendo.2022.1043543

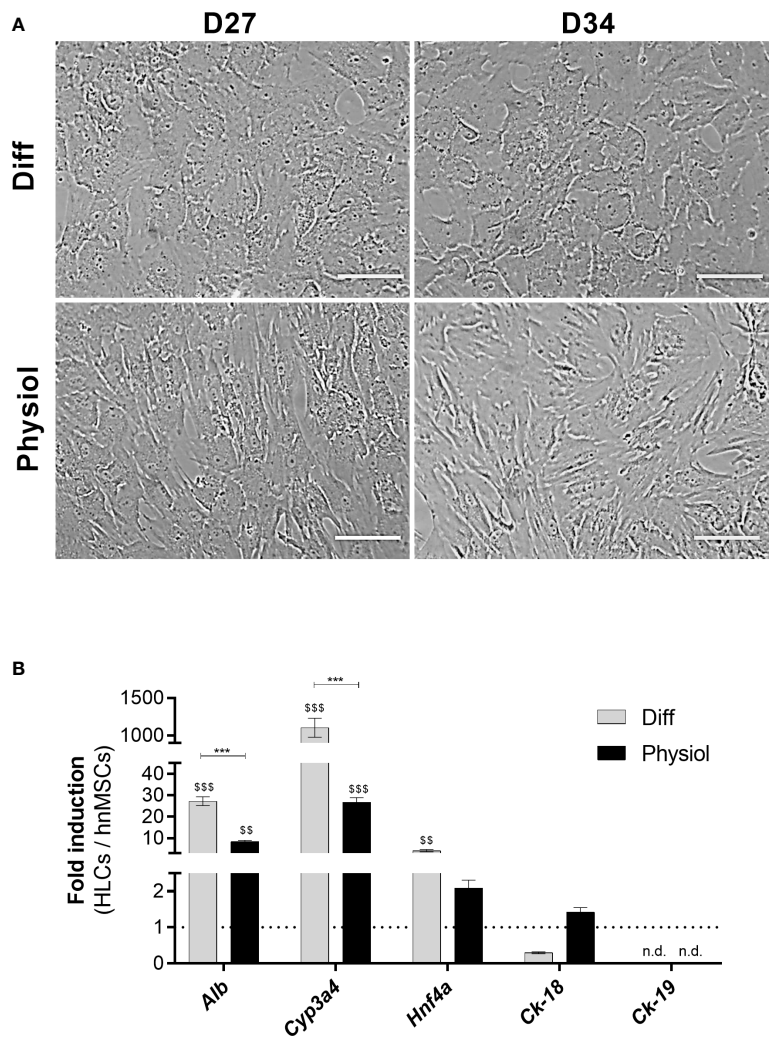

FIGURE 1
Physiol maintained the typical polygonal hepatocyte-like morphology and the induction of *Alb*, *Cyp3a4* and *Hnf4a* in HLCs. **(A)** Morphology in HLCs maintained in Diff and Physiol, at D27 and D34. Scale bar = 100 µm. **(B)** Hepatic-specific gene expression in HLCs at D34. Data are expressed as fold induction relative to hnMSCs and represented as Average ± SEM (n = 3-6). *** significantly differs from the other conditions with $p < 0.001$. $$ and $$$ significantly induced with $p < 0.01$ and $p < 0.001$, respectively (two-way ANOVA). D27, D34, day 27, day 34 of the differentiation protocol; HLCs, hepatocyte-like cells; hnMSCs, undifferentiated human neonatal mesenchymal stem cells; *Alb,* albumin; *Cyp3a4,* cytochrome P450, 3A4; *Hnf4a,* hepatocyte nuclear factor-4α; *Ck-18,* cytokeratin-18; *Ck-19,* cytokeratin-19; n.d., non-determined.

G6pase), FA oxidation (*Ppara*, *Cpt1a* and *Acox1*), bile acid metabolism (*Fxr*) and mitochondrial function (*Ppargc1a*) was also evaluated (Figure 6D).

All conditions displayed glycogen storage capacity (Figure 6A and Supplementary Figure 5). Most importantly, we could only observe insulin-stimulated AKT phosphorylation in HLCs kept in Physiol (Figure 6B). Moreover, upon insulin exposure, *Irs2* expression was downregulated in HLCs in Physiol (Figure 6C, $p < 0.001$). Likewise, HLCs in Physiol exposed to insulin presented a downregulation of *Pdk4*, *G6pase*, *Ppara*, *Cpt1a*, *Acox1*, *Fxr* and *Ppargc1a*, indicating an induction of glycolysis and bile acid metabolism (*Pdk4* and *Fxr* are negative regulators of these pathways, respectively) and inhibition of gluconeogenesis and FA oxidation (Figure 6D). *Ppargc1a* enhances the expression of genes related to mitochondrial function and induces gluconeogenesis and, herein, its downregulation also reinforces gluconeogenesis inhibition. On the other hand, upon insulin incubation, HLCs in Diff maintained the expression of *Pdk4* and *G6pase* and increased the expression of *Cpt1a*, *Acox1* and *Ppargc1a* which is associated to FA oxidation and mitochondrial function induction. Overall, our data suggest that HLCs in Physiol were more sensitive to insulin stimulation than hpHep.

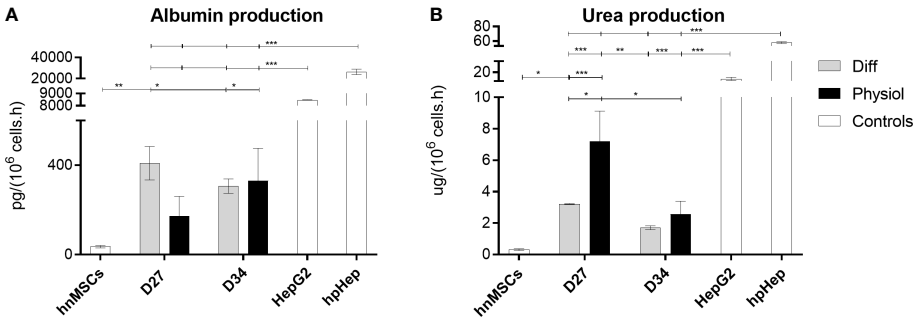

FIGURE 2
Albumin production was similar in both conditions while urea synthesis was improved with Physiol. Effect of Diff and Physiol and culture time on **(A)** albumin and **(B)** urea production. Data are represented as Average ± SEM (n = 3). Undifferentiated hnMSCs and HepG2 cell line and cryopreserved hpHeps are negative and positive controls, respectively (white bars). *, **, *** significantly differs from the other conditions with $p < 0.05$, $p < 0.01$ and $p < 0.001$, respectively (two-way ANOVA). hnMSC, undifferentiated human neonatal mesenchymal stem cells; hpHep, human primary hepatocytes; D27, D34, day 27, day 34 of the differentiation protocol.

Discussion

Stem-cell based hepatic *in vitro* models have demonstrated potential for studying and modeling metabolic-related diseases (30, 31). However, most hepatic differentiation protocols maintain differentiated HLCs in micromolar concentrations of insulin and dexamethasone and millimolar concentrations of glucose that reduce insulin sensitivity. Thus, this work focused on the modulation of insulin signaling and the metabolism of glucose and the synthetic glucocorticoid dexamethasone towards the development of a human-based hepatic *in vitro* model suitable for studying insulin signaling pathway.

As such, prior to the evaluation of the insulin-regulated metabolism, the MSC-derived HLC basal hepatic phenotype and functionality in more physiological concentrations of insulin, glucose and dexamethasone was compared to Diff (4), and the typical hepatic polygonal shape morphology, overexpression of hepatic-specific genes, albumin production and mitochondrial function confirmed.

As for hepatic specific genes, the expression of the hepatic marker, *Ck-18*, was detected in HLCs and in hnMSCs, possibly due to the presence of early endodermal markers in umbilical cord matrix-derived MSCs populations (32); whereas the cholangiocyte marker *Ck-19* was not expressed in HLCs in Physiol confirming the hepatocyte lineage commitment. Additionally, overexpression of *Alb* or *Hnf4a* in HLCs showed that the concentrations of glucose, insulin and dexamethasone

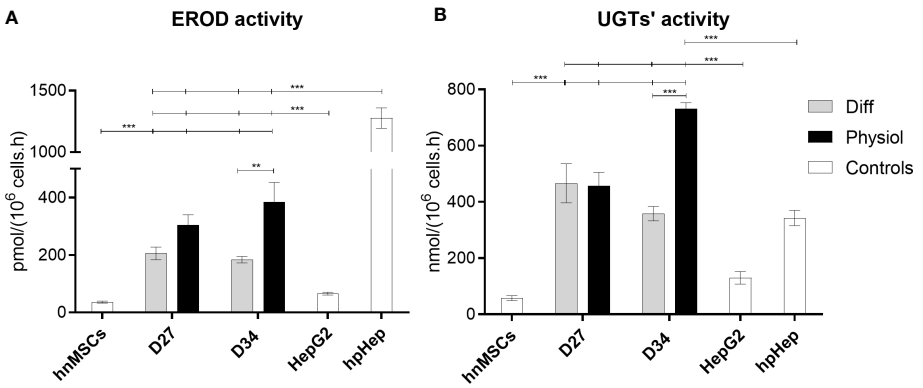

FIGURE 3
EROD and UGTs' activities were improved with Physiol. Effect of culture time and medium composition on **(A)** EROD (phase I) and **(B)** UGTs' (phase II) activities. Data are represented as Average ± SEM (n = 3-4). Undifferentiated hnMSCs and HepG2 cell line and cryopreserved hpHep are negative and positive controls, respectively (white bars). **, *** significantly differs from the other conditions with $p < 0.01$ and $p < 0.001$, respectively (two-way ANOVA). EROD, 7-ethoxyresorufin-O-deethylase; UGTs, uridine 5'-diphosphate glucuronosyltransferases; hnMSC, undifferentiated human neonatal mesenchymal stem cells; hpHep, human primary hepatocytes; D27, D34, day 27, day 34 of the differentiation protocol.

herein used maintained the HLC differentiated status without interfering with HLC viability and adherence, as previously demonstrated for human primary hepatocytes (8). Likewise, albumin production was similar in HLCs in both conditions, while Physiol could improve ammonia detoxification as demonstrated by urea production. It was previously reported that lower glucose concentrations result in higher urea production in HepG2-C3A (33) and in this work, we could also observe that media with lower glucose concentrations (Physiol and Diff $^{-glu}$) demonstrated the same trend (Supplementary Figure 2B). Moreover, glucagon was shown to increase urea production in hpHeps (34). Since glucagon and insulin are antagonistic hormones, media with lower insulin concentrations may have a positive impact in HLC ammonia detoxification.

As for the biotransformation ability, *Cyp3a4* expression level of HLCs was increased in all Diff conditions when compared to Physiol (Physiol and Physiol $^{+glu}$), which may be a consequence of the higher concentrations of dexamethasone in Diff media, a known CYP3A4 inducer (Supplementary Figure 1B) (35). In addition, phase I and phase II activities were evaluated through EROD (CYP1A1/2) and UGT assays, respectively. In Physiol, both activities were enhanced, further supporting the improvement of HLC hepatic features under these conditions. This is in accordance with previous observations showing that dexamethasone decreases CYP1A1 and CYP1A2 activity in hpHeps (12). Herein, glucose may also have negatively regulated EROD activity, given that at D34, EROD activity in HLCs kept in low glucose levels (Physiol and Diff $^{-glu}$) was higher than HLCs in Physiol $^{+glu}$ and Diff (media with 25 mM of glucose), as seen in Figure 3A and Supplementary Figure 3A. Indeed, Davidson et al. reported that hypoglycemic conditions (~0.4 – 0.5 mM of glucose) significantly increased the expression of *Cyp1a2*, as compared to a normoglycemic control (~5 mM)

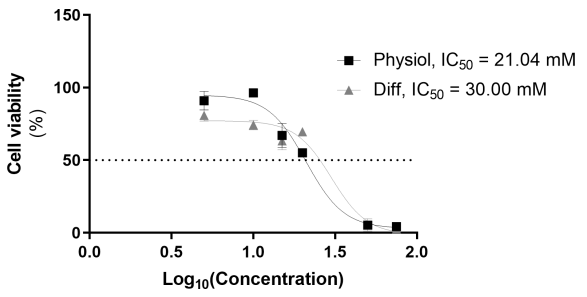

FIGURE 4
HLCs in Physiol presented higher sensitivity to paracetamol-induced cytotoxicity. Comparison of paracetamol cytotoxicity in HLCs maintained in Diff and Physiol at D34 evaluated by MTS mitochondrial activity assay. HLCs were incubated with 0, 5, 10, 15, 20, 50 and 75 mM of paracetamol. The percentage of viable cells is calculated relative to non-treated HLCs (mean ± SEM) (n = 3).

(14). Interestingly, in our protocol, cells maintained in lower glucose concentrations also showed higher CYP1A1/2 activities.

To further validate the usefulness of our model for hepatotoxicity studies, HLCs were exposed to paracetamol, a drug known to cause hepatotoxicity in overdose (36–38) and whose toxicity is dependent on phase I and II metabolism. At high-dose paracetamol exposure, the metabolic pathway switches from the detoxifying phase II metabolism to phase I metabolism, generating the toxic intermediate *N*-acetyl-*p*-benzoquinone imine (NAPQI). Paracetamol is mainly metabolized through conjugation with sulphate and glucuronic acid and, to a lesser extent, through oxidation by CY2E1, CYP1A2 and CYP3A4 (36). Accordingly, cell viability upon paracetamol exposure was assessed as an indirect measure of HLC metabolic competence. Indeed, the higher paracetamol cytotoxicity observed in Physiol is an indicator of higher biotransformation ability. Our results demonstrate that decreased concentrations of insulin, glucose and dexamethasone improved the sensitivity of HLCs to paracetamol toxicity, suggesting a higher phase I activity, in accordance with EROD activity results, and consequently higher formation of the toxic metabolite NAPQI. Moreover, changes in the metabolic cell status can result in different drug efficacy and safety. Therefore, the observed differences between Diff and Physiol in drug metabolism suggest that our HLC model could be able to recapitulate differences in CYP450 activities observed in numerous metabolic pathologies, namely NAFLD (39, 40).

Insulin regulates glucose and lipid metabolism in hepatocytes and mitochondria are the central hub for controlling metabolic homeostasis and energy production. Disturbances in mitochondrial function mediate hepatocyte injury, affect cell viability, and are associated with NAFLD, drug-induced hepatotoxicity, and cholestasis (37, 41). Herein, Physiol maintained HLC mitochondrial functionality under basal conditions, as well as the mitochondrial contribution for ATP production, flexibility to respond to energetic demands and the maximum operation capacity when compared to Diff. These results can also confirm that Physiol could maintain the hepatic differentiation degree as it was reported that glycolysis is the main provider of ATP in stem cells while mitochondrial oxidative phosphorylation is the most predominant source of ATP in differentiated cells (42).

Finally, carbohydrate metabolism and insulin signaling were specifically assessed in HLCs as the liver regulates blood glucose levels through glycogen synthesis and gluconeogenesis. Upon insulin binding to the insulin receptor, there is a cascade of phosphorylation of downstream enzymes: insulin receptor substrate proteins, PI3K and AKT. AKT phosphorylation is an important event in the insulin transduction pathway as it will then mediate the effects of insulin on glucose, glycogen, protein and lipid metabolism (43). Herein, HLCs were indeed able to form glycogen stores in both conditions. Moreover, in response to insulin exposure, only HLCs in Physiol exhibited AKT

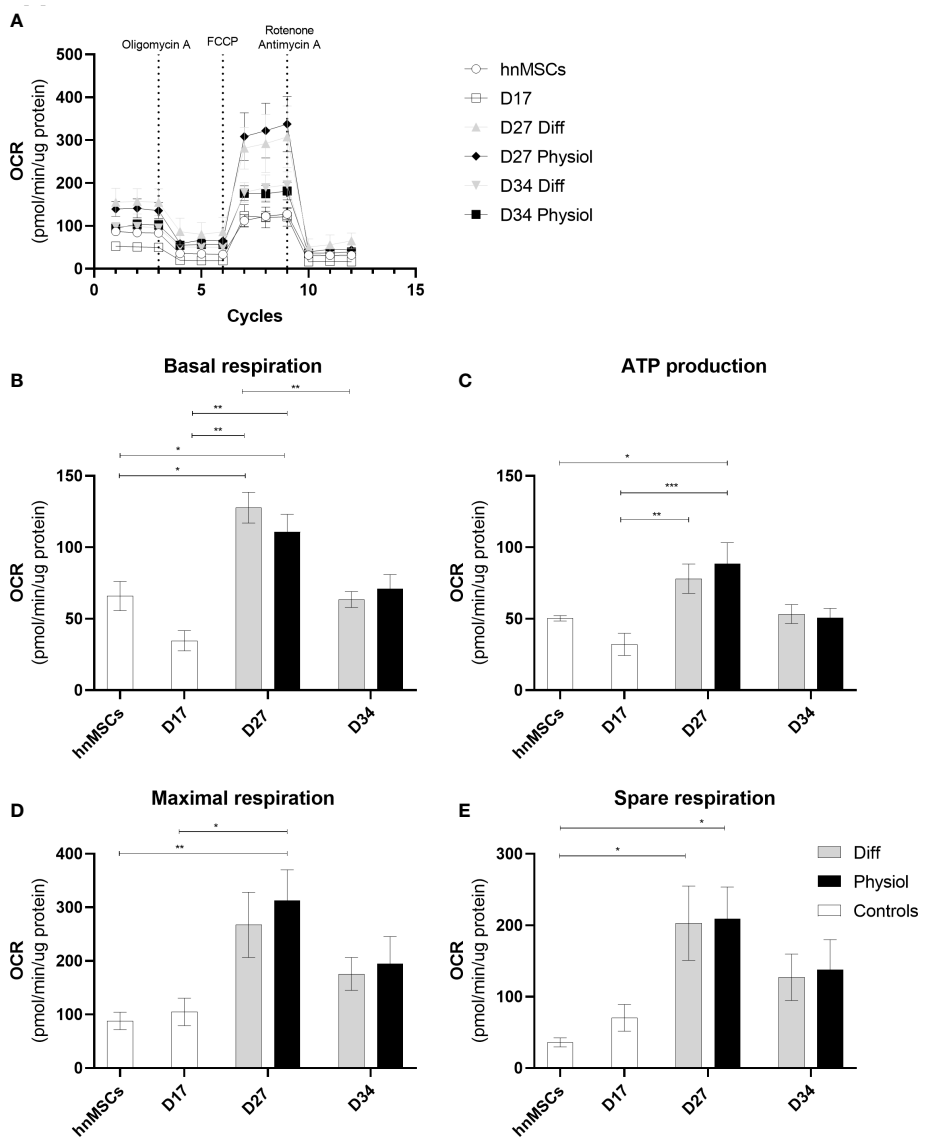

FIGURE 5
Physiol maintained HLC mitochondrial function. Evaluation of mitochondrial function by directly measuring the OCR of cells at different stages of differentiation and exposed to different media. **(A)** OCR in the presence of 1.5 µM of oligomycin, 1.25 µM of FCCP, 2 µM of antimycin and 2 µM of rotenone. **(B)** Basal respiration. **(C)** ATP production. **(D)** Maximal respiration. **(E)** Spare respiration. Data are represented as Average ± SEM (n = 3-5). *, **, *** significantly differs from the other conditions with $p < 0.05$, $p < 0.01$ and $p < 0.001$, respectively (two-way ANOVA). hnMSC, undifferentiated human neonatal mesenchymal stem cells; OCR, oxygen consumption rate; D17, D27, D34, day 17, day 27, day 34 of the differentiation protocol.

phosphorylation. The absence of AKT phosphorylation in HLCs in Diff, a signal of insulin resistance development, may be related to the chronic exposure to high insulin concentrations (1.72 µM), as previously reported (44, 45). IRS2 plays a major role in hepatic energy homeostasis in fasting conditions, mediating insulin effects through the AKT cascade. *Irs2* expression increases in the fasting state and immediately decreases after food intake which is accompanied by an increase in insulin blood levels (46). Accordingly, after subjecting HLCs to fasting and subsequent exposure to insulin, only HLCs in Physiol presented a downregulation of *Irs2* as previously described (46–48). In particular, under non-pathological conditions, insulin will induce glycolysis and lipid synthesis while inhibiting gluconeogenesis and FA oxidation (49). Accordingly, a RT-qPCR analysis showed that HLCs, maintained under lower concentrations of insulin, dexamethasone and glucose throughout the maturation phase (Physiol), were more sensitive to insulin stimuli, upregulating

10.3389/fendo.2022.1043543

glycolysis and bile acid metabolism and downregulating gluconeogenesis, FA oxidation and mitochondrial function-related pathways as observed *in vivo*. On the other hand, HLCs maintained in higher and non-physiological concentrations of insulin, dexamethasone and glucose (Diff) were not responsive to insulin insult, keeping the expression of genes involved in glycolysis and gluconeogenesis while FA oxidation is induced. Therefore, lower concentrations of those supplements are best suited for maintaining cells for energy metabolism regulation studies by maintaining insulin responsiveness.

Importantly, the activation of glycolysis and bile acid synthesis along with the inhibition of gluconeogenesis and FA oxidation accompanied by increased biotransformation activity are zonation features characteristic of perivenous hepatocytes (50). Therefore, overall, these results may suggest the modulation of HLCs towards a perivenous-like phenotype, important when studying metabolic diseases. NAFLD, in particular, has a perivenous predominance due to reduced FA oxidation gene expression that will lead to faster lipid accumulation in this region (51). In particular, we observe that our HLC model displays glycogen storage capacity and modulates gluconeogenic gene expression, which was a limitation found by Nagarajan and colleagues in different hepatocyte lines (1).

Moreover, in contrast, to other works that use FBS, insulin at micromolar concentrations, glucose concentrations above 10 mM and dexamethasone concentrations superior to 100 nM, which may affect insulin action (30, 31, 52–54), the model herein developed represents a more physiological system that can be

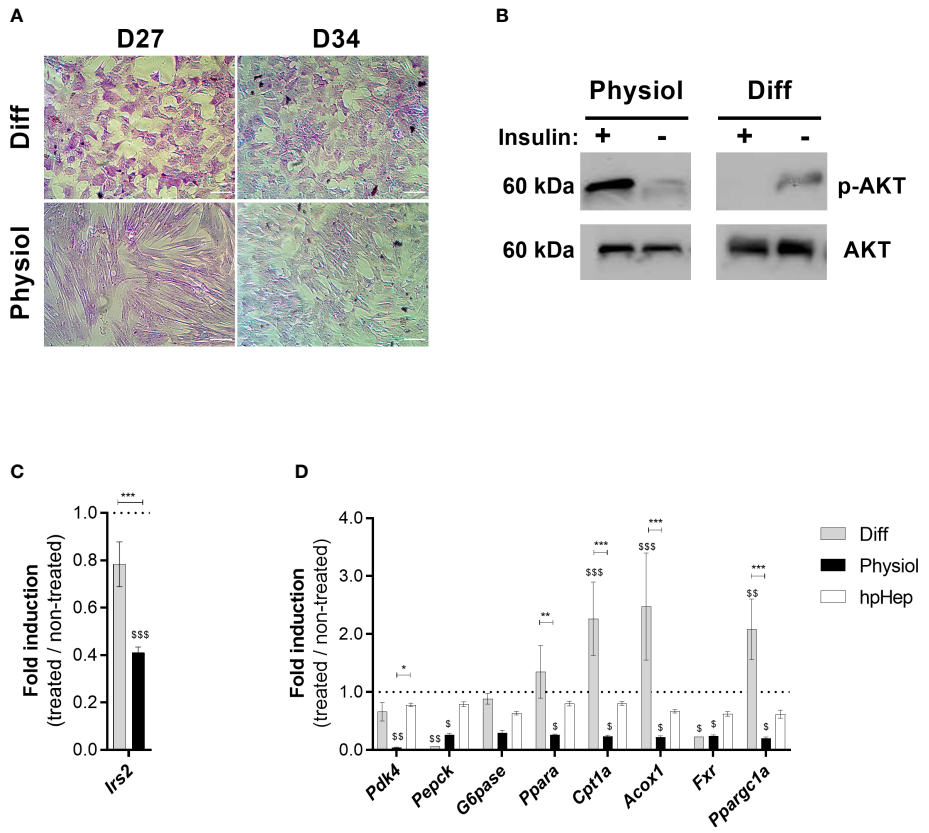

FIGURE 6
Physiol maintained glycogen storage ability and improved HLC responsiveness to insulin stimuli. **(A)** Glycogen storage ability evaluated by PAS staining at D27 and D34. Scale bar = 100 µm. **(B)** AKT phosphorylation confirmed in HLCs kept in Physiol in response to insulin by Western Blot analysis. **(C)** Effect of insulin in *Irs2* expression in HLCs subjected to fasting, evaluated by RT-qPCR. **(D)** Effect of insulin in HLC gene expression. Genes involved in glycolysis (*Pdk4*), gluconeogenesis (*Pepck* and *G6pase*), fatty acid oxidation (*Ppara*, *Cpt1a* and *Acox1*), bile acid metabolism (*Fxr*) and mitochondrial function (*Ppargc1a*) were evaluated by RT-qPCR. RT- qPCR data are expressed as fold induction relative to non-treated cells (n = 3-6). *, **, *** significantly differs from the other conditions with $p < 0.05$, $p < 0.01$ and $p < 0.001$, respectively. $, $$ and $$$ significantly induced or repressed with $p < 0.05$, $p < 0.01$ and $p < 0.001$, respectively (two-way ANOVA). hpHep, human cryopreserved hepatocytes; *Pdk4*, pyruvate dehydrogenase kinase 4; *Pepck* phosphoenolpyruvate carboxylase; *G6pase*, glucose-6-phosphatase; *Ppara*, peroxisome proliferator-activated receptor α; *Cpt1a*, carnitine palmitoyltransferase 1α; *Acox1*, acyl-CoA oxidase 1; *Fxr*, Farnesoid X receptor; *Ppargc1a*, peroxisome proliferator-activated receptor γ coactivator 1-α; *Irs2*, insulin receptor substrate 2.

used in the future to induce NAFLD and study disease mechanisms. Indeed, to our knowledge, it is shown for the first time the AKT phosphorylation, downregulation of *Irs2* and of genes related to glucose and lipid metabolism upon insulin exposure in a HLCs *in vitro* model.

In sum, our data reveal that more physiological levels of insulin, glucose and dexamethasone regulate insulin signaling and energy metabolism in HLCs as it improves insulin sensitivity along with ammonia detoxification, biotransformation activity and mitochondrial function while retaining albumin production and overexpression of hepatic-specific genes. Therefore, manipulating glucose homeostasis and glucocorticoid concentration can be a strategy for developing relevant hepatic *in vitro* models for drug metabolism studies, hepatotoxicity assessment and disease modeling of energy metabolism-related disorders.

Data availability statement

The original contributions presented in the study are included in the article/Supplementary Material. Further inquiries can be directed to the corresponding author.

Author contributions

JM, JRu and VM developed the study concept and the study design. JRo, AF-P, SC and AS performed the experiments and data collection. JRo and AF-P performed the data analysis and interpretation under the supervision of JM and VM. JM and JRo drafted the manuscript. JRu and VM provided critical revisions. All authors contributed to the article and approved the submitted version.

Funding

The work was financially supported by Fundação para a Ciência e a Tecnologia (FCT) through SFRH/BD/144130/2019 to JRo; PD/BD/114113/2015 and IMM/BI/76-2019 to AF-P; IF/01693/2014 and IMM/CT/27-2020 to VM; PTDC/MED-TOX/29183/2017; UIDB/04138/2020; UIDP/04138/2020 and PTDC/BIACEL/31230/2017. This project has received funding from the European Horizon´s research and innovation programme HORIZON-HLTH-2022-STAYHLTH-02 under agreement No 101095679; from the European Molecular Biology Organization (EMBO-IG#3309); and was also supported by COST actions CA17112, CA20121 and CA20140.

Conflict of interest

The authors declare that the research was conducted in the absence of any commercial or financial relationships that could be construed as a potential conflict of interest.

Publisher's note

Supplementary material

The Supplementary Material for this article can be found online at: https://www.frontiersin.org/articles/10.3389/fendo.2022.1043543/full#supplementary-material

References

1. Nagarajan SR, Paul-Heng M, Krycer JR, Fazakerley DJ, Sharland AF, Hoy XAJ. Lipid and glucose metabolism in hepatocyte cell lines and primary mouse hepatocytes: A comprehensive resource for *in vitro* studies of hepatic metabolism. *Am J Physiol - Endocrinol Metab* (2019) 316(4):E578–89. doi: 10.1152/ajpendo.00365.2018

2. Afshari A, Shamdani S, Uzan G, Naserian S, Azarpira N. Different approaches for transformation of mesenchymal stem cells into hepatocyte-like cells. *Stem Cell Res Ther* (2020) 11(1):1–14. doi: 10.1186/s13287-020-1555-8

3. Chen C, Soto-Gutierrez A, Baptista PM, Spee B. Biotechnology challenges to *In vitro* maturation of hepatic stem cells. *Gastroenterology* (2018) 154(5):1258–72. doi: 10.1053/j.gastro.2018.01.066

4. Cipriano M, Correia JC, Camões SP, Oliveira NG, Cruz P, Cruz H, et al. The role of epigenetic modifiers in extended cultures of functional hepatocyte-like cells derived from human neonatal mesenchymal stem cells. *Arch Toxicol* (2017) 91(6):2469–89. doi: 10.1007/s00204-016-1901-x

5. Cipriano M, Freyer N, Knöspel F, Oliveira NG, Barcia R, Cruz PE, et al. Self-assembled 3D spheroids and hollow-fibre bioreactors improve MSC-derived hepatocyte-like cell maturation *In vitro*. *Arch Toxicol* (2017) 91(4):1815–32. doi: 10.1007/s00204-016-1838-0

6. Cipriano M, Pinheiro PF, Sequeira CO, Rodrigues JS, Oliveira NG, Antunes AMM, et al. Nevirapine biotransformation insights: An integrated *in vitro* approach unveils the biocompetence and glutathiolomic profile of a human hepatocyte-like cell 3D model. *Int J Mol Sci* (2020) 21(11):1–18. doi: 10.3390/ijms21113998

7. Fraczek J, Bolleyn J, Vanhaecke T, Rogiers V, Vinken M. Primary hepatocyte cultures for pharmaco-toxicological studies: At the busy crossroad of various anti-dedifferentiation strategies. *Arch Toxicol* (2013) Vol. 87:577–610 p. doi: 10.1007/s00204-012-0983-3

8. Damm G, Schicht G, Zimmermann A, Rennert C, Fischer N, Kießig M, et al. Effect of glucose and insulin supplementation on the isolation of primary human hepatocytes. *EXCLI J* (2019) 18:1071–91. doi: 10.17179/excli2019-1782

9. Takayama K, Inamura M, Kawabata K, Katayama K, Higuchi M, Tashiro K, et al. Efficient generation of functional hepatocytes from human embryonic stem cells and induced pluripotent stem cells by HNF4α transduction. *Mol Ther* (2012) 20(1):127–37. doi: 10.1038/mt.2011.234

10. Campard D, Lysy PA, Najimi M, Sokal EM. Native umbilical cord matrix stem cells express hepatic markers and differentiate into hepatocyte-like cells. *Gastroenterology* (2008) 134(3):833–48. doi: 10.1053/j.gastro.2007.12.024

11. Snykers S, Vanhaecke T, Papeleu P, Luttun A, Jiang Y, Vander Heyden Y, et al. Sequential exposure to cytokines reflecting embryogenesis: The key for *in vitro* differentiation of adult bone marrow stem cells into functional hepatocyte-like cells. *Toxicol Sci* (2006) 94(2):330–41. doi: 10.1093/toxsci/kfl058

12. Vrzal R, Stejskalova L, Monostory K, Maurel P, Bachleda P, Pavek P, et al. Dexamethasone controls aryl hydrocarbon receptor (AhR)-mediated CYP1A1 and CYP1A2 expression and activity in primary cultures of human hepatocytes. *Chem Biol Interact* (2009) 179(2–3):288–96. doi: 10.1016/j.cbi.2008.10.035

13. Ferris HA, Kahn CR, Barnes P, Cristancho A, Lazar M, Biddinger S, et al. New mechanisms of glucocorticoid-induced insulin resistance: make no bones about it. *J Clin Invest.* (2012) 122(11):3854–7. doi: 10.1172/JCI66180

14. Davidson MD, Ballinger KR, Khetani SR. Long-term exposure to abnormal glucose levels alters drug metabolism pathways and insulin sensitivity in primary human hepatocytes. *Sci Rep* (2016) 6:1–11. doi: 10.1038/srep28178

15. Martins JP, Santos JM, De AJM, MA F, De Almeida MVT, Almeida SCP, et al. Towards an advanced therapy medicinal product based on mesenchymal stromal cells isolated from the umbilical cord tissue: Quality and safety data. *Stem Cell Res Ther* (2014) 5(1):1–15. doi: 10.1186/scrt398

16. Santos JM, Camões SP, Filipe E, Cipriano M, Barcia RN, Filipe M, et al. Three-dimensional spheroid cell culture of umbilical cord tissue-derived mesenchymal stromal cells leads to enhanced paracrine induction of wound healing. *Stem Cell Res Ther* (2015) 6(1):90. doi: 10.1186/s13287-015-0082-5

17. Rajan N, Habermehl J, Coté MF, Doillon CJ, Mantovani D. Preparation of ready-to-use, storable and reconstituted type I collagen from rat tail tendon for tissue engineering applications. *Nat Protoc* (2007) 1(6):2753–8. doi: 10.1038/nprot.2006.430

18. Wilkening S, Stahl F, Bader A. Comparison of primary human hepatocytes and hepatoma cell line HepG2 with regard to their biotransformation properties. *Drug Metab Dispos* (2003) 31(8):1035–42. doi: 10.1124/dmd.31.8.1035

19. Chiarolini A, Donato MT, Gómez-Lechón MJ, Pala M, Valerio F, Ferro M. Comparison of rat hepatocyte and differentiated hepatoma cell line cultures as bio-indicators of CYP 1A1 inducers in urban air. *Biomarkers* (1997) 2(5):279–85. doi: 10.1080/135475097231508

20. Ács A, Liang X, Bock I, Griffitts J, Ivánovics B, Vásárhelyi E, et al. Chronic effects of carbamazepine, progesterone and their mixtures at environmentally relevant concentrations on biochemical markers of zebrafish (Danio rerio). *Antioxidants* (2022) 11(9):1776. doi: 10.3390/antiox11091776

21. Jönsson EM, Abrahamson A, Brunström B, Brandt I. Cytochrome P4501A induction in rainbow trout gills and liver following exposure to waterborne indigo, benzo[a]pyrene and 3,3′,4,4′,5-pentachlorobiphenyl. *Aquat Toxicol* (2006) 79 (3):226–32. doi: 10.1016/j.aquatox.2006.06.006

22. Monostory K, Kohalmy K, Prough RA, Kóbori L, Vereczkey L. The effect of synthetic glucocorticoid, dexamethasone on CYP1A1 inducibility in adult rat and human hepatocytes. *FEBS Lett* (2005) 579(1):229–35. doi: 10.1016/j.febslet.2004.11.080

23. Vieira Silva A, Chu I, Feeley M, Bergman, Håkansson H, Öberg M. Dose-dependent toxicological effects in rats following a 90-day dietary exposure to PCB-156 include retinoid disruption. *Reprod Toxicol* (2022) 107:123–39. doi: 10.1016/j.reprotox.2021.09.012

24. Bhandari RNB, Riccalton LA, Lewis AL, Fry JR, Hammond AH, Tendler SJB, et al. Liver tissue engineering: A role for co-culture systems in modifying hepatocyte function and viability. *Tissue Eng* (2001) 7(3):345–57. doi: 10.1089/10763270152044206

25. Ringel M, Von Mach MA, Santos R, Feilen PJ, Brulport M, Hermes M, et al. Hepatocytes cultured in alginate microspheres: An optimized technique to study enzyme induction. *Toxicology* (2005) 206(1):153–67. doi: 10.1016/j.tox.2004.07.017

26. Donato MT, Gómez-Lechón MJ, Castell JV. A microassay for measuring cytochrome P450IA1 and P450IIB1 activities in intact human and rat hepatocytes cultured on 96-well plates. *Anal Biochem* (1993) 213(1):29–33. doi: 10.1006/abio.1993.1381

27. Miranda JP, Rodrigues A, Tostões RM, Leite S, Zimmerman H, Carrondo MJT, et al. Extending hepatocyte functionality for drug-testing applications using high-viscosity alginate–encapsulated three-dimensional cultures in bioreactors. *Tissue Eng Part C Methods* (2010) 16(6):1223–32. doi: 10.1089/ten.tec.2009.0784

28. Gomez-Lechon MJ, Donato MT, Ponsoda X, Fabra R, Trullenque R, Castell J. Isolation, culture and use of human hepatocytes in drug research. In: Castell JV, Gómez-Lenchón MJ, editors. *In vitro methods in pharmaceutical research*. California, USA: Academic Press (1997). p. 368.

29. Correia JC, Massart J, de Boer JF, Porsmyr-Palmertz M, Martínez-Redondo V, Agudelo LZ, et al. Bioenergetic cues shift FXR splicing towards FXRα2 to modulate hepatic lipolysis and fatty acid metabolism. *Mol Metab* (2015) 4(12):891–902. doi: 10.1016/j.molmet.2015.09.005

30. Gurevich I, Burton SA, Munn C, Ohshima M, Goedland ME, Czysz K, et al. iPSC-derived hepatocytes generated from NASH donors provide a valuable platform for disease modeling and drug discovery. *Biol Open* (2020) 9(12):1–9. doi: 10.1242/bio.055087

31. Collin de l'Hortet A, Takeishi K, Guzman-Lepe J, Morita K, Achreja A, Popovic B, et al. Generation of human fatty livers using custom-engineered induced pluripotent stem cells with modifiable SIRT1 metabolism. *Cell Metab* (2019) 30(2):385–401.e9. doi: 10.1016/j.cmet.2019.06.017

32. La Rocca G, Anzalone R, Corrao S, Magno F, Loria T, Lo Iacono M, et al. Isolation and characterization of Oct-4+/HLA-G+ mesenchymal stem cells from human umbilical cord matrix: Differentiation potential and detection of new markers. *Histochem Cell Biol* (2009) 131(2):267–82. doi: 10.1007/s00418-008-0519-3

33. Iyer VV, Yang H, Ierapetritou MG, Roth CM. Effects of glucose and insulin on HepG2-C3A cell metabolism. *Biotechnol Bioeng* (2010) 107(2):347–56. doi: 10.1002/bit.22799

34. Winther-Sørensen M, Galsgaard KD, Santos A, Trammell SAJ, Sulek K, Kuhre RE, et al. Glucagon acutely regulates hepatic amino acid catabolism and the effect may be disturbed by steatosis. *Mol Metab* (2020) 42:101080. doi: 10.1016/j.molmet.2020.101080

35. Pascussi JM, Drocourt L, Gerbal-Chaloin S, Fabre JM, Maurel P, Vilarem MJ. Dual effect of dexamethasone on CYP3A4 gene expression in human hepatocytes. sequential role of glucocorticoid receptor and pregnane X receptor. *Eur J Biochem* (2001) 268(24):6346–58. doi: 10.1046/j.0014-2956.2001.02540.x

36. Athersuch TJ, Antoine DJ, Boobis AR, Coen M, Daly AK, Possamai L, et al. Paracetamol metabolism, hepatotoxicity, biomarkers and therapeutic interventions: A perspective. *Toxicol Res (Camb).* (2018) 7(3):347–57. doi: 10.1039/c7tx00340d

37. Serras AS, Rodrigues JS, Cipriano M, Rodrigues AV, Oliveira NG, Miranda JP. A critical perspective on 3D liver models for drug metabolism and toxicology studies. *Front Cell Dev Biol* (2021) 203. doi: 10.3389/fcell.2021.626805

38. Anundi I, Lähteenmäki T, Rundgren M, Moldeus P, Lindros KO. Zonation of acetaminophen metabolism and cytochrome P450 2E1-mediated toxicity studied in isolated periportal and perivenous hepatocytes. *Biochem Pharmacol* (1993) 45(6):1251–9. doi: 10.1016/0006-2952(93)90277-4

39. Chalasani N, Christopher Gorski J, Asghar MS, Asghar A, Foresman B, Hall SD, et al. Hepatic cytochrome P450 2E1 activity in nondiabetic patients with nonalcoholic steatohepatitis. *Hepatology* (2003) 37(3):544–50. doi: 10.1053/jhep.2003.50095

40. Donato MT, Jiménez N, Serralta A, Mir J, Castell JV, Gómez-Lechón MJ. Effects of steatosis on drug-metabolizing capability of primary human hepatocytes. *Toxicol Vitr.* (2007) 21(2):271–6. doi: 10.1016/j.tiv.2006.07.008

41. Grattagliano I, Russmann S, Diogo C, Bonfrate L, J. Oliveira P, Q.-H. Wang D, et al. Mitochondria in chronic liver disease. *Curr Drug Targets.* (2011) 12 (6):879–93. doi: 10.2174/138945011795528877

42. Hopkinson BM, Desler C, Kalisz M, Vestentoft PS, Juel Rasmussen L, Bisgaard HC. Bioenergetic changes during differentiation of human embryonic stem cells along the hepatic lineage. *Oxid Med Cell Longev* (2017) 2017:1–11. doi: 10.1155/2017/5080128

43. Haeusler RA, McGraw TE, Accili D. Metabolic signalling: Biochemical and cellular properties of insulin receptor signalling. *Nat Rev Mol Cell Biol* (2018) 19 (1):31–44. doi: 10.1038/nrm.2017.89

44. Ning J, Hong T, Yang X, Mei S, Liu Z, Liu H-Y, et al. Insulin and insulin signaling play a critical role in fat induction of insulin resistance in mouse. *Am J Physiol Metab* (2011) 301(2):E391–401. doi: 10.1152/ajpendo.00164.2011

45. Kearney AL, Norris DM, Ghomlaghi M, Wong MKL, Humphrey SJ, Carroll L, et al. Akt phosphorylates insulin receptor substrate to limit pi3k-mediated pip3 synthesis. *Elife* (2021) 10:1–32. doi: 10.7554/eLife.66942

46. Kubota N, Kubota T, Kajiwara E, Iwamura T, Kumagai H, Watanabe T, et al. Differential hepatic distribution of insulin receptor substrates causes selective insulin resistance in diabetes and obesity. *Nat Commun* (2016) 7:1–16. doi: 10.1038/ncomms12977

47. Hirashima Y, Tsuruzoe K, Kodama S, Igata M, Toyonaga T, Ueki K, et al. Insulin down-regulates insulin receptor substrate-2 expression through the phosphatidylinositol 3-kinase/Akt pathway. *J Endocrinol* (2003) 179(2):253–66. doi: 10.1677/joe.0.1790253

48. Zhang J, Ou J, Bashmakov Y, Horton JD, Brown MS, Goldstein JL. Insulin inhibits transcription of IRS-2 gene in rat liver through an insulin response element (IRE) that resembles IREs of other insulin-repressed genes. *Proc Natl Acad Sci U S A* (2001) 98(7):3756–61. doi: 10.1073/pnas.071054598

49. Rui L. Energy metabolism in the liver. *Compr Physiol* (2014) 4(1):177–97. doi: 10.1002/cphy.c130024

50. Godoy P, Hewitt NJ, Albrecht U, Andersen ME, Ansari N, Bhattacharya S, et al. Recent advances in 2D and 3D *in vitro* systems using primary hepatocytes, alternative hepatocyte sources and non-parenchymal liver cells and their use in investigating mechanisms of hepatotoxicity, cell signaling and ADME. *Arch Toxicol* (2013) 87(8):1315–530. doi: 10.1007/s00204-013-1078-5

51. Ben-Moshe S, Itzkovitz S. Spatial heterogeneity in the mammalian liver. *Nat Rev Gastroenterol Hepatol* (2019) 16(7):395–410. doi: 10.1038/s41575-019-0134-x

52. Graffmann N, Ring S, Kawala M-A, Wruck W, Ncube A, Trompeter H-I, et al. Modeling nonalcoholic fatty liver disease with human pluripotent stem cell-derived immature hepatocyte-like cells reveals activation of PLIN2 and confirms regulatory functions of peroxisome proliferator-activated receptor alpha. *Stem Cells Dev* (2016) 25(15):1119–33. doi: 10.1089/scd.2015.0383

53. Graffmann N, Ncube A, Martins S, Fiszl AR, Reuther P, Bohndorf M, et al. A stem cell based in vitro model of NAFLD enables the analysis of patient specific individual metabolic adaptations in response to a high fat diet and AdipoRon interference. *Biol Open* (2021) 10(1):bio054189. doi: 10.1242/bio.054189

54. Parafati M, Kirby RJ, Khorasanizadeh S, Rastinejad F, Malany S. A nonalcoholic fatty liver disease model in human induced pluripotent stem cell-derived hepatocytes, created by endoplasmic reticulum stress-induced steatosis. *Dis Model Mech* (2018) 11(9):dmm033530. doi: 10.1242/dmm.033530

Frontiers in Endocrinology

Explores the endocrine system to find new therapies for key health issues

The second most-cited endocrinology and metabolism journal, which advances our understanding of the endocrine system. It uncovers new therapies for prevalent health issues such as obesity, diabetes, reproduction, and aging.

Discover the latest Research Topics

See more →

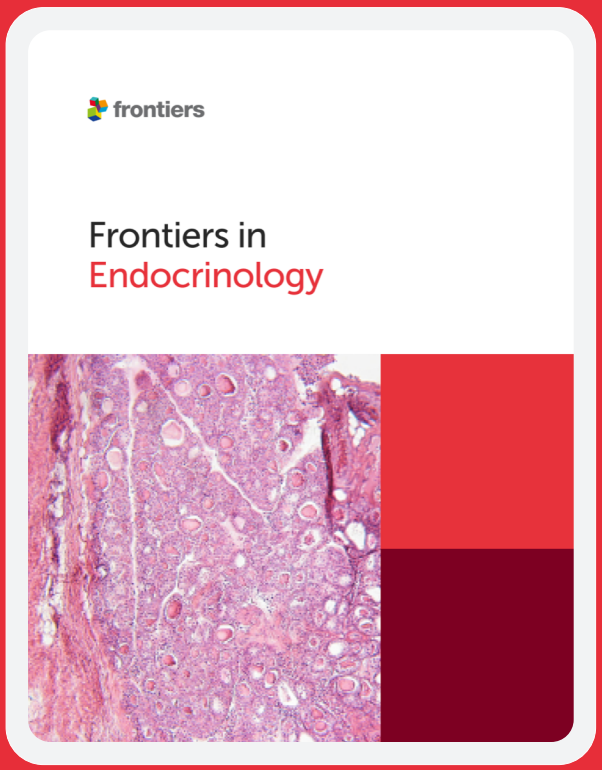

Frontiers

Avenue du Tribunal-Fédéral 34
1005 Lausanne, Switzerland
frontiersin.org

Contact us

+41 (0)21 510 17 00
frontiersin.org/about/contact